TECHNISCHE UNIVERSITÄT MÜNCHEN

Lehrstuhl für Lebensmittel- und Bio-Prozesstechnik

Immobilized enzyme technology for the production of whey protein hydrolysates

- Design of flow-through immobilized trypsin reactors, influence of hydrolytic environment, and comparison with free trypsin

Yuhong Mao

Vollständiger Abdruck der von der Fakultät Wissenschaftszentrum Weihenstephan für Ernährung, Landnutzung und Umwelt der Technischen Universität München zur Erlangung des akademischen Grades eines

Doktors der Naturwissenschaften (Dr. rer. nat.)

genehmigten Dissertation.

Vorsitzende: Prof. Dr. -Ing. Mirjana Minceva

Prüfende der Dissertation:

1. Prof. Dr.-Ing. Ulrich Kulozik
2. Prof. Dr. rer. nat. Wilfried Schwab

Die Dissertation wurde am 17.01.2019 bei der Technischen Universität München eingereicht und durch die Fakultät Wissenschafts zentrum Weihenstephan für Ernährung, Landnutzung und Umwelt am 10.04.2019 angenommen.

Acknowledgement

This thesis arose from my work at the Chair of Food and Bioprocess Engineering, (formerly Chair of Food Process Engineering and Dairy Technology), Technical University of Munich. It was encouraged and supervised by Prof. Dr.-Ing. Ulrich Kulozik, to whom I would like to express special gratitude. I appreciate all the support and encouragement from him during my life in Germany. Particularly, I do appreciate his TRUST to accept me as a PhD candidate.

Many thanks to Elena Leeb and Dr. Seronei Chelulei Cheison for their inspiration on my research work, to Claudia Hengst and Heidi Wohlschläger for their friendly support with the HPLC analysis, to Dr. Jannika Dombrowski for her help with the correction of my “Zusammenfassung”, to Friederike Schöpflin, Sabine Becker for their nice support with various chores, etc. Warm thanks to all my colleagues for so many interesting and lovely parties, as well as for training me how to drink beer☺, especially to “handsome” Hansi and “sweet” Annette. In particularly, I want to thank my very nice office colleague Melli, who did help me a lot and answered me at least hundreds of questions. I do enjoy the warm atmosphere here.

I would like to thank all my students, Daniel Kremer, Maria Krischke, Fabian Dick, who contributed to this work, for their great commitment and the pleasant collaboration.

I also thank Dr. Urh Černigoj from BIA Separations (Ajdovščina, Slovenia) for his technical help in developing the CIM-MITR, as well as for his helpful scientific discussion.

At the end, I want to thank my family, teachers and lovely friends in China for their wonderful support, encouragement and motivation. At their convenience, I would like to express my appreciation in Chinese.

亲爱的爸爸妈妈，谢谢你们对我的支持，在远方的我不仅没有办法照顾你们，还时常让你们为我担心。回想过去的四年多，自己确实不懂事，时常说一些让你们为我担忧的话。谢谢你们对我永无止境的包容和爱。

谢谢敬爱的杨老师，一直以来对我的关心，指导和鼓励，以及师姐李超对我申请博士职位的帮助。还有我可爱的小伙伴们，仲仲，淑萍，郑局长，etc., 无论多久没联系，每一次见面都毫无陌生感。特别感谢在德国认识的庄昱师兄，so nice!!! 也因为他，我认识了人生很重要的一个人。

最后，薛同学，谢谢你☺☺☺

Danke Deutschland.

明心见性

Abbreviations

ALD	/	Aldehyde
A	Au	Spectrophotometer absorbance
B	m^2	Permeability
BA		N_α-Benzoyl-L-arginine
BAEE	/	N_α-Benzoyl-L-arginine ethyl ester
BAHC	/	Benzamidine hydrochloride
c	mg/mL	Concentration
Ca^{2+}	/	Bivalent calcium ions
$CaCl_2$	/	Calcium chloride
CDI	/	Carbonyldiimidazole
CIM	/	Convective interaction media
D	cm	Outer diameter
d	cm	Inner diameter
d_{10}	nm	Diameter at which 10% of the sample's mass is comprised of particles with a diameter less than this value
d_{50}	nm	Diameter at which 50% of the sample's mass is comprised of particles with a diameter less than this value
d_{90}	nm	Diameter at which 90% of the sample's mass is comprised of particles with a diameter less than this value
Di	/	Dilution factor
DH		Degree of hydrolysis
DHAP		2,5-dihydroxyacetophenone
EDA	/	Ethylendiamine
EDA-GLA	/	Ethylendiamine-glutaraldehyde
F	mL/min	Flow rate
HCCA		α-cyano-4-hydroxycinnamic acid
HCl	/	Hydrochloride acid
H (h)	cm	Height
h	/	Number of hydrolyzed peptide bonds
h_{tot}	/	Total number of peptide bonds in one gram protein substrate
IMER	/	Immobilized enzyme reactor
IMTR	/	Immobilized trypsin reactor

K_m	µmol/mL	Michaelis-Menten constant
K_m"	µmol/min	Modified Michaelis-Menten constant
K_{cat}	/	Turnover number
LC-ESI		Liquid chromatography-electrospray source ionization-tandem
MS		Mass spectrum
MALDI-ToF		Matrix-assisted laser desorption/ionization time-of-flight
MITR	/	Monolith based immobilized trypsin reactor
MES	/	2-(n-morpholino)-ethanesulfonic acid
Na^+	/	Sodium ion
NaCl	/	Sodium chloride
NaOH	/	Sodium hydroxide
N_b		Normality of the base
OPA	/	Trinitrobenzenesulphonic acid
PI	/	Isoelectric point
2-PB	/	2-picoline borane
ΔP	mPa	Pressure drop/backpressure
R	mg/min or %	Depleting rate of protein
RP-HPLC	/	Reversed phase high performance liquid chromatography
$NaBH_4$	/	Sodium borohydride
$NaCNBH_3$	/	Sodium cyanoborohydride
t	min or h	Time
TGase	/	Transglutaminase
TNBS		Trinitrobenzenesulphonic acid
Tris	/	(hydroxymethyl)-aminomethane
U*	µmol/min	Enzymatic activity, the amount of BAEE converted to BA in 1 min
V_{max}	µmol/min	Maximal velocity
v/v	/	Volume/volume
WP	/	Whey protein
WPC	/	Whey protein concentrate
WPI	/	Whey protein isolate
α	/	Average degree of dissociation of the amine groups
α-La	/	α-lactalbumin

β-Lg	/	β-lactoglobulin
ε	mol^{-1} cm^{-1}	Molar extinction coefficient
$\dot{\gamma}$	s^{-1}	Shear rate
η	Pa·s	Viscosity
σ	Pa	Shear stress
γ_{load}	mg/mL	Concentration of trypsin in the loading solution
γ_n	mg/mL	Concentrations of trypsin in washing and deactivation fractions after the immobilization
v	meqv/min	Rate of reaction

Content

1 General Introduction

Whey is the fluid by-product resulting from the precipitation of casein in milk. The precipitation can be facilitated by the growth of microorganisms, the addition of acid or enzymes (Kilara & Vaghela, 2018). Whey contains high-quality proteins that not only can benefit consumers from nutritional perspectives, but also are very important to the textural and sensory quality of food products. The processing of whey proteins, including heat treatment, extrusion, gelation, chemical and enzymatic modification, etc., significantly affects their structural, nutritional, and functional properties. Among these processing techniques, the enzymatic modification of proteins represents an attractive way due to fast reaction rates, mild conditions, and high specificity. Proteases and transglutaminase are the most frequently used enzymes for modifying whey proteins (Kilara & Vaghela, 2018).

Trypsin (EC 3.4.21.4), a serine protease in the digestive system of human and animals, was discovered by Wilhelm Kühne (1877). This enzyme is widely used in proteomic research, due to its high specificity, which preferably cleaves the C-terminal peptide bonds of Arg and Lys (Olsen, Ong & Mann, 2004). Except in proteomic research, trypsin is also one of the most widely used enzymes in food processing, where trypsin or a trypsin preparation (mixed with other enzymes) has been used to improve both functional and nutritional properties of food proteins. To reduce the cost of large-scale use of trypsin in solution and improve its industrial implementation, the enzyme immobilization represents an attractive technique due to the possibility of reusing enzymes and producing enzyme-free hydrolysates. In this chapter, a general introduction on the processing of whey proteins, the enzyme trypsin, and the immobilization of enzymes will be provided. Since the interaction between the substrate and the enzyme depends on a variety of factors influencing structure of both the enzyme and substrate, these factors will be varied in this study so that the basics are required to be discussed first.

1.1 Processing of whey proteins

Whey proteins products are concentrated from whey by removing minerals and lactose. The most common protein levels in whey protein concentrates (WPCs) are 35%, 55%, and 80%. The highest form of whey purification yields whey protein isolates (WPIs) with >90% protein on a dry weight basis (Kilara & Vaghela, 2018). The processing of whey proteins is attracting more and more attention, and innovative manufacturers are adding processed whey proteins to everything from desserts, snacks and frozen entrees to sauces, dips, dressings and more.

1.1.1 Compositions of whey proteins

The composition of whey proteins from cow milk is illustrated in Table 1-1, where the amount of each whey protein is compared with that in human milk. In cow milk, β-lactoglobulin (β-Lg) and α-lactalbumin (α-La) represent the major whey proteins, which accounts for 80% of the total amount of whey proteins. In human milk, β-Lg does not

exist while α-La shows a much higher amount. Thus, β-Lg in cow milk is considered to act as a primary allergen, especially in infant formulae (Selo, Clement, Bernard et al., 1999). Among minor whey proteins, lactoferrin and lysozyme present only traceable amount, which are significantly lower than those in human milk. This thesis mainly considered the major whey proteins β-Lg and α-La in bovine milk, thereby, their structural and functional properties are described in detail.

Table 1-1. Comparison of whey protein compositions between human and cow milk.

Protein	Human milk (g/L)	Cow milk (g/L)
Whey proteins	6.4	5.8
α-Lactalbumin	2.6	1.1
β-Lactoglobulin	/	3.6
Lactoferrin	1.7	trace
Serum albumin	0.5	0.4
Lysozyme	0.5	trace
Immunoglobulins	0.8 (IgA)	0.5 (IgG)

1.1.1.1 β-lactoglobulin

As shown in Fig. 1-1, β-Lg contains 162 amino acids and has a molecular weight (MW) of 18.3 kDa and a isoelectric point (PI) of 5.35 (Edwards, 2008). β-Lg, classified into the family of lipocalin, has been isolated with endogenously bound fatty acids and has been shown to bind a variety of hydrophobic molecules in vitro, but its true function remains unclear (Brownlow, Cabral, Cooper et al., 1997). There are three variants, labeled as A, B and C, commonly occur in cow's milk (Qin, Bewley, Creamer et al., 1999). Among three variants, β-Lg A and B are the most abundant (Edwards, 2008), which differ at two sites: Asp_{64} in A is changed to Gly in B, and Val_{118} in A is changed to Ala in B. Furthermore, β-Lg contains five cysteine residues, four of whom form two intramolecular disulfide bridges (Cys_{66}–Cys_{160} and Cys_{106}–Cys_{119}). The secondary structure of native β-Lg, marked in Fig. 1-1, consists of about 7–11% α-helix, 52–54% β-sheet, 27% β-turn and 9–10% of random coil (Yang, Yang, Kong et al., 2015).

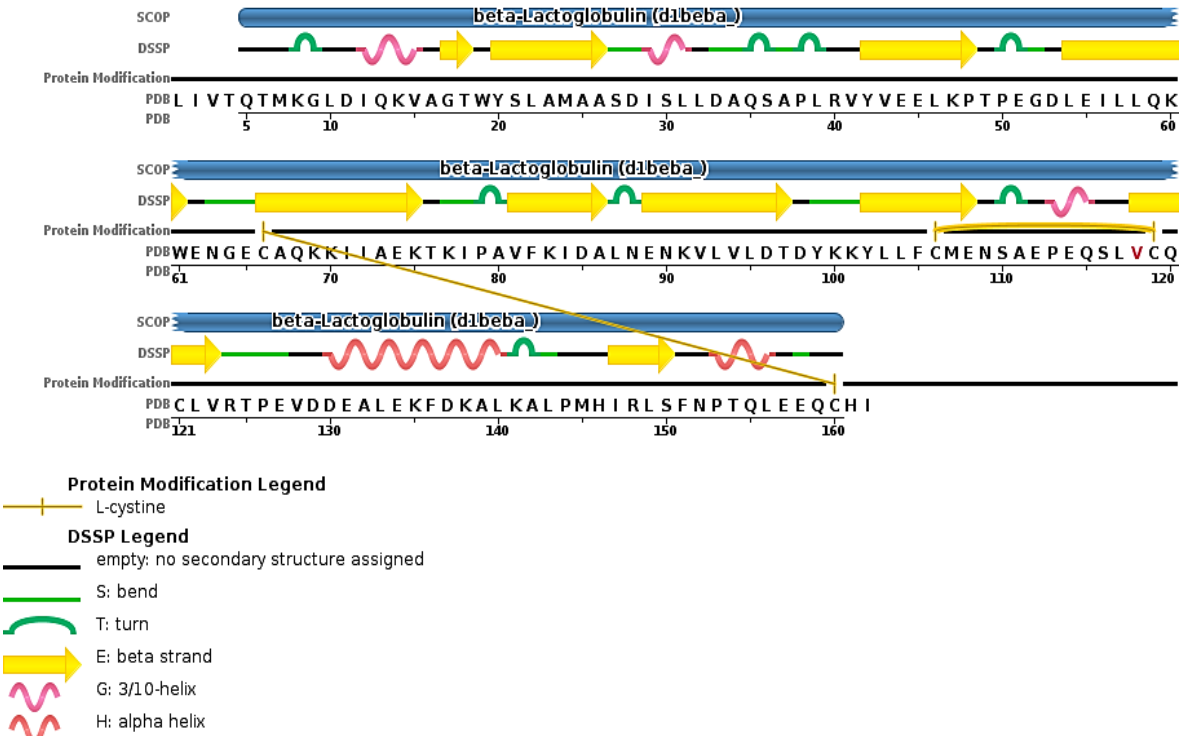

Fig. 1-1. Primary and secondary structures of β-lactoglobulin. Image from the RCSB PDB (www.rcsb.org) with PDB ID 1BEB.

The first tertiary structure of β-Lg at the medium-resolution determined by Papiz and Sawyer (1986) illustrates that the molecular structure consists of eight stranded antiparallel β-sheets flanked on one side by an α-helix constituting a hydrophobic pocket (Fig. 1-2). The remaining free thiol group (Cys_{121}) is buried inside this hydrophobic pocket within the globular structure and thus, is not accessible at the native state. Regarding the two very common genetic variants, β-Lg A and B, the Asp64Gly substitution results in the CD loop adopting a different conformation, whereas the Val118Ala substitution causes no detectable change in structure (Qin et al., 1999). However, a previous research suggests that the lower thermal stability of the B variant is mainly due to the substitution of Val118Ala, which results in the hydrophobic core being less well packed. In contrast to the thermal stability, β-Lg B displayed a higher resistance to tryptic digestion (Creamer, Nilsson, Paulsson et al., 2004).

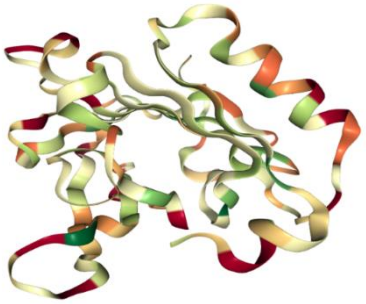

Fig. 1-2. 3D structure of β-lactoglobulin, colored from red (hydrophilic) to green (hydrophobic). Image from the RCSB PDB (www.rcsb.org) of PDB ID 1BEB.

The quaternary structure of β-Lg varies from monomer to dimer or oligomer, which depends on pH, temperature and ionic strength (Casal, Kohler & Mantsch, 1988), as shown in Fig. 1-3. The dimer interface is described in Figure 1-4 by Brownlow et al. (1997). Namely, twelve hydrogen bonds have been identified; four of these are main chain bonds between β strand I of adjacent monomers (N Arg_{148} → O Arg_{148}* and N Ser_{150} → O His_{146}*, and the complement of both). The largest number of interactions occurs between the AB loops of each monomer, where the following mainly sidechain hydrogen bonds exist: N Ala_{34} → OD1 Asp_{33}*, NH1 Arg_{40} → OD1 Asp_{33}*, NH1 Arg_{40} → OD2 Asp_{33}* and NH2 Arg_{40} → OD2 Asp_{33}* and the complement of each.

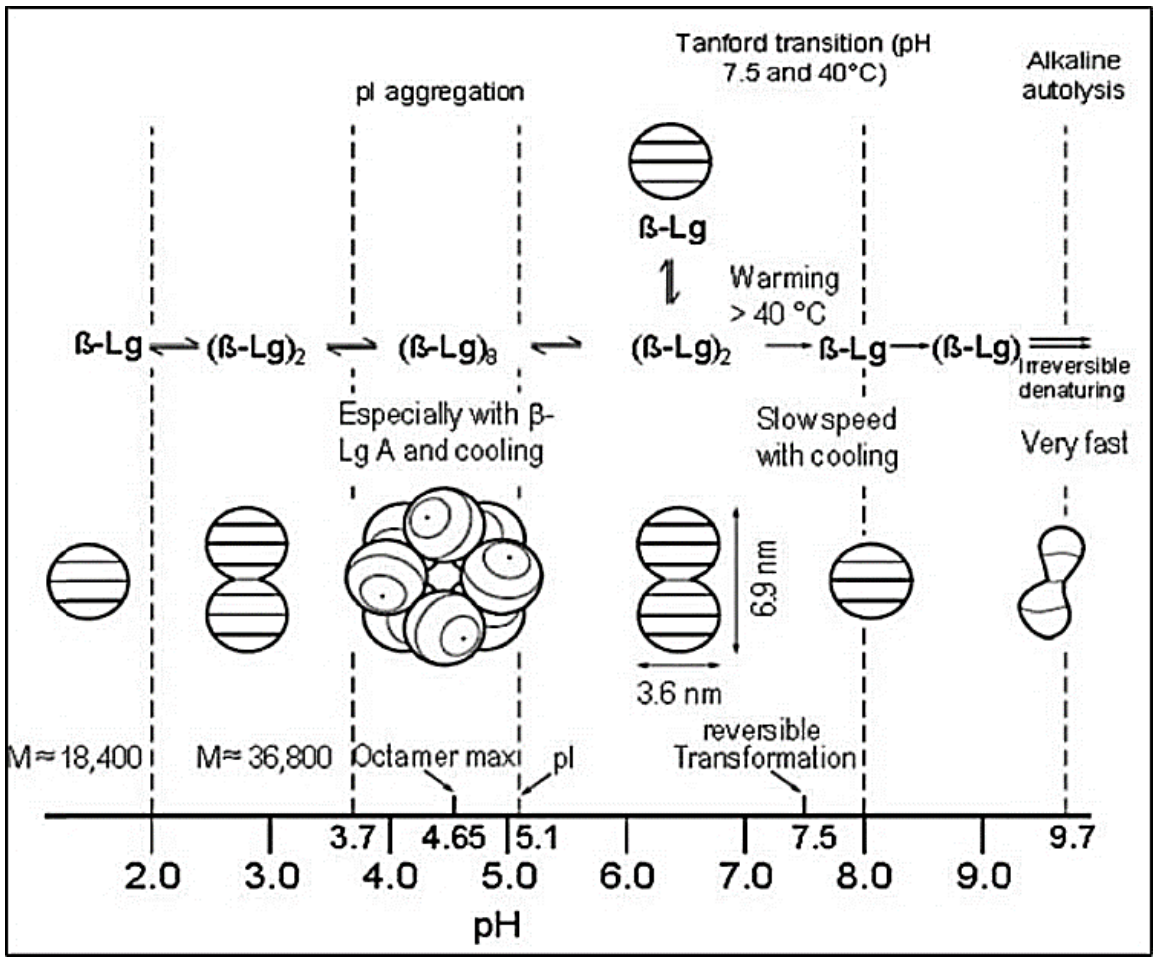

Fig. 1-3. Influence of the temperature and pH on the molecular structure of β-lactoglobulin (Cheison & Kulozik, 2017).

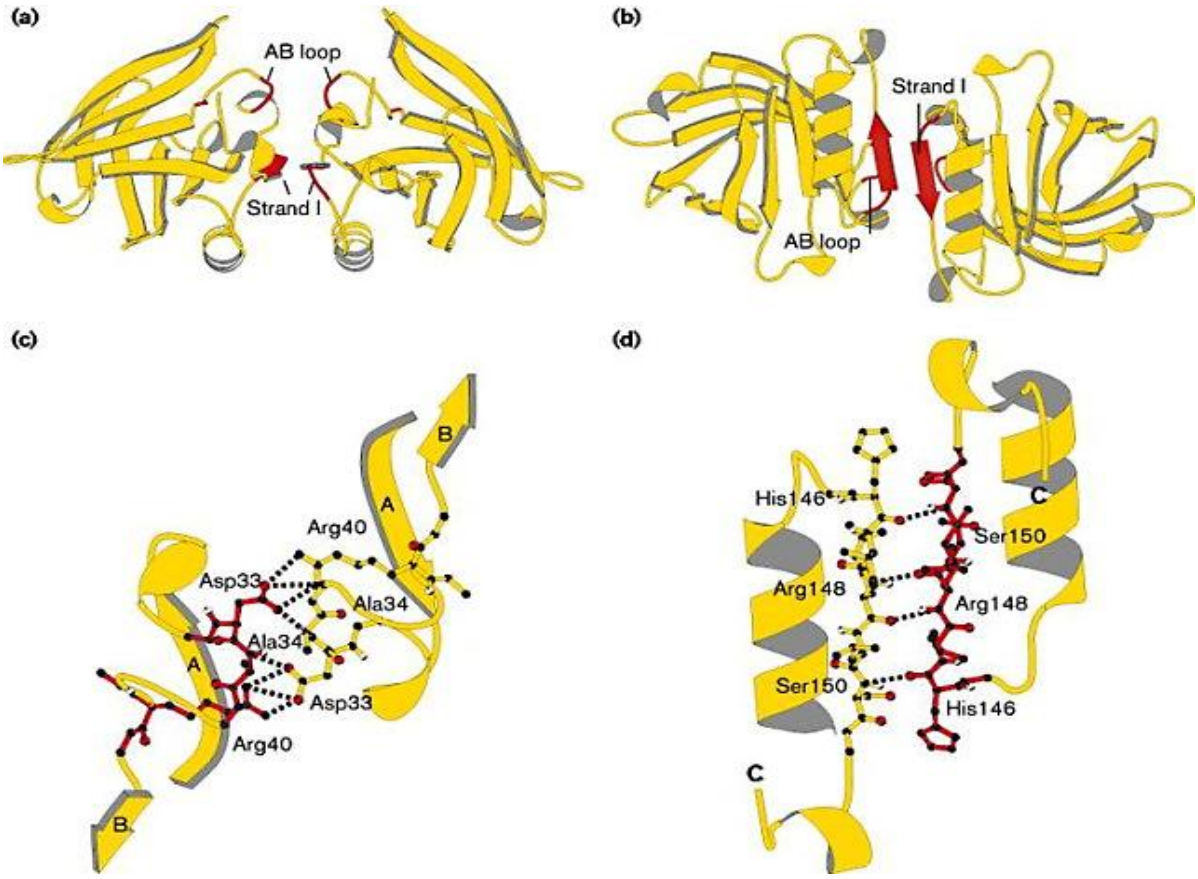

Fig. 1-4. The dimer interface of β-lactoglobulin. Regions involved in the interface are coloured red. (a) The interface is viewed along β strand I and (b) rotated through 90°. The hydrogen bonds between adjacent AB loops are shown in (c) and the hydrogen bonds between adjacent β strands are shown in (d). Hydrogen bonds are represented by dashed lines (Brownlow et al., 1997).

Influence of pH on β-Lg structures

Under physiological conditions β-Lg exists as a dimer, and decreasing pH to 3.5–5.5 β-Lg, especially the genetic variant A, forms octamers at low temperatures. The octamer is supposed to be a closed ring, consisting of four dimers associated symmetrically about a tetrad axis (Pessen, Purcell & Farrell, 1985). By further decreasing pH to 2, it tends to dissociate into monomers, and increasing pH above 6.8 also leads to dissociation of the dimers. In addition, the most remarkable effect of increasing pH on β-Lg structural changes is reported by Tanford, Bunville and Nozaki (1959). They observed that a general conformational transition occurred at the pH near 7.5, where a buried carboxyl group was released, leading to an increase in the reactivity of a free sulfhydryl group and a change of the exposure of a tyrosine moiety. They also found that this reversible structural transition at pH 7.5 was not an unfolding, rather like a new folding. Further increasing pH up to 9.5, β-Lg undergoes a more generally slow and irreversible denaturation. Regarding the pH effects on the secondary structures of β-Lg, Casal, Kohler and Mantsch (1988) calculated the proportion of each motif at increasing pH values, as summarized in Table 1-2.

Table 1-2. Influence of pH on the secondary structures of β-lactoglobulin (Casal, Kohler & Mantsch, 1988).

pH	Observed wavenumber (cm^{-1}) [a]	Proportion (%) [b]	Assignment
2	1682	1	ß-sheet
	1667	11	turns
	1653	32	α-helix + random
	1637	25	d-sheet
	1626	30	ß-sheet
3	1682	4	d-sheet
	1666	15	turns
	1652	27	α-helix + random
	1637	28	ß-sheet
	1627	25	d-sheet
7	1680	6	ß-sheet
	1664	19	turns
	1649	22	α-helix + random
	1636	32	ß-sheet
	1624	21	ß-sheet
10	1676	8	ß-sheet
	1660	18	turns
	1647	25	random
	1633	35	ß-sheet
	1622	14	ß-sheet
13	1674	19	ß-sheet
	1658	22	turns
	1640	60	random
	1629	8	ß-sheet

[a] *After deconvolution;* [b] *Percent areas obtained by curve-fitting: estimated error ± 10%.*

Influence of temperature on β-Lg structures

Close to natural pH, bovine β-Lg presents as dimmers at room temperature, while the dimer dissociation occurs between 30 and 55°C (Sawyer, 1969). Moreover, higher temperatures causes unfolding and increases thiol reactivity (Sawyer, 2003). The thermal denaturation of β-Lg occurs in two stages: (1) at about 60°C, it turns into the intermediate structure, which is the same as that found in the alkaline denaturation; (2) the final stage at around 90ºC does not unfold β-Lg to a random coil before aggregating and polymerizing, which is clearly distinct from the alkaline denaturation. Surprisingly, the secondary structure of β-Lg is more affected by decreasing temperatures to minus degree, e.g., one at –15°C involves primarily changes in the β-strands (Casal et al., 1988). In addition, the effects of temperature highly depend on the processing time. Fang and Dalgleish (1997) indicated that heating at lower temperatures (70 and 80ºC) for a longer time caused extensive denaturation, as heating at higher temperature (90ºC) for a short time. However, the structure of the denatured protein was different in the two cases. Namely, more β-structure remained when denatured at lower temperatures, whereas evidence for extensive intermolecular β-structure was found on the sample heated at a higher temperature.

Influence of salts on β-Lg structures

The ion-specific effect of salts on proteins is firstly reported in a systematic way by Franz Hofmeister (1888), who ranked the ability of ions at a fixed ionic strength to affect the properties of proteins in aqueous solutions. He differentiated between chaotropes and kosmotropes, i.e., salts that induced either disorder or more order in the protein conformation. Renard, Lefebvre, Griffin et al. (1998) found that β-Lg favored dimerization in the presence of NaCl. Furthermore, ions also affect the tertiary structure of β-Lg, e.g., Trp exposure increases in the presence of high concentration of NaCl, indicating that more hydrophobic groups are exposed (Zhao, Li & Li, 2017). In addition, the influence of salts on β-Lg is intensively investigated under the thermal processing, as salts are suggested to prevent β-Lg from denaturation (Baussay, Bon, Nicolai et al., 2004; Renard et al., 1998).

Influence of organic solvents on β-Lg structures

Organic solvents are wildly used for the cold gelation of β-Lg (Kundu, Aswal & Kohlbrecher, 2017; Nikolaidis & Moschakis, 2018; Renard, Lefebvre, Robert et al., 1999). In the study of Dufour et al. (1993), the secondary structure transformation of β-Lg from a predominantly β-structure into the α-helical one is influenced by solvent polarity changes, and the mid-points of the observed structural transformation occur at dielectric constant ≈ 60 (30–40% ethanol). These structural changes are not a sudden, rather a gradual transformation depending on the ethanol concentration, as well as on pH, temperature. Some studies (Dufour, Bertrand & Haertlé, 1993; Dufour & Haertlé, 1990; Mousavi, Chobert, Bordbar et al., 2008; Renard et al., 1999) suggest that β-Lg exhibits an intermediate state around 20% ethanol, where it starts unfolding and binds an additional second retinol molecule. Besides, β-Lg in 50% ethanol shows a higher α-helix content at pH 8 than at pH 7 (Renard et al., 1999). These conformational changes lead to the exposure of hydrophobic residues in the core of β-Lg to the solvent. Aggregation or gelation due to hydrophobic interactions may subsequently take place (Renard et al., 1999). Dufour, Robert, Bertrand et al. (1994) found that at concentrations above 0.5 mM (≈ 10 mg/mL), β-Lg had the potential to aggregate and gel in hydroalcoholic solutions.

1.1.1.2 α-lactalbumin

α-La is the second most abundant whey protein in bovine milk, which is composed of 123 amino acids (Fig. 1-5). This protein has a MW of 14.17 kDa and a PI of 4.8 (Edwards, 2008). There are two predominant genetic variants (A and B) for α-La, and the B variant presents in the milk of most *Bos taurus* cattle, while the variant A presents at a low frequency in the milk of some Italian and Eastern European *Bos taurus* breeds. These two genetic variants differ only at one position, Glu_{10} in variant A is substituted by Arg in B (Stanciuc & Râpeanu, 2010). A-La binds Ca^{2+}, with the holo form being the more abundant form in milk, whereas it presents as apo form when Ca^{2+} is liberated (Edwards, 2008). In the mammary gland, α-La participates in lactose synthesis, thereby creating an osmotic “drag” to facilitate milk production and secretion. It binds divalent cations (Ca^{2+}, Zn^{2+}) and may facilitate the absorption of essential minerals.

Furthermore, it provides a well-balanced supply of essential amino acids to the growing infant (Lonnerdal & Lien, 2003). Delavari, Saboury, Atri et al. (2015) suggest that α-La can be introduced as a suitable carrier for vitamin D3.

The secondary structures of α-La are illustrated in Fig. 1-5. Its native state consists of two domains: a large α-helical domain and a small β-sheet domain, which are connected by a calcium binding loop. The α-helical domain is composed of three major α-helices (residues 5–11, 23–24, and 86–98) and two short 3/10 helices (residues 18–20, and 115–118). The small domain is composed of a series of loops, consisting of a small three-stranded antiparallel β-pleated sheet (residues 41–44, 47–50, and 55–56) and a short 3/10 helix (three residues per turn and an intra chain hydrogen bond loop containing 10 atoms; residues 77–80) (Permyakov & Berliner, 2000). The globular tertiary structure of α-La is stabilized by four disulfide bridges, i.e., Cys_{6}–Cys_{120}, Cys_{61}–Cys_{77}, Cys_{73}–Cys_{91} and Cys_{28}–Cys_{111}, among which the cysteine bridge between residues 73 and 91 holds the aforementioned two domains, forming the Ca^{2+} binding loop (Permyakov & Berliner, 2000). Thus, α-La shows high affinity toward Ca^{2+}, which stabilizes its native structures as the holo- form. This form is compared with its apo- form (without binding Ca^{2+}) using NMR spectroscopy by Wijesinha-Bettoni, Dobson, and Redfield (2001). Their results show that the rearrangements of the structure associated with the conversion of the holo to apo form of the protein do not involve the detectable population of partially unfolded intermediates. Chrysina, Brew and Acharya (2000) compared the crystal structures of these two forms in a great detail, as shown in Fig. 1-6. The ions (Ca^{2+} and Zn^{2+}) binding sites are marked in Fig. 1-6 A and the structures of α-La in apo-, holo- and recombinant forms are illustrated in Fig. 1-6 B. A conformational change is found at the inter-lobe interface (which connects the Ca^{2+} binding site and the cleft involving Tyr_{103} through a channel containing trapped water molecules) located on the opposite face of the apo- form. Thus, after the removal of Ca^{2+} from holo α-La, the protein adopts a molten globular structure which is a compact conformer with a large proportion of native secondary structure but little fixed tertiary structure (Chrysina, Brew & Acharya, 2000). In addition, interactions between α-La and calcium strongly depend on pH values, i.e., such interactions are insignificant at pH values < 4.0, whereas an increase in pH toward neutrality entails the binding of one or possibly two calcium ions (Patocka & Jelen, 1991). Regarding the influence of environmental conditions on α-La structures, it is very important to point out that any conditions inducing conformational transitions, such as temperature, pressure, denaturant concentration, depend upon metal ion concentration, especially that of calcium ion (Permyakov & Berliner, 2000).

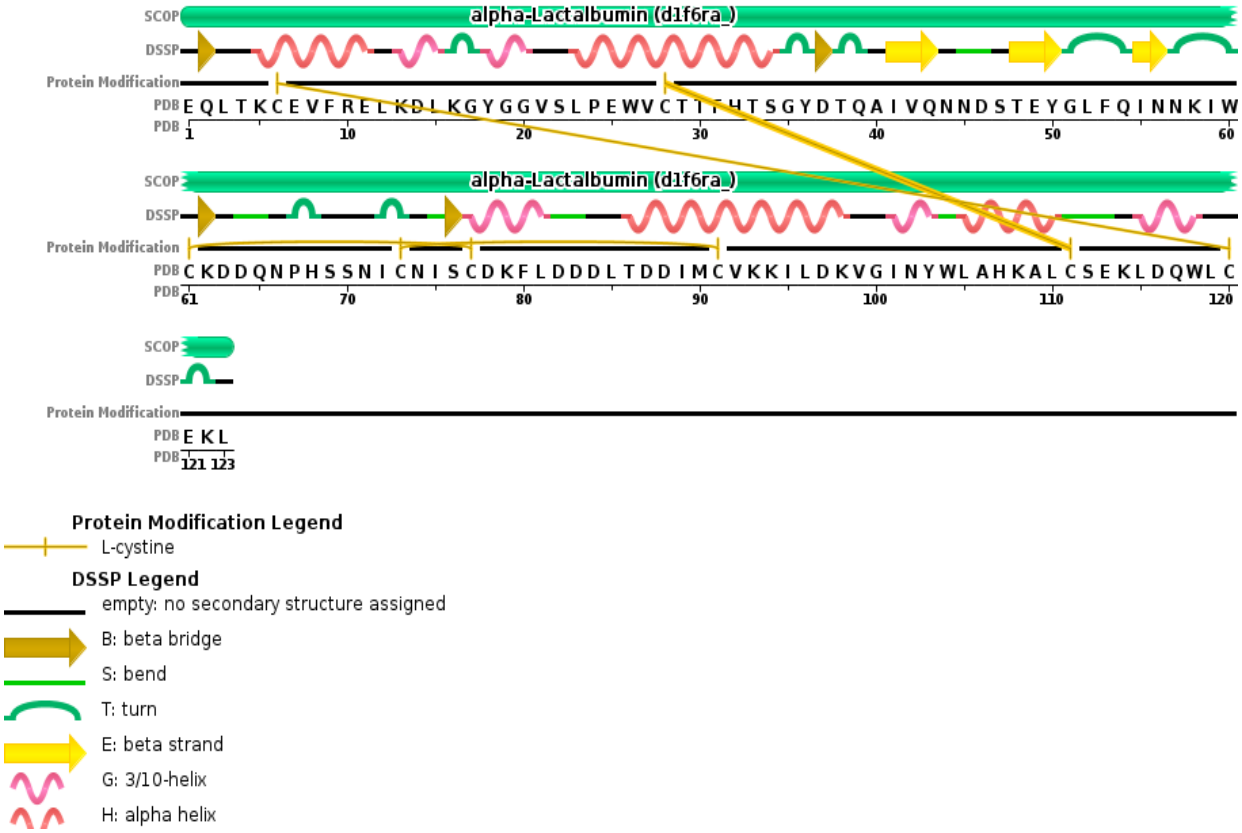

Fig. 1-5. Primary and secondary structures of α-lactalbumin. Image from the RCSB PDB (www.rcsb.org) with PDB ID 1F6R.

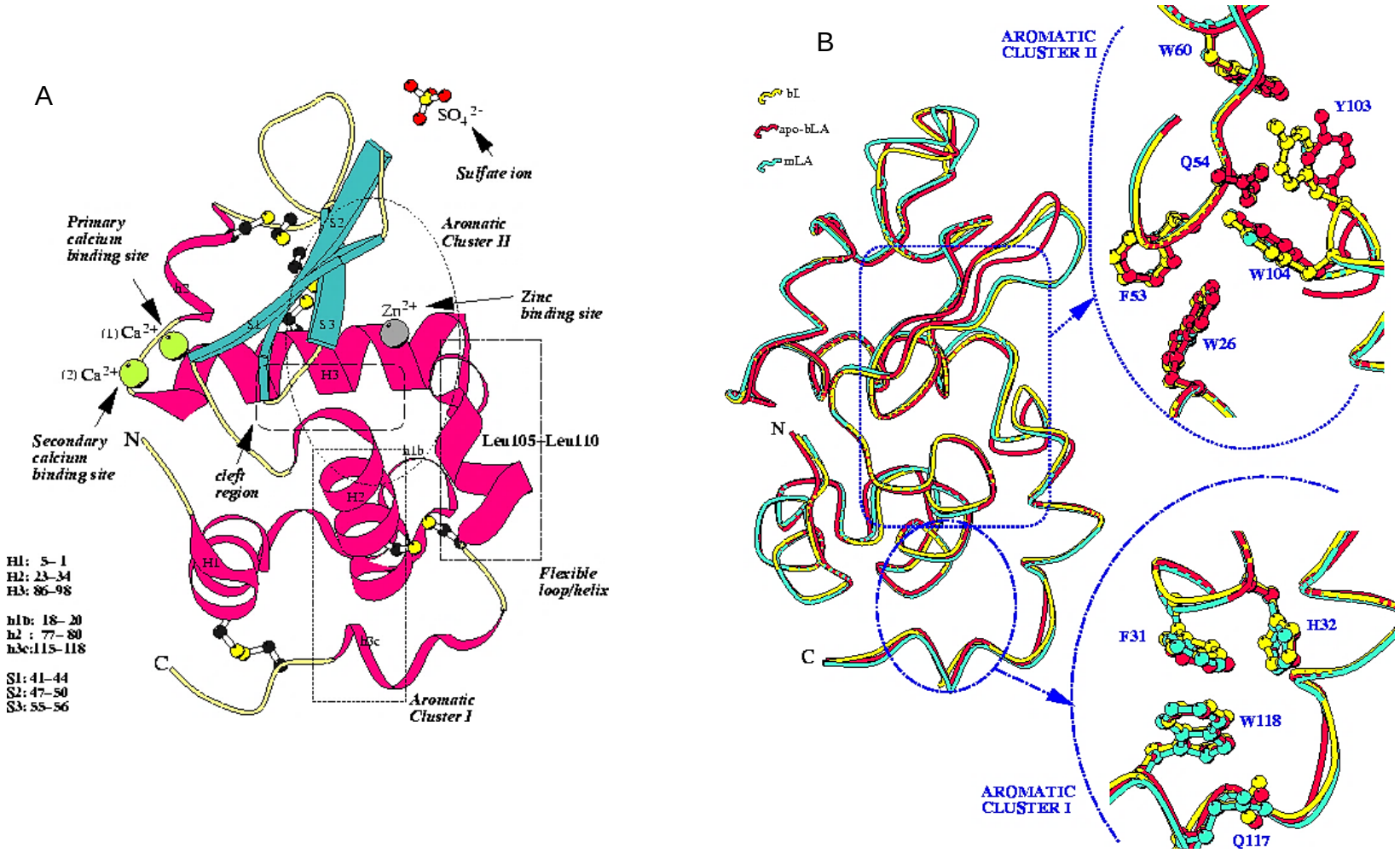

Fig. 1-6. (A) Structure of α-lactoglobulin and its functional regions showing the location of metal ions. Secondary structural elements (S, b-strand; H, a-helix; h, 310 helix) are marked; (B) Superposition of α-La structures. The Ca^{2+} free (apo α-La) structure is shown in red, the native α-La (holo α-La) structure is shown in yellow, and recombinant α-La in green. The insets show the details of packing interactions in aromatic clusters I and II (the hydrophobic box) (Chrysina, Brew & Acharya, 2000).

1.1.2 Processing state of whey proteins

Whey proteins present various functionalities, such as foaming, emulsification, gelation, etc., as well as provide high-quality nutrition to consumers. To further improve the nutritional or functional properties of whey proteins, protein modifications are necessary. Generally, physical treatments and enzymatic modifications are the most popular and are wildly implemented. Chemical modifications of proteins are also possible but are not generally practiced, due to the necessity to prove the processing safety to humans (Kilara & Vaghela, 2018).

1.1.2.1 Physical processing

Whey proteins are physically processed by various separation/fractionation techniques to get each component from the mixtures for specific applications, as well as by thermal treatment, extrusion, etc., to create ideal particle sizes for using as innovative ingredients or substitutions in various food products.

Separation and fractionation

Many research groups are working on the separation and fractionation of whey proteins by membrane filtration or chromatographic methods (Aguero, Bringas, Román et al., 2017; Geng, Tolkach, Otte et al., 2015; Heidebrecht, Kainz, Schopf et al., 2018; Konrad & Kleinschmidt 2008; Toro-Sierra, Tolkach & Kulozik, 2011). The two major whey proteins α-La and β-Lg have similar protein sizes and PI values, which are considered as a challenge to be separated from each other. Kamau, Cheison, Chen et al. (2010) summarized the available methods for isolating α-La from milk (based on studies before 2010), as shown in Fig. 1-7. Later, combing thermal treatment with membrane filtration, these two proteins were obtained separately at high overall yields and purities, i.e. yields are 60.7–80.4% for α-La at a purity of 91.3%, and 80.2– 97.3% for β-Lg at a purity of 97.2% (Toro-Sierra et al., 2011). Geng et al. (2015) developed a method by using anion exchange chromatography in combination with ultrafiltration to obtain kilogram-scale amounts of α-La of 100% purity from α-La enriched WPC at a high recover rate of 85%. With the respect to separating minor whey proteins, such as immunoglobulin class G (IgG), Heidebrecht et al. (2018) developed a mixed-mode chromatographic method and obtained 130–150 g pure IgG from 3 L colostrum within five hours.

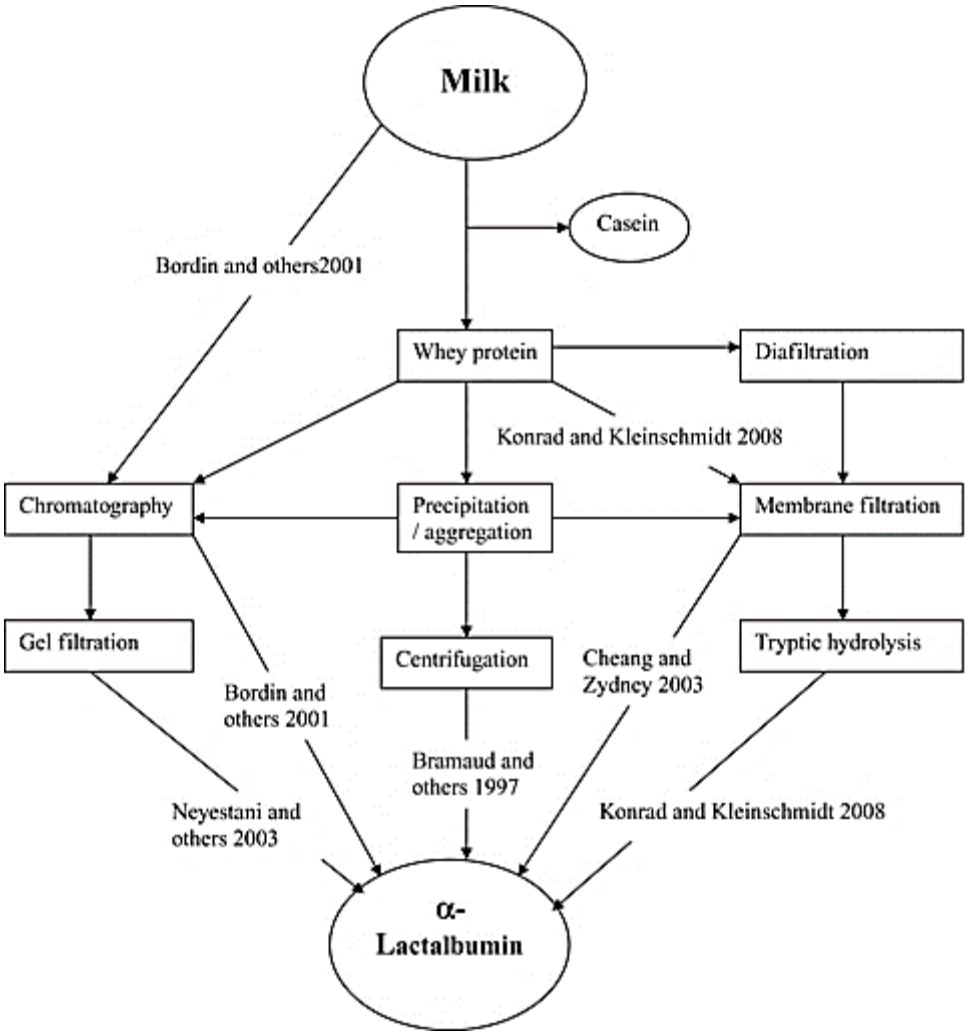

Figure 1-7. A summary of the available methods for the isolation and manufacture of α-La from milk based on studies until 2010 (Kamau et al., 2010).

Thermal treatment

Conventionally, thermal processing is usually employed to enhance sensorial and nutritional quality of whey proteins, as well as to extend the shelf life of final products. Generally, heat treatment modifies proteins via denaturation, restructuring of disulfide bonds and generation of new intra/inter molecular bonds, leading to changes in protein structures or contributing to the increase in practical size. Klarenbeek (1984) summarized effects of various heat treatments (up to 150°C) on structure and solubility of whey proteins. It is pointed out that mild heat treatments up to 60°C may affect reversibly the solubility and foaming properties of whey proteins. Conformational changes are observed above 60°C for α-La and near 80 and 140°C for β-Lg, exerting more serious effects on the functional properties of whey proteins. Modifications of cysteine-residues in the polypeptide chain are detected above 100°C under identical heating conditions. Except for the applied temperature, the addition of salts and the heating modes (direct versus indirect) significantly affect the outcome of thermally processed whey proteins. For instance, in the work of Kelleher, Mahony, Kelly et al. (2018), direct and indirect heat treatment were applied to WPI solutions, resulting in

significantly different final products in terms of appearance, physical characteristics and volatile profile, and many enhanced properties were observed for the products by direct heat treatment. Baussay et al. (2004) explored the influence of ionic strength on the heat-induced aggregation of β-Lg at pH 7, and found that density of the aggregates increased with increasing ionic strength. In addition, the thermal treatment is combined with shear processing, to obtain ideal particle sizes. For example, Wolz and Kulozik (2017) used heated co-rotating twin screw extruder to particulate whey proteins.

Non-thermal treatment

With the developments of non-thermal processing techniques, such as pulsed light, high-pressure processing (HPP), irradiation, cold plasma, ultrasound and pulsed electric field (PEF), these processing techniques can induce changes in protein conformation, and mitigate the allergenicity of certain proteins while retaining the original characteristics of the food materials (Ekezie, Cheng & Sun, 2018). For example, an ultra high-pressure homogenizer (up to 300 MPa) was used to treat WPI solutions (3%, w/w), which dissociated large protein aggregates leading to the unmasking of buried hydrophobic groups without affecting protein solubility, so that enhancing the viscoelasticity of air-water interfaces and improving foam stability (Bouaouina, Desrumaux, Loisel et al., 2006). Besides, it is suggested that surface hydrophobicity of the soluble WPI aggregates is significantly increased by ultrasound treatment (Shen, Fang, Gao et al., 2017). Veerman, Baptist, Sagis et al. (2003) developed a new multistep Ca^{2+}-induced cold gelation process for β-Lg, by which the critical percolation concentration was an order of magnitude lower than in the conventional cold gelation method.

1.1.2.2 Enzymatic processing

Schmidt and Poll (1991) investigated the sensitivity of major whey proteins to various enzymes, i.e., serine proteinases, cysteine proteinases, aspartic proteinases and metallo proteinases, in total 14 types of proteases, providing important information on the selection of enzymes to hydrolyze whey proteins. The enzymatic processing of whey proteins mainly aims at: (1) reducing allergenicity; (2) improving functionalities, such as gelling, foaming, emulsifying properties; and (3) obtaining bioactive peptides. Following descriptions will give more details on each respect.

Reduction of allergenicity

Allergy to bovine milk is one of the most common types of food allergy, especially in infants. Thus, the application of hypoallergenic formulae is recommended. Hypoallergenic formulae are frequently manufactured from the whey protein fraction, which contains a high amount of β-Lg, a major allergen absent from human milk (Lozano-Ojalvo, Pérez-Rodríguez, Pablos-Tanarro et al., 2017). In several works (Cheison, Leeb, Toro-Sierra et al., 2011; Lisak, Toro-Sierra, Kulozik et al., 2013), this major allergen β-Lg is selectively digested by trypsin or chymotrypsin, and the other major whey protein α-La which presents in human milk, is able to be remained at a large extent.

With respect to reducing allergenicity, enzymatic processing mainly destroys the linear epitopes by extensively or partially hydrolyzing the allergens. Both extensively (eHF) and partially (pHF) hydrolyzed formulae are used in allergy prevention nutrition. eHF is almost allergen free, and most of its residual oligo-peptides have MWs below 3 kDa. The pHF is more palatable and less expensive than most eHF formulae, and typically has MWs in the range of 3 to 10 kDa. Besides, the low residual content of allergen in pHF suggests that they may induce oral tolerance without sensitization (Exl, 2001). Regarding eHF, Lakshman, Toyokawa, Tachibana et al. (2011) applied several enzymes to produce hypoallergenic bovine whey protein hydrolysates, and found that the lowest antigenicity was observed in the WPC hydrolysates treated with acid proteinases from *Monascus pilosus* and trypsin. In the study of Kim, Ki, Khan et al. (2007), it is suggested that incubation of heated WPC with 1% pepsin and then with 1% trypsin was the most effective way for producing low-antigenic hydrolysates from WPC. Lozano-Ojalvo et al. (2017) provided a process to produce pHF and their results show that a hydrolysate of whey proteins by pepsin under high pressure, containing 50% of peptides with molecular masses between 3 and 10 kDa, retains sufficiently immunogenicity to stimulate Th2 responses, but is not enough to generate specific IgE or IgG1 antibodies that could mediate systemic anaphylaxis.

Improvement of functionalities

Enzymatic processing of whey proteins results in the reduction of MW, thus, in an increased solubility as well as in the exposure of hydrophobic groups previously buried inside the protein. Therefore, whey protein hydrolysates may present higher rate of diffusion to the oil/water interface and better ability to cover a larger area of the interface than the intact protein, affecting the functionalities, such as foaming, emulsifying, and gelling capacities. A study indicates that glycation of β-Lg with galactose followed by limited hydrolysis presents exceptional foam stability, which might allow extending the use of this protein as a foaming agent. Besides, whey proteins derived peptides are suggested as both emulsifiers and bioactive compounds in nanoemulsion delivery systems (Adjonu, Doran, Torley et al., 2014). Regarding the gelling ability, Chen, Swaisgood, and Foegeding (1994) found that the partially hydrolyzed β-Lg had a lower gel point and gelled more rapidly than the intact protein at 80°C.

Production of bioactive peptides

Enzymatic hydrolysis of whey proteins liberates fragments that can promote health benefits in the immune, cardiovascular, nervous and gastrointestinal systems, which are the so-called bioactive peptides (Dullius, Goettert & Souza, 2018). Some commercially sold functional ingredients based on bioactive peptides derived from whey proteins are summarized by Dullius et al. (2018), which are reproduced in Table 1-3. Various enzymes are used for the production of bioactive peptides, such as trypsin (Leeb, Gotz, Letzel et al., 2015), alcalase (Peng, Kong, Xia et al., 2010), thermolysin (Contreras, Hernández-Ledesma, Amigo et al., 2011), etc.. Pretreatment of whey proteins followed by enzymatic hydrolysis is suggested to be an approach for

controlling the release of peptides (Adjonu, Doran, Torley et al., 2013; Leeb et al., 2015; Costa, Gontijo & Netto, 2007; Okamoto, Rikimaru, Enomoto et al., 2014).

Following production process, peptides with different functionalities must be separated and enriched to achieve high-yield products. Membrane separation methods, such as ultrafiltration and nanofiltration (Arrutia, Rubio & Riera, 2016; Quintieri, Monaci, Baruzzi et al., 2017), are commonly applied in current food industry due to the feasible cost. To increase the selectivity of membrane filtration, electro membrane separation technologies are suggested, which use electric charge and molecular mass to affect peptide separation in one-step (Leeb, Holder, Letzel et al., 2014). In addition, with high selectivity, membrane adsorption chromatographic techniques are attractive due to the largely improved fractionation efficiency by increasing process capacity and flow rates, compared with conventional bead-based chromatography.

Among whey proteins, the hydrolysis of β-Lg attracts particular attentions (Hernandez-Ledesma, Recio & Amigo, 2008). As mentioned previously, this protein is considered as a major allergen protein, and simultaneously it works as a precursor for several identified peptides with interesting bio-functionalities. For instance, peptides f(9–14), f(71–75), f(78–83), f(92–100) and f(142–148), generated by tryptic hydrolysis of β-Lg, are reported with ACE-inhibiting, bactericidal or hypocholesterolemic properties, respectively (Leeb et al., 2015).

Table 1-3 Commercially sold functional food ingredients based on bioactive peptides derived from whey proteins, reproduced from the work of Dullius, Goettert and Souza (2018).

Product name	Manufacture	Type of product	Peptide	Health claim
BioZate® Product line	Davisco, USA	Hydrolysed whey protein isolate	β-lactoglobulin fragments	Reduction of blood pressure
BioPureGMP™	Davisco. USA	Whey protein isolate (WPI)	GMP f(106–169)	Prevention of dental caries, blood clotting, antibacterial, antivirus
Vivinal® ALPHA	Borculo Domo Ingredients (BDI), the Netherlands	Ingredient/hydrolysate	Whey-derived peptide	relaxation and sleep
Praventin™	DMV International, the Netherlands	Food supplement/capsule	Lactoferrin enriched whey protein hydrolysate	Acne reduction
Dermylex™	Advitec Inc., Canada	Food supplement/ tablet	Whey protein extract XP-828L	Reduces symptoms of psoriasis
Hilmar™8390	Hilmar Ingeredient, USA	Food suuplement	Whey protein hydrolysate	ACE inhibition, DPP-IV enzyme inhibition
NOP-47™	Glanbia Nutritionals, USA	Food supplement and pharmaceutical applications	Whey derived peptide	Anti-inflammatory properties

Abbreviations: GMP: glycomacropeptide, ACE: angiotensin-converting enzyme, DPP-IV: dipeptidylpeptidase IV.

1.2 The enzyme Trypsin

The protease trypsin and its inactive precursor, trypsinogen, were first obtained in crystalline form from bovine pancreatic tissue. With the cleavage of peptide bond Lys_6–Ile_7 on trypsinogen, this precursor is transformed into the active form β-trypsin (Walsh, 1970). The activation process is catalyzed by a variety of enzymes, including enterokinase, mold proteases, and trypsin itself (Walsh, 1970). As shown in Fig. 1-8, β-trypsin (from bovine pancreas) contains 223 residues and has a MW of 23.3 kDa (Walsh, 1970). Six disulfide bridges in trypsin stabilize its tertiary structures. Further autolysis of β-trypsin (cleaved at Lys_{131}–Ser_{132}) results in α-trypsin which is held together by disulfide bridges. In addition, calcium ions are very important to the activity, heat stability, and structure of trypsin. As shown in Fig. 1-9, the position on trypsin for the calcium ion binding is illustrated. With formation of calcium-trypsin complex, an altered form of trypsin with a more compact structure possesses greater enzyme activity than calcium-free trypsin (Sipos & Merkel, 1970).

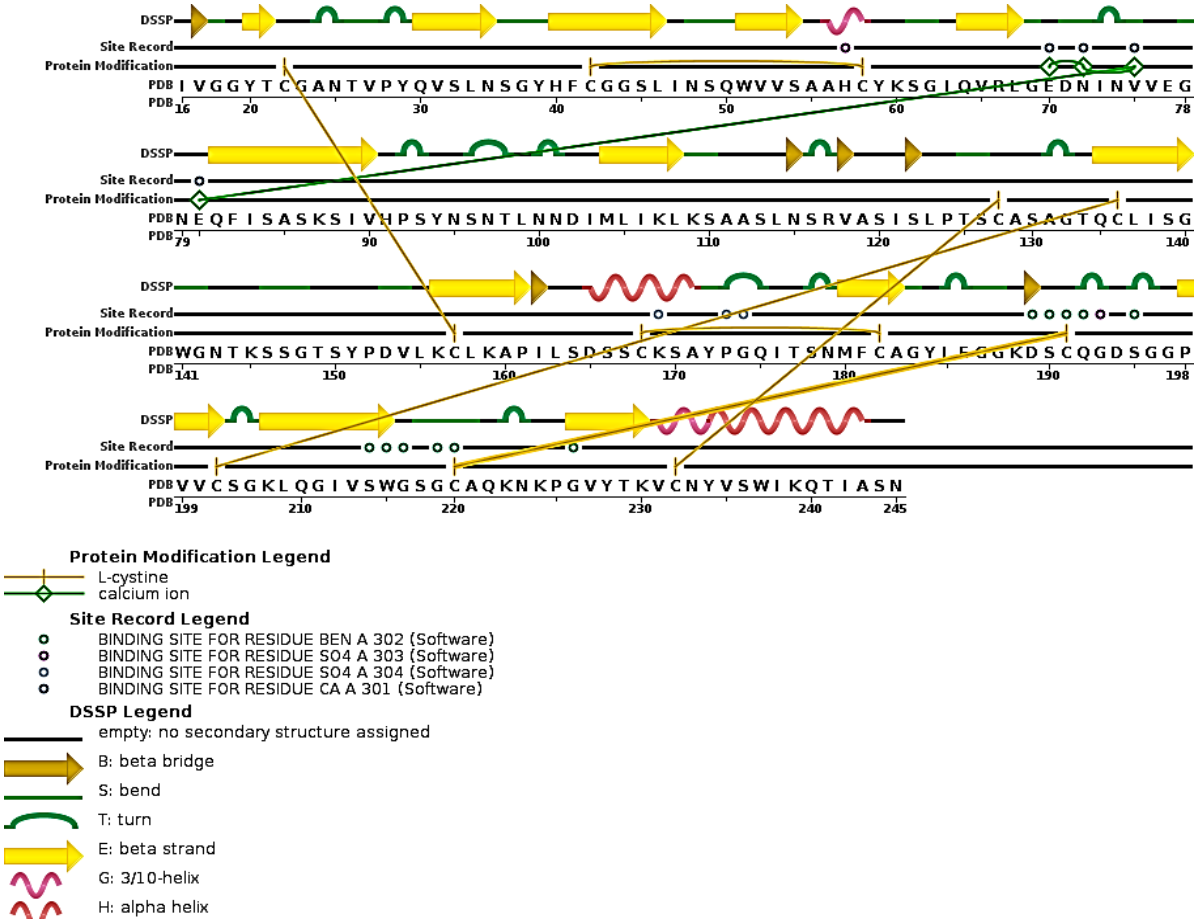

Fig. 1-8. Primary and secondary structures of bovine trypsin. Image from the RCSB PDB (www.rcsb.org) with PDB ID 4I8H.

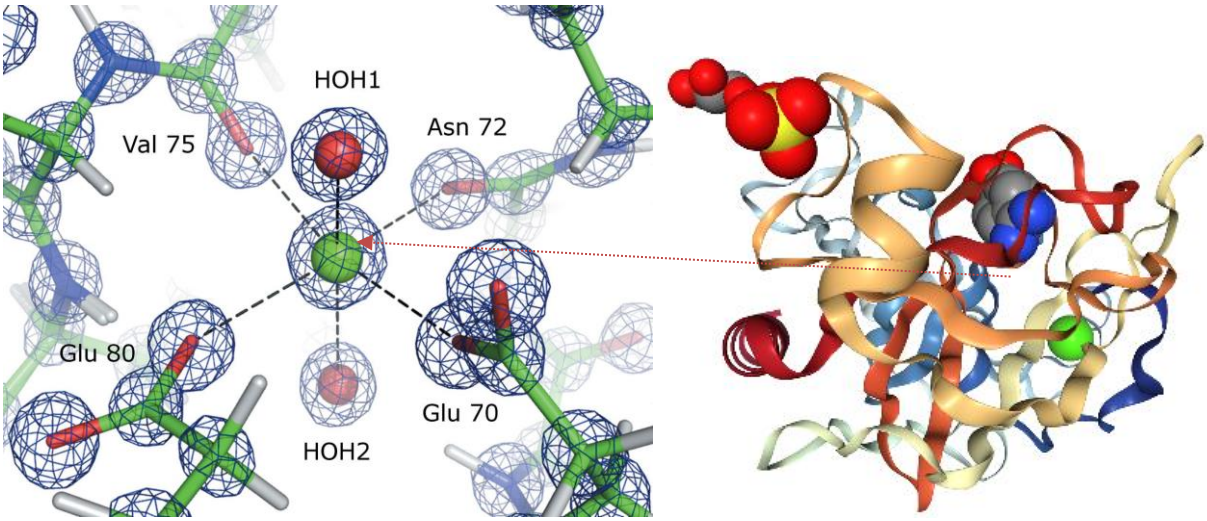

Figure 1-9. 3D structure of bovine trypsin (blue is the N-terminus and red is the C-terminus). The calcium ion binding site on trypsin is highlighted on left. Image from the RCSB PDB (www.rcsb.org) with PDB ID 4I8H.

1.2.1 Specificity and selectivity

As the member of serine protease family, trypsin shares about 40% amino acid homology with chymotrypsin, and both contain a catalytic triad consisting of His_{57}, Asp_{102}, and Ser_{195} (Polgar, 2005). In addition to the catalytic triad, the binding pocket on trypsin, also called S1 pocket, constitutes by Asp_{189}, Gly_{226} and Gly_{216}, which dominantly decides its specificity (Fig. 1-10). This S1 pocket is deeper and narrower, compared with the binding pocket on chymotrypsin. Besides, a negatively charged Asp, locating at the bottom of this binding pocket, binds basic amino acids via ionic interactions. Hence, target amino acids for cleavage need to have long side chains and be positively charged to allow formation of the enzyme/substrate complex. Only Arg and Lys meet these criteria, and therefore trypsin is considered to cleave exclusively C-terminal to Arg and Lys residues (Olsen, Ong & Mann, 2004). However, previous studies (Asao, Tsuji, Tashiro et al., 1992; Cheison, Brand, Leeb et al., 2011; Cheison, Leeb, Letzel et al., 2011) report that cleavage at Tyr-Ser on several substrates is a common feature, even when the purest possible trypsin is used. In addition, as trypsin has, within its sequence, 14 Lys and 2 Arg residues, which are potential attack sites for trypsin, it might undergo autolysis during the hydrolysis process.

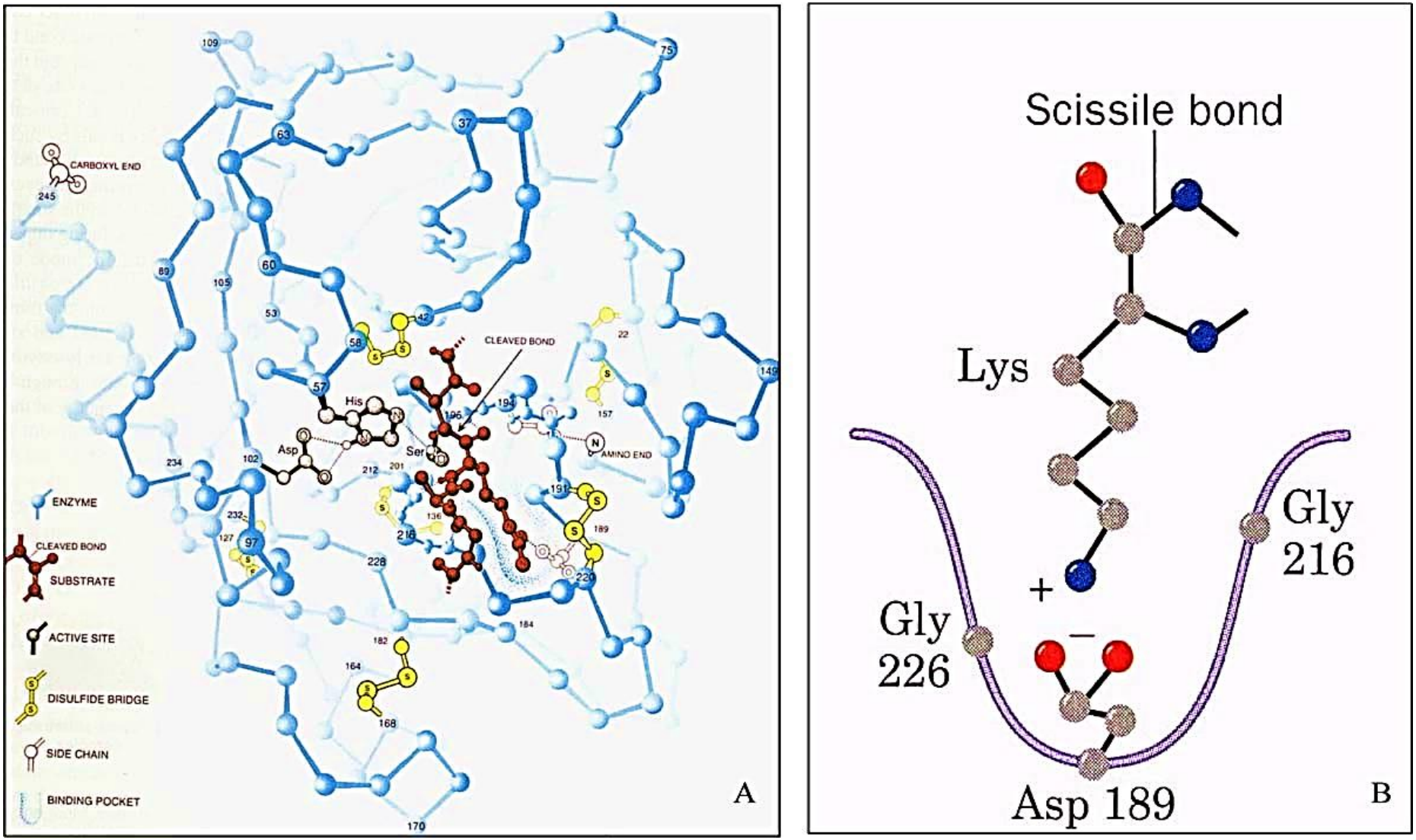

Figure 1-10. The catalytic triad and binding pocket on trypsin (Linenberger & Bretz, 2015).

The specificity of a proteolytic enzyme describes the type of amino acid, after which it can hydrolyze a peptide bond (e.g., Lys and Arg for trypsin). Regardless of the specificity of the enzyme for individual cleavage sites, not all cleavable sites are hydrolyzed at the same time. To clearly describe this preference in protein hydrolysis, Butre, Sforza, Gruppen et al. (2014) introduced the criteria “selectivity”, referring to the rate at which individual cleavage sites in a protein substrate are hydrolyzed relative to other cleavage sites. The ability to discriminate the selectivity of an enzyme is considered essential for understanding enzymatic hydrolysis of proteins, especially in terms of obtaining hydrolysates consisting of desired properties.

Some groups indicate that the selectivity an enzyme is decided by the primary structure of a substrate (Abramowitz, Schechter & Berger, 1967; Deng, Veer, Sforza et al., 2017). Abramowitz et al. (1967) defined the residue, after which following the scissile bond, as the P_1 residue, and the neighbouring amino acids toward N-termini of the protein were P_2 to P_n and those toward the C-termini side were P_1' to P_n'. They indicated that the selectivity of an enzyme toward a cleavage site was modulated by five or six residues surrounding the cleavage site (from P_3 to P_3'). For instance, it is suggested that trypsin shows very low selectivity toward a cleavage site if an acidic residue is on either side of this site and no cleavage occurs if a Pro residue is after the cleavage site. In the conclusion of Deng et al. (2017), when both amino acids on neighbor positions of the binding site are charged, this cleavage site is considered to have a low accessibility to trypsin, such as Lys_{100} and Lys_{135} on β-Lg.

Except the influence of substrate primary structure, the secondary, tertiary, even quaternary structures of a substrate protein might make it difficult for the enzyme to access certain scissile bonds, which is the so-called steric hindrance. Wright (1977) reports evidence for the secondary and conformational specificities of trypsin, and suggests that the secondary specificity of trypsin is not sequence-specific, but is peptide main chain in the third and fourth positions, which is determined by the tertiary structure of the substrate. Some studies (Cheison et al., 2011; Fernández & Riera, 2013) found that f(76-138) on β-Lg constituted a resistant core to tryptic attack. In addition, the holo- α-La is resistant to tryptic hydrolysis, while its apo- form does not (Schmidt & Poll, 1991).

1.2.2 Sources of trypsin

The natural trypsin, found in the digestive system of many vertebrates, is formed in the small intestine from the trypsinogen produced by the pancreas (Rawlings & Barrett, 1994). Commonly, trypsin is extracted and purified from animal pancreas such as bovine, ovine and porcine. Recently, the extraction and characterization of trypsin from several fish species attracts considerable attention (Castillo-Yanez, Pacheco-Aguilar, Garcia-Carreno et al., 2005; Kishimura, Hayashi, Miyashita et al., 2006; Klomklao, Benjakul, Visessanguan et al., 2007; Klomklao, Benjakul, Visessanguan et al., 2006). However, the production of trypsin based on extraction from animal sources suffers a series of disadvantages, particularly, the supply of raw material and the low content of trypsin in the raw material.

An alternative way to produce food enzymes is via microbial fermentation, which can be better controlled than extractions from animal organs. Microbial enzymes used in food processing are commonly as a form of enzyme preparations which typically contain other enzymes and metabolites of the production strain except the desired enzyme (Mullally et al., 1994). Furthermore, it is necessary to consider the safety to apply such enzyme preparations in food processing, particularly, the toxigenic potential of the enzyme producing strain. Some commercially available enzyme preparations containing trypsin activity include alcalase, protamex, and pronase, etc..

With the development of recombinant technology in biology, many enzymes now used in food processing are produced from recombinant microorganisms. Some patents disclosing the production of trypsin or trypsinogen by recombinant several microbial strains are summarized in Table 1-4. However, the expression of mammalian trypsin in microbial systems is not easy to achieve in commercially relevant levels. Recently, Novozymes Bio- tech, inc. has commercialized the microbial trypsin based on strain *Fusarium venenatum* (gene modified) and named as Formea™. They indicate that this microbial trypsin shows the specificity very close to the ones extracted from the porcine source.

Table 1-4. Summary on patents disclosing the production of trypsin or trypsinogen by several recombinant microbial strains.

Patent	**Trypsin type**	**Microbial system**	**Assignee**	**Priority date**
US5945328A	porcine trypsin	*Aspergillus Oryzae host Strain*	Novo Nordisk As	1995
WO01/55429	human trypsinogen and trypsin	*E. coli*	Polymun Scientific Immunbiologische Forschung Gmbh	2000
WO2000017332A1	trypsin and trypsinogen analogs	*E. coli*	Eli Lilly And Company, Universite Louis Pasteur	1998
WO1999010503A1	trypsinogen	*E. coli*	Roche Diagnostics Gmbh	1997
US0043455A1	mammalian trypsin	*Fusarium venenatum*	Novozymes Biotech, Inc.	2004

1.2.3 Applications of trypsin in food protein processing

In the processing of food proteins, trypsin is applied to (1) improve the functional properties, such as solubility, emulsification, foaming and gelling properties of food proteins; (2) improve the digestibility of vegetable and seed proteins; (3) produce protein hydrolysates and bioactive peptides that are used in infant formulae and for people with special health problems such as hypertension; and (4) reduce the concentration of allergens in some foods (Yu & Ahmedna, 2012).

An extensive hydrolysis of food proteins easily leads to a bitter tasting, as well as to the loss of certain functionalities, such as foaming, emulsifying, gelling properties. Contrast to an extensive hydrolysis, limited or partially proteolysis exposes hydrophobic and hydrophilic residues, enhances the amphiphilic characteristics of proteins, and probably improves the functionalities of treated proteins. Due to the strict specificity of trypsin, a tryptic hydrolysis of most proteins is relatively easy to be controlled as a limited hydrolysis, thus, trypsin is popular in the enzymatic modification of food proteins. For instance, it is reported that tryptic treatment of casein results in a higher emulsion activity and emulsion stability compared to those treatments by papain and pancreatin (Luo, Pan & Zhong, 2014). Banach, Lin and Lamsal (2013) observed that milk protein concentrate increased its emulsion activity and stability after the hydrolysis by trypsin or chymotrypsin, while not by papain. In addition, trypsin is wildly applied to produce food-derived bioactive peptides. According to the source of protein, some identified bioactive peptides derived from various food proteins by trypsin or the combination of trypsin with other proteases, are sorted out in Table 1-5.

Table 1-5. Summary on identified bioactive peptides derived from various food proteins by trypsin or the combination of trypsin with other proteases.

Protein sources		Identified Peptides	Activity	Reference
Milk protein	Casein	FFVAP	ACE-inhibition	Migliore-Samour and Jolles (1988)
		GLF	Immunomodulation	Fiat, Migliore-Samour, Jolles et al. (1993)
	β-Lg	IPAVF	Dipeptidyl peptidase-IV inhibitory	Silveira, Martinez-Maqueda, Recio et al. (2013)
		GLDIQK	ACE-inhibitor	Pihlanto-Leppälä, Rokka, and Korhonen (1998)
		IIAEK	Hypocholesterolemic	Nagaoka, Futamura, Miwa et al. (2001)
		IPAVFK	Bactericidal	Pellegrini, Dettling, Thomas et al. (2001)
		VLVLDTDYK	Bactericidal	
		ALPMHIR	ACE-inhibitor	Mullally, Meisel, and FitzGerald (1997)
	α-La	GLF	Immune-modulating	Jaziri, Migliore-Samour, Casabianca-Pignede et al. (1992)
		EQLTK	Antimicrobial	Pellegrini, Thomas, Bramaz et al. (1999)
		GYGGVSLPEWVCTTF	Antimicrobial	
Soy protein		MLPSYSPY	Anticancer	Kim, Kim, Kim et al. (2000)
		LLPHH	Antioxidative	Korhonen and Pihlanto (2003)
		RPLKPW	Antihypertensive	
Rice albumin		GYPMYPLPR	Immunostimulation	Takahashi, Moriguchi, Ikeno et al. (1996)

1.3 Immobilization of enzymes

The adsorption of invertase observed by Nelson and Griffin (1916) is considered as the first scientific observation leading to the discovery of immobilized enzymes (Homaei, 2015). Over 100 years, immobilized enzymes consistently attract considerable attention due to their numerous benefits over free enzymes and their increasing applications. Namely, the immobilization of enzymes provides merits like: (1) the convenient storage and shipment of enzymes; (2) saves on enzyme cost due to recycle possibilities; (3) the improvement of enzyme stability against harsh physical and chemical conditions, such as high temperature, denaturant agent, extreme shear force, etc.; (4) production of enzyme-free hydrolysates, minimizing downstream product processing; (5) high potential for industrial adaptation. However, the immobilization process might change enzyme structures, leading to the loss of enzymatic activity even to the inactivation of the enzyme. In addition, limitations by mass transfer could be another major concern while using immobilized enzymes, due to the used supports that might cause hindrance for the substrate to contact the immobilized enzyme molecules. Thus, the immobilization technology is extremely important to obtain an immobilized enzyme system with desired properties.

1.3.1 Immobilization technology

Immobilization technology generally comprises the development of suitable supports, the immobilization pathways (covalent binding, adsorption, physical entrapment, etc.), as well as the immobilization protocols, including environmental conditions and agents.

1.3.1.1 Support materials

The support materials play a crucial role in enzyme immobilization, because these materials might significantly affect the properties of catalytic systems containing immobilized enzymes. For example, in the work of Hernandez, Garcia-Galan and Fernandez-Lafuente (2011), where lipase B is immobilized on different commercial porous beads, a much higher specific activity is observed for the systems using support of MCI GEL CHP20P than those using decaoctyl Sepabeads. In the review of Homaei (2015), the supports commonly used in enzyme immobilization are classified into inorganic and organic materials according to their chemical compositions, as well as into porous and none porous materials based on their morphological properties. In this review, eight support materials are illustrated in detail, i.e., biopolymers, synthetic polymers, hydrogels, inorganic supports, smart polymers, conducting polymers, gold nanoparticles and magnetic nanoparticles. Recently, Zdarta, Meyer, Jesionowski et al. (2018) also provide a general overview on support materials for enzyme immobilization, where these support materials are divided into two main groups, classic and new materials. Classic materials are usually abundant in nature (mineral, biopolymers) or are easy to synthesize, which makes them relatively cheap; and materials belonging to the new materials group can facilitate easy separation of biocatalytic systems from reaction mixtures (magnetic nanoparticles) or enable the avoidance of enzyme particles overloading on the surface of the carrier (Zdarta et al., 2018).

The characteristics of support materials include basic chemical compositions (e.g., SiO_2, polystyrene with various percentages of divinyl benzene), type and density of functional groups (e.g., -COOH, $-NH_2$, etc.), and morphological properties, such as pore size and distribution, the size of beads if available, as well as the specific surface area, and/or specific pore volume (Buchholz & Klein, 1987). These characteristics at a large extent decide how enzymes can be immobilized (adsorption, covalent binding, entrapment, etc.), as well as how substrate molecules interact with the immobilized enzyme (limited by diffusion or not).

Diffusion is the movement of molecules (mass transfer properties), which is only driven by a concentration gradient. When the substrate has to diffuse from the bulk solution into pores, reaching the active site of the immobilized enzyme, the apparent enzymatic reaction velocity V", limited by the diffusion velocity $V"_{diff}$, is commonly lower than the kinetic velocity $V"_{kin}$ of the immobilized enzyme, as shown in Fig. 1-11 (Engasser & Horvath, 1976). The diffusion efficiency depends on substrate and pore sizes, as well as on the diffusion coefficient of a substrate (Vlakh & Tennikova, 2013a).

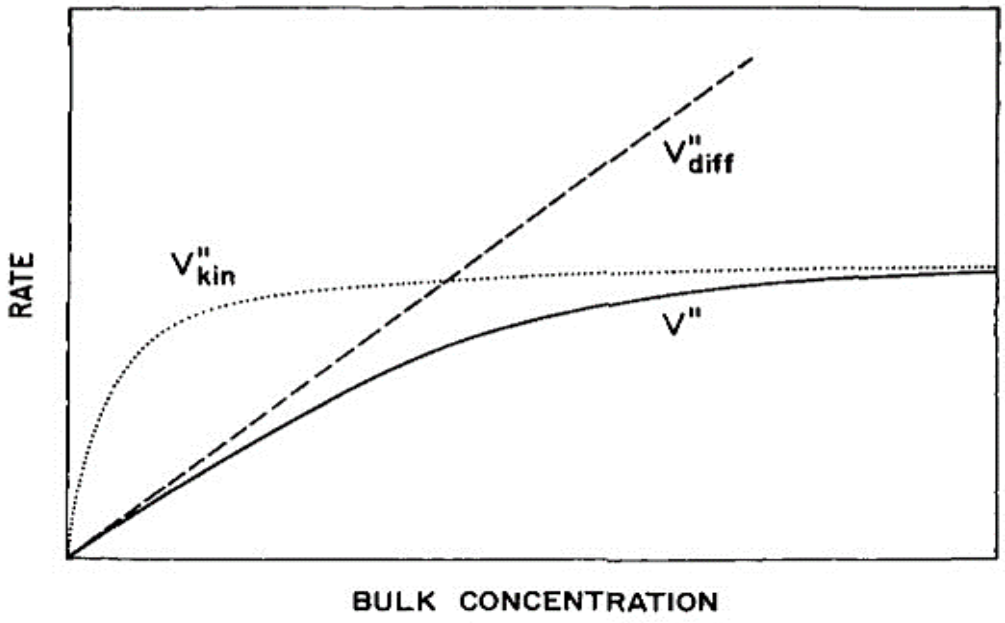

Figure 1-11. Overall rate of a reaction, V", catalyzed by a surface-bound enzyme against the substrate concentration in the bulk solution. In this case, V is determined by both the inherent rate of enzymatic reaction at the surface, $V"_{kin}$, and the maximum possible rate of substrate diffusion to the surface, V_{diff} (Engasser & Horvath, 1976).

According to the presence or absence of diffusional limitations for a substrate to reach the active site of an immobilized enzyme in a catalyst system, the available supports are generally classified into two groups, as shown in Fig. 1-12, where some typical representatives are cited. Generally, a diffusional limit for substrates commonly presents in porous particles based systems, while is negligible in nano particles, membrane and monolith based systems.

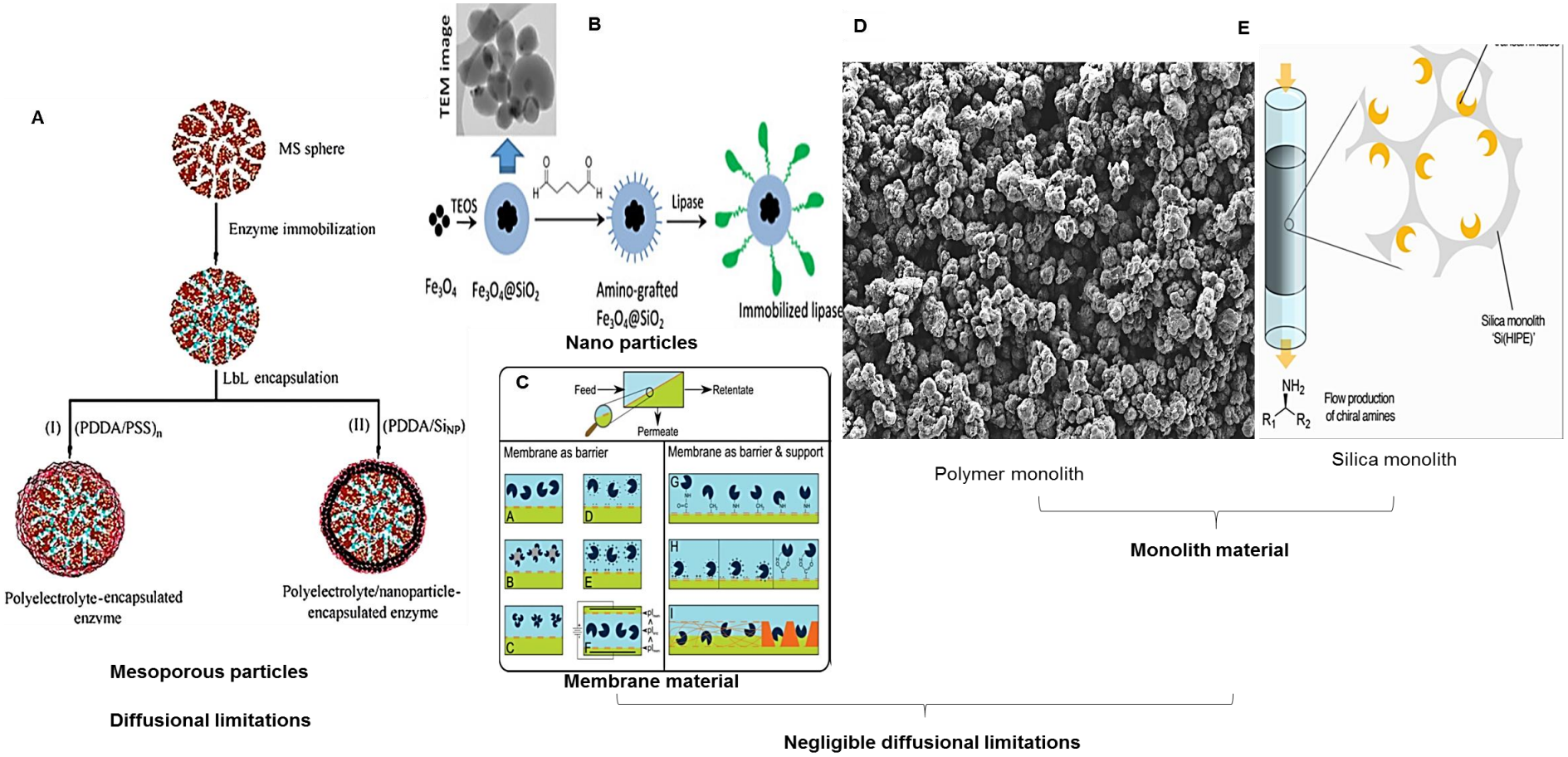

Figure 1-12. (A) Mesoporous particles based immobilized enzyme system (Zhou & Hartmann, 2013); (B) Nano particles based system (Karimi, 2016); (C) Membrane materials based systems (Jochems, Satyawali, Diels et al., 2011); (D) Polymeric monolith based system (from BIA separations); and (E) Silica monolith based system (Biggelaar, Soumillion & Debecker, 2017).

Mesoporous particles

Porous particles include microporous (e.g., zeolites) and mesoporous materials, with a pore size of ≤ 2 nm or 2–50 nm, respectively. The size of mesopores matches the size of most enzymes, and many mesoporous particles contribute to a high surface areas like 1500 m^2/g, as well as to a large pore volumes of around 1.5 cm^3/g (Hartmann, 2005). Therefore, mesoporous particles are suitable supports for various enzymes. The immobilization of enzymes on such mesoporous particles has been studied for almost two decades, which is well summarized in the review of Zhou and Hartmann (2013).

In view of water insolubility, thermal and chemical stability, hydrophilicity and the presence of sufficient chemical groups for the binding of enzyme molecules, various mesoporous particles fulfil most of the requirements for an effective immobilization support (Yiu, Wright & Botting, 2001). However, diffusional limitations happen frequently in porous particles based catalysts, leading to the restriction on the mass transport of substrates and products. Such limitations might not only decrease the enzymatic efficiency, but also result in a unique selectivity toward various substrates, as the access of a substrate to the enzyme confined in porous particles host might be orientation selective (Hartmann, 2005). To reduce such limitations, the increase of pore size represents an approach, while with sacrificing the available surface area, which leads to a decrease in the amount of immobilized enzyme. A compromise between low diffusional limitations and large surface area has to be made. Another approach by transforming one-dimensional pores to three-dimensional interconnected pores in porous particles, can also reduce potential diffusional limitations while still retaining a relatively large surface area (Zhou & Hartmann, 2013).

Up to date, many mesoporous particles are commercially available for the enzyme immobilization, such as Amberlite®, Bio-Rex®, Emphaze™ azlactone beads, Sepharose®, Eupergit® C, etc. (Dwevedi, 2016; Katchalski-Katzir & Kraemer, 2000; Zhou & Hartmann, 2013). To perform the hydrolysis by mesoporous particles based immobilized enzymes, batch based and packed column based reactors are used. In addition to diffusional limitations for both types of reactors, the high backpressure and low flow rate commonly happen to the packed column based reactor. For instance, catalase was immobilized onto Eupergit® C, consisting of beads with a diameter of 100–250 µm and an average pore diameter 25 nm. This immobilized catalase beads packed column is only allowed to be continuously operated up to 82 min at a substrate flow rate of 2.3 mL/min, after which the remaining activity was about 50% of its original activity (Alptekin, Tükel, Yıldırım et al., 2010).

Nonporous nanoparticles

The enormous progress achieved in the nanotechnology field has led to the development of nanoparticles with diameters of up to 30 nm which have been extensively studied in recent years as candidates for enzyme immobilization such as magnetic nanoparticles, nano gold particles or graphene, etc. (Dwevedi, 2016; Naldi, Tramarin & Bartolini, 2018). Nonporous nanoparticles provide a large surface area, on

which enzyme molecules are attached. The greatest advantage of nanoparticles over other porous particles is their ability to minimize diffusional limitations.

The recovery of immobilized enzymes from the reaction mixture after the hydrolysis in a batch is a crucial problem that must be solved when nanoparticles are used. One possible solution is the application of magnetic nanoparticles, such as iron, cobalt and nickel and their chemical compounds, which can be easily recovered from the reaction mixture (Cao, Li, Wang et al., 2012). Among various magnetic nanoparticles, Fe_3O_4 nanoparticle attracts considerable attention, because it has no toxicity, good biocompatibility and do not retain residual magnetism after the removal of external magnetic field (Atacan, Cakiroglu & Ozacar, 2016b). Atacan et al. (2016b) used Fe_3O_4 nanoparticles, pre-treated with gallic acid, as the support for the covalent immobilization of trypsin. Their results show that Michaelis-Menten kinetic constant (K_m) and maximum reaction velocity (V_{max}) of the immobilized trypsin are 54% higher and 20% lower than those of free trypsin respectively, indicating a relatively small decrease in enzymatic efficiency. Other inorganic nanomaterials such as nano gold particles (Kotal, Srivastava & Maiti, 2011) and graphene (Bolibok, Wiśniewski, Roszek et al., 2017) are studied as matrices for enzyme immobilization as well. As a new type of support material, carbon nanotubes, which are characterized by an ordered, nonporous structure, large surface area and biocompatibility, have been widely used in recent years (Feng & Ji, 2011). Unlike other materials, carbon nanotubes enhance the transfer of electrons between the substrate and the immobilized enzyme, which renders them for the immobilization of oxidoreductases (Feng & Ji, 2011). Other groups of enzymes (transferases and hydrolases) have also been immobilized with the use of carbon nanotubes (Markiton, Boncel, Janas et al., 2017).

Membranes

Regarding membranes based immobilized enzyme reactors, membranes are used either as a barrier to retain enzymes, or as a support to stabilize enzymes. As a barrier, enzyme molecules can be retained by various ways, such as size exclusion, charge or hydrophilic repulsion (Jochems et al., 2011). For instance, ultrafiltration membranes have been reported as an enzyme barrier to build catalyst systems for hydrolyzing several proteins (Cheison, Wang & Xu, 2007). By such applications, enzyme molecules are not modified, rather are physically retained, so that enzymes still preserve intrinsic characteristics and activity as the free form, while their stability against harsh environmental conditions is not improved either. Therefore, such membranes based enzyme reactors are only able to be reused for several times, due to the leakage or autolysis of enzymes (Cheison, Wang & Xu, 2007; Jochems et al., 2011).

To chemically stabilize enzymes on membranes, binding sites where the membrane is able to form chemical bonds with the enzyme molecules are necessary to be introduced by different surface modification techniques, as essentially such enzyme binding sites are not always present on the native membranes. Surface modifications on membranes can be achieved in three different ways, grafting, etching and coating

(Jochems et al., 2011). To hydrolyze lactose in milk, biocatalytic membranes were obtained by using nylon membranes grafted with glycidyl methacrylate (GMA) and activated by hexamethylenediamine (HMDA) and glutaraldehyde, respectively (Grano, Diano, Rossi et al., 2004). As enzyme molecules are immobilized on the surface of such membranes, diffusional limitations are always absent while the limited surface area on such single layer membranes commonly leads to the insufficient amount of immobilized enzymes.

Monoliths

Monolithic materials that can be regarded as a further development of membrane materials, are a kind of a single piece unit containing flow-through pores (Vodopivec, Podgornik, Berovič et al., 2003). In past decades, the application of monolithic materials has rapidly expanded thanks to significant advantages they offer over conventional porous particles. Monoliths provide several unique features such as very high porosity, high binding capacity, and low dispersion for very large molecules. The void structure of monoliths consists of open pores forming a network of channels through which the mobile phase flows. Thus, mass transfer in most monolithic channels can be exclusively guided by convective flow (Podgornik, Savnik, Jancar et al., 2014). Recently, reports dealing with the enzyme immobilization on monoliths have consistently increased (Kawakami, Sera, Sakai et al., 2005; Naldi, Tramarin & Bartolini, 2018; Vodopivec et al., 2003). Generally, monolith materials can be divided into two major groups, inorganic and organic monoliths.

To date, inorganic monoliths are mainly the silica-based monoliths that exhibit micrometer-size flow-through pores, constituting a macroporous network and nanometersize mesopores on the skeleton (Ma, Zhang, Liang et al., 2007). These monoliths have a hierarchically-structured permanent pore space, i.e. a typical bimodal pore size distribution (Causon & Nischang, 2014). Silica-based monoliths are commonly fabricated via a sol–gel process, and might be following a chemical modification of the matrix with different silylation reagents (Ma et al., 2007). Enzymes can be either simply entrapped in the silica monolithic matrix, or covalently immobilized on the modified surface of silica monoliths (Krenkova & Svec, 2009). With the respect to entrapping enzymes, Kawakami et al. (2005) developed a micro-bioreactor consisting of silica monolith immobilized protease derived using an in situ sol-gel method. Their results indicate that it is necessary to reduce this mass-transfer resistance in order to improve the reactor performance. This mass transfer resistance is probably due to the morphological drawbacks of certain silica based monoliths, such as the large size distribution, variable geometry, random spatial distribution of the macropores, and a radially heterogeneous morphology (Hormann, Mullner, Bruns et al., 2012). With the development, the new generation of silica monoliths possess not only smaller macropores, a more homogeneous macropore space, and a thinner silica skeleton, but also radial homogeneity of these structural parameters as well as of the local external or macroporosity (Hormann et al., 2012). Monoliths with modified surface have been used to immobilize proteolytic enzymes such as trypsin, chymotrypsin, and

pronase (Krenkova & Svec, 2009). For example, transaminase was immobilized on the structured silica monoliths by either adsorption or covalent grafting using amino-functionalized silica monoliths and glutaraldehyde as a coupling agent (Biggelaar, Soumillion & Debecker, 2017). In the work of Calleri, Temporini, Perani et al. (2004), trypsin was immobilized on an epoxy-modified silica monolithic support provided by Merck (Darmstadt, Germany). They concluded that these modified silica monolithic material was suitable for enzyme immobilization in terms of repeatability of the grafting reaction, long-term stability of the bioreactor and catalytic efficacy. Nevertheless, the surface modification for silica monoliths is still considered as a laborious work, which is limited, difficult, and always leaves residual surface silanol groups that can interact with solute molecules in an undesirable fashion (Mullner, Zankel, Holtzel et al., 2017).

Organic monoliths, consisting by organic polymers, such as polymethacrylate, polyacrylamide, and polystyrenes, can be generally prepared by in situ polymerization of organic monomers and crosslinkers in the presence of porogenic solvents (Ma et al., 2007). In contrast to common silica based monoliths, polymeric monoliths exhibit a monomodal pore-size distribution (Causon & Nischang, 2014). For methacrylate based materials, it is possible to prepare monoliths in broad ranges of porosity and pore size, which can be realized by changing porogen composition or porogen to monomer ratio and polymerization temperature (Podgornik et al., 2014). The work of Han et al. (2014) describes immobilization of horseradish peroxidase (HRP) onto a polymethacrylate-based monolith which was fabricated by thermally induced phase separation (TIPS) method. This monolith was reacted with N-hydroxysuccinimide (NHS) to activate the carboxyl groups on the monolith and further modified with HRP.

Molded rigid organic polymer based monoliths have been regarded as popular supports for enzyme immobilization, due to the high chemical stability over a wide pH range, good biocompatibility, and ease of modification with various functional groups (Svec & Fréchet, 1999). In the work of Vodopivec et al. (2003), enzymes citrate lyase, malate dehydrogenase, isocitrate dehydrogenase and lactate dehydrogenase were immobilized through epoxy groups on the methacrylate-based monoliths, commercialized under the trademark of Convective Interaction Media® (CIM®). Their results indicate the absence of a diffusional limitation in these monolith based immobilized enzymes reactors. To covalently immobilize enzymes on monoliths, the functional groups introduced to the monolith surface are crucially important. Hence, the ease to be modified with various functional groups renders organic monoliths attractive to be the support for enzyme immobilization. Nicoli, Gaud, Stella et al. (2008) investigated epoxy, carbonyldiimidazole (CDI) and ethylenediamine (EDA) functionalized CIM® monolithic disks for the immobilization of trypsin, and found that the most efficient immobilized trypsin reactor was obtained by immobilizing trypsin on a EDA disk. Recently, Naldi, Černigoj, Štrancar et al. (2017) compared immobilization yields of trypsin achieved with two CIM® monolithic disks. Namely, one disk was firstly modified by spacer glutaraldehyde and then functional group EDA, and the other disk is only modified with functional group aldehyde (ALD) without any spacer arm. Their

results show that a three times higher amount of immobilized trypsin is noted for the ALD monolith without any spacer arm.

1.3.1.2 Immobilization pathways and conditions

Based on various immobilization strategies, thousands of protocols on enzyme immobilization have been reported in literature. Immobilization protocols involve intensive optimization of immobilizing conditions (solvents, pH, time, temperature etc.) to control the interaction between matrix and enzyme, as well as the proper orientation of the enzyme to maintain its catalytic properties (Dwevedi, 2016). According to the summarized immobilizing strategies from Homaei (2015), an adapted classification of main immobilizing pathways is illustrated in Fig. 1-13. When a matrix is provided, the enzyme can be either physically entrapped, or stabilized through non-covalent or covalent bonds. Besides, enzyme molecules can also form cross-linked aggregates. Generally, the strength of the binding is usually inversely related to the ease with which it can be reversed. In other words, these two conflicting objectives, stability and reversibility, are difficult to meet simultaneously (Homaei, 2015). Each method has both merits and demerits, i.e., covalent binding and cross-linking are effective and durable, but time-consuming and easily affecting enzyme conformations; adsorption is simple and cheap to perform, but always unstable; diffusional limitations are inherent in entrapment and micro-encapsulations.

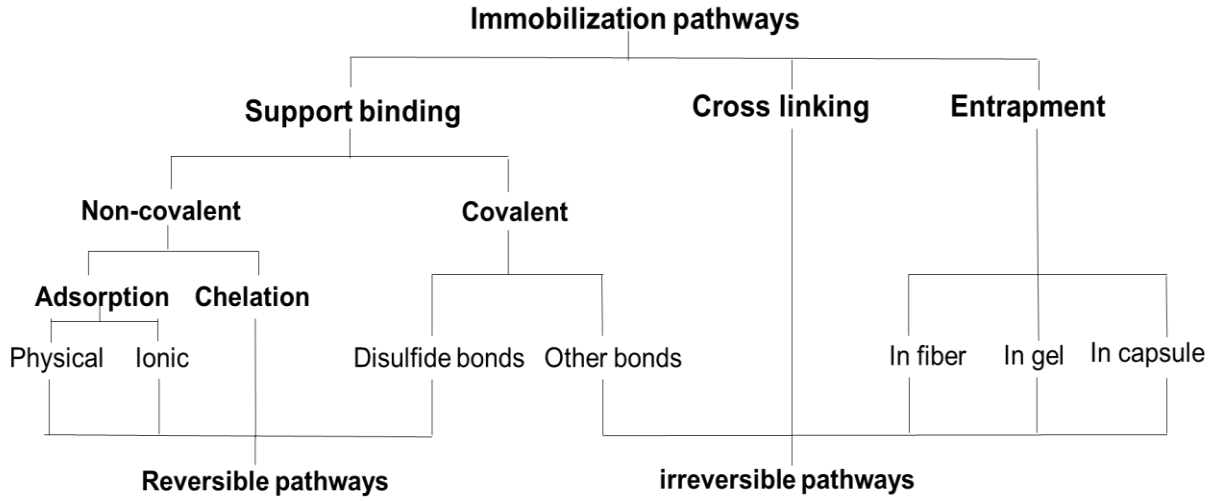

Figure 1-13 Summary on immobilization pathways, adapted from Homaei (2015).

Subramanian, Kennel, Oden et al. (1999) investigated the immobilization of enzyme on the silica monolith via (1) covalent coupling either through a metal link reagent or silica reagents containing pendant amino or epoxide linkers; (2) an entrapment technique using a thin layer of gelatin; or (3) an adsorption technique using poly-L-lysine. According to their results, the covalent immobilization techniques resulted in high surface loadings, while were relatively time consuming and caused irregularities on the silicon surface; the gelatin-based entrapment method was found to be unreliable; adsorption was simple to perform and was a mild coupling treatment that results in a smooth layer on the silicon surface. In addition, the obtained biocatalyst

systems performed very differently from each other, due to the different immobilizing methods. Barbosa, Torres, Ortiz et al. (2012) developed five immobilized lipase B biocatalysts by changing the immobilizing agents (detergents and salts). Namely, using high ionic strength, ionic adsorption is avoided, lipase B is adsorbed on the support via interfacial activation; using non-ionic detergents (e.g., Triton X-100), the enzyme becomes ionically adsorbed on the activated support; if detergent and salt are simultaneously present during immobilization, a covalent attachment to the support is first produced; in absence of detergent and high ionic strength, a mixture of all of the previous immobilization reasons coexisted. They also found that these produced biocatalysts showed very different features, and their performance varied significantly due to the changes in experimental conditions.

To sum up, the choice of immobilization methods or conditions is still a case-by-case decision, depending on the characteristics of supports, the target enzyme, as well as practical applications.

1.3.2 Factors affecting the performance of immobilized enzymes

It is well know that the enzymatic performance of free enzymes strongly depends on environmental factors, such as temperature, pH, salts, etc.. Generally, the tendency of such factors coincides for free and immobilized enzymes (Vlakh & Tennikova, 2013b). Immobilized enzymes, probably, exhibit higher resistance than their free forms against harsh conditions (higher temperature, extreme pH, organic detergents, etc.) due to the stabilization through various immobilization techniques, especially via the covalent binding.

Compared with the hydrolysis by free enzymes, the performance of an immobilized enzyme reactor (IMER) is determined not only by enzymatic activity but also by mass transfer properties. Environmental conditions might exert considerable influence on the mass transfer to and from the immobilized enzyme. In addition to free enzymes, the micro- and nano-environment around immobilized enzyme molecules might be different from the bulk environment, which is particularly remarkable for the diffusion-limited IMERs. Regarding the performance of an IMER toward a specific substrate, the influence of environmental conditions on the substrate must be considered as well, but it is a case-by-case study, which will not be discussed here in detail.

1.3.2.1 Effects of temperature

Temperature is one of the main parameters, exerting influence on the activity and stability of immobilized enzymes, as well as on the mass transfer properties in IMERs.

Like most chemical reactions, the reaction rate of a catalyst system increases with the raising temperature, as the components in this catalyst system move faster and collide into each other more frequently in a given time. However, the excessive increase in temperature might inactivate enzymes due to the thermal denaturation. The immobilization of enzyme reduces the degree of structural freedom of protein macromolecule and, thus, protects it from this potential denaturation (Vlakh &

Tennikova, 2013b). For example, the relative activity of free organophosphorus hydrolase (OPH) decreased about 92% after the incubation at 55°C for 24 h, whereas at the same conditions, the immobilized OPH onto epoxy and 1,1′-Carbonyldiimidazole (CDI) modified cellulose retain 35% and 26.4% of its initial activity, respectively (Sharifi, Robatjazi, Sadri et al., 2018). The similar conclusion was reported for other IMERs, such as immobilized trypsin on modified Fe_3O_4 magnetic nanoparticles (Atacan, Cakiroglu & Ozacar, 2016b), immobilized papain on magnetic poly(HEMA-GMA) nanoparticles (Alpay & Uygun, 2015), and β-galactosidase covalently immobilized on silica (Bernal, Sierra & Mesa, 2014), etc..

Except the improvement in thermal stability, the optimal temperature, where enzymes show the highest activity, might change due to the immobilization. For instance, the optimal temperature of the previously mentioned invertase increased from 45°C to 60°C after its immobilization (Uygun, Uygun, Ozcaliskan et al., 2012). An increase in the optimal temperature was also observed for trypsin immobilized on Fe_3O_4 magnetic nanoparticles, i.e. 37°C for free trypsin versus 45–55°C for immobilized trypsin (Atacan, Cakiroglu & Ozacar, 2016b). Delattre, Michaud, and Vijayalakshmi (2008) observed the same optimal temperature 30°C for both free lyase and its immobilized form on CIM®-epoxy disk. Interestingly, Benčina, Benčina, Štrancar et al. (2005) found that the activity of deoxyribonuclease (DNase) immobilized on CIM®-epoxy disk was not significantly changed when temperature was decreased from 37 to 25°C, whereas its free form decreased 40% activity at 25°C compared with that at its optimal temperature 37°C. Thus, it seems that immobilized DNase showed a broader optimal temperature range (25–37°C) than the free one.

In most studies, the increase in thermal stability of immobilized enzymes is attributed by the structural stabilization due to the immobilization technique. However, reasons, why the optimal temperature range for enzymes increased or broadened after the immobilization, are seldom discussed. The mechanism of increased enzymatic activity with raising temperature is based on the fundamentals of molecular motion. The immobilization of enzyme significantly reduces the motion of enzyme molecules, thus, a higher temperature is required to achieve the maximum activity as the motion of substrate molecules can be enhanced at increasing temperature. This phenomenon happens quite often for batch based IMERs, especially those with diffusional limitations, because substrate molecules have to initiatively come to the immobilized enzyme in these IMERs. Contrast to these catalyst systems, substrate molecules in some flow-through IMERs can be driven to the immobilized enzyme by flow (shear force), which can be enhanced via increasing the flow rate. Hence, temperature exerts much less influence on the optimal activity of such IMERs.

1.3.2.2 Effects of pH

pH is another important parameter for a biocatalyst system, as enzymes are active only in certain pH range and mostly each enzyme has strongly defined pH optimum where its activity reaches the maximum (Vlakh & Tennikova, 2013b). The increase or decrease in pH leads to the changes in charge of different amino acids, then probably

in the average surface charge of substrate and enzyme molecules. Hence, the interactions between enzyme and substrate, especially those strongly depending on the electrostatic interactions, might significantly alter. Finally, not only the enzymatic activity, but also the selectivity of an enzyme toward various substrates might change because of the varied pH values.

At extreme pH, most enzymes lose their enzymatic activity due to pH-induced conformational distortion. This conformational distortion can be largely reduced by the immobilization of an enzyme, particularly via covalent binding. A broader working pH range, i.e., a pH range in which the enzyme is activated and functioning, has been observed for various enzymes after their immobilization (Bernal, Sierra & Mesa, 2014; Sanjay & Sugunan, 2006; Vlakh & Tennikova, 2013b). For example, Xie, Svec, and Fréchet (1999) found that the trypsin immobilized on poly(2-vinyl-4,4-dimethylazlactone-co-acrylamideco-ethylene-di-methacrylate) monolith remained 62% of its maximum activity at pH 10, whereas free trypsin only remained 20% activity of its maximum value at pH 9 and even lost all activity at pH 10. Analogous results were obtained in the study of Delattre, Michaud and Vijayalakshmi (2008), where 10–20% activity higher for pectin lyase immobilized on CIM®-epoxy disk was found than that for its free form at pH 4, 5.5 and 7. In addition to stabilize the structure of enzyme, immobilization can also prevent certain enzymes from autodigestion at the working pH range, such as trypsin that is a representative of unstable enzymes known to be susceptible to autodigestion (Benčina, Podgornik, Štrancar et al., 2004). However, it is also reported that no substantial expansion in the working pH range of immobilized enzymes is observed, compared with their free forms (Atacan, Cakiroglu & Ozacar, 2016b). Trypsin immobilized on modified Fe_3O_4 magnetic nanoparticles exhibited a similar activity profile as a function of pH like its free form (Atacan et al., 2016b). Another example lactase (β-galactosidase) encapsulated into κ-carrageenan-based hydrogel beads, was deactivated very fast at low pH like its free form (Zhang, Zhang, Chen et al., 2016). The authors concluded that hydrogel beads could not prevent acid-induced loss of enzymatic activity, and postulated that the small H^+ ions could readily diffuse into the enzyme-loaded beads through the pores within the hydrogel matrix and were, therefore, still able to alter the properties of the active site.

Generally, the immobilization increases the stability against extreme pH and broadens the working pH range of certain enzymes, which highly depends on the immobilization approach. Regarding the optimum pH range, theoretically, immobilized enzymes coincide with their free forms if the active site on the enzyme is not affected during the immobilization process (Vlakh & Tennikova, 2013b). Practically, the optimum pH range of an immobilized enzyme might differ from its free form, even from that immobilized via another approach. In the study of Sanjay and Sugunan (2006), free invertase exhibited maximum activity at pH 5, so did the covalently bound one, while the invertase immobilized via adsorption showed its highest activity at pH 6. The authors suggested that the surface characteristics of supports affected the optimum pH by means of charge interactions. An increase in optimum pH was also observed for

invertase entrapped on CA–ZrO_2 and CA–TiO_2 gel fibers (Nakane, Ogihara, Ogata et al., 2001). Other enzyme like Lactozym™, who has an optimum pH of 6.5 at its free form, increased this value to 7 after its immobilization on cellulose beads (Roy & Gupta, 2003). As previous studies said, due to the charge characteristic on the matrix surface used for immobilization, a pH gradient might form between the micro-/nano-environment around enzyme molecules and the bulk environment.

1.3.2.3 Effects of salts

The effects of salts on immobilized enzymes have not received enough attention, while salt-effect studies have proven useful for determining the intrinsic properties of free enzymes (Endo, Kurinomaru & Shiraki, 2016, 2018; Garajova, Balogova, Dusekova et al., 2017; Quan, Wei, Jiang et al., 2008; Salis, Bilanicova, Ninham et al., 2007). Most of these studies interpret the salt-effect based on ionic properties and ion specificity. Ionic properties refer to the effects of any salt ion, including charge shielding/electrical double layer effects and stoichiometric ion binding to a charged protein (Tsumoto, Ejima, Senczuk et al., 2007). These effects are always independent of the salt type but dependent on the salt concentration (ionic strength). Ionic properties are important in regulating enzyme–substrate interactions, thereby affecting enzyme activity and selectivity. This factor is particularly important in hydrolysis reactions that depend on the movement of charged molecules relative to each other. Thus, both the binding of charged substrates to the enzyme and then the movement of charged groups within the catalytic active site will be influenced by ionic composition of the medium (Chaplin & Bucke, 1990). The ion-specific effect of the medium on proteins was first reported in a systematic way by Franz Hofmeister (1888), who ranked the ability of ions at a fixed ionic strength to affect the properties of proteins in aqueous solutions. He differentiated between chaotropes and kosmotropes, salts that induced either disorder or more order in the protein conformation. Hofmeister ions are reported to influence the properties of numerous enzymes (Endo, Kurinomaru & Shiraki, 2016; Garajova et al., 2017; Tougu, Tiivel, Talts et al., 1994). In many cases, the ion-specific influence on enzyme activity follows the Hofmeister series, with kosmotropes activating enzymes and chaotropes inhibiting enzyme activity (Garajova et al., 2017). Enzyme activation by kosmotropes occurs because these salts increase both the structural stability of the enzyme and the hydrophobic interactions between the enzyme and its substrate (Endo, Kurinomaru & Shiraki, 2016). Besides, a bell-shaped dependence of enzyme activity on ions in the Hofmeister series has been observed, indicating that both chaotropic and kosmotropic ions can inactivate enzymes (Žoldák, Sprinzl & Sedlák, 2004). For instance, chymotrypsin exhibits the unusual property of increased activity with the addition of 3 M NaCl to the medium but no significant increase in the presence of 3 M LiCl or KCl (Wesolowska, Krokoszynska, Krowarsch et al., 2001). Another study observed that the addition of 0.5 M NaCl decreased K_m and increased K_{cat} of chymotrypsin, with the opposite results for trypsin (Endo, Kurinomaru & Shiraki, 2018).

Regarding the effects of salts on immobilized enzymes, most studies focus on the role of salts in the immobilization process (Betancor, López-Gallego, Hidalgo et al., 2006;

Essa, Magner, Cooney et al., 2007; Muzzarelli, Barontini & Rocchetti, 1976), and the effects of salts on the activity or performance of immobilized enzymes are seldom discussed. In the study of Carrea, Bovara, Pasta et al. (1982), three enzymes, alcohol dehydrogenase, gly-ceraldehyde-3-phosphate dehydrogenase, and 20-β-hydroxysteroid dehydrogenase were immobilized on CNBr-activated Sepharose 4B, and the results suggested that 1 M phosphate and 0.5 M sulfate dramatically stabilized both free and immobilized enzymes against inactivation by temperature and urea. In addition, it is reasonable to assume that the mass transfer properties in IMERs may change after the addition of salts due to their effects at least on charge-based attraction or repulsion between substrate molecules and immobilization supports.

1.3.2.4 Effects of organic solvent

A general consequence of adding organic solvent is the decrease of the bulk dielectric constant of a solvent. This shifts significantly the balance of electrostatic charges on the protein and changes the organization of dipolar moments, resulting in protein structural changes (Dufour, Bertrand-Harb & Haertlé, 1993). Therefore, enzymes might undergo structural distortion in the presence of organic solvent, leading to decreased activity even inactivation. After the incubation in 20% ethanol at room temperature for hours, trypsin remained only 20% activity at pH 8 (Tchorbanov & Iliev, 1993). The immobilization of enzymes is an approach to stabilize enzymes against denaturing conditions, i.e., reducing inactivation by preventing protein from unfolding (Mozhaev, Melik-nubarov, Sergeeva et al., 1990). In 30% ethanol solution (40^{o}C & 30 min), free trypsin lost 40% of its activity, while the covalently immobilized trypsin retained around 90% (Kang, Kan, Yeung et al., 2005).

The addition of organic solvent affects the performance of IMERs from various respects, i.e., (i) nonspecific interactions between substrate molecules and the matrix surface might be suppressed, especially for those matrixes with hydrophobic surface; (ii) the presence of organic solvents influences the enzyme activity; (iii) the mass transfer properties in an IMER are probably altered in the presence of organic solvent. In the study of Bartolini, Greig, Yu et al. (2009), butyrylthiocholine was hydrolyzed by butyrylcholinesterase (BChE) immobilized on the surface of CIM® disk modified with ethylene diamine (EDA). To explore the influence of organic solvents on the performance of immobilized BChE reactor, methanol, ethanol, 1-propanol, 2-propanol, and DMSO were selected and 1% of each solvent was added in the mobile phase. Among the selected solvents, the addition of 1% 2-propanol led to 34% increase in activity, and further increasing its concentration to 3–5%, a growth of product yield to 41% was observed. In order to minimize nonspecific interaction with solid matrix without affecting the activity of β-secretase immobilized on CIM®-EDA disk, Mancini, Naldi, Cavrini et al. (2007) optimized the mobile phase composition. DMSO was found as a suitable organic modifier and was used in the mobile phase at low percentage (5%) without affecting the enzymatic activity, whereas acetonitrile markedly decreased the activity of this IMER.

1.3.2.5 Effects of flow rate

Flow rate is an important and unique factor influencing the performance of flow-through IMERs. The influence of flow rate on the performance of IMERs differs on a case-by-case basis, which depends on the type of IMERs such as particles-based packed bed reactors or monolith/membrane based reactors, on the enzyme nature, as well as on the flow approach, i.e. single flow-through at zonal or continuous approach versus recirculated flow approach.

Regarding particle based packed bed IMERs, the enzymatic rate is reported to increase firstly and then decrease with the raising flow rate in the study of Petro, Svec, and Fréchet (2000), where trypsin was immobilized on poly (glycidyl methacrylate-co-ethylene dimethacrylate) beads with a mean particle size of 10 µm and a median pore size of 10.9 nm. In their study, trypsin was also immobilized onto "molded" macroporous rods of the same material, and the activity of immobilized trypsin on this rods based IMER increased firstly and reached a plateau with the increasing flow rate. The authors interpreted the different dependences of activity on flow rate for beads- and rods- based IMERs by the diffusional limitations, as the substrate molecules must diffuse into the small pores from the main stream of the mobile phase in a beads-based IMER, a relatively low flow rate was required to ensure efficient diffusion time.

In the work of Giorno, Drioli, Carvoli et al. (2001), an enzyme membrane reactor with immobilized fumarase was developed and they found that the axial flow rate did not influence reactor performance. However, this study evaluated the performance of this reactor based on the conversion degree that is calculated by the concentration of the converted substrate in a ratio to the initial substrate concentration. In fact, an increasing flow rate reduced the processing time while contributed to a same conversion degree. Thus, the enzymatic efficiency (defined in a unit of time) was actually enhanced with the increasing flow rate.

As the void structure of monoliths consists of open pores forming a network of channels, mass transfer in most monolithic channels can be exclusively guided by convective flow (Podgornik et al., 2014). Therefore, monolithic IMERs can always be used at a high flow rate, and simultaneously at a low back pressure. Compared with particles based IMERs, the influence of flow rate on the performance of monolithic IMERs attracts more attention (Bartolini, Cavrini & Andrisano, 2005, 2007; Mancini et al., 2007; Naldi et al., 2017; Nicoli et al., 2008; Vodopivec et al., 2003; Yao, Qi, Hu et al., 2011). However, the results of these studies seem differ drastically, which is mainly due to the fact that each study evaluated the IMER standing from different points, i.e., enzymatic activity, kinetic parameters, product/substrate conversion rate, or even the sequence coverage in the proteomic application.

With the respect to kinetic parameters, some conflicting results are obtained. A decreased V_{max} and an increased K_m depending on increasing flow rates was observed in several works (Bartolini et al., 2007; Mancini et al., 2007). CIM® monolith was used as support in both studies, acetylcholinesterase and β-secretase were studied in the

works of Bartolini et al. (2007) and Mancini et al. (2007), respectively. Bartolini et al. (2007) used the index of micromoles of product formed per minute, while the evaluation of Mancini et al. (2007) was based on the percent of product obtained from enzymatic hydrolysis oversighting the unit time (actually, the enzymatic activity expressed as picomol of substrate hydrolysed per min was found to be increasing at higher flow rate), although both studies get the similar conclusion. Namely, an increase in K_m value indicates the lower substrate affinity, which is attributed by the reduced accessibility of the substrate to the bound enzyme. This phenomenon is considered to be more evident in a flow-through system at increasing flow rates. Regarding the decrease in V_{max} with increasing flow rates, both studies do not give clear reason. Apart from above two studies, K_m and the turnover number k_3 of the enzymes immobilized on CIM® monolithic supports, such as citrate lyase, malate dehydrogenase, isocitrate dehydrogenase and lactate dehydro-genase, were reported to be flow-unaffected (Vodopivec et al., 2003). The authors further concluded that the mass transfer of the substrate in CIM-IMERs is not diffusional limited. Because of that, a higher flow rate results in higher conversion rates and shorter reaction times. Yao et al. (2011) developed a Trypsin-IMER based on sub-micron skeletal polymer monolith, and they found that with increasing flow rates, V_{max} values decreased, while K_m was independent on the flow rate.

Most of aforementioned studies used CIM® monolith as immobilization support for different enzymes, these inconsistent results are probably due to the different natures of enzymes and the experimental conditions, such as the explored flow rate range. It is a possibility that the studied range of flow rate in some studies are insufficient. In a recent study (Naldi et al., 2017), the influence of flow rate on the enzymatic activity of IMERs (trypsin immobilized on various CIM® disks) was compared using zonal and continuous flow approaches. An underestimation of the apparent active units of immobilized trypsin seemed to occur when a zonal approach was applied, due to the insufficient supplement of substrate. By using continuous flow approach, at low flow rates the amount of substrate supplemented to each IMER per minute is a rate-limiting factor. Indeed, increasing the flow rate the amount of hydrolyzed substrate per minute increases up to a plateau. Higher the amount of active units in an IMER, higher the flow rate required to reach the steady state, i.e., the maximum conversion rate. Hence, the maximum enzymatic activity of an IMER should be evaluated in steady-state conditions, where enough substrate is supplied.

As discussed previously, another reason for the inconsistent results on the influence of flow rate is due to the applied the index. In studies of Bartolini et al. (2005) and Mancini et al. (2007), where the obtained product (normally the product peak area) was used as the index, a flow dependent of the obtained product was always observed in exponential decay mode. In addition, Nicoli et al. (2008) directly correlated the result of sequence recovery rate of trypsin-IMER with its enzymatic activity, and indicated that the use of high digestion flow rates up to certain value (0.4 mL/min, and a lower

sequence recovery rate was observed at 0.8 mL/min in their study) increased the enzymatic activity, which is quite disputable.

Regarding the mechanisms underlying the positive effects of increasing flow rates, higher flow rate is presumably attributed to the increase in mass transfer of substrate molecules toward the immobilized enzyme. Besides, the quick and non-restricted removal of product might be another reason. With the respect to the decrease in enzyme activity with increasing flow rate, it is explained as a result of reduced contact time between substrate and enzyme molecules. In addition, Bartolini et al. (2009) speculated that at higher flow rates, the increasing friction between liquid and solid phases occurred, negatively influencing the enzyme catalytic efficiency by reversibly modifying the 3D structure of immobilized enzyme (Vlakh & Tennikova, 2013b).

1.3.3 State of trypsin immobilization

Due to the exclusive specificity of trypsin, this enzyme is wildly applied in proteomic researches. Hence, numerous immobilized trypsin reactors (IMTRs) are developed to accelerate the digestion step for proteomics analysis. Vlakh and Tennikova (2013b) summarized monolith based immobilized trypsin reactors up to year 2013 for the application in proteomics. Recently, Naldi et al. (2018) reviewed monolith based, micro and nano particles based IMTRs for the same application. In addition, several commercialized IMTRs have been launched in past years, including beads based and columns based IMTRs. Namely, various beads are used as supports, such as magnetic (Mag-Trypsin™ from Takara Bio Europe) and non-magnetic beads (Thermo Scientific Pierce), as well as agarose (Sigma-Aldrich). Columns based IMTRs are micro spin columns containing highly purified, TPCK-treated porcine trypsin (Sigma-Aldrich), Poroszyme™ Immobilized Trypsin Cartridge from Applied Biosystems, Perfinity™ Trypsin Column and NoRA™ Trypsin Column from Perfinity Biosciences (Naldi et al., 2018). However, these micro reactors are designed for the application in the proteomic research, which deal with micro gram substrate each time, and is far away from the production of food protein hydrolysates.

Except high enzymatic efficiency, to reach a higher space-time yield (the amount of substrate converted per biocatalyst reactor), the crucial requirements for enzymatic hydrolysates production are a need for processing larger amount of substrate, and the achievement of longer continuous digestion time in each cycle. These requirements might cause a blockage problem. To reach a relatively high processing capacity, enzymatic membrane reactors were developed (Prata-Vidal, Bouhallab, Henry et al., 2001), while trypsin was not able to be recovered and reused. In past decades, the immobilization of trypsin onto different stationary supports has been studied for the potential application in food industry, as summarized in Table 1-6. Generally, trypsin was immobilized on porous particles, such as chitosan beads, cellulose beads, or pore glass beads, etc.. Thus, diffusional limitations are discussed in most studies. Besides, the reusability of most IMTRs is still below 10 times. Processing capacities, either by batch based reactor, or by flow-through approach with packed bed column, only ranged from micro liters to milli liters, except for one study by Lee, Senyk and Shipe

(1975), in which liters of samples were processed each time while an obvious decrease of flow rate was observed due to plugging of the column. To sum up, available systems still suffer from low processing stability and low capacity in terms of volume throughput. In addition, no commercialized IMTRs are indicated for the production of food protein hydrolysates.

Table 1-6. Summary on immobilized trypsin reactors for the application in the food processing.

Immobilization support and pathway	Application	Hydrolysis Capacity	Stability and reusability	Reference
Trypsin–chymotrypsin mixture was immobilized onto modified polyvinyl chloride (PVC) microspheres, which were activated by the subsequent treatment of PVC microspheres with ethylene- diamine and glutaraldehyde (I-CT)	Hydrolysis of protein in hairtail surimi wash water to produce antioxidant peptides.	(1) Activity: 1340 ± 50 U/g (2) 11.2 g I-CT was packed in a glass column (bed volume 15 mL) (3) Single flow through at 0.5 – 3 mL/min (4) protein concentration: N/A	Stability: half-life of the packed column reactor was 6 h at 30^{o}C and 1 h at 60^{o}C. Reusability: N/A	Zhou, Ding, Li et al. (2016)
Trypsin was immobilized onto chitosan using a covalent binding	Hydrolysis of degrade egg yolk phosvitin for the production of phosphopeptides	(1) Activity: N/A (2) Batch based hydrolysis (3) 10 mg/mL protein solution with a E/S ratio of 1:20 (w/w) at 50^{o}C for 2 h	Activity was retained well after trypsin five times' repeat	Zhong, Li, Hu et al. (2016)
Trypsin was immobilized on Fe_3O_4 magnetic nanoparticles that had been pre-treated with gallic acid (GA)	Hydrolysis of bovine serum albumin (BSA) within 1 h	(1) Activity: V_{max} 18.3 mM/min (2) Batch based hydrolysis (3) 100 µL 1 mg/mL degraded BSA + 900 µL immobilized trypsin (1 mg/mL), at 37^{o}C for 1 h	Stability: preserved 92% of its initial activity after 120 days of storage at 4^{o}C Reusability: preserved 54.5% of its initial activity after eight times successive reuse	Atacan, Cakiroglu and Ozacar (2016a)
Trypsin was covalently immobilized on activated glyoxyl-agarose support (0.2–0.3 mg/g support)	Hydrolysis of casein and β-Lg	(1) Activity: 32.80% of its free form (2) 24 mg/mL casein + 6 mg/mL β-Lg, at a E/S ratio of 1:100	N/A	Pessato and Tavano (2015)
Trypsin was immobilized on activated porous chitosan resin	One-step affinity purification of trypsin inhibitor (TI) from soybean	(1) Activity: N/A (2) Single flow through with a packed column (3) 60 mL 20 mg/mL	Stability: preserved 90% initial activity after 20 days Reusability: retained 90% activity after six cycles	Zhang, Zhang, Wang et al. (2011)

Trypsin was covalently immobilized on highly activated glyoxyl-Sepharose 4B-CL gel supports	Hydrolysis of crude extracts of *E. coli* and cheese whey	(1) Activity: N/A (2) Batch based hydrolysis (3) 10 mL, 6 mg/mL whey proteins + 0.7 g immobilized trypsin for 6 h	Preserved more than 90% of their initial activity after 20 days usage.	Marques, Pessela, Betancor et al. (2011)
Trypsin was immobilized on glyoxyl and amine spent grains	Hydrolysis of whey proteins	(1) Activity: 44.3 ± 2.2 U /g supports (2) Batch based hydrolysis (3) 50 mL, 50 mg/mL WPI solution; E/S N/A	Stability: preserved 90% activity after 60 days at 4ºC Reusability: no loss of activity after 4 cycles	Rocha, Gonçalves and Teixeira (2011)
Trypsin was immobilized on activated chitosan beads.	Purification of trypsin inhibitor in the soybean processing	(1) Activity: N/A (2) Single flow through with 5 g immobilized trypsin packed in a column, 40 mL (3) 3 mg/mL trypsin inhibitor solution	N/A	Zhang, Zhang, Lin et al. (2008)
Trypsin was covalently immobilized on the cellulosic support using a spacer of diaminoalkanes.	Hydrolysis of β-Lg	(1) Activity: toward substrate BApNA V_{max} 0.31 (free form 66) (2) Batch based hydrolysis (3) Recirculated flow through hydrolysis with a packed-bed column at 0.5 mL/min for 20 h	Stability: Remained 90% activity after 10 days Reusability: Activity decreased 25% after five repeats. Packed reactor showed a decrease in the β-Lg hydrolysis yield to 40% after 9 days	Yamamoto, Imamura, Susanti et al. (2005)
Biotinylated trypsin was adsorbed on avidin-biotinylamino activiated cellulose beads and controlled-pore glass (CPG) beads	N/A	(1) Activity: on cellulose 9.91 U/mg and on CPG 8.78 U/mg (2) Batch based hydrolysis	N/A	Janolino and Swaisgood (2002)

Trypsin was was immobilized on succinamidopropyl glass beads	Hydrolysis of α(s)-Casein or β-Casein	(1) Activity: 49.4 U/g of beads (2) Flow through: A fluidized bed bioreactor containing 2 ml of immobilized trypsin beads was used to recirculate 8 ml of αs-CN or β-CN solution (10 mg/mL) for 2 or 1.5 h,	N/A	Park, Swaisgood and Allen (1998)
Trypsin was covalently im-mobilized on succiamidopropyl controlled-pore glass beads	Hydrolysis of β-Lg	(1) Activity: N/A (2) Flow through: 6 mL 5 mg/mL β-Lg was recirculated through a fluidized bed bioreactor containing 2 ml of immobilized trypsin beads at 4 ^{o}C for 20 min	N/A	Huang, Catignani and Swaisgood (1994)
Trypsin was immobilized on controlled pore glass beads	Hydrolysis of β-Lg for gelation	(1) Activity: N/A (2) Batch based hydrolysis: 12 mL, 5 mg/mL + 2 mL immobilized trypsin beads	N/A	Chen, Swaisgood, and Foegeding (1994)
Trypsin was immobilized on a polyacrylamide matrix	Hydrolysis of β-casein	N/A	N/A	Reimerdes (1979)
Trypsin was immobilized on acetone-silanized porous 96% silica glass particles	Hydrolysis of cold raw milk to reduce the oxidation	(1) Activity: N/A (2) Flow through: 5 c reservoir through the packed column reactor at room temperature at a flow rate of 2 liters/h for 5 h	Reusability: preserved 90% of its initial activity after 14 days (stored in 20% ethanol)	Lee, Senyk and Shipe (1975)

2 Objective and Outline

Whey as a by-product of cheese manufacture is a valuable source of proteins and functional peptides. In past decades, whey proteins have been subject to extensive investigations regarding enzymatic processing using various enzymes. Trypsin (EC 3.4.21.4), a serine protease, is found in the digestive system of humans and many other vertebrates, where it hydrolyzes proteins. As mentioned previously, tryptic hydrolysis of whey proteins results in reduced allergenicity, improved functionalities as well as enhanced nutritional values. Besides, tryptic hydrolysis has the potential of being well controlled because of its exclusive specificity, which might contribute to a highly reproducible hydrolysate profile. However, the costly production and purification of trypsin seriously limits its implementation in the food industry. As an alternative approach, immobilization of trypsin has attracted more and more attention due to the possibility of reusing the enzyme and producing enzyme-free hydrolysates. To date, numerous reactors containing immobilized trypsin are available. However, most of them still suffer from several problems, namely, low reusability because of gradual blockages during processing, diffusional limitations for those reactors based on porous particles, enzyme leakage due to non-covalent bonding, and low capacity in terms of volume throughput. Moreover, the majority of conducted studies only focuses on the immobilized reactor per se, i.e. the amount of immobilized enzyme, its stability and reusability, etc.. Although the specificity of immobilized trypsin was verified in IMTRs designed for proteomics analysis, investigations hardly ever encompass the selectivity of immobilized trypsin (i.e. peptides evolution patterns), let alone correlating to various hydrolytic conditions. However, to exert more control over the hydrolysis process, it is important to elucidate the influence of the hydrolytic environment on the selectivity of an enzyme, allowing hydrolysis to be driven by the reaction speed as well as the desired peptide profiles, obtained at various stages during hydrolysis.

Therefore, the aim of this thesis was to develop an IMTR with improvements over available reactors as well as to systematically and comprehensively study the hydrolysis of whey proteins using this IMTR. In view of previous efforts in the development of IMTRs, monolithic columns, specifically, polymethacrylate monolithic columns commercialized under the trademark Convective Interaction Media® (CIM®), were chosen as immobilization supports. For the first time, the CIM column with a pore size of 6 µm, theoretically less prone to pore blockage, was used as an immobilization support and compared with a 2.1 µm pore size. The IMTRs were systematically evaluated in terms of immobilization yields, activity, stability, permeability, etc.. To clarify the influence of various hydrolytic conditions on the selectivity of immobilized trypsin, the hydrolysis of a single protein — β-Lg by this immobilized trypsin was compared with that using free trypsin. At the end, a mixture of proteins — WPI was hydrolyzed by an IMTR with upscaled bed volume. In addition, kinetic studies as functions of flow rate and substrate resource were undertaken.

3 Results and Discussion

3.1 Production of β-lactoglobulin hydrolysates by monolith based immobilized trypsin reactors

Summary and contribution of the doctoral candidate

Tryptic hydrolysis of β-Lg is attracting more and more attention due to the reduced allergenicity and the functionality of resulting hydrolysates. To produce hydrolysates in an economically viable way, for the first time, trypsin was immobilized on monolith with pore size 6 µm (N2), which is less prone to pore blockage, and its efficiency was compared with pore size 2.1 µm (N1). The developed immobilized trypsin reactors (IMTRs) were characterized in terms of permeability and enzymatic activity during intensive usage. N1 showed twice the activity compared with N2, correlating well with its almost two times higher amount of immobilized trypsin. N2 showed high stability over 18 cycles, as well as during more than 30 weeks' storage, compared with N1. The efficiency of IMTRs on hydrolyzing β-Lg was compared with free trypsin. Namely, the final DH by N1 reached 9.68% (86.58% cleavage sites) within 4 h, while only around 6% (53.67% cleavage sites) by 1.5 mg free trypsin. Immobilized trypsin and free trypsin showed different preferences toward individual cleavage sites on β-Lg.

It is noted that hydrolysis conditions, such as pH, ionic strength, temperature, etc., are not optimized in this study. The efficiency of these IMTRs in production of β-Lg hydrolysates is highly potential to be improved after the optimization of processing parameters.

Most significant contribution to this manuscript was made by the doctoral candidate. This comprised (i) the conception and design of experiments based on preceded critical literature review; (ii) experimental conduction on the characterization of IMTRs, protein hydrolysis, and hydrolysates analysis; (iii) data analysis and data interpretation. In addition, writing and revising of the manuscript was done by the doctoral candidate.

Note: N1 and N2 in this study used to distinguish developed IMTRs, refer to N3 and N4 in the chapter Overall Discussion.

Adapted original manuscript[1]

Production of β-Lactoglobulin hydrolysates by monolith based immobilized trypsin reactors

Yuhong Mao[1], Urh Černigoj[3], Viktor Zalokar[3], Aleš Štrancar[3], Ulrich Kulozik[1,2]
Technical University of Munich, [1]Chair for Food and Bioprocess Engineering,
[2]Institute for Food and Health (ZIEL) – Technology Unit,
Weihenstephaner Berg 1, D-85354, Freising-Weihenstephan, Germany
[3]BIA Separations d.o.o., Mirce 21, 5270 Ajdovščina, Slovenia

Abstract: Tryptic hydrolysis of β-Lactoglobulin (β-Lg) is attracting more and more attention due to the reduced allergenicity and the functionality of resulting hydrolysates. To produce hydrolysates in an economically viable way, immobilized trypsin reactors (IMTRs), based on polymethacrylate monolith with pore size 2.1 µm (N1) and 6 µm (N2), were developed and used in a flow-through system. IMTRs were characterized in terms of permeability and enzymatic activity during extensive usage. N1 showed twice the activity compared with N2, correlating well with its almost two times higher amount of immobilized trypsin. N2 showed high stability over 18 cycles, as well as over more than 30 weeks during storage. The efficiency of IMTRs on hydrolyzing β-Lg was compared with free trypsin, and the resulting hydrolysates were analyzed by MALDI-TOF/MS. The final hydrolysis degree by N1 reached 9.68% (86.58% cleavage sites) within 4 h, while only around 6% (53.67% cleavage sites) by 1.5 mg of free trypsin. Peptides analysis showed the different preference between immobilized trypsin and free trypsin. Under the experimental conditions used in this study, the potential cleavage site Lys^{135}–Phe^{136} was resistant against the immobilized trypsin in N1.

Key words: monolith, trypsin, immobilized enzyme reactor, β-Lactoglobulin

[1] Adaptions refer to formatting issues: e.g., numbering of sections, figures, tables and equations, abbreviations, manufacturer specifications, axis labeling, figure captions and style of citation.

[1] Originally published in: *Electrophoresis* (2017), Vol. 38. Issue: 22-23, pp. 2947-2956. Permission for reuse of this article was granted by Wiley Online Library.

3.1.1 Introduction

Among the major whey proteins β-Lactoglobulin (β-Lg) is the main antigen. Enzymatic hydrolysis of this protein is a common approach to reduce allergenicity. The use of the serine protease Trypsin (EC 3.4.21.4), which preferably cleaves the C-terminal peptide bonds of Arginine (Arg/R) and Lysine (Lys/K), not only can significantly reduce its allergenicity (Jost, Meister & Monti, 1991), but also leads to the release of five biofunctional peptides (Leeb et al., 2015). In addition, Schmidt and Poll (1991) showed that native α-Lactalbumin (α-La) was highly resistant to tryptic digestion while native β-Lg was not. Indeed, Konrad and Kleinschmidt (2008), taking advantage of this selective susceptibility of β-Lg, used a combination of membrane technology and trypsin hydrolysis to obtain a yield of α-La of 90–95% in purity. However, the cost of large-scale use of trypsin in solution is very high, which severely limits its industrial application. Correspondingly, immobilized trypsin represents an alternative approach due to the possibility of reusing the enzyme and producing enzyme-free hydrolysates.

During the past few decades, the immobilization of trypsin onto different stationary supports has been studied resulting in the development of various immobilized trypsin reactors (IMTRs). These IMTRs can generally be divided into three groups: (1) trypsin is immobilized on nano- or microparticles (Atacan, Cakiroglu & Ozacar, 2016b; Wang, Jiao, Gao et al., 2017; Yamaguchi, Miyazaki, Honda et al., 2009); (2) trypsin is retained by membrane (Prieto, Guadix & Guadix, 2010); or (3) trypsin is immobilized onto surface of monolithic materials (Liang, Tao, Ma et al., 2011; Meller, Pomastowski, Szumski et al., 2017; Naldi et al., 2017; Nicoli et al., 2008; Svec, 2006). However, available systems still suffer from low processing stability, i.e. high pressure drop over time (Cheison, Zhang, Wang et al., 2009), enzyme leakage due to non-covalent bonding (Atacan, Cakiroglu & Ozacar, 2016b; Cheison et al., 2009), and low capacity in terms of volume throughput (Bassan, Bezerra, Peixoto et al., 2016).

Among the different immobilization supports, monoliths have been of recent interest, because they generally allow for a higher mass flow, and mass transfer of target molecules with the enzyme bound to the monolithic channel surfaces is primarily governed by the mobile phase convective flow. Furthermore, the surface of monoliths can be modified with various functional groups, which makes covalent bonding of enzyme much easier. However, most of the developed monolithic IMTRs are designed to accelerate the digestion step for proteomics analysis, which differs from the application of producing protein hydrolysates. Besides high enzymatic efficiency, to reach a higher space-time yield (the amount of substrate converted per biocatalyst reactor), the crucial requirements for enzymatic hydrolysates production are a need for processing larger amount of substrate and longer continuous digestion time in each cycle. These requirements may cause a blockage problem. Theoretically, monoliths with very large pores can minimize this issue (Bencina, Bencina, Podgornik et al., 2007), but at the expense of the decreased surface area, resulting in significant reduction of the amount of immobilized trypsin.

Based on these considerations, for the first time, we immobilized trypsin on monolith with pore size 6 µm (N2), which is less prone to pore blockage, and compared its efficiency with that with pore size 2.1 µm (N1). This allows us to conclude on the effect of convective flow through the pores at longer operation times in a continuous mode. Short polymethacrylate monolithic columns, commercialized under the trademark Convective Interaction Media® (CIM®), were used as the stationary supports. The immobilized trypsin yield was compared in these two IMTR systems and correlated with their digestion activities. The efficiencies of these two CIM-IMTRs in hydrolyzing β-Lg were compared with each other, as well as with free trypsin. Furthermore, long-term stability of these two IMTRs was monitored throughout the whole study.

In addition, differences in the hydrolysates may arise from the use of an immobilized enzyme instead of the free one. In fact, immobilization can change, e.g., the accessibility of the enzyme to the substrate or even the affinity of the enzyme towards a specific substrate. In this study, we also explored the peptides compositions in the hydrolysates resulting from immobilized and free trypsin, separately.

3.1.2 Materials and methods

3.1.2.1 Materials

Bovine β-Lg was fractionated from WPI, a product from Fonterra Co-operative Group Ltd (Auckland, New Zealand) as described by Tolkach et al. (2011). Trypsin from bovine pancreas (Type I, ~10,000 BAEE units/mg protein), Nα-Benzoyl-L-arginine ethyl ester (BAEE, B4500), Tris (hydroxymethil)-aminomethane (TRIS), sodium cianoborohydride ($NaCNBH_3$), ethanolamine, sodium chloride (NaCl), benzamidine hydrochloride (BAHC), 2-(N-morpholino)-ethanesulfonic acid (MES), sodium hydroxide, sulphuric(VI) acid, calcium chloride and sodium eriodate were purchased from Sigma–Aldrich (St Louis, MO, USA). Deionized water was from MilliQ System (Millipore Corporation, Bedford, USA).

3.1.2.2 Preparation of CIM-IMTRs and frame of flow-through system

CIM-IMTRs preparation

Aldehyde activated CIM radial columns (CIM-ALD, tube dimensions: outer diameter (D) – 1.86 cm, inner diameter (d) – 0.67 cm, height (h) – 0.42 cm; volume 1.0 mL) with nominal pore size diameter of 2.1 and 6 µm were provided by BIA Separations d.o.o. (Ajdovščina, Slovenia).

The specific surface area of the monoliths before trypsin immobilization was measured via nitrogen adsorption by TriStar II 3020 (Micromeritics Instrument Corporation, Norcross, GA, USA). Nitrogen of 99.999% purity was used. Before analysis the monolith samples were dried in nitrogen flow at 70°C for 1 hour.

Pore size distribution was measured by a Pascal 440 (Thermo-Quest Italia, Rodano, Italy) mercury porosimeter within a range of 15–10,000 nm. Approximately 0.1 g of dried monolith sample was measured before immobilization.

Trypsin was covalently immobilized on CIM-ALD monolithic columns using the following coupling protocol. The immobilization was done in duplicate. 5.0 mg of trypsin was dissolved in 5 mL of immobilization buffer, composed of 0.1 M MES, pH 5.6, $NaCNBH_3$ (3.0 mg/mL) and BAHC (0.4 mg/mL). The CIM-ALD column was washed with 20 mL of 0.1 M MES buffer at pH 5.6, followed by 10 mL of immobilization buffer. Then the trypsin solution was continuously recirculated for 3 h at a flow rate of 0.5 mL/min. Aliquots of trypsin solution were collected at the beginning, during and at the end of the immobilization procedure for subsequent trypsin mass balance analysis. The residual aldehyde groups were deactivated by treating the columns with ethanolamine and $NaCNBH_3$ solution as it is described in Naldi et al. (2017). Afterwards, the column was washed with 20 mL of Tris-HCl buffer (20 mM pH 7.4 containing 1 M NaCl). Before use the prepared CIM-IMTRs were stored at 4°C in aqueous solution of 20 mM acetic acid, pH 3.5 containing 1.0 mM $CaCl_2$.

Determination of immobilized trypsin density

The amount (mg) of immobilized trypsin was calculated according to Eq. 3.1-1.

$$m_{immobilized}(trypsin) = \gamma_{load}(trypsin) \times V_{load} - \sum \gamma_n(trypsin) \times V_n \quad (3.1\text{-}1)$$

Where, γ_{load}(trypsin) is the concentration of trypsin in the loading solution; γ_n(trypsin) are concentrations (mg/mL) of trypsin in washing and deactivation fractions after the immobilization; V_{load} is the volume of trypsin solution applied to the column and V_n is the sum of the washing and deactivation fraction volumes, in mL. The determination of trypsin concentration was performed chromatographically as described by Naldi et al. (2017).

Frame of the flow-through system

IMTR was inserted in ÄKTA system (GE Healthcare Bio Sciences) consisting of sample pump (P-960), system pump, auto-sampler and detectors for UV, pH, temperature and conductivity. The whole system was controlled by Unicorn Software 5.31.

3.1.2.3 Pressure drop and permeability calculation

The backpressure without and with IMTR was recorded at increasing flow rates, namely 0.5, 2.0, 5.0, 10 and 15 mL/min, by pumping deionized water. The difference between these two values at a defined flow rate was considered to be the pressure drop created by the inserted reactor. According to the study of Podgornik et al. (2014), the permeability of monolith was calculated according to Eq. 3.1-2:

$$B = \frac{F}{\Delta P} \times \frac{\eta \times ln(\frac{D}{d})}{2\pi h} \quad (3.1\text{-}2)$$

Where, ΔP (MPa) is the pressure drop; η is the viscosity of mobile phase (0.87685 MPa*s for deionized water); B (m^2) is the calculated permeability of monolith; F (mL/min) is the volumetric flow rate; D (m) and d (m) are outer and inner tube diameters, and h (m) is monolith height.

3.1.2.4 Activity measurements of free and immobilized trypsin

The activity measurement is a spectrophotometric rate determination (A_{253nm}, Light path = 1 cm) in buffer solution based on the following reaction:

$$BAEE + H2O \xrightarrow{Trypsin} N\alpha - Benzoyl - L - arginine\ (BA) + ethanol$$

All the measurements were conducted at 25 ± 1°C. 0.1 M Tris-HCl buffer was used, and its pH was adjusted to different values, namely 7.2, 7.8, 8.1, 8.5 and 9.2, to assess the effect of pH.

Free trypsin activity measurement

For measuring free trypsin activity, a continuous spectrophotometric rate determination was performed following the protocol given by the manufacturer (Sigma-Aldrich, 2016). The activity of free trypsin was expressed as BAEE units. One BAEE unit is defined to produce a ΔA253 of 0.001 per minute in a reaction volume of 3.20 mL.

Immobilized trypsin activity measurement

Inserted IMTR was washed by deionized water firstly and then equilibrated by 0.1 M Tris-HCl buffer (varied pHs) at 5 mL/min. 10 mM BAEE in 0.1 M Tris-HCl buffer was continuously pumped through this IMTR at 10 mL/min. The first 4 mL of sample was discarded because of the dead volume of Äkta system and following 2 mL was collected by the auto-sampler. The collected samples were diluted and further measured by spectrophotometer at 253 nm. The activity unit U* (μmol/min), defined as the amounts of BAEE one CIM-IMTR converted to BA in 1 min at specific conditions, was calculated using Eq. 3.1-3:

$$U^* = \frac{\Delta A \times F \times Di \times 10^3}{L \times \varepsilon} \quad (3.1\text{-}3)$$

ΔA (Au) is the absorbance difference of BAEE solution before and after hydrolysis; Di is dilution factor; L is the light path, here is 1 cm; ε is the molar extinction coefficient, corresponding to the differential molar absorbance of BAEE against BA at 253 nm, here is 808 mol^{-1} cm^{-1} determined by Kedzy et al (1965). U* can be easily converted to BAEE units, using the conversion factor 270 determined by Bergmeyer et al. (1974).

3.1.2.5 Hydrolysis of β-Lg

Between experiments IMTRs were stored at 4°C in storage solution (19 mM $CaCl_2$ in 10% ethanol/water solution, pH 3 adjusted by 0.1 M HCl). This solution was required to be washed out prior to starting the next cycle. Therefore, before each hydrolysis experiment, the CIM-IMTR was washed by deionized water. The washing step was also used to characterize the IMTR in terms of the pressure drop as described in 2.3. If the pressure drop would be higher than base line, this would have been an indication of pore blockage. Afterwards, it was equilibrated by 0.1 M Tris-HCl buffer at pH 7.8 (this step was excluded when pH-stat method was applied). After each hydrolysis of β-Lg, a cleaning step using an alkaline solution (0.5 mM NaOH + 5 mM NaCl, pH 10.8) was used, and deionized water was applied to remove the alkaline prior to filling the

system with storage solution. All the hydrolysis experiments were conducted at 25 ± 1°C.

Single flow-through approach

Native β-Lg in 0.1 M Tris-HCl buffer (1.5, 3 and 6 mg/mL) at pH 7.8 was continuously pumped through the IMTR (N1 or N2) at different flow rates, ranging from 0.5 to 10 mL/min. The first 4 mL of hydrolysates were discarded. The following 6 mL were collected by the auto-sampler for the native protein content measurement. The amount of native β-Lg was determined using RP-HPLC as described by Tolkach et al. (2011). The depleting rate of β-Lg was calculated according to Eq. 3.1-4:

$$R = \frac{C_d \times v}{v/F} = C_d \times F \qquad (3.1\text{-}4)$$

Where, R (mg/min) is the depleting rate of β-Lg, C_d (mg/mL) is the difference of β-Lg concentration before and after hydrolysis, v (mL) is the collected volume, and F (mL/min) is the flow rate.

Recirculation flow approach

50 mL of native β-Lg in 0.1 M Tris-HCl buffer (3 mg/mL) at pH 7.8 was recirculated through N1 for 2 h at 0.5, 5, 10 and 15 mL/min, respectively. Samples at different time intervals (0, 10, 20, 30, 60, 90, 120 min) were drawn for native protein content analysis (Tolkach et al. 2011).

Comparison of IMTRs and free trypsin on hydrolyzing β-Lg

Native β-Lg dissolved in deionized water (25 mL, 10 mg/mL, pH was adjusted to 7.8 using 1M NaOH) was hydrolyzed by free trypsin or IMTRs. For the hydrolysis by IMTRs, the recirculation flow approach at 10 mL/min was applied.

TitroLine alpha plus autotitrator (Schott AG, Mainz, Germany) measured the change of pH every 3 s during the hydrolysis process and kept pH constant by addition of 0.1 M NaOH. The data was acquired by the TitriSoft 2.5 software. The degree of hydrolysis (DH) is defined as the percentage of peptide bonds cleaved (h) compared to the total available peptide bonds (h_{tot}) in the protein substrate (Eq. 3.1-5). Instantaneous DH at any given time was calculated using Eq. 4 according to the pH-stat method (Adler-Nissen, 1986).

$$DH = \frac{h}{h_{tot}} \times 100\,\% = \frac{V_b \times N_b}{\alpha \times M_p \times h^*_{tot}} \times 100\% \qquad (3.1\text{-}5)$$

where, V_b (mL), base consumption; N_b, normality of the base; α, average degree of dissociation of the NH groups; M_P (g), mass of protein; h^*_{tot}, total number of peptide bonds in one gram protein substrate, in this work we calculated this value to be 7.63 meqv/g for β-Lg.

From Eq. 3.1-5, h was derived directly, and the velocity of reaction was calculated by Eq. 3.1-6.

$$V = \frac{dh}{dt} \qquad (3.1\text{-}6)$$

Where, V (meqv/min) is the rate of reaction; h (meqv) is the amount of peptide bonds cleaved; t (min) is the hydrolyzing time.

3.1.2.6 Peptides composition analysis using MALDI-TOF mass spectrometry

Collected samples were analyzed for mass composition using MALDI-TOF/MS system (ultrafleXtreme MALDI-TOF/TOF, Bruker Daltonics, Bremen, Germany) with two matrices separately, α-Cyano-4-hydroxycinnamic Acid (HCCA, Bruker Part-No. #201344) and 2,5-Dihydroxyacetophenone (DHAP, Bruker Part no. #201346). Generally, HCCA is used for the measurement of peptides and proteins in the low mass range (≤ 4,000 Da), whereas DHAP is mainly used for proteins in the higher mass range. The detailed method is described in supporting information.

3.1.3 Results and discussion

3.1.3.1 IMTRs characterization

Yield of immobilized trypsin in IMTRs

Development of CIM-IMTR for proteomic applications clearly demonstrated that decrease of pore size down to 0.6 µm was preferable due to higher immobilized trypsin density on the monolithic surface and consequently higher enzymatic conversion (Naldi et al., 2017). Unfortunately, the decrease of pore size by a factor of 2 results in a 4 times higher pressure drop and a drastic decrease of permeability, which is not an option for hydrolysates production. Therefore, an alternative approach was considered, where monoliths were with larger pores and consequently higher permeabilities. The monolithic surface area is one of the most important parameters influencing the maximum amount of immobilized protein. BET surface areas of CIM monoliths (before trypsin immobilization) were measured to be 5.0 and 2.0 m^2 per g of dry monolith for 2.1 µm (N1) and 6 µm (N2) pore sizes, respectively. In our immobilization protocol, 5 mg of trypsin was available for binding to a monolith with volume of 1 mL. Mass balance calculations showed a complete depletion of trypsin from the immobilization solution for N1, while 2 mg of trypsin remained unbound with the N2. Correlating BET surface area and amount of immobilized trypsin, at least 2 mg more trypsin could be additionally bound to the monolithic surface in case of N1 to obtain the maximum possible ligand density.

Considering BET surface areas and the molar mass of trypsin from bovine pancreas (23.8 kDa), each trypsin molecule in N1 and N2 occupies approximately 17 and 11 nm^2 of surface, respectively. Based on Saha et al. (2015), the molecular dimension of native trypsin from porcine pancreas is 4.8 nm x 3.7 nm x 3.2 nm. Assuming that the spatial dimensions of bovine-derived trypsin are similar and that enzyme molecules are surrounded by a hydration layer of approximately 0.2 nm, one trypsin molecule would occupy between 10 and 20 nm^2 surface. It is concluded that the highest possible surface density of immobilized trypsin was achieved with N2 (100 ± 15%), while approximately 65 ± 10% coverage was obtained for N1.

Initial pressure drop and permeability

The pressure drop created by freshly prepared N1 and N2 at different flow rates was recorded in Figure 3.1-S1. A linear increase of pressure drop depending on flow rates for both reactors was observed as expected for constant permeability, proving that porous monolithic structure is stable and no compression occured even when the flow rate was up to 15 mL/min. According to Eq. 3.1-2, the calculated initial permeabilities of N1 and N2 were 2.45 x 10^{-12} m^2 and 1.91 x 10^{-11} m^2, respectively. Due to the same porosity of N1 and N2 (60%), 7.80 times higher permeability of N2 could be attributed mainly to the pore size difference. According to the Blake–Kozeny equation, the permeability of a porous bed depends on the particle size forming the bed, as well as on its porosity. Instead of particle diameter a pore size (d_v) is used, and the expression takes the following form (Podgornik et al., 2014):

$$B = K_v \times \varepsilon \times d_V^2 \qquad (3.1\text{-}7)$$

Where, K_v is a structural constant of particular bed. Assuming same porosity and structural constant for N1 and N2, an Eq. 3.1-8 is derived:

$$\frac{B_{N1}}{B_{N2}} = \frac{d_{V1}^2}{d_{V2}^2} \qquad (3.1\text{-}8)$$

The exact pore sizes of both monoliths were determined by mercury porosimetry before the immobilization (2.15 µm for N1 and 5.80 µm for N2) as described above. The measured permeability ratio (N1/N2 = 7.80) fits very well with the squares of the experimentally determined d_v ratio, thus confirming that N1 and N2 were structurally similar materials.

Activity measurements at increasing pH values

Figure 3.1-1. Activity profiles for IMTRs and free trypsin at increasing pH values and

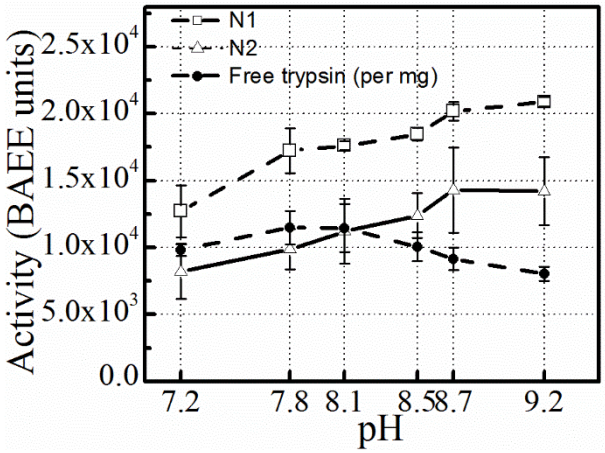

10 mL/min. The activity measurements at each pH value was repeated at least for three times.

BAEE was dissolved in 0.1 M Tris-HCl buffer and used as substrate to assess the activity of immobilized and free trypsin at increasing pH values. As shown in Fig. 3.1-1, N1 showed almost twice the activity compared with N2, which correlates well with the almost two times higher amount of immobilized trypsin in N1. With increasing pH up to 9.2, the activity of both IMTRs was quite stable and even exhibited a slight

increment. Actually, the immobilized trypsin could survive without any decrease of activity at pH 10.8, which was decided to be the pH of washing solution applied in this study. On the contrary, the activity of free trypsin started to decrease above pH 8.1.

Not surprisingly, such stabilization of immobilized trypsin with pH increase was attributed to the applied multipoint covalent immobilization, which has been claimed by Fernandez-Lafuente et al. (1995). However, immobilization often results in a decrease of enzymatic activity due to steric hindrance and reduced accessibility to the trypsin active site. Comparing the specific activity of per mg immobilized trypsin in IMTRs with per mg free one, a decrease of 74–48% for N1 and 73–41% for N2 at varied pH values was observed.

Based on these results, the characteristics of CIM-ALD columns and corresponding IMTRs are summarized in Table 3.1-1.

Table 3.1-1: Characteristics of CIM-ALD columns (column volume 1 mL) and corresponding IMTRs

Column	Pore size (μm)	BET surface (m^2/g)	Permeability in di-water (m^2)	Amount of immobilized trypsin (mg per mL)	Trypsin surface density (molecules per nm^2)	Activity U* (μmol/min) (substrate BAEE) at pH 7.8 and 10 mL/min
N1	2.15±0.1	5.0±0.4	$2.45x10^{-12}$	5.0±0.2	11±4	63.86±6.08
N2	5.80±0.3	2.0±0.2	$1.91x10^{-11}$	3.0±0.3	17±5	36.56±5.56

3.1.3.2 Hydrolysis of β-Lg

Efficiency evaluation of IMTRs at different flow rates

The flow rate is one of the most important factors influencing the flow-through bioreactor performance. To evaluate the performance of IMTRs in depleting β-Lg at different flow rates, both single flow-through approach and recirculation flow approach were applied, which are more practical to improve the hydrolysates yield compared with a classical zonal approach (with injection volume only up to microliter or milliliter).

For the immobilized trypsin, the optimal pH is 8.7 or even higher, while activities of the free one started to decrease when the pH value was above 8.1 (see Fig. 3.1-1). To compare the efficiencies between the free and the immobilized trypsin, we decided to perform the hydrolysis at pH 7.8.

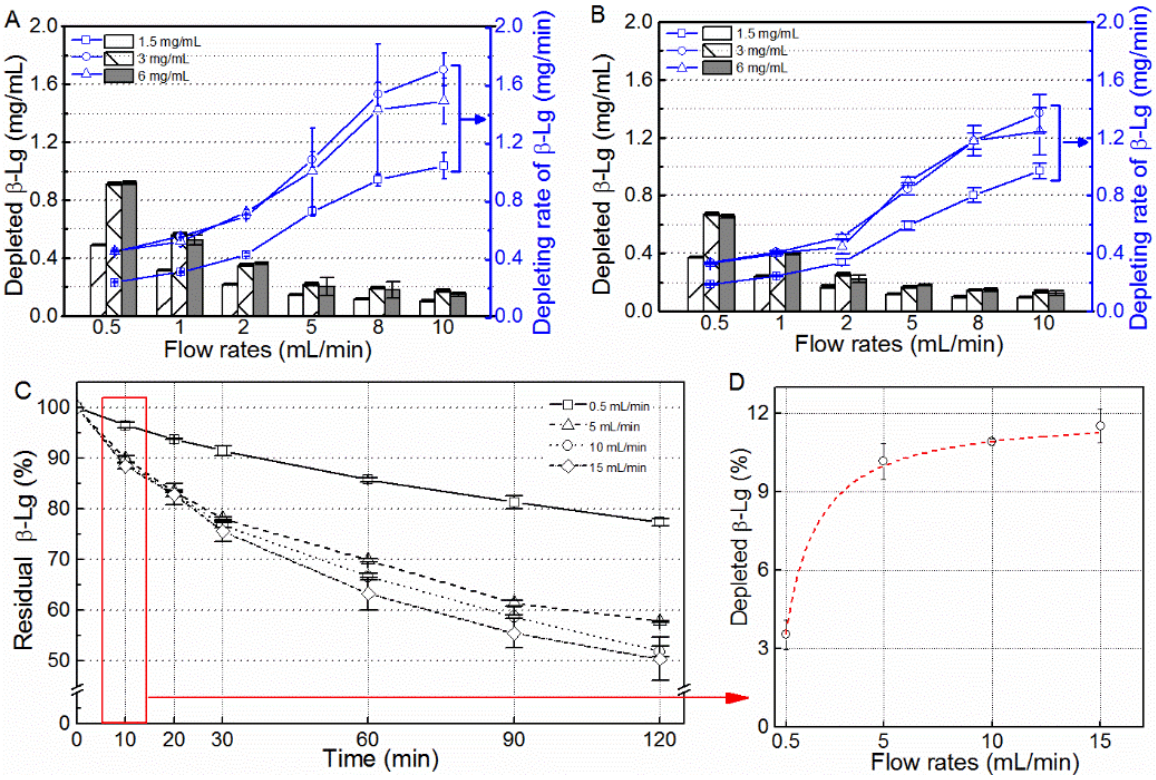

Figure 3.1-2. Efficiency of IMTRs in depleting β-Lg: (A) & (B) the depleted amount of β-Lg by N1 and N2 depending on flow rates in single flow-through approach; (C) the residual amount of β-Lg during recirculation at different flow rates by N1; (D) The depleted amount of β-Lg by N1 in first 10 min during recirculation at different flow rates.

In a single flow-through approach, β-Lg solutions (in 0.1 M Tris-HCl buffer, pH 7.8) with stepwise increased concentrations were used to avoid underestimation of IMTRs' performance due to the insufficient replenishment of substrate. As shown in Fig. 3.1-2 A and B, 3 mg/mL native β-Lg was found already to be a saturating concentration for all explored flow rates, since no more β-Lg was depleted when the substrate concentration further raised to 6 mg/mL. As expected, for both N1 and N2 more native β-Lg was depleted at lower flow rates because of the corresponding longer contact time between immobilized trypsin and substrate. However, regarding to the efficiency (i.e. the depleting rate of β-Lg) at each flow rate, a clear increasing dependence on flow rate was found, as can be seen from the curves in Fig. 3.1-2 A and B. As compared to IMTRs used in proteomic applications, in continuous operation we rate the performance of IMTR technology from a different perspective. A higher depleting rate would be a decisive criteria regarding processing efficiency. To further assess the effects of flow rates on IMTR's efficiency, a recirculation flow approach within a long given time is preferred, which provides the possibility to compare the depleted β-Lg limited to the same given time while at different flow rates. According to the results in Fig. 3.1-2 A and B, the efficiency values at 5 mL/min seem to be in the middle range. Hence, 50 mL of β-Lg solution (in 0.1 M Tris-HCl buffer, pH 7.8) at 3 mg/mL were recirculated through N1 at 0.5, 5, 10 and 15 mL/min for 2 h, respectively. The residual native β-Lg in substrate solution at different time intervals, as shown in Fig. 3.1-2 C, decreased significantly faster when flow rates were at or above 5 mL/min during

recirculation, compared with that at 0.5 mL/min. The growth of depleting efficiency with increasing flow rates is presumably attributed to the increased mass transfer of β-Lg molecules towards the immobilized trypsin (Vlakh & Tennikova, 2013b). In addition, the work of Jungreuthmayer et al. (2015) demonstrated that the flow in monolith showed a lateral velocity component, which may contribute to the transport of molecules to the monolith wall. This confirmed lateral velocity can be speculated to promote the contact between substrate and fixed trypsin. From this result, it is assumed that the fluctuating flow behavior in monolith may be more severe at higher flow rates, since the efficiency in depleting β-Lg was higher at increased flow rates. However, this increase of efficiency depending on flow rates can reach a plateau, as shown in Fig. 3.1-2 C, no increment was found when the flow rate further raised to 15 mL/min from 10 mL/min. Actually, a clear plateau was observed in Fig. 3.1-2 D, where the depleted β-Lg in first 10 min was plotted versus applied flow rates. This dependence of efficiency on flow rates is quite different from that in the single flow-through approach (Fig. 3.1-2 A & B), where the efficiency improved significantly with increasing flow rates. It was noted that the substrate concentration was assumed constant in the calculation by single flow-through approach, while it declined continuously in a recirculation flow approach. Hence, for further experiments, the recirculation flow rate was fixed at 10 mL/min.

Comparison of the hydrolysis efficiency by IMTRs and free trypsin

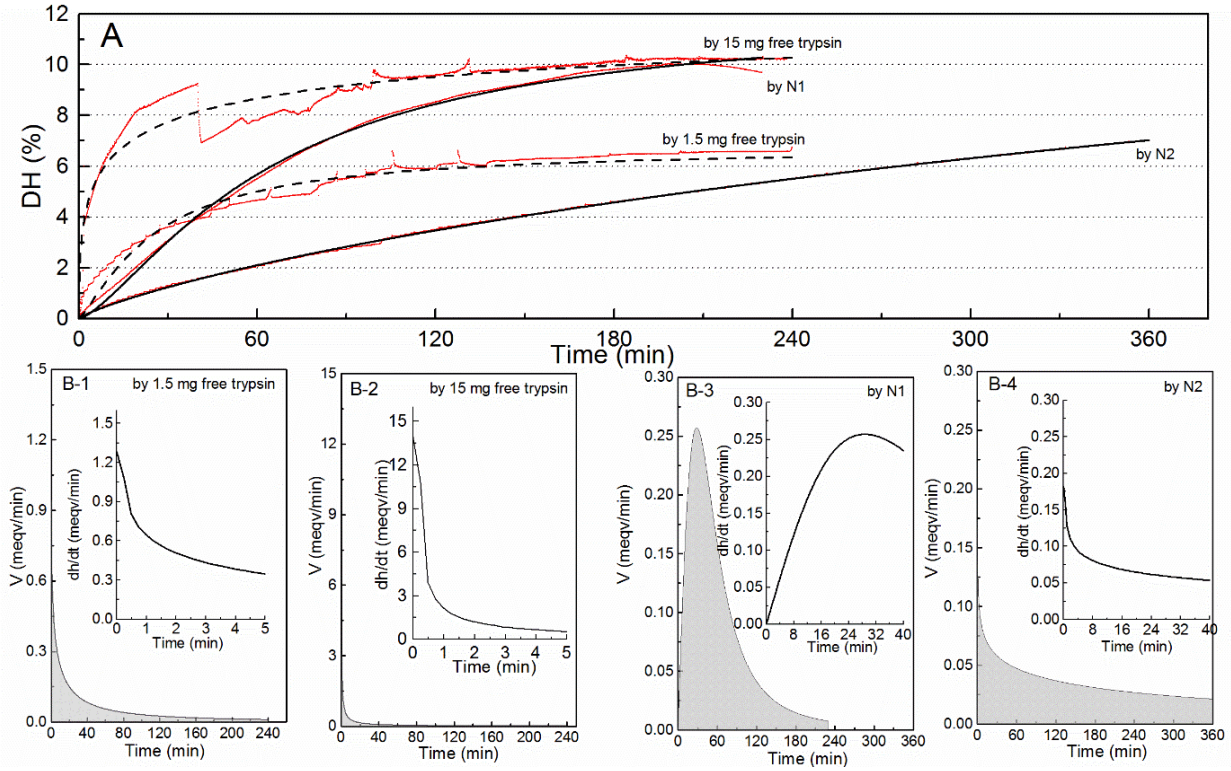

Figure 3.1-3. (A): the evolution of DHs depending on time for four hydrolysis experiments; (B): the velocities of these four hydrolysis processes, B-1 ~ B-4 refer to the hydrolysis by 1.5 free trypsin, 15 mg free trypsin, N1 and N2, respectively, in addition, the first 5 min for free trypsin and 40 min for IMTRs were highlighted.

The efficiencies of IMTRs in producing β-Lg hydrolysates at recirculation flow approach were compared with each other, as well as with free trypsin (1.5 mg and 15 mg) in a stirred solution. The same amount of substrate (25 mL, 10 mg/mL β-Lg in water, pH 7.8) was used. Additionally, it was noted that the activity of 1.5 mg free trypsin equals the activity of N1 in term of BAEE units (Fig. 3.1-1).

As shown in Fig. 3.1-3 A, the DH using 1.5 mg free trypsin increased much faster at the beginning than that using N1 or N2. From the curves of velocity versus time in Fig. 3.1-3 B-1, B-3 and B-4, the maximum reaction velocity (V) by free trypsin at the given conditions in this study reached around 1.28 meqv/min, 5-fold of that by N1 and 7-fold of that by N2, respectively. Obviously, free trypsin is more flexible to contact with β-Lg compared with immobilized trypsin in IMTRs, forming enzyme-substrate complex, and then contributed to a significantly higher reaction velocity. On the other hand, the steric effects that are involved by non-oriented immobilization can also lead to a lower velocity.

Normally, the maximum velocity at given conditions is determined by measuring the initial reaction velocity in a catalyst system, because it requires a high concentration of substrate. As shown in Fig. 3.1-3 B-1, in a system with free trypsin, the maximum velocity was achieved immediately once the reaction started. However, it took around 30 min to reach the maximum velocity for N1 (Fig. 3.1-3 B-3). Since the measurements of DH depended on consumed volumes of NaOH, it is assumed that the initial delay of calculated DH in N1 case is not because of a slower enzymatic reaction, rather because of the residual charge on monolithic surface. The surface of N1 has properties of a weak base (secondary amine) due to ethanolamine deactivation of residual aldehyde groups after trypsin immobilization (Lendero, Vidic, Brne et al., 2008). The DH experiments were performed in water, therefore the monolith charge was not shielded by the buffer and obviously it served as the neutralizing agent or as a buffering agent in the beginning of the reaction, thus decreasing the consumption of NaOH. In Fig. 3.1-2 C, where β-Lg was dissolved in 0.1 M Tris-HCl buffer, no delay of β-Lg depletion was observed with N1 in the beginning of the reaction, indirectly confirming the interpretation of DH experiment in Fig. 3.1-3 C. We also developed two IMTRs using another approach, where ethanolamine was excluded during deactivation, and no delay of initial reaction velocity was observed (data not shown here). One would expect similar observations with N2 as well, but the amount of ethanolamine groups on the N2 surface was considerably lower, which almost eliminated this delay. The reasons are: 1) higher surface coverage by trypsin, leading to lower amount of residual aldehyde available for the reaction with ethanolamine; 2) 2.5 times lower surface area of N2 leading to at least 2.5 times lower amount of charged functional groups.

Along the hydrolysis process, the reaction velocity continuously decreased, especially using free trypsin. The final DH within 4 h by 1.5 mg free trypsin was only around 6%, while its theoretical DH_{max} is 11.18% (Leeb et al., 2015). The effects of autodigestion, reduction of substrate and potential inhibition of products can account for this result. Correspondingly, the decrease of reaction velocity by immobilized trypsin was much

slower mainly because of the absence of autodigestion. Since autodigestion of enzyme is a time-dependent process, more trypsin provided, longer effective hydrolyzing time can be achieved. Hence, 10-fold amount of free trypsin was used to hydrolyze the same amount of substrate. A sharp increase of maximum reaction velocity was observed (Fig. 3.1-3 B-2) and DH increased extremely fast in a short time, close to the theoretical DH_{max}. The DHs by 15 mg free trypsin and N1 finally reached plateaus so that they were considered as the practical maximum DHs. Accordingly, the hydrolysates were collected for further analysis. In N2, the DH gradually increased, reaching 7% after 6 h. Presumably, this hydrolysis process can reach its maximum DH when enough time is provided.

Peptides compositions analysis

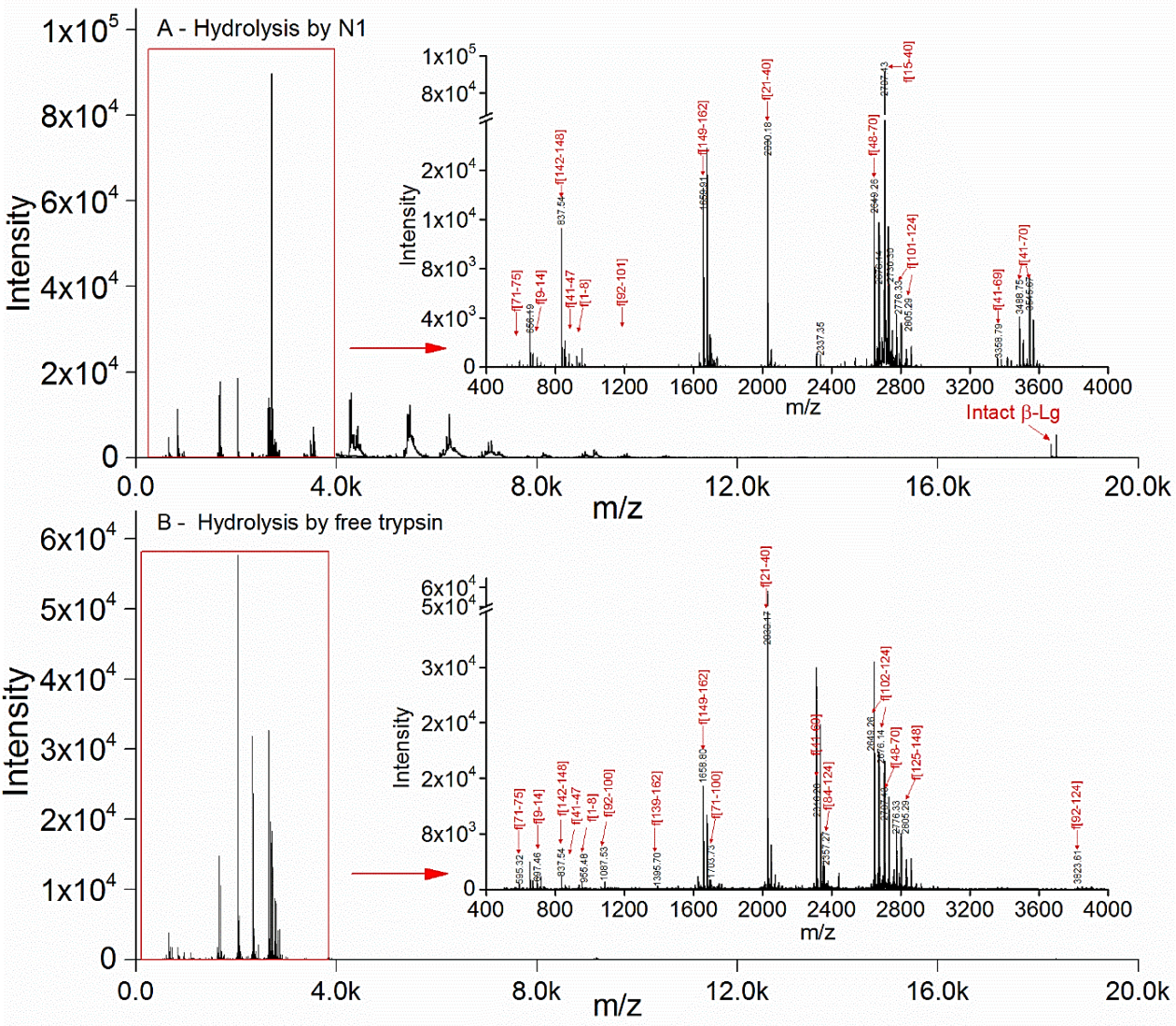

Figure 3.1-4. Mass spectra of samples analyzed using the α-Cyano-4-hydroxycinnamic Acid (HCCA) and 2,5-Dihydroxyacetophenone (DHAP) matrix: (A) sample hydrolyzed by N1; (B) sample hydrolyzed by 15 mg free trypsin.

The peptides compositions in collected samples were analyzed using MALDI-TOF/MS, as shown in Fig. 3.1-4. (the mass spectrum exported directly from flex analysis software is shown in Fig. 3.1-S2). Mass signals in the range between 500 and 8,000 Da were clearly observed in the sample from N1, even intact β-Lg peaks around 18,000 Da were still visible (Fig. 3.1-4 A). On the contrary, most peaks were below 4,000 Da in the sample hydrolyzed by free trypsin. Correlating to the practical DH_{max}, the final DH by N1 (9.68%) was indeed lower than that by free trypsin (11.07%).

β-Lg contains 161 peptide bonds, of which 18 peptide bonds are theoretically cleavable by trypsin, leading to the release of 19 peptides after complete trypsinolysis, as shown in Fig. 3.1-S3. However, the masses below 500 Da are not possible to be detected by our method in this study. Regarding other detectable peptides, only f(48–60) was missing in both samples, f(125–135) and f(61–69) only missed in the sample hydrolyzed by N1. By searching polypeptides in the hydrolysates from N1, no matched peptide starting from Phe_{136} or end at Lys_{135} was found. Hence, it is speculated that the potential cleavage site Lys_{135}–Phe_{136} was resistant against the immobilized trypsin in N1 under our experimental conditions.

Along the hydrolysis process, it is important to point out the competition for the active site between the original protein substrate and the released polypeptides. Analysis of these polypeptides in the final hydrolysates provides information on the preference between immobilized and free trypsin. From the mass spectrum in Fig. 3.1-4, f(41–60), f(71–100) and f(70–75) remained in final hydrolysates by free trypsin, as well as by N1. The existence of f(125–138) and f(92–138) further confirms Lys^{135}–Phe^{136} was indigestible by N1. Other polypeptides with quite high intensity, such as f(41–70), f(41–69), f(101–124) and f(92–101), only existed in the hydrolysates from N1. By calculating the content of hydrophobic amino acids, these four polypeptides contain 39.9%, 41.38%, 41.7% and 60.0%, respectively. These high contents of hydrophobic amino acids may account for the non-digestion. Because the hydrolysis by immobilized trypsin in methacrylate monolith requires a transportation of the substrate to the monolith wall, these hydrophobic peptides seem less prone to be transported and then are hard to contact with the active site of immobilized trypsin.

3.1.3.3 Operational stability

During operation of IMTRs, pressure drop and activity were monitored through the whole study. To confirm the durability of IMTRs in one cycle, 10 mg/mL β-Lg solution was continuously recirculated through N1 or N2 at 10 mL/min for 6 h, respectively. As shown in Fig. 3.1-S4, a slight increment of recorded pressure drop was noted for N1, namely from 0.30 MPa to 0.33 MPa, whereas the pressure drop by N2 completely kept constant. The adsorption of β-Lg molecules on the surface of monolith should be responsible for this slight increase of N1.

On the other hand, cumulative action from each cycle to the next one is a potential issue. N2 was used to hydrolyze β-Lg (10 mg/mL) for 18 cycles (except for 6 h in the first cycle, others were continued for 3 h each time), both enzymatic activity and

pressure drop remained constant (the monitored permeability and activity was recorded in Fig. 3.1-S5). Regarding to N1, the same substrate solution and recirculation time in each cycle were applied. Fig. 3.1-S6 records the pressure drop, calculated permeability and activity over 18 cycles. No decrease was observed of either permeability or activity in the first 10 cycles. Hereafter, the permeability declined gradually while the enzymatic activity was still unchanged until the 18_{th} cycle. Because of the continuous increase of pressure drop, 20 mL of 0.05 M NaOH solution was used to flash N1 at 5 mL/min after the 18th cycle, which resulted in an increase of permeability, while accompanied by a complete loss of activity. After the application of 1 M NaOH, the permeability nearly returned to its initial value. This result confirms the blockage problem in N1 due to the cumulative action. It should be noted that the cycles were not always conducted over consequent days, and IMTRs were stored at 4°C in storage solution between cycles. After these operations, N2 was completely stable during storage over 30 weeks, in terms of BAEE activity and pressure drop, monitored over 3 weeks.

3.1.4 Concluding remarks

Trypsin immobilized on CIM monolith columns showed significant activity towards β-Lg. Different from hydrolysis by free trypsin in stirred solution, the efficient contact time between immobilized trypsin and substrate is much shorter than the recirculation time due to 0.6 mL pore volume of IMTRs. Nevertheless, the hydrolysis by N1 reached a much higher DH (9.68%) than that by 1.5 mg free trypsin (6.02%) in 4 h, mainly due to the autodigestion of free trypsin. To avoid this problem, a higher amount of enzyme is necessary to achieve DH_{max}, leading to higher costs. Furthermore, monoliths with large pores and consequently higher permeabilities make long-term use of IMTRs possible. At least 18 times' reuse of N1 significantly reduces costs in total. In order to additionally improve the operational stability, IMTR based on CIM monolith with pore size of 6 µm (N2) was developed and characterised as highly permeable alternative.

It is noted that hydrolysis conditions, such as pH, ionic strength, temperature, etc., are not optimized in this study. The efficiency of these IMTRs in production of β-Lg hydrolysates is highly potential to be improved after the optimization of processing parameters. Furthermore, these parameters play great roles not only in the effectiveness, but also in the selectivity. For example, Cheison's work (2011) confirms that trypsin hydrolysis in solution at pH 8.5 and 25°C offers the complete removal of β-Lg while the retention of 67.87% native α-La. Hence, optimization of these parameters for IMTRs could allow a better process control such that the desired hydrolysis of the target β-Lg would preferably take place, while α-La remained largely unaffected, at lower levels of denaturation.

Acknowledgements

The first author thanks China Scholarship Council (CSC) for the support of her personal cost. This work was partially supported by Slovenian Research Agency within the research program P4-0369.

3.1.5 Supporting Information

3.1.5.1 Peptides composition analysis using Matrix-assisted laser desorption/ionization time-of-flight (MALDI-TOF) mass spectrometry

Sample preparation

Bovine β-Lg has five Cys residues, four of them form disulfide bridges between Cys_{66} and Cys_{160}, and between Cys_{106} and Cys_{119}. Cys_{121} is free and therefore available for reaction. It is well documented that MALDI-TOF mass spectra often shows the expected peaks corresponding to the disulfides accompanied by their reduction products. To avoid the interference from disulfide bonds, reduction with Dithiothreitol (DTT) and Cys-alkylation with Chloroacetamide (CAA) were processed to all samples.

Samples were diluted in water to a protein concentration around 0.5 mg/ml, and the pH after dilution stayed between 7 and 8. 128.6 µl 80 mM DTT was given to 900 µl diluted sample, the mixture was shaked at 37^{o}C for 45 min, afterwards 141 µl 400 mM CAA was added and samples were stored in dark for 30 min. To acidify the reduced samples, 6 µl 0.5% formic acid was mixed with each sample. The final pH of samples ready for spotting was below 3. A blank sample (using 900 µl distilled water instead of protein solution) was prepared following same steps as well.

HCCA was dissolved in solvent containing 60% ACN diluted in distilled water and 0.1% TFA. The mixture was ultrasonicated for 10 min to achieve maximum solubility and then centrifuged (3 min, 10,000 rpm) to separate the saturated solution and the rest of the insoluble HCCA. The supernatant was used for spotting. Exactly same procedure was applied to prepare DHAP matrix.

The external standards (protein standard I and PAS, Bruker Daltonics GmbH, Bremen, Germany) were dissolved in 500 µL of the same solvent that was used for the DHAP and HCCA. For the calibration.

1 µl sample (including blank sample) or standards was mixed with 1 µl HCCA matrix or DHAP matrix directly on anchor target (stainless steel MTP 384) by pipetting up and down several times. Every sample was spotted at least three times. Spots on target were dried in fume hood at room temperature.

Mass Spectrometry

MALDI-TOF/MS was managed using flexControl 3.0 Software (Bruker Daltonics, Bremen, Germany). Spectra based on the HCCA-matrix were obtained at reflectron mode, and the method PepMix.par was chosen and modified. The samples with DHAP-matrix was analyzed at linear mode by method ProtMix.par. The laser strength was optimized at 30% for HCCA-matrix and 60% for DHAP-matrix. Each spot was shot at least 5 times manually at different parts.

Peptides analysis

The peaks in blank sample was picked using flexAnalysis 3.0 (Bruker Daltonics, Bremen, Germany) firstly and imported into mass control list of theoretical trypsin auto digests, then this new mass control list was set as background peaks. These background peaks were removed from the picked peaks of samples before analysis. A theoretical peptides database from β-Lg digested by trypsin was built using the Sequence Editor (Bruker Daltonics, Bremen, Germany). By comparing the mass of picked peaks in sample with this database using a written code in software R 3.3.3 (open source software), the sequences were assigned to each peak.

3.1.5.2 Supporting information tables

Table 3.1-S1A Identification of peptides obtained by free trypsin hydrolysis of β-Lg

Calculated mass [a)]	Observed mass [b)]	S/N	Intensity	Assigned Sequence
595.36	595.38	48.80	1053.26	[71- 75]
674.42	674.45	18.50	405.58	[78- 83]
695.39 [Na]	695.39	51.00	1126.14	[9- 14]
739.46 [K]	739.34	14.30	320.95	[70- 75]
837.48	837.49	124.60	2983.49	[142-148]
880.02	881.44	29.80	729.78	[41- 47]
938.47	938.46	38.10	958.32	[84- 91]
955.54 [Na]	955.53	68.20	1739.05	[1- 8]
1064.13 [B]	1064.45	13.10	364.25	[61- 69]
1087.58	1087.57	55.30	1571.36	[92-100]
1122.17 [A]	1122.46	11.10	325.95	[61- 69]
1245.59	1245.82	17.10	1055.66	[125-135]
3178.64	1395.64 *	14.10	553.41	[139-162]
1679.78 [Na]	1680.77	266.20	14016.42	[149-162]
3401.93	1702.75 *	30.10	1596.03	[71-100]
2029.06	2030.07	895.90	55472.75	[21-40]
2313.26	2313.24	451.60	30620.22	[41- 60]
4716.30 [B]	2357.20 *	62.20	4136.44	[84-124]
4744.33 [A]	2373.16 *	11.40	754.73	[84-124]
2646.06 [B]	2647.15	517.60	27628.98	[102-124]
2674.11 [A]	2675.18	313.10	16361.50	[102-124]
2705.32 [Na]	2705.23	193.10	9817.88	[48- 70]
2707.38	2708.33	103.20	5252.95	[15- 40]
2804.45 [k]	2803.28	148.00	6964.99	[125-148]
3821.43 [B]	3821.68	10.10	119.51	[92-124]
3849.48 [A]	3849.70	14.20	161.92	[92-124]
3873.33 [B]	3873.78	11.40	731.00	[102-135]
3901.39 [A]	3901.63	12.10	130.30	[102-135]

Table 3.1-S1B Identification of peptides obtained by N1 hydrolysis of β-Lg

Calculated mass [a)]	Observed mass [b)]	S/N	Intensity	Assigned Sequence
573.36	573.50	22.80	3804.20	[71- 75]
673.39	673.53	15.90	2696.44	[9- 14]
674.42	674.55	19.00	3183.10	[78- 83]
739.456 K	739.38	11.80	160.99	[70- 75]
837.48	837.53	159.80	2240.08	[142-148]
880.02	881.48	36.90	525.56	[41- 47]
903.57	925.59	43.30	628.99	[76- 83]
933.54	933.68	22.10	3344.63	[1- 8]
938.47	938.49	17.70	260.71	[84- 91]
1087.58	1087.70	25.80	3442.63	[92-100]
1193.68	1193.84	20.60	1420.95	[92-101]
1635.78	1635.86	13.90	316.23	[125-138]
1680.83 Na	1680.86	154.80	3520.47	[149-162]
3401.93	1702.848 *	25.70	597.50	[71-100]
2029.06	2030.18	27.50	7352.10	[21-40]
2313.26	2313.36	18.70	569.61	[41- 60]
2647.31 B	2647.19	276.90	7653.24	[48- 70]
2707.38	2707.39	1460.10	38111.90	[15- 40]
5435.60 B	2719.221 *	13.50	556.91	[92-138]
2722.98 A	2723.38	21.00	748.42	[48- 70]
2707.38	2729.37	214.20	5708.41	[15- 40]
5463.63 A	2733.271 *	101.40	2807.11	[92-138]
2772.27 B	2772.33	17.60	562.44	[101-124]
2802.28 A	2803.34	77.60	1997.31	[101-124]
3357.68 B	3358.63	25.30	439.38	[41- 69]
3415.68 A	3416.64	19.40	322.41	[41- 69]
3485.78 B	3486.72	98.30	1401.68	[41- 70]
3543.78 A	3544.74	166.60	2226.37	[41- 70]
18265.39 B	9142.34*	9.10	1834.00	Intact β-Lg
18351.42 A	9183.16*	7.30	1456.00	
18265.39 B	18282.29	8.10	425.00	
18351.42 A	18367.33	6.40	338.00	

a): Monoisotopic mass with single charge, calculated from amino acid sequence. A represents this sequence particularly from β-Lg A, and B is from β-Lg B. There are two amino acids different as shown in Fig. 3.1-S3. Na and K represent sodium and potassium adduct, respectively.

*b): Observed mass with single charge except for those marked with *, * means double charged mass.*

3.1.5.3 Supporting information figures

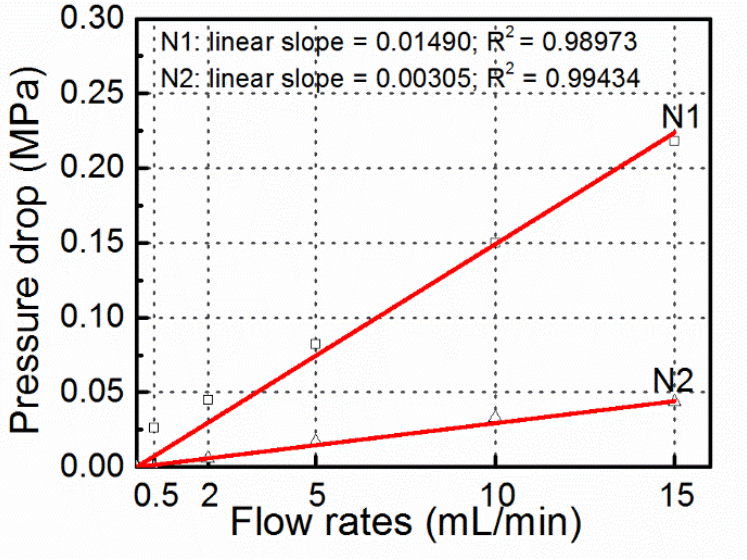

Figure 3.1-S1. Pressure drop of freshly prepared IMTRs depending on flowrates

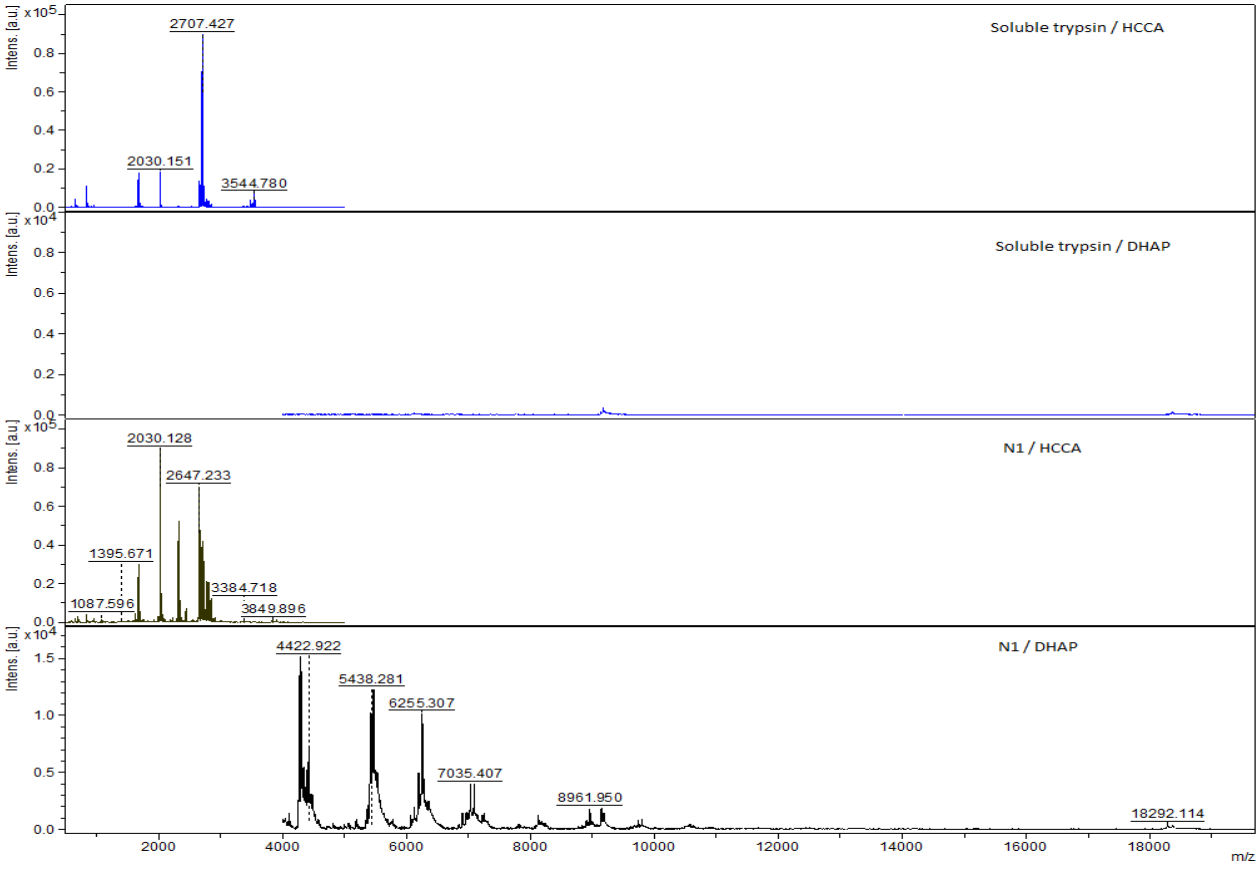

Figure 3.1-S2. Mass spectrum of samples in different matrix exported directly from Flex analysis software.

β-Lactoglobulin (genetic variant B inscribed at position 63 and 118)

Leu Ile Val Thr Gln Thr Met Lys Gly Leu Asp Ile Gln Lys Val Ala Gly Thr Trp Tyr[20]

Ser Leu Ala Met Ala Ala Ser Asp Ile Ser Leu Leu Asp Ala Gln Ser Ala Pro Leu Arg

Val Tyr Val Glu Glu Leu **Lys** **Pro** Thr Pro Glu Gly Asp Leu Glu Ile Leu Leu Gln Lys[60]

Trp Glu Asp(Gly)Gly Glu Cys Ala Gln Lys Lys Ile Ile Ala Glu Lys Thr Lys Ile Pro Ala

Val Trp Lys Ile Asp Ala Leu Asn Glu Asn Lys Val Leu Val Leu Asp Thr Asp Tyr Lys[100]

Lys Tyr Leu Leu Phe Cys Met Glu Asn Ser Ala Glu Pro Glu Gln Ser Leu Val(Ala)Cys Gln

Cys Leu Val Arg Thr Pro Glu Val Asp Asp Glu Ala Leu Glu Lys Phe Asp Lys Ala Leu[140]

Lys Ala Leu Pro Met His Ile Arg Leu Ser Phe Asn Pro Thr Gln Leu Glu Glu Gln Cys

His Ile[162]

Figure 3.1-S3. Amino acid sequence of bovine β-Lg (variants A and B). The cleavage sites for trypsin (Lys and Arg) are highlighted.

3.2 Comparison of the influence of pH on the selectivity of free and immobilized trypsin for β-lactoglobulin hydrolysis

Summary and contribution of the doctoral candidate

The hydrolysis conditions, e.g., pH, ionic strength, temperature, influence the reaction rate, and lead to different product profiles. No prior study discusses in sufficient detail whether these influences will differ once the enzyme is immobilized. In this study, we compared the selectivity of free and immobilized trypsin toward β-Lg with a focus of environmental pH. Although, no significant difference in the evolution of DH at pH 7.8 and 8.7 was observed, both free and immobilized trypsin exhibited greater accessibility to intact β-Lg at increasing pH values. The pH increase from 7.8 to 8.7 even shifted the model of the depletion of native protein by free trypsin from “one-by-one” to “zipper,” whereas this influence on immobilized trypsin was limited. Regarding the two genetic variants, β-Lg A was more accessible than variant B under all experimental conditions, while the differences between these two variants are insignificant above pH 8.5. In addition, free trypsin exhibited greater differences in this preference than the immobilized one. The quantification of the selected peptides during the hydrolysis process showed that free trypsin preferentially attacked the cleavage sites located at the C-terminus at pH 7.8, whereas an opposite preference was observed at pH 8.7. For the immobilized trypsin, no significant preference regarding the C- or N-terminus was noted, only a slight increase in preference for Lys_8 was identified at pH 8.7.

Based on the findings in this study, obviously, immobilization does lead to the changes in selectivity, which is also affected by pH. However, the influence of pH is hard to predict, thus, particular attention should be paid to hydrolysates compositions when studying the optimal pH of the hydrolysis to obtain the desired products.

Most significant contribution to this manuscript was made by the doctoral candidate. This comprised (i) the conception and design of experiments based on preceded critical literature review; (ii) experimental conduction on protein hydrolysis and hydrolysates analysis; (iii) data analysis and data interpretation. In addition, writing and revising of the manuscript was done by the doctoral candidate.

Adapted original manuscript[2]

Comparison of the influence of pH on the selectivity of free and im-mobilized trypsin for β-lactoglobulin hydrolysis

Yuhong Mao[a*], Maria Krischke[a], Claudia Hengst[a], Ulrich Kulozik[a,b]
Technical University of Munich, aChair of Food and Bioprocess Engineering, bInstitute of Food and Health (ZIEL)–Technology Unit,
Weihenstephaner Berg 1, D-85354, Freising-Weihenstephan, Germany

Abstract: Although immobilized trypsin is a viable alternative to the free enzyme in solution for producing protein hydrolysates, the change of selectivity introduced by immobilization is unclear. In this study, we compared the selectivity of free and immobilized trypsin for β-lactoglobulin (β-Lg) with a focus on the impact of environmental pH. Both free and immobilized trypsin exhibited greater accessibility to native β-Lg at elevated pH (from pH 7.2 to 8.7). Additionally, free trypsin preferred to attack cleavage sites located at the C-terminus at pH 7.8, whereas an opposite preference for the N-terminus was observed at pH 8.7. Regarding the immobilized trypsin, the pH did not significantly influence its preference for the C- or N-terminus. Generally, immobilization of trypsin resulted in more focused cleavage within its specificity during the initial stage of hydrolysis, and some peptides were formed more rapidly by the immobilized trypsin.

Keywords: β-lactoglobulin, tryptic hydrolysis, immobilization, pH, selectivity

[2] Adaptions refer to formatting issues: e.g., numbering of sections, figures, tables and equations, abbreviations, manufacturer specifications, axis labeling, figure captions and style of citation.

[2] Originally published in: *Food chemistry* (2018), Vol. 253, pp. 194-202. Permission for reuse of this article was granted by Elsevier.

3.2.1 Introduction

Enzymatic hydrolysis of β-lactoglobulin (β-Lg) produces peptides with reduced allergenicity (Selo et al., 1999) and improved functionality (Leeb et al., 2015). However, the cost of the large-scale use of enzymes in solution is very high, which severely limits their implementation at industrial scale. Correspondingly, immobilized enzymes represent an alternative approach due to the possibility of reusing enzymes and producing enzyme-free hydrolysates.

Enzyme immobilization has been exploited over the last four decades to enhance enzymatic activity and stability, which strongly depend on support properties, binding orientation, the number of formed bonds, the microenvironment of the enzyme, and other variables. Aside from measuring stability and activity, some researchers (Atacan, Cakiroglu & Ozacar 2016b; Naldi et al., 2017) analyzed the peptide profiles of the resulting hydrolysates to assess the enzyme specificity after immobilization. The specificity of a proteolytic enzyme describes the type of amino acid, after which it can hydrolyze a peptide bond (e.g., Lys and Arg for trypsin). Regardless of the specificity of the enzyme for individual cleavage sites, not all cleavable sites are hydrolyzed at the same time. Cheison et al. (2011) followed the release of peptides as a function of hydrolysis time from β-Lg hydrolyzed by free trypsin during the first 10 min. They found that the N- and C-termini (Lys_8-Gly_9, Lys_{141}-Ala_{142}, and Arg_{148}-Leu_{149}) of β-Lg were cleaved early (15 s), implying the ease of trypsinolysis at the exposed termini. The results of Fernández and Riera (2013) also show the existence of areas within the intact β-Lg with different susceptibility to tryptic attack. To describe this preference in protein hydrolysis, Butre et al. (2014) introduced the criteria “selectivity”, referring to the rate at which individual cleavage sites in a protein substrate are hydrolyzed relative to other cleavage sites. The ability to discriminate the selectivity of an enzyme is considered essential for understanding enzymatic protein hydrolysis, especially in terms of obtaining hydrolysates consisting of preferred properties.

Upon immobilization of an enzyme, its conformation may change, thus affecting its intrinsic properties (V_{max}, k_{cat}, or K_m), especially when the enzyme is firmly fixed by multipoint covalent immobilization (Duggal & Bucholz, 1982). In addition, the properties of the supports used for immobilization, such as the charge of the stationary phase, hydrophobicity/hydrophilicity, may influence the intrinsic properties of the immobilized enzyme, particularly when charged substrates or products molecules are involved in the enzymatic process. Duggal and Bucholz (1982) presented clear evidence for significant shifts in the association constants for substrates and inhibitors due to the covalent binding of trypsin to a rigid support. Changes of the intrinsic properties of immobilized enzymes may lead to changes in selectivity. Furthermore, the mass transfer properties of an immobilized biocatalyst may affect the competition for the active site of the enzyme between the original protein substrate and released polypeptides, which influences the selectivity to some extent, especially in a diffusion-limited step. Thus, more attention should be devoted to comparing selectivity between free and immobilized enzymes. Rocha, Gonçalves and Teixeira (2011) compared

peptide profiles of whey protein hydrolysates from free and immobilized trypsin by reversed-phase high-performance liquid chromatography (RP-HPLC) and concluded that no significant difference was observable. However, the sensitivity of HPLC, in our eyes, is not sufficient to make this statement. Mass spectroscopy would be required to identify and quantify the resulting peptides not only in the final hydrolysates, but also during the hydrolysis. Hence, many important aspects remain uncharacterized or not well understood, especially the evolutions of peptides, which should be affected by alterations in the selectivity of an enzyme after immobilization.

Additionally, the process of hydrolysis should be performed with a focus on the holistic influence of the hydrolytic environment, including pH, ionic strength, and temperature et al., as these parameters play important roles regarding effectiveness and selectivity of enzymes. To exert more control over the process, it is important to elucidate the influence of the hydrolytic environment on peptide composition, i.e., the selectivity of the enzyme, allowing hydrolysis to be driven by both the “speed” and the desired peptide profiles obtained at various stage along the hydrolysis process.

Among these parameters, pH is easy to adjust while dramatically affecting the process. The effect of pH on enzymes varies, but it is prominently represented by the fact that each enzyme has an optimal pH range (e.g., pH 7.8–8.1 for free trypsin) in which the highest activity is observed. Meanwhile, changes in pH disrupt hydrogen bonding and affect salt bridges, leading to changes of the secondary and tertiary structures of the substrate as well as the enzyme. In fact, evidence of the influence of pH on enzyme selectivity was revealed in a study of the hydrolysis of whey protein isolate (WPI) by *Bacillus licheniformis* (Butré, Sforza, Wierenga et al., 2015), in which large differences in enzyme selectivity for different cleavage sites of β-Lg were observed at pH 7.0, 8.0, and 9.0 (optimal pH for *Bacillus licheniformis* is 8.0).

Our previous work (Mao, Cernigoj, Zalokar et al., 2017) developed a monolith-based immobilized trypsin reactor (MITR), which has been confirmed as an effective alternative tool for producing β-Lg hydrolysates. This previous work also evaluated the effects of pH on the activity of both immobilized and free trypsin using a model substrate Nα-benzoyl-L-arginine ethyl ester (BAEE). Specifically, the free trypsin showed the highest activity at pH 7.8–8.1, and remained around 80% and 60% activity at pH 7.2 and pH 8.7, respectively. The MITR exhibited 70% activity at pH 7.2 compared with that at its optimal pH range (pH 8.5–8.7). In the present study, we aimed at clarifying the selectivity of the immobilized trypsin for β-Lg hydrolysis in comparison with free trypsin. The influence of pH ranging from pH 7.2 to pH 8.7, was investigated, i.e. somewhat broader than the optimum for free trypsin, in order to also include the pH range optimal for the immobilized one. The hydrolysis was characterized using three descriptors: (i) degree of hydrolysis (DH); (ii) the amount of depleted or remaining intact β-Lg as a function of DH (two genetic variants, β-Lg A and B, were compared); and (iii) the peptide profiles and molecular mass distribution depending on DH. Peptides with a mass of less than 4000 Da were assigned to specific sequences, and the selected peptides were further quantified to follow their dynamic evolutions.

3.2.2 Materials and methods

3.2.2.1 Materials

Bovine β-Lg was fractionated from WPI, a product developed by Fonterra Co-operative Group Ltd (Auckland, New Zealand), as described by Toro-Sierra, Tolkach, and Kulozik (2011). The obtained β-Lg powder had a protein content of 98.6% relative to the dry matter, and native β-Lg represented >99% of the total protein content. Trypsin from bovine pancreas (Type I, approximately 10,000 BAEE units/mg protein), BAEE (B4500), Tris (hydroxymethyl)-aminomethane (TRIS), NaCl, $CaCl_2$, and NaOH were purchased from Sigma–Aldrich (St Louis, MO, USA). Deionized water was acquired using the Milli-Q System (Millipore Corporation, Bedford, USA).

The MITR was prepared as described in our earlier work (Mao et al., 2017). Aldehyde-activated Convective Interaction Media® radial column (outer diameter (D), 1.86 cm; inner diameter (d), 0.67 cm; height (h), 0.42 cm; volume, 1.0 mL) with a nominal pore size diameter of 2.1 μm was used as the immobilization support. The amount of immobilized trypsin was 5.0 ± 0.2 mg/mL monolith, and the trypsin surface density was 11 ± 4 molecules per nm^2. After immobilization, the permeability of the MITR was approximately 2.45×10^{-12} m^2 measured using deionized water.

3.2.2.2 Hydrolysis of β-Lg

Hydrolysis by free trypsin

β-Lg solution (50 mg/mL) was hydrolyzed by free trypsin with an enzyme-substrate ratio (E/S) of 0.1% (w/w) at 25 ± 1°C. An additional experiment was conducted at E/S of 1% and pH 7.8 to reach the maximum DH. The pH of substrate solution was adjusted to 7.2, 7.8, 8.1, 8.5, and 8.7. A TitroLine alpha plus auto-titrator (Schott AG, Mainz, Germany) was used for the pH-stat hydrolysis. The detailed calculation of DH and reaction velocity was described in our published work (Mao et al., 2017).

Hydrolysis by immobilized trypsin

The MITR was integrated into an ÄKTA system (GE Healthcare Bio Sciences). In the single flow-through approach, a native β-Lg solution with a concentration of 3 mg/mL was pumped through the MITR at a flow rate of 0.5 or 10 mL/min. The pH of the applied solution was adjusted to 7.2, 7.8, 8.1, 8.5, and 8.7. Using the recirculation flow approach, 100 mL of a native β-Lg solution (10 mg/mL) were recirculated through the MITR at 10 mL/min, pH 7.8 and 8.7 were investigated. The pH-stat method was used to maintain a constant pH and to follow the evolution of DH.

3.2.2.3 Analysis of hydrolysates

1-mL samples were taken at different intervals (0, 5, 10, 20, 30, 45, 60, 90, 120, and 180 min) during the pH-stat process and stored at −20°C. When free trypsin was used, 0.5 mL of the trypsin inhibitor solution (from soybean, 10 mg/mL) was mixed with each sample immediately to stop the hydrolysis. Samples (5 mL) produced by MITR using the single flow-through approach were stored at −20°C for further analysis.

Quantification of residual native β-Lg

The native β-Lg content in samples was quantitatively determined via RP-HPLC using an Agilent 1100 series HPLC system (Agilent Technologies) and a PLRP-S 300A-8µm Latek column (150 × 4.6 mm). The detail on the gradient was previously described by Leeb et al. (2015). β-Lg A (99% purity, Sigma Aldrich, L7780) and β-Lg B (99% purity, Sigma Aldrich, L8005) were used as standards to build a calibration curve.

Separation and quantification of select peptides

The separation of hydrolysates was performed by RP-HPLC using the system described above. All samples were diluted only with the deionized water to a concentration of 4 mg/mL, excluding the sample with the maximum DH for free trypsin that was initially incubated with dithiothreitol (DTT) for 45 min at 37°C and then mixed with chloroacetamide in dark for 30 min. A mobile phase of solvent A containing 0.1% (v/v) trifluoroacetic acid (TFA) dissolved in Milli-Q water and solvent B consisting of 0.0555% (v/v) TFA dissolved in 80% (v/v) acetonitrile (diluted in Milli-Q water) was applied. The entire analysis was conducted at 40°C and 1 mL/min, and the eluting time was extended to 45.5 min with a gradient from 3% to 57% solvent B. The standard sample injection volume was 20 µL, and the elution was monitored at 214 nm. Selected peaks were collected using a fraction collector for peptide composition analysis. Peaks containing a single peptide were chosen for further quantification, and the molar concentration of each specific peptide was calculated from the peak area according to Eq. 3.2-1 (Fernández & Riera, 2013) as follows:

$$X_i = 1 \times 10^6 \left(\frac{A_i}{\varepsilon_i \times l \times v}\right) \times f \times D \qquad (3.2\text{-}1)$$

where x_i (µM) is the concentration of peptide i, A_i (AU min) is the peak area, l (0.6 cm) is the path length of the UV cell, v is the injection volume (20 µL), f is the flow rate (1 mL/min), D is the dilution factor of the sample before injection, and ε_i (AU M^{-1} cm^{-1}) is the molar extinction coefficient of peptide i at 214 nm calculated according to the work of Kuipers and Gruppen (2007).

Identification of peptides using matrix-assisted laser desorption/ionization time-of-flight mass spectrometry (MALDI-TOF-MS)

Mass compositions of collected samples were analyzed using a MALDI-TOF-MS system (ultrafleXtreme MALDI-TOF-TOF, Bruker Daltonics, Bremen, Germany) with two matrices separately, α-cyano-4-hydroxycinnamic acid (HCCA, Bruker Part-No. #201344) and 2,5-dihydroxyacetophenone (DHAP, Bruker Part no. #201346). Generally, HCCA was used to measure peptides in a low mass range (≤4000 Da), whereas DHAP was for the higher mass range. The detailed method was described in our previous work (Mao et al., 2017).

Identification of peptides by liquid chromatography-electrospray source ionization-tandem MS (LC-ESI-MS/MS) analysis

To further confirm the peptide composition, the fractions from the maximally hydrolyzed β-Lg, were further analyzed via LC-ESI-MS/MS, which was conducted at the center BayBioMs (Freising, Germany). The samples were completely dried in the SpeedVaC

(Thermo Scientific, Germany) and resuspended in 500 µl 0.1% FA water. 0.1 µg sample was injected and re-chromatographed by an analytical column (75 µm x 40 cm, C18 column, Reprosil Gold, 3 µm, Dr. Maisch, Ammerbuch, Germany) in 60 min. The gradient was 4 to 32% solvent B (0.1 % FA and 5% DMSO in ACN) in A (0.1% FA and 5% DMSO) at a flow rate of 300 nL / min. The MS measurement was performed on the LTQ Orbitrap Velos in a data-dependent mode whereby the ten most prominent precursor ions of the entire MS spectrum were automatically extracted and fragmented at higher energy collisional dissociation (HCD) at 30% collision energy. The dynamic exclusion was set to 30 s. Both survey scans and product ion scans were recorded in the Orbitrap. Inlet capillary temperature was held at 275°C. A label-free quantification with MaxQuant (version 1.5.3.30, Cox and Mann, 2008) was carried out by the MS data against a Bos taurus UniProt reference database (version 09.07.2016, 24217 entries, contains both β-Lg A and B).

3.2.2.4 Statistical analysis

All hydrolysis experiments were performed in triplicate. Mean values ± 95% confidence levels are reported. Data were plotted using Origin Pro 9.0 or R 3.3.3 (open source software).

3.2.3 Results and discussion

3.2.3.1 Characterization of the hydrolysates: Chromatographic profile and peptide identification

Some semi-quantitative techniques, i.e. techniques based on the peak area of MS-extracted ions (Leeb et al., 2015) or examining the peak area integrated from the chromatography spectrum (Tauzin, Miclo, Roth et al., 2003), were used to monitor peptide formation. However, these methods do not permit the comparison of the abundance between peptides in terms of the absolute concentration due to differences in the ionization efficiency of different peptides. In this study, the molar extinction coefficient of each identified peptide was calculated and used for the absolute quantification.

Fig. 3.2-1 shows typical chromatographic profiles of samples resulting from the hydrolysis by free trypsin and MITR. One profile corresponds to the initial substrate, and the two main genetic variants of β-Lg (A and B) eluted with retention times of 45.71 and 46.13 min, respectively, are presented. The second profile shows the final step (sample was processed with DTT) in the course of hydrolysis by free trypsin, during which the DH plateaued at 10.02%. As shown in the figure, all peptides present in the final hydrolysates eluted before 25 min. β-Lg contains 161 peptide bonds, of which 18 are theoretically cleavable by trypsin, leading to the release of 19 or 21 (considering the two genetic variants) final peptides after complete trypsinolysis. However, there were 26 peaks observed, indicating the existence of intermediate peptides or nonspecific cleavage. The other two profiles refer to the samples produced via intermediate hydrolysis at pH 7.8 by free trypsin (DH 6.12%) and MITR (DH 4.01%). Different from the maximally hydrolyzed sample, some peaks eluted after 25 min in

these samples, and the peaks corresponding to intact β-Lg were still visible in the sample hydrolyzed for 3 h using MITR.

The peaks appearing before 25 min for three samples are highlighted in Fig. 3.2-1B. As can be seen, the good resolution allowed the monitoring of peptides formation on the basis of their peak areas, if no co-elution occurred. To assess the composition of individual peaks with identical or similar retention times from different hydrolysates, the peaks resulting from these samples, which were baseline separated, were collected separately. The peak numbers on the chromatogram in Fig. 3.2-1B refer to the peptide identification obtained via MALDI-TOF-MS, as reported in Table 3.2-1. In addition, the fractions from maximally hydrolyzed β-Lg were further analyzed by ESI-MS/MS (see Table 3.2-1) to ensure the correct identification of peptides.

According to previous works (Butré et al., 2015; Cheison et al., 2011) nonspecific cleavage of Tyr_{20}-Ser_{21} (f(21–40)) in β-Lg is a common feature, even when the purest possible trypsin is used. As the proposed fragment was assigned to the detected mass in the MALDI spectrum using a written code in software R 3.3.3 with a built-in database (Mao et al., 2017), peptides f(21–40) and f(15–20) were manually transferred into this database. However, this nonspecific cleavage was not included in the LC-ESI-MS/MS measurement. As shown in Table 3.2-1, peptide f(21–40) was detected by MALDI in both peaks P8 and P9 for all three samples. Additionally, peptide f(92–100) co-eluted in P8, which was confirmed by both MALDI and ESI. The polypeptide f(41–60) with one miscleavage site (Lys_{47}) was found in P10. Lys_{47} is linked to a proline amino acid, and it is potentially resistant to trypsinolysis, as observed by Olsen et al. (2004) as well. In addition, P10 from the maximally hydrolyzed sample contained peptide f(21–40), mainly due to the large amount of this peptide in the final hydrolysates.

Regarding peaks P2–P7, peptide f(71–75) was detected only by MALDI. It appears that this peptide is not detectable by ESI in this study. Another mass detected by MALDI referring to f(76–83) exhibited extremely strong intensity in the samples produced via intermediate hydrolysis. However, this mass was not observed in the maximally hydrolyzed sample, mainly due to the insufficient amount of this peptide, correlating with the small chromatographic peak shown in Fig. 3.2-1, as it is an intermediate peptide with the missed cleavage site Lys_{78}. Finally, six peaks (P2–P7) could be confidently used for further quantification.

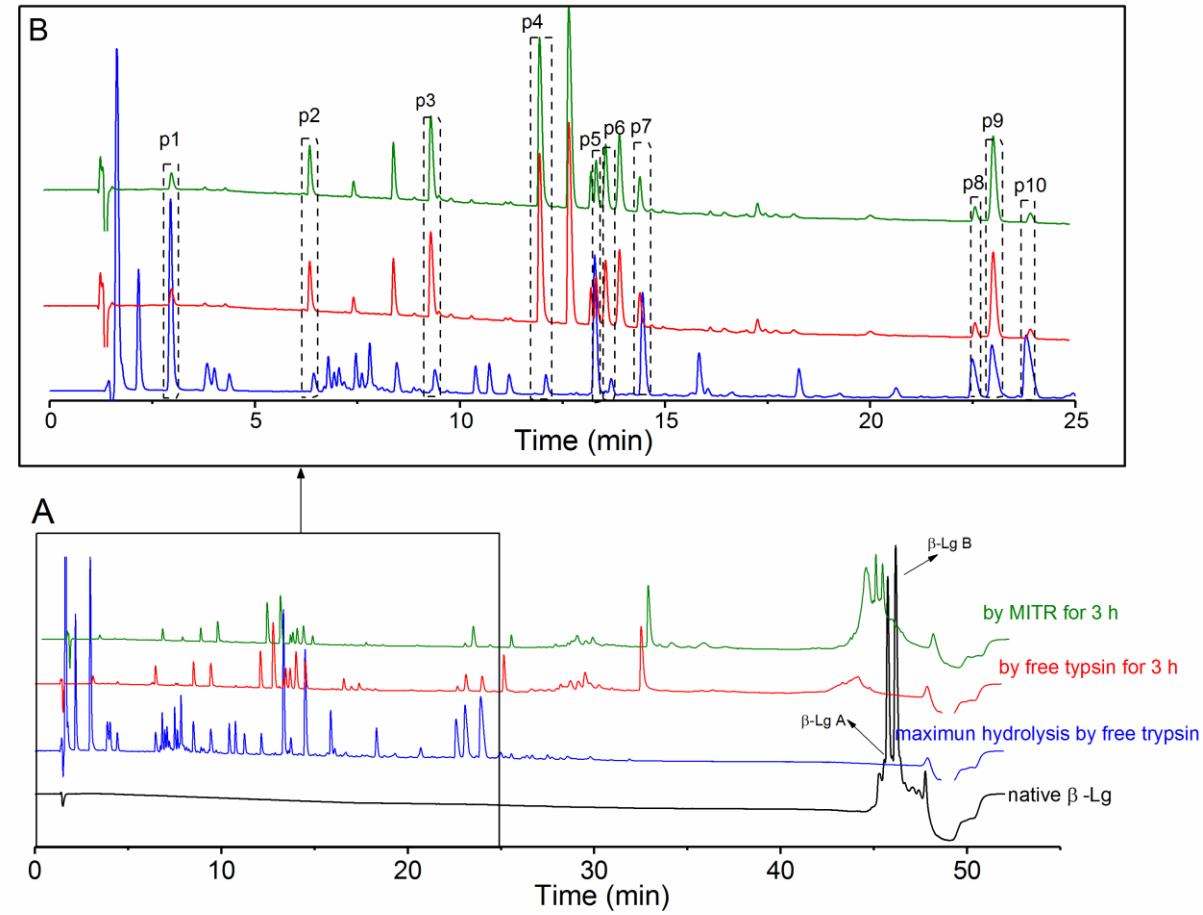

Figure 3.2-1 Chromatographic profiles of intact β-lactoglobulin (β-Lg), the final product of free trypsin hydrolysis, and products generated via intermediate hydrolysis by free trypsin and a monolith-based immobilized trypsin reactor (MITR) (A). The chromatogram before 25 min for the latter three samples are highlighted in B.

3.2.3.2 Comparison of selectivity as a function of pH

Samples with pH values ranging from pH 7.2 to 8.7 were hydrolyzed by free trypsin for 5 min or by MITR at 0.5 and 10 mL/min using single flow-through approach.

Depletion of native β-Lg

The first medium-resolution structure of β-Lg determined by Papiz and Sawyer (1986) illustrates that the molecular structure consists of an antiparallel β-sheet formed by nine strands (A–I) and loops connecting the strands. The work of Qin, Bewley, Creamer et al. (1998) indicates that at pH 6.2, the EF loop is closed over the top of the barrel, burying Glu_{89} (the carboxylic acid with the anomalous pK_a) inside the calyx, whereas at pH 8.1, this loop is articulated away from the barrel such that the formerly buried glutamic acid becomes exposed in the carboxylate form. Furthermore, further increases of pH to values exceeding 8.0 induce further structural changes because the charge states of the side groups of a protein depend on the pH. The pH-dependent structural characteristics can explain the observed result, i.e. the fact that the intact protein was generally more accessible with increasing pH values for both free and immobilized trypsin. For free trypsin, a sharp increase in hydrolyzed β-Lg levels was

observed when the pH was increased from 7.8 to 8.1 (see Fig. 3.2-2), whereas no obvious increment was noted at higher pH values. Concerning the hydrolysis by MITR at 0.5 mL/min, the hydrolyzed β-Lg content significantly increased as the pH was raised from 7.2 to 7.8, as well as from 8.1 to 8.5, as shown in Fig. 3.2-2. For the MITR operated at 10 mL/min, a significant increase was observed when the pH exceeded 7.2, while no difference in the levels of the hydrolyzed native protein from pH 7.8 to pH 8.7 was noticeable. It should be noted that the hydrolyzing time (the time for each substrate molecule remained in MITR) at 10 mL/min is extremely short, theoretically corresponding to 0.06 min because of the 0.6-mL pore volume. The enzymatic activity of free trypsin decreased significantly above pH 8.5 (Mao et al., 2017), this can explain why no more protein was hydrolyzed by free trypsin at pH 8.5 and 8.7 whereas the hydrolytic activity of immobilized trypsin was highest at these pH values. However, it is surprising that no significant difference in the depletion of native protein was observed for free trypsin at pH 7.2 and 7.8, as its activity at pH 7.8 was significantly higher than that at pH 7.2.

The applied β-Lg in this study contains two variants A and B, which differ by two amino acid substitutions, namely Asp64Gly and Val118Ala. The Asp64Gly substitution results in the CD loop adopting a different conformation, whereas the Val118Ala substitution causes no detectable change in the structure (Qin et al., 1999). However, their previous research also suggests that the lower thermal stability of the B variant is mainly due to the substitution of Val118Ala, which results in the hydrophobic core being less well packed. In contrast to the thermal stability, β-Lg B displayed a higher resistance to tryptic digestion (Creamer et al., 2004), which was also confirmed in the present study. As shown in Fig. 3.2-2 B–C, β-Lg A was hydrolyzed faster than the B variant at all applied pH values for both free and immobilized trypsin, and both β-Lg A and β-Lg B were more accessible to trypsin with increasing pH.

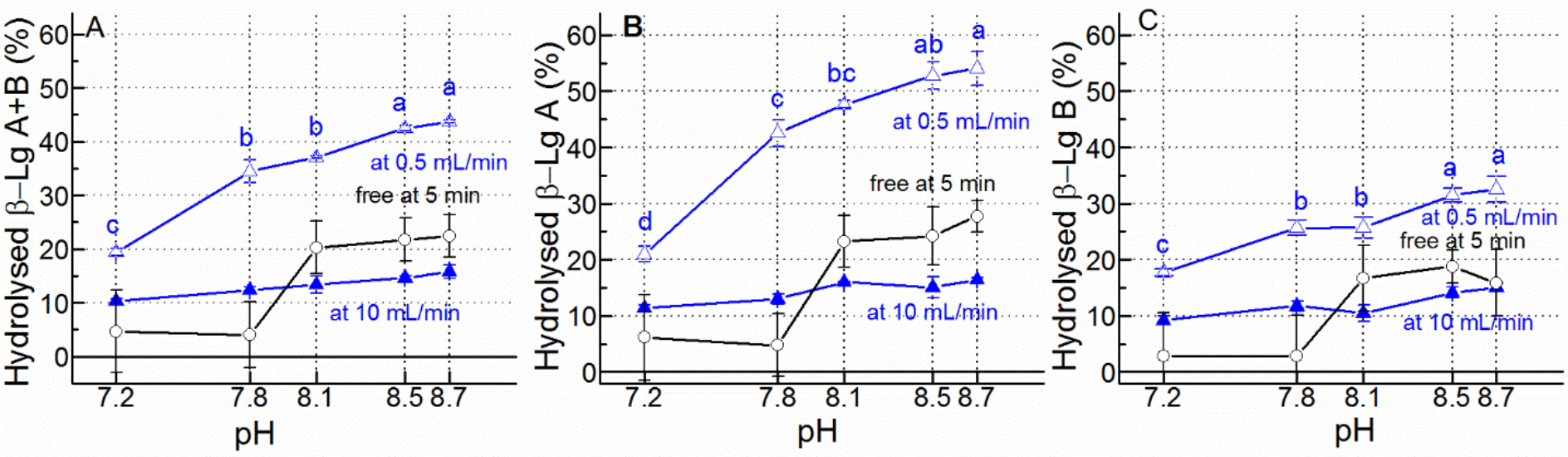

Figure 3.2-2 Hydrolyzed native protein (%) at increasing pH values. A shows the total amount of β-Lg, including the two genetic variants. B and C refer to hydrolyzed β-Lg A (%) and B (%), respectively. A significant difference is presented only for the hydrolysis by MITR at 0.5 mL/min. Data concerning significance for the other two cases are described directly in the text.

Analysis of the composition of hydrolysates

The accessibility of the intact protein is important, but it does not provide information about selectivity among different potential cleavage sites. Hence, the peptide compositions were analyzed by MALDI-TOF-MS, which provides details concerning the mass distribution in a range from 500 Da to the mass of intact β-Lg. As shown in the Venn diagrams (Fig. 3 A1, B1, and C1), detected masses smaller than 4000 Da were assigned to specific fragments, and those larger than 4000 Da were directly distributed in Fig. 3.2-3 A2, B2, and C2.

Peptides lacking miscleavage sites f(1–8), f(9–14), f(15–40), f(142–148), and f(149–162) were detected in all samples. This confirms the strong preference of both free and immobilized trypsin for cleavages at the two C-terminal lysines and N-terminal Lys_{141}, Arg_{148}, and Arg_{40} irrespective of the pH at which the hydrolysis was performed (pH 7.2–8.7). It is already known that arginyl residues are up to 25-fold faster hydrolyzed by trypsin than lysyl residues (Cheison & Kulozik, 2017). There are three arginyl residues among 18 potential cleavable sites in β-Lg. Excluding the aforementioned two cleavable sites, both free and immobilized trypsin preferred Arg_{124}, as peptide f(125–138) with one miscleavage site, Lys_{135}, existed in all samples. Another final peptide, f(71–75), was detectable in the samples from pH 7.8 to 8.7 for free trypsin and for MITR at 0.5 mL/min, whereas this peptide was only found in the sample at pH 8.7 hydrolyzed by the MITR at 10 mL/min. This peptide, located on β-strand D, is exposed to tryptic attacks in the native form of β-Lg, and this attack is considered to be directly associated with enzymatic degradation of the β-Lg molecule (Leeb et al., 2015). Correlating with the depleted intact protein content, it is reasonable to find f(71–75) in the samples hydrolyzed at higher pH values. The last detected peptide without a missed cleavage site was f(84–91) in the sample produced by the MITR at 0.5 mL/min and pH 8.7. It is noted that masses smaller than 500 Da cannot be detected by the method applied in this study, leading to the absence of information at least on five final peptides.

Notably, the nonspecific peptide f(21–40) was present in all samples except that produced by the MITR at pH 7.2 and 10 mL/min. An earlier work of Fernández and Riera (2013) indicated that f(21–40) was released from f(15–40); thus, f(15–20) was a companion product. However, f(15–20) was only found in selected samples in this study, specifically in those hydrolyzed by the free trypsin at pH 7.2 and 7.8, as well in those hydrolyzed by the MITR at pH 8.5 (0.5 mL/min) and pH 8.7 (0.5 and 10 mL/min). This finding suggests that f(21–40) can also be directly generated from f(1–40) or f(9–40), as f(9–40) was detected in all samples. A completely different behavior concerning f(15–20) release was observed upon hydrolysis by free trypsin versus the immobilized one. Namely, free trypsin preferentially further hydrolyzed f(15–40) to release f(21–40) at lower pH values, whereas MITR exhibited this preference at pH 8.5 and 8.7. In addition, Lys_{69} and Lys_{70} displayed different accessibilities; e.g., Lys_{70} was cleavable at all experimental pH values, whereas Lys_{69} was preferentially attacked at higher pH values. Because these two lysines have a similar physical accessibility, this difference

is mainly due to the modulation by the different residues surrounding the cleavage sites.

Regarding the mass distribution for samples containing peptides larger than 4000 Da, peaks for intact β-Lg were visible in all samples as shown in Fig. 3.2-3 A2, B2, and C2. In the samples hydrolyzed by the MITR at 0.5 mL/min, more peaks were in the range of 4000–10,000 Da with increasing pH, indicating that more intact β-Lg was attacked directly at higher pH values. Regarding free trypsin, no significant differences in peptide composition were noted between pH 7.2 and 7.8, as well as in the pH range of 8.1–8.7, correlating well with the depleted amounts of native protein as shown in Fig. 3.2-2.

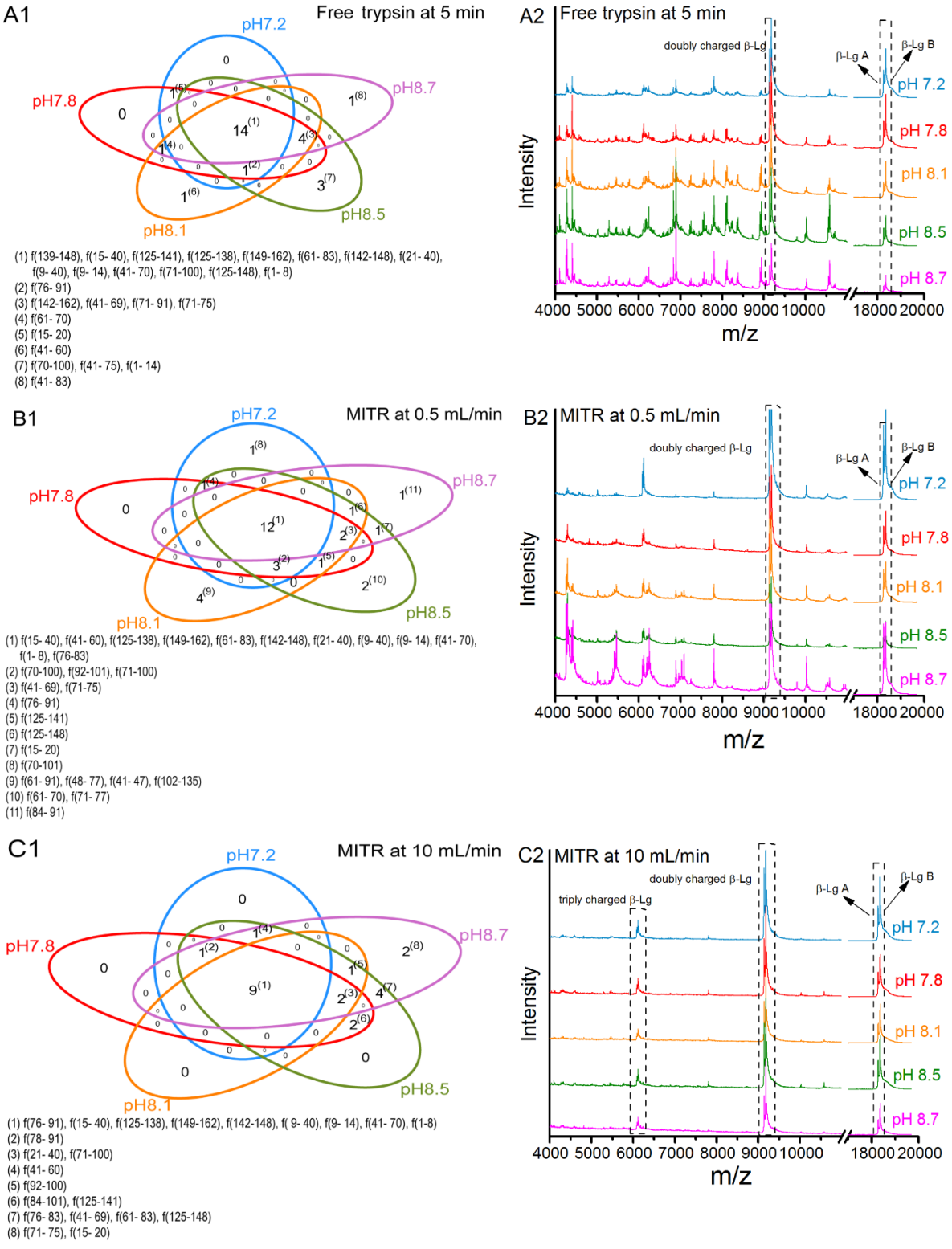

Figure 3.2-3 Comparisons of peptide patterns for masses smaller than 4000 Da at five pH values are shown in A1, B1, and C1, and the mass distributions for larger peptides are presented in A2, B2, and C2. A refers to the samples hydrolyzed by free trypsin for 5 min, and B and C describe samples hydrolyzed by the monolith-based immobilized trypsin reactor (MITR) at 0.5 and 10 mL/min, respectively.

3.2.3.3 Comparison of selectivity as a function of DH

The comparison in section 3.2.3.2 illustrates that differences in the selectivity between free and immobilized trypsin depend on the pH. To identify the differences in a dynamic hydrolysis process, i.e., which and when peptides are formed, a more detailed analysis based on the evolution of DH was conducted. According to the results in section 3.2, pH 7.8 and 8.7 were chosen for further experiments.

Analysis of residual native protein as a function of DH

Fig. 3.2-4 A presents the evolutions of DH as a function of time. As expected, the increase of DH in the initial phase using free trypsin was much faster than that using MITR. As shown in Fig. 3.2-4 B1 and B2, the maximum reaction velocities for free trypsin reached approximately 7.5 and 4 meqv/min at pH 7.8 and 8.7, respectively, which were much higher than those achieved using MITR. Obviously, free trypsin is more flexible in making contact with substrate β-Lg than the immobilized one, contributing to the higher reaction velocity, which has been discussed in many cases of immobilized catalysts (Duggal & Bucholz, 1982; Mao et al., 2017; Rocha et al., 2011). During hydrolysis by free trypsin, a sharp decrease of the reaction velocity within 30 min was observed, and after 3 h, the DH reached 6.10% at pH 7.8 and 5.82% at pH 8.7. The effects of autodigestion, reduction of the substrate, and potential inhibition by products can explain this result. Correspondingly, the decrease of the reaction velocity for immobilized trypsin was less pronounced, mainly because of the absence of autodigestion, as well as the fast removal of products. It is noted that no significant difference in the DH at pH 7.8 and 8.7 was observed for both free and immobilized trypsin.

The decrease of residual native β-Lg content as a function of DH indicates the preference for the hydrolysis of intact protein molecules versus the intermediate peptides and thereby the selectivity. In the Linderstrøm-Lange theory on protein hydrolysis, two models were distinguished: zipper and one-by-one (Adler-Nissen, 1976). As shown in Fig. 3.2-4 C1 and C2, for the free and the immobilized trypsin, a similar linear rate of hydrolysis of the intact protein depending on DH was observed at pH 7.8, which met the “one-by-one” model. This rate was faster at pH 8.7 for both forms of trypsin. Especially for the free one, a sharp increase of the depletion rate was noted in the initial stage of hydrolysis, during which the increase in DH from 0 to 1% corresponded to a depletion of 40% of the intact protein content, in agreement with the “zipper” model. For hydrolysis by the MITR at pH 8.7, the intact protein level decreased linearly as a function of DH. As discussed in the 3.2.1, β-Lg exhibits a pH-dependent structure, making it more tryptic accessible at pH 8.7 than that at pH 7.8. In addition, the thermal stability of β-Lg, decreases from 76^{o}C at pH 7.0 to 58^{o}C at pH 9.0 measured by Haug, Skar, Vegarud et al. (2009). This decrease of thermal stability has been suggested to contribute to the increase of hydrolysis rate of the intact protein as well (Cheison et al., 2011).

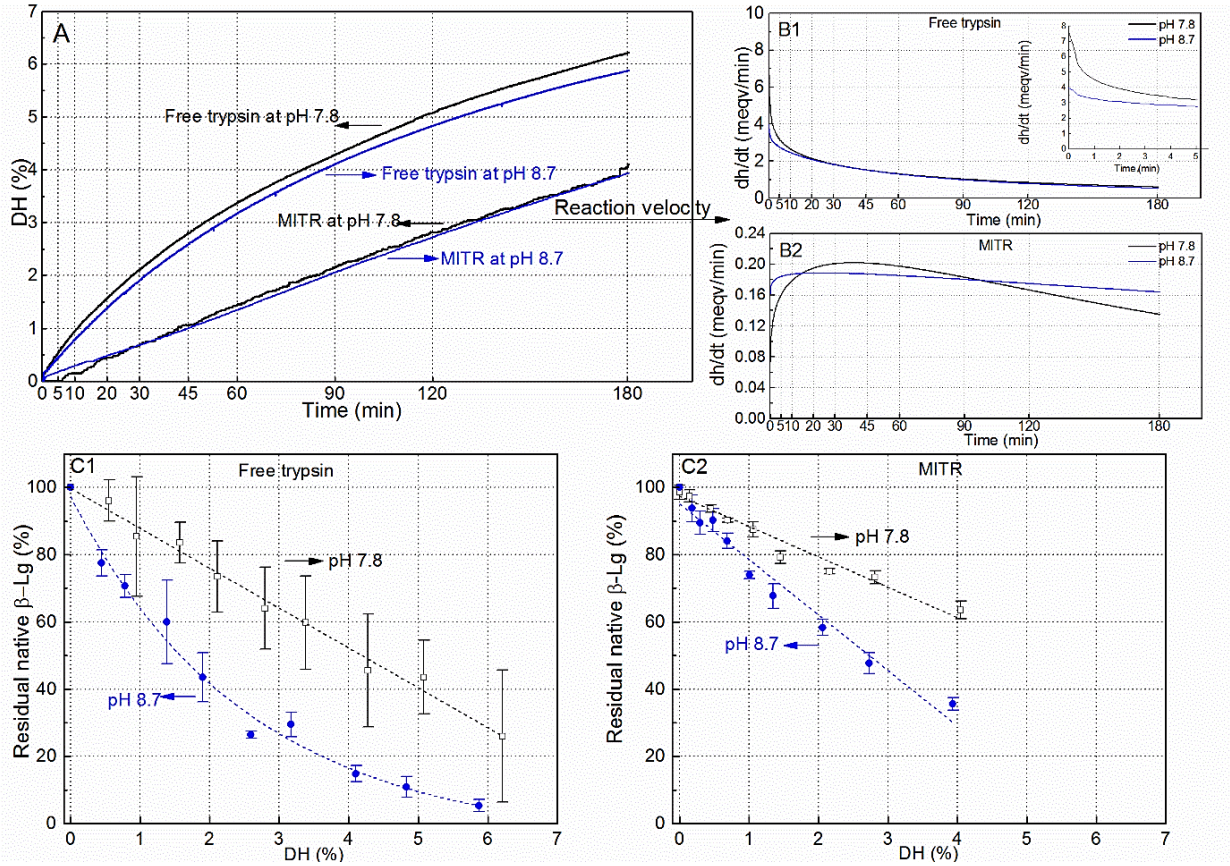

Figure 3.2-4 The evolution of the degree of hydrolysis (DH) depending on time is shown in A. B1 and B2 illustrate the reaction velocities for free and immobilized trypsin, respectively. The inset shows the initial velocity (the first 5 min) of hydrolysis by free trypsin. C1 and C2 show the residual native protein content (%) as a function of DH during hydrolysis by free and immobilized trypsin, respectively.

Peptide formation

As shown in Figs. 3.2-S1 and S2, the evolution of peptides as a function of DH was compared at pH 7.8 and 8.7 for free (Fig. 3.2-S1) and immobilized trypsin (Fig. 3.2-S2). The formed peptides can be classified into three main groups: (i) the final peptides for which their formation is directly linked to the breakdown of intact β-Lg, i.e., normally with high physical accessibility; (ii) some intermediate peptides that are formed rapidly during the first stage of hydrolysis but are then further hydrolyzed, leading to (iii) the smaller or final peptides.

In the first group of peptides, the cleavage sites located at the C- and N-termini, e.g., Lys_{8}, Lys_{14}, Arg_{40}, Arg_{141} and Lys_{148}, are considered the most physically accessible; as expected, peptides corresponding to the cleavages at these sites were released in the initial stage of hydrolysis by both free and immobilized trypsin. Another peptide f(71–75) typically presents a quick release during tryptic hydrolysis because of its external position in the three-dimensional structure of β-Lg and its amino acid composition, both which favor the action of trypsin (Fernández & Riera, 2013). In this study, it formed during the initial stage of hydrolysis using free trypsin as well, whereas it was only

detected in samples with a DH exceeding 2% for the MITR. Regarding the second group, f(125–138) was not further hydrolyzed until the DH reached at least 4% for immobilized trypsin and even 6% for free trypsin, given that f(125–135) was not found. Concerning other intermediate peptides, f(76–91) appeared earlier at pH 7.8 than that at pH 8.7 for both free and immobilized trypsin. The resulting final peptide f(84–91) was also released earlier at pH 7.8 than at pH 8.7, namely at DH values of 0.69% (pH 7.8) and 1.35% (pH 8.7) for immobilized trypsin and 1.84% (pH 7.8) and 5.87% (pH 8.7) for free trypsin. Other studies (Cheison et al., 2011; Fernández & Riera, 2013) indicate that f(76–138) constitutes a resistant core to tryptic attack, which is in accordance with the result using free trypsin in this study, as the cleavage sites within this sequence were less preferred. However, the immobilization of trypsin improved the attack to this area to some extent.

The evolution of polypeptides with high molecular masses, in particular those between 4000 and 10,000 Da, is directly linked to the breakdown of the intact protein. As shown in Figs. 3.2-S1 and S2, for both free and immobilized trypsin, the number of peaks with masses between 4000 and 10,000 increased much faster at pH 8.7 than that at pH 7.8, correlating well with the depletion rate of the intact protein (see Fig. 3.2-4). Regarding hydrolysis by free trypsin at pH 8.7, which was considered to agree with the “zipper” model, hydrolysis of the intact protein was initially rapid, leading to a large number of intermediate peptides, after which the depletion rate of the protein was slower. Likewise, these polypeptides were further hydrolyzed into smaller peptides.

Quantification of selected peptides

The quantification of selected peptides illustrates the dynamics of their formations, in which the concentration of each peptide relative to the theoretical maximum molar concentration is expressed as a function of DH, as shown in Fig. 3.2-5.

The peptides located at the C- and N-termini, e.g., f(1–8), f(9–14), and f(142–148), formed more rapidly at pH 8.7 than at pH 7.8 for both forms of trypsin, especially for the free one. As previously discussed, these peptides can be formed from cleavage of the intact protein, being directly linked to the depletion rate of β-Lg. Another peptide, f(71–75), located at the outside of the protein, was released more rapidly at pH 8.7 with free trypsin, whereas no significant difference in its release was noted between pH 7.8 and 8.7 for the immobilized trypsin. Comparing the formation rates of these four peptides, differences in selectivity were identified, and these differences depended on the pH as well as the use of free or immobilized trypsin. For instance, at pH 8.7, the preferred order of formation of these peptides by free trypsin was f(1–8) > f(142–148) > f(9–4) ≈ f(71–75), whereas at pH 7.8, this order was changed to f(142–148) > f(1–8) ≈ f(9–14) ≈ f(71–75). For the immobilized trypsin, no obviously different preference at pH 7.8 concerning the release of these different peptides was found, and only at pH 8.7, f(1–8) formed significantly faster than the other three peptides.

f(76–83) and f(125–138) are two intermediate peptides, and their relatively slow liberation in the initial stage of hydrolysis is the result of their release from intermediate

products opposed to the substrate molecule itself. With the accumulation of intermediate products, the formation rates of these two peptides increased, reaching approximately 30% for the free trypsin at DH 6% and approximately 20% for the immobilized one at DH 4%, which were much lower than the rates for four more physically accessible peptides. An interesting result was that the immobilized trypsin showed the same trends to form the peptide f(76–83) at pH 7.8 and 8.7, which is faster than that for the free trypsin. Whereas the pH had a great influence on the release of f(76–83) and f(125–138) for free trypsin, both peptides were formed faster at pH 7.8 than at pH 8.7. In addition, there was no decreasing trend observed for these two intermediate peptides, as no final peptide released from these two was detected in any samples (see Figs. 3.2-S1–2).

Generally, pH exerted more pronounced effects on the selectivity of free trypsin than the immobilized one. In this study, trypsin was rigidified by the multipoint covalent immobilization, which can keep its conformation quite stable when the pH is altered. Whereas, the free trypsin may suffer some structural distortion introduced by the increase of pH values, and this distortion always correlates to the changes of its selectivity (Rodrigues, Ortiz, Berenguer-Murcia et al., 2013).

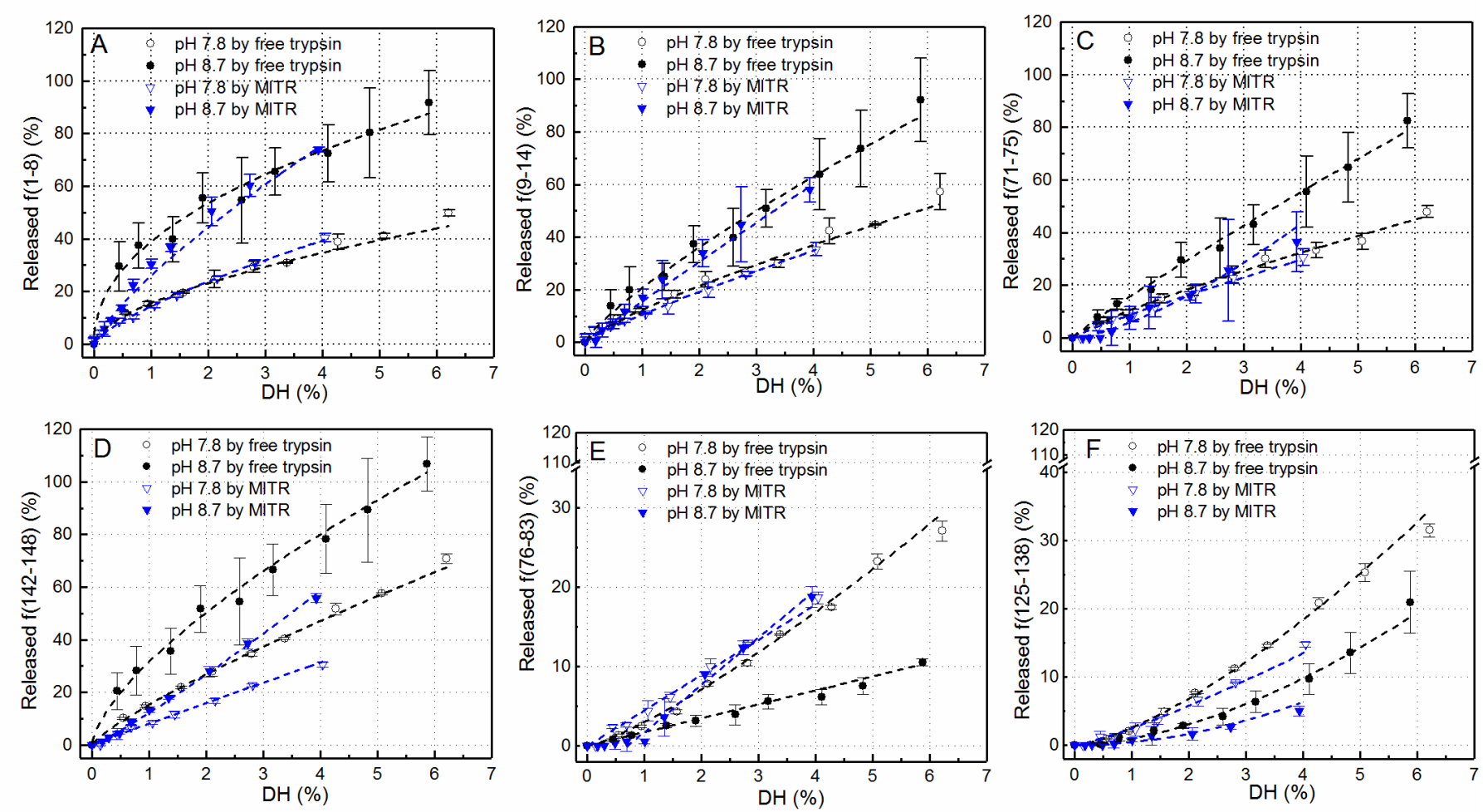

Figure 3.2-5 Formation of six select peptides (%) as a function of the degree of hydrolysis (DH). A, B, C, D, E, and F present data for peptides f(1–8), f(9–14), f(71–75), f(142–148), f(76–83), and f(125–138), respectively.

3.2.4 Conclusion

The hydrolysis conditions, e.g., pH, ionic strength, temperature, influence the hydrolysis rate and lead to different product profiles. No prior study discusses in sufficient detail whether these influences will differ once the enzyme is immobilized. In this study, the hydrolysis of β-Lg by free and immobilized trypsin was compared in detail with a focus on the influence of pH. In addition, the performance of the applied MITR, e.g., activity, permeability, remained nearly constant throughout all conducted experiments.

Although no significant difference in the evolution of DH at pH 7.8 and 8.7 was observed, both free and immobilized trypsin exhibited greater accessibility to intact native β-Lg at increasing pH values. The increase of pH from 7.8 to 8.7 even shifted the model of the depletion of native protein by free trypsin from “one-by-one” to “zipper,” whereas this influence on the hydrolysis by immobilized trypsin was limited. Regarding the two genetic variants, β-Lg A was more accessible than variant B under all experimental conditions, and free trypsin exhibited greater differences in this preference than the immobilized one.

The comparison of peptide profiles in the Venn diagrams clearly illustrated the different influences of pH over the range of 7.2–8.7 on the hydrolysis of β-Lg by free and immobilized trypsin. Generally, the immobilization of trypsin led to more focused cleavage sites within its specificity at the initial stage of hydrolysis compared with the findings for free trypsin. The quantification of the selected peptides during the hydrolysis process showed that free trypsin preferentially attacked the cleavage sites located at the C-terminus at pH 7.8, whereas an opposite preference was observed at pH 8.7. However, for the immobilized trypsin, no significant preference regarding the C- or N-terminus was noted, only a slight increase in preference for Lys_8 was identified at pH 8.7.

Based on the findings of this study, obviously, immobilization does lead to the changes of selectivity, which is also affected by pH. However, the influence of pH is hard to predict; thus, particular attention should be paid to hydrolysates compositions when studying the optimal pH of the hydrolysis to obtain the desired products.

Financial support

This research did not receive any specific grant from funding agencies in the public, commercial, or not-for-profit sectors.

Acknowledgements

The first author thanks China Scholarship Council (CSC) for the support of her personal cost. The authors would like to thank Urh Černigoj from BIA Separations (Ajdovščina, Slovenia) for his technical help in developing the MITR.

3.2.5 Supporting Information

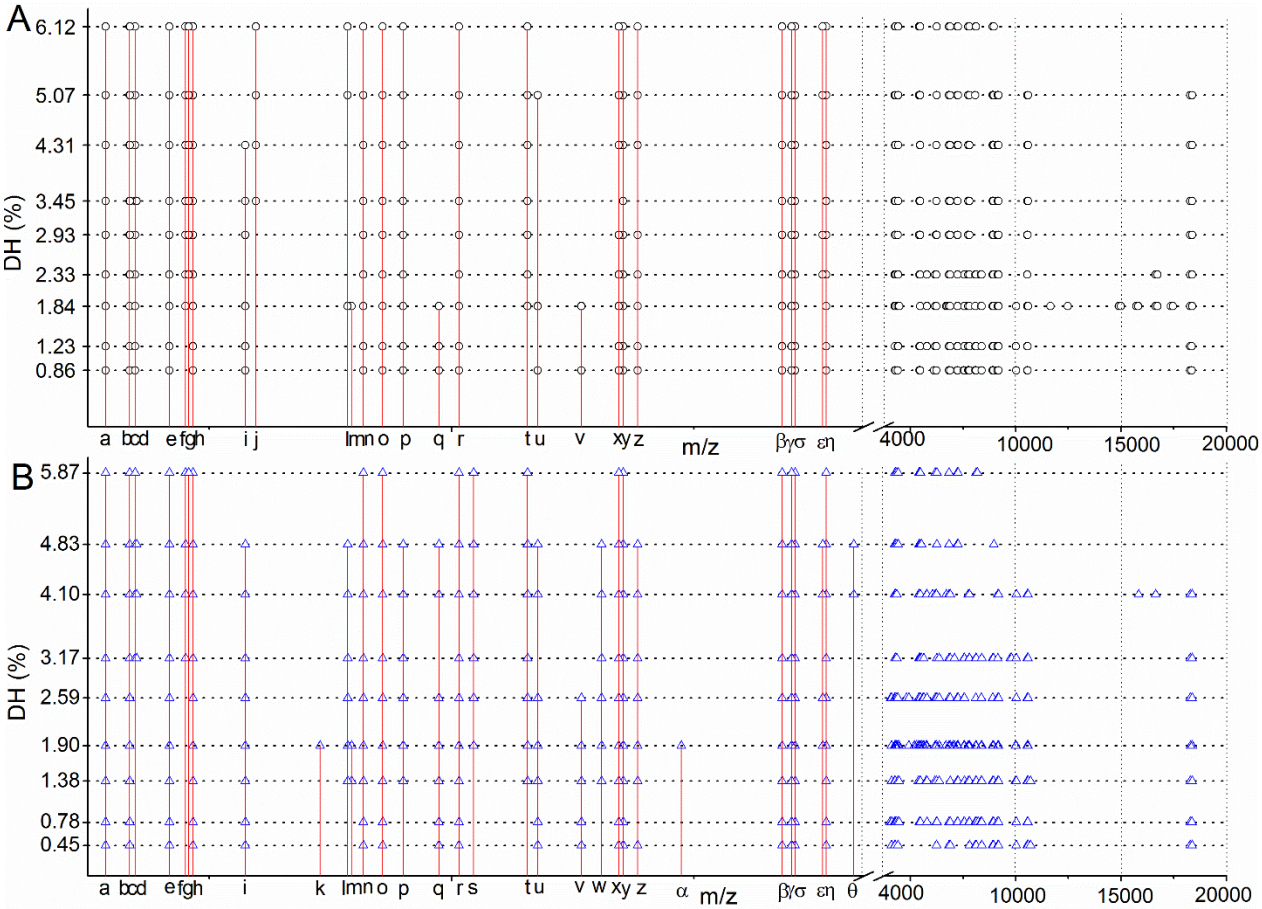

a=f(71-75); b=f(9-14); c=f(15-20); d=f(70-75); e=f(142-148); f=f(76-83); g=f(84-91); h=f(1-8); i=f(139-148); j=f(92-101); k=f(71-83); l=f(78-91); m=f(1-14)
n=f(125-138); o=f(149-162); p=f(76-91); q=f(125-141); r=f(21-40); s=f(84-101); t=f(41-60); u=f(71-91); v=f(142-162); w=f(78-100); x=f(61-83); y=f(15-40)
z=f(125-148); α=f(101-124); β=f(9-40); γ=f(71-100); δ=f(41-69); ε=f(70-100) / f(71-101); η=f(41-70); θ=f(70-101)

Figure 3.2-S1 Peptides profiles (below 4 000 Da) and mass distribution (above 4 000)

resulting from the hydrolysis by free trypsin as a function of DH, A is at pH 7.8 and B is at pH 8.7.

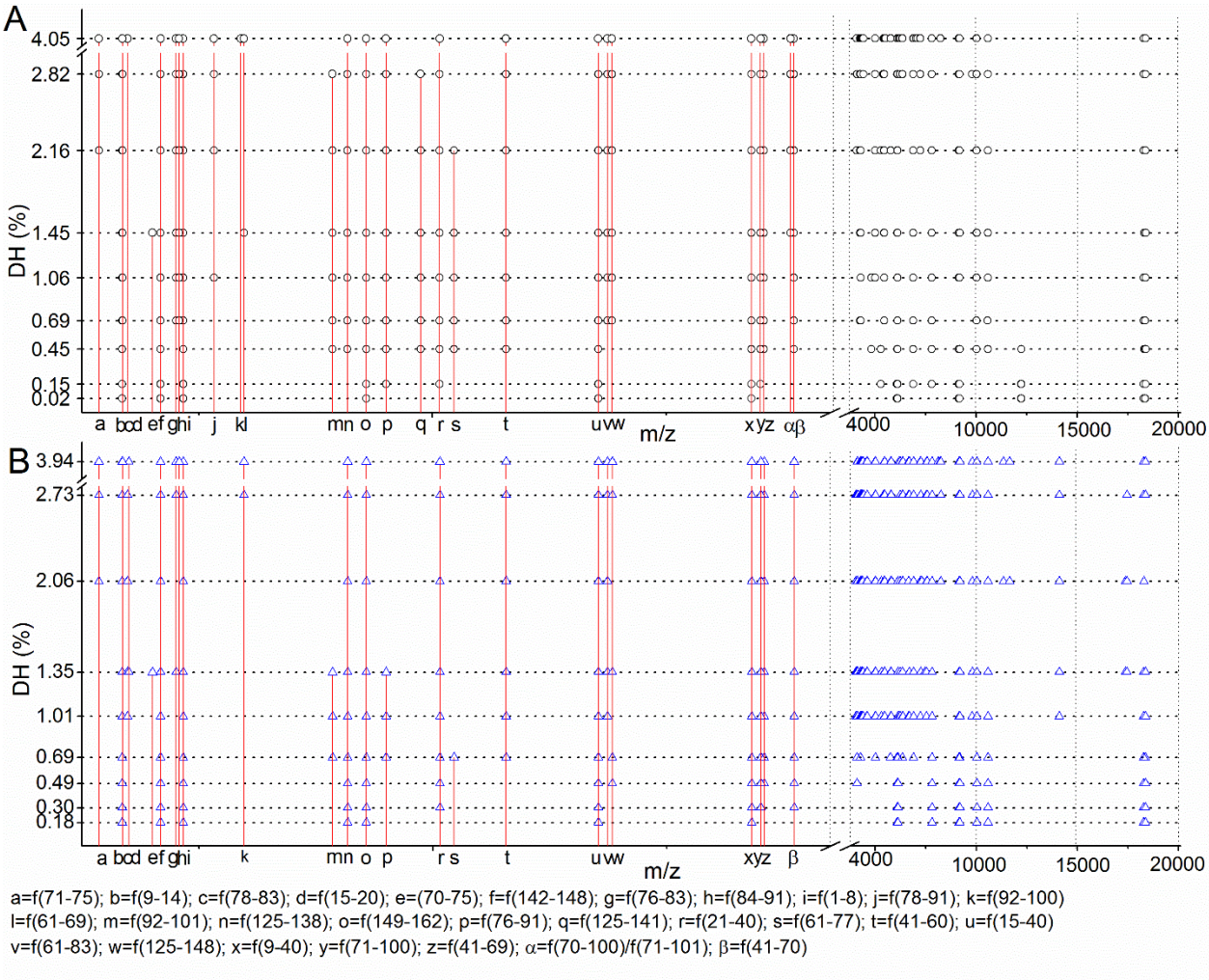

Figure 3.2-S2 Peptides profiles (below 4 000 Da) and mass distribution (above 4 000) resulting from the hydrolysis by MITR as a function of DH, A is at pH 7.8 and B is at pH 8.7.

3.3 Influence of salts on hydrolysis of β-lactoglobulin by free and immobilised trypsin

Summary and contribution of the doctoral candidate

Salt-effect studies have proven useful for regulating enzymatic hydrolysis to influence the efficiency and hydrolysate profiles. This study compares the influence of Tris and NaCl on the hydrolysis of β-lactoglobulin (β-Lg) by free and immobilized trypsin. For both forms of trypsin, 0.1 M Tris accelerated the release of most final peptides except peptide f(71–75) and showed no significant effect on the depletion of intact β-Lg. Regarding NaCl, increasing its concentrations retarded the release of peptides associated with the breakdown of intact protein, corresponding to a decreasing depletion of intact β-Lg, which was more pronounced for immobilized trypsin. Besides, both free and immobilized trypsin preferentially hydrolyzed certain intermediate peptides upon the addition of NaCl, with an increase in the degree of hydrolysis by 22.37% (0.02 M) for free trypsin and 62.09% (0.02 M) & 44.27% (0.1 M) for immobilized trypsin over those without NaCl. Potential mechanisms underlying the observed salt effects are discussed in detail.

Generally, the hydrolysis efficiency and hydrolysates profiles can be regulated by adding different salts at varied concentrations. This effect results from the varied interactions between different salts and proteins. As some desired results are obtained by adding salts into the hydrolysis medium, this study may provide some hints on the choices of buffers or other salts to regulate the hydrolysis process, improving the hydrolysis efficiency or obtaining the desired product profiles.

Most significant contribution to this manuscript was made by the doctoral candidate. This comprised (i) the conception and design of experiments based on preceded critical literature review; (ii) experimental conduction on protein hydrolysis and hydrolysates analysis; (iii) data analysis and data interpretation. In addition, writing and revising of the manuscript was done by the doctoral candidate.

Adapted original manuscript[3]

Influence of salts on hydrolysis of b-lactoglobulin by free and immobilised trypsin

Yuhong Mao[a*], Maria Krischke[a], Claudia Hengst[a], Ulrich Kulozik[a,b]
Technical University of Munich, aChair of Food and Bioprocess Engineering, bInstitute of Food and Health (ZIEL)–Technology Unit,
Weihenstephaner Berg 1, D-85354, Freising-Weihenstephan, Germany

Abstract: Immobilized trypsin is an alternative to free trypsin for producing protein hydrolysates with increased functionalities. However, the influence of hydrolytic conditions on this process remains unclear. This study compares the influence of salts on β-lactoglobulin (β-Lg) hydrolysis by free and immobilized trypsin. For both forms of trypsin, 0.1 M Tris accelerated the release of most final peptides except f(71–75), and had no significant effects on the hydrolysis of intact β-Lg. Increasing NaCl concentrations from 0 to 0.02 M increased the degree of hydrolysis (DH) by 22.37% for free trypsin and by 62.09% for immobilized trypsin. The presence of 0.1 or 0.5 M NaCl hindered the release of peptides associated with the breakdown of intact protein. This led to 2–4 fold decreases in depleting intact β-Lg and DH, except immobilized trypsin at 0.1 M NaCl (DH increased by 44.27% compared without NaCl). Potential mechanisms underlying the effects of salts are discussed.

[3] Adaptions refer to formatting issues: e.g., numbering of sections, figures, tables and equations, abbreviations, manufacturer specifications, axis labeling, figure captions and style of citation.

[3] Originally published in: *International Dairy Journal* (2019), Vol. 93, pp. 106-115. Permission for reuse of this article was granted by Elsevier.

3.3.1 Introduction

In past decades, bovine β-lactoglobulin (β-Lg), a major allergen absent from human milk, has been subject to extensive investigations regarding enzymatic processing via various enzymes (Hernández-Ledesma, Recio & Amigo, 2008). Trypsin (EC 3.4.21.4), a serine protease, is found in the digestive system of humans and many other vertebrates. Tryptic hydrolysis of β-Lg results in reduced allergenicity (Selo et al., 1999) and enhanced nutritional values (Hernández-Ledesma et al., 2008; Leeb, Gotz, Letzel, Cheison & Kulozik, 2015). However, the costly production and purification of trypsin seriously limits its implementation in the food industry (Yu & Ahmedna, 2012). As an alternative approach, immobilization of trypsin has attracted more and more attention due to the possibility of reusing the enzyme and producing enzyme-free hydrolysates.

In our previous work (Mao, Černigoj, Zalokar, Štrancar & Kulozik, 2017), a monolithic column-based immobilized trypsin reactor (MITR) showed significant activity toward β-Lg. The immobilization of an enzyme can alter its intrinsic properties (V_{max}, k_{cat} or K_m) (Duggal & Bucholz, 1982), leading to changes in enzyme selectivity, i.e., the rate at which individual cleavage sites in a protein substrate are hydrolyzed relative to other cleavage sites (Butré, Sforza, Gruppen & Wierenga, 2014). Consistent with these observations, we compared the selectivity of free and immobilized trypsin for β-Lg hydrolysis focusing on the impact of hydrolytic pH, and found that pH had a greater effect on the selectivity of free trypsin compared with immobilized trypsin (Mao, Krischke, Hengst & Kulozik, 2018). Except for pH, the influence of salts on hydrolysis process is also important, because the production of food protein hydrolysates is never conducted in a pure aqueous media, but rather in a complex system with various ions.

Salt-effect studies have proven useful for determining the intrinsic properties of enzymes (Endo, Kurinomaru & Shiraki, 2016, 2018; Garajova et al., 2017; Quan et al., 2008; Salis, Bilanicova, Ninham & Monduzzi, 2007). Most of these studies interpret the salt-effect data based on ionic properties and ion specificity. Ionic properties refer to the effects of any salt ion, including charge shielding/electrical double layer effects and stoichiometric ion binding to a charged protein (Tsumoto, Ejima, Senczuk, Kita & Arakawa, 2007). These effects are always independent on the salt type but dependent on the salt concentration (ionic strength). Ionic properties are important in regulating enzyme–substrate interactions, thereby affecting enzyme activity and selectivity. This factor is particularly important in hydrolysis reactions that depend on the movement of charged molecules relative to each other. In tryptic hydrolysis. Asp_{189}, located in the catalytic pocket of trypsin, attracts and stabilizes positively charged Lys and Arg residues on substrates (Evnin, Vásquez & Craik, 1990). Thus, both the binding of charged substrates to the enzyme and then the movement of charged groups within the catalytic active site will be influenced by the ionic composition of medium (Chaplin & Bucke, 1990).

The ion-specific effect of medium on proteins was first reported in a systematic way by Franz Hofmeister (1888), who ranked the ability of ions at a fixed ionic strength to affect the properties of proteins in aqueous solutions. Hofmeister differentiated between

chaotropes and kosmotropes, salts that induced either disorder or more order in protein conformation. Hofmeister ions are reported to influence the properties of numerous enzymes (Endo et al., 2016; Garajova et al., 2017; Tougu et al., 1994). Mostly, the ion-specific influence on enzyme activity follows the Hofmeister series, with kosmotropes activating enzymes and chaotropes inhibiting enzyme activity (Garajova et al., 2017). Enzyme activation by kosmotropes occurs because these salts increase both the structural stability of the enzyme and the hydrophobic interactions between the enzyme and its substrate (Endo et al., 2016). A bell-shaped dependence of enzyme activity on ions in the Hofmeister series has been observed, indicating that both chaotropic and kosmotropic ions can inactivate enzymes (Žoldák, Sprinzl & Sedlák, 2004). Chymotrypsin exhibits increased activity with the addition of 3 M NaCl, but no significant increase in the presence of 3 M LiCl or KCl (Wesolowska, Krokoszynska, Krowarsch & Otlewski, 2001). Another study observed that with the addition of 0.5 M NaCl, the K_m of chymotrypsin decreased and its K_{cat} increased, while trypsin showed the opposite results (Endo et al., 2018). In addition, weak electrolytes are widely applied as buffers in enzyme technology. Tris (hydroxymethyl) aminomethane (Tris) solution is one such buffer, which is reported to stabilize BSA molecules (Taha & Lee, 2010) and interact with lysozyme molecules through hydrogen-bonding (Quan et al., 2008).

Previous studies regarding salt effects on enzymes have used primarily low–molecular-mass substrates (Endo et al., 2016, 2018; Tougu et al., 1994). These results may not apply to enzymatic reactions involving proteins as substrates, e.g., β-Lg in this study, as salts may influence β-Lg structure, thus, affecting the enzymatic process. For instance, Renard, Lefebvre, Griffin and Griffin (1998) found that β-Lg favored dimerization in the presence of NaCl. Furthermore, ions also affect the tertiary structure of β-Lg, e.g., Trp exposure increases in the presence of NaCl (> 0.1 M), indicating that more hydrophobic groups are exposed (Zhao, Li & Li, 2017). Therefore, the influence of salts on the enzymatic hydrolysis of a specific substrate should be investigated systematically on a case-by-case basis.

It is not able to find studies dealing with the influence of salts on the protein hydrolysis in a flow-through reactor using immobilized trypsin. In the present study, trypsin was covalently immobilized on an aldehyde-activated monolith through multiple attachment points. This covalent immobilization is the most common approach to stabilize the enzyme against different denaturing conditions (Mozhaev, Melik-nubarov, Sergeeva, Šikšnis & Martinek, 1990). Hence, compared with free trypsin, the ion-induced conformational effects on immobilized trypsin, in theory, should be significantly reduced. Additionally, substrates are convectively transported to immobilized trypsin in a flow-through MITR. This critical step is largely decided by the mass transfer properties in MITR. It is reasonable to assume that the mass transfer properties in MITR might change with the addition of salts, due to their effects at least on charge-based attraction or repulsion between substrate molecules and the monolith surface.

Therefore, the aim of this study was to determine the influence of salts on immobilized trypsin for the β-Lg hydrolysis, and simultaneously to compare with free trypsin. Specifically, the following parameters were investigated: (i) ion-specific effects, i.e., buffer salt (weak organic electrolyte, Tris) versus neutral salt (strong inorganic electrolyte, NaCl); and (ii) ionic strength effects (ionic properties) using different salt concentrations. The influence of these factors was evaluated by measuring the hydrolysis efficiency and analyzing the hydrolysates profiles.

3.3.2 Materials and methods

3.3.2.1 Materials

Bovine β-Lg was fractionated from whey protein isolate (WPI), a product developed by Fonterra Co-operative Group Ltd (Auckland, New Zealand), as described by Toro-Sierra, Tolkach and Kulozik (2011). The obtained β-Lg powder had a protein content of 98.6% relative to the dry matter. β-Lg powder was dissolved in deionized water at 4°C overnight. After the removal of denatured β-Lg by adjusting the pH to 4.6 and centrifugation (6000 × g for 10 min), the supernatant was filtered through a cellulose membrane with a cut-off of 0.45 µm (Macherey-Nagel, Düren, Germany). After the pH adjustment to 8.7, β-Lg solution was mixed with pre-dissolved NaCl or Tris buffer solution to reach a final concentration of 10 mg mL^{-1} native protein, and the final pH of the mixed solutions was adjusted to 8.7.

Trypsin from bovine pancreas (Type I, approximately 10 000 Nα-benzoyl-L-arginine ethyl ester [BAEE] units mg^{-1} protein), BAEE (B4500), Tris (hydroxymethyl)-aminomethane (Tris), NaCl, and NaOH were purchased from Sigma Aldrich (St Louis, MO, USA). Deionized water was acquired using the Milli-Q System (Millipore Corporation, Bedford, MA, USA).

An aldehyde (ALD) activated CIMmultus™ column (1 mL-bed volume, BIA Separations, Ajdovščina, Slovenia)-based MITR with 2.15 ± 0.1 µm pore size was developed in our earlier work (Mao et al., 2017). The amount of immobilized trypsin was 5.0 ± 0.2 mg per MITR, and the MITR permeability was approximately 2.45×10^{-12} m^2 using deionized water.

3.3.2.2 Trypsin activity toward BAEE substrate

The enzymatic activity of trypsin was measured at pH 8.7 using the model substrate BAEE in three buffers, 0.1 M Tris buffer, 0.1 M Tris + 0.1 M NaCl, 0.5 M Tris buffer. The measurement was a spectrophotometric determination as described previously (Mao et al., 2017). The activity of free trypsin is expressed as BAEE units mg^{-1}. One BAEE unit produces a ΔA_{253} of 0.001 per minute in a reaction volume of 3.20 mL. The activity of MITR was calculated as the unit U* (µmol min^{-1}), which is the amount of BAEE converted to BA by the MITR in 1 min. U* can be easily converted to BAEE units, using the conversion factor 270, as determined by Bergmeyer (1974).

3.3.2.3 Hydrolysis of β-Lg

To A previous study (Cheison, Leeb, Toro-Sierra & Kulozik, 2011) indicated that at the optimal temperature of free trypsin, i.e., 37°C, the enzyme selectivity was little controlled by other environmental conditions, as temperature was the dominating influence. It is expected to regulate the trypsin selectivity with the addition of salts. On the other hand, both free trypsin and MITR already showed significant activity toward β-Lg at ambient temperature (Mao et al., 2017). Hence, all hydrolysis experiments were conducted at 25 ± 1°C.

To assess the effects of salts, 25 mL β-Lg solution (native protein, 10 mg mL^{-1}) in Tris buffer (0.1 or 0.5 M) or Tris-NaCl buffer (0.1 M Tris + 0.1 M NaCl) was hydrolyzed by free trypsin or immobilized trypsin for 1 h. The hydrolysis of β-Lg by free trypsin was conducted at an enzyme/substrate ratio of 0.1% (w/w). Thus, the hydrolysis reaction was ensured to be performed at similar ratios of activity units (BAEE units) to per gram β-Lg for both free trypsin and MITR.

To further explore the effects of salts, 100-mL β-Lg solution (10 mg mL^{-1}) in 0.1 M Tris, or in 0, 0.02, 0.1, or 0.5 M NaCl was hydrolyzed by free trypsin or immobilized trypsin for 3 h. During hydrolysis 1-mL samples were taken out at intervals (0, 5, 10, 20, 30, 45, 60, 90, 120, and 180 min). A TitroLine alpha plus auto-titrator (Schott AG, Mainz, Germany) was used to maintain a constant pH of 8.7 throughout the course of the reaction. The degree of hydrolysis (DH) was calculated according the amount of NaOH consumed, as described previously (Mao et al. 2017). In addition, because 18 of the 161 peptide bonds of β-Lg are potential cleavage sites for trypsin, a theoretical DH_{max} of 11.18% can be achieved during trypsinolysis. The practical DH_{max} values were reached and discussed in our previous work (Mao et al., 2017). In this study, all hydrolysis processes were stopped at intermediate stages to save time. Also, it makes more sense to focus on the release of peptides at the early stage of hydrolysis to explore the enzymatic selectivity.

For the hydrolysis by free trypsin, a constant enzyme–substrate (E/S) ratio of 0.1% (w/w) was applied, and the hydrolysis of 1-mL aliquots was stopped by the addition of 0.5 mL trypsin inhibitor solution (10 mg mL^{-1}, from chicken egg white, Sigma Aldrich). Hydrolysis by MITR was realized in a flow-through system (Äkta explorer, GE Healthcare Europe GmbH, Freiburg, Germany) controlled by Unicorn Software 5.31.

3.3.2.4 Analysis of hydrolysates

Hydrolysates profiles were quantitatively analyzed for residual native protein content and peptide composition.

Quantification of residual native β-Lg

The native β-Lg content of samples was determined via reversed-phase high-performance liquid chromatography (RP-HPLC) using an Agilent 1100 series HPLC system (Agilent Technologies, California, USA) and a PLRP-S-300Å-8µm column (150 × 4.6 mm, Latek, Eppelheim, Germany). Each sample was diluted with deionized water

to ≈ 4 mg mL^{-1}. After adjusting the pH to 4.6, the sample was filtered through a cellulose membrane with a cut-off of 0.45 µm and a volume of 20 µL was injected. Detailed gradient information was previously described by Leeb et al. (2015). The protein concentration was calculated from the detected peak area and a calibration curve using standards β-Lg A (99% purity, Sigma Aldrich) and β-Lg B (99% purity, Sigma Aldrich).

Chromatographic separation and quantification of peptides

All samples were diluted to approximately 4 mg mL^{-1}, and 1-mL aliquots of the diluted solution were firstly incubated with 150 µL 80 mM dithiothreitol (DTT) at pH 8 and 37°C for 45 min, and then mixed with 200 µL 400 mM chloroacetamide (CAA) and stored in the dark for 30 min. The pre-treated samples were analyzed on the Agilent 1100 series HPLC system coupled with a Kinetex_XB-C18-100Å column (100 x 4.6 mm, Phenomenx, California, USA). The mobile phase of solvent A containing 0.1% (v/v) trifluoroacetic acid (TFA) dissolved in Milli-Q water and solvent B consisting of 0.0555% (v/v) TFA dissolved in 80% (v/v) acetonitrile (diluted in Milli-Q water) was applied. The entire analysis was conducted at 60°C and 1.5 mL min^{-1}. The gradient was increased multi-linearly from 1 to 45% of solvent B in 60 min. The sample injection volume was 60 µL, and the elution was monitored at 214 nm. The samples with the highest DH at each condition were further fractionated. Peaks eluted before 45 min were automatically collected separately based on the slope, and peaks after 45 min were collected based on time with a unit of 1 min. The collected fractions were analyzed by matrix-assisted laser desorption/ionization time-of-flight mass spectrometry (MALDI-TOF-MS) to determine the peptide composition.

The molar concentration of each specific peptide was calculated from the peak area according to Eq. (3.3-1) (Fernández & Riera, 2013) as follows:

$$X_i = 1 \times 10^6 \left(\frac{A_i}{\varepsilon_i \times l \times v}\right) \times f \times D \quad (3.3\text{-}1)$$

where x_i (µM) is the concentration of peptide i, Ai (AU min) is the peak area, l (0.6 cm) is the path length of the UV cell, v is the injection volume (60 µL), f is the flow rate (1.5 mL/min), D is the dilution factor of the sample before injection, and ε_i (AU M^{-1} cm^{-1}) is the molar extinction coefficient of peptide i at 214 nm, as calculated according to Kuipers and Gruppen (2007). To quantitatively compare the released peptides, the following indexes were calculated:

$$R_1(\%) = \frac{The\ amount\ of\ released\ peptide\ (\mu M)}{The\ \ amount\ of\ hydrolyzed\ protein\ (\mu M)} \quad (3.3\text{-}2)$$

$$R_2(\%) = \frac{The\ relative\ amount\ of\ released\ peptide\ (\%)}{The\ relative\ DH\ (\%)} = \frac{\frac{The\ amount\ of\ the\ released\ peptide\ (\mu M)}{The\ theoretical\ maximun\ amount\ of\ each\ peptide\ (\mu M)}}{\frac{The\ reached\ DH\ Value\ (\%)}{The\ theoretical\ maximum\ DH\ value\ (\%)}} \quad (3.3\text{-}3)$$

MALDI-TOF-MS

The obtained fractions were analyzed for mass composition using a MALDI-TOF-MS system (ultrafleXtreme MALDI-TOF-TOF, Bruker Daltonics GmbH, Bremen, Germany). Matrix α-cyano-4-hydroxycinnamic acid (HCCA) and 2,5-dihydroxyacetophenone (DHAP) were used separately. HCCA is sufficient to measure peptides and proteins in the low mass range from 500 to 4000 Da, and DHAP is commonly used for the high mass range up to 20 000 Da. 1-µl samples (including blank sample) or standards (PAS with HCCA and Protein Calibration Standard I with DHAP, Bruker Daltonics GmbH) were mixed with 1-µl matrices directly on the anchor target (stainless steel MTP 384, Bruker Daltonics GmbH). Each sample was spotted at least three times. The MALDI-TOF-MS was run in a positive reflection mode for mass ranges of 400–4000 Da (sample with HCCA) and 3000–10000 Da (sample with DHAP), or in a positive linear model for the mass range of 4000–20000 Da (sample with DHAP). The process was managed using flexControl™ 3.0 Software (Bruker Daltonics GmbH). Peptides were identified by comparing the detected mass/charge (m/z) with the theoretical m/z as described previously (Mao et al., 2017).

Statistical analysis

All experiments were performed in triplicate and in a staggered manner (for MITR) to reduce bias. Mean values ± standard deviation are reported. Analysis of variance was performed to estimate differences between mean values where the significance level was established as $P < 0.05$. The Tukey-test was used to evaluate the significance of differences. Data were plotted using Origin Pro 9.0 or R 3.3.3 (open-source software).

3.3.3 Results and discussion

3.3.3.1 General comparison of salt effects on free and immobilized trypsin

The conductivities of the applied buffers were 3.82 mS cm-1 (0.1 M Tris), 10.85 mS cm-1 (0.1 M Tris + 0.1 M NaCl), and 9.61 mS cm-1 (0.5 M Tris), respectively. The enzymatic activity toward BAEE (342.82 Da) and the depletion of intact β-Lg in these buffers were investigated. In all reactions, applied buffers kept pH in 8.6–8.7.

As shown in Fig. 3.3-1, either the addition of 0.1 M NaCl or increasing Tris concentration from 0.1 to 0.5 M did not significantly affect the enzymatic activity of free and immobilized trypsin, although the conductivity of the reaction medium increased greatly. Wesolowska et al. (2001) found that the activity of free trypsin toward BAEE was nearly unaffected by the presence of NaCl up to 3 M. Contrastively, the amount of hydrolyzed intact β-Lg decreased significantly for both forms of trypsin due to the addition of salts, as shown in Fig. 3.3-2. For free trypsin, around 63% of intact protein was hydrolyzed in 0.1 M Tris, which decreased by 40% with the addition of 0.1 M NaCl. For immobilized trypsin, the hydrolyzed amount of intact β-Lg decreased by 18% with the presence of 0.1 M NaCl or 0.5 M Tris.

The surface charge of β-Lg is much more complex than BAEE. Thus, the influence of salts on electrostatic interactions between substrate and enzyme appears to be greatly strengthened, when β-Lg substituted the substrate BAEE. In addition, salts may

stabilize or destabilize β-Lg. For instance, Tris buffer is reported to stabilize macromolecules such as BSA (Taha & Lee, 2010). Increasing concentrations of NaCl (up to 2 M) are reported to increase the thermal stability of β-Lg (Vardhanabhuti & Foegeding, 2008). Stabilization of substrate molecules may prevent them from hydrolysis.

Although Tris and NaCl did not affect enzymatic activity significantly, they exerted considerable influences on the interactions between β-Lg and trypsin. To interpret the mechanism, Tris and NaCl were introduced to the reaction medium separately, and the hydrolysis without the addition of salts was conducted as well.

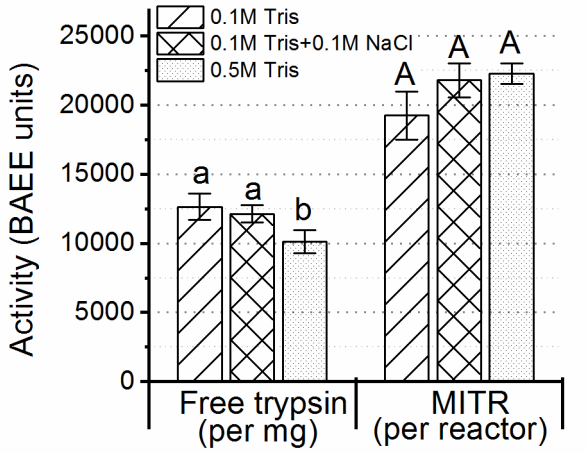

Figure 3.3-1. Effects of Tris buffer and NaCl on trypsin activity. Hollow bars, bars with crossed lines and dots represent the hydrolysis of β-Lg in 0.1 M Tris, 0.1 M Tris + 0.1 M NaCl, and 0.5 M Tris, respectively. Data values represent mean values of three replicates with a 95% confidence interval. Values with the same lowercase letter (for free trypsin) or with the same uppercase letter (for monolith-based immobilized trypsin reactor) are not statistically different ($P \geq 0.05$).

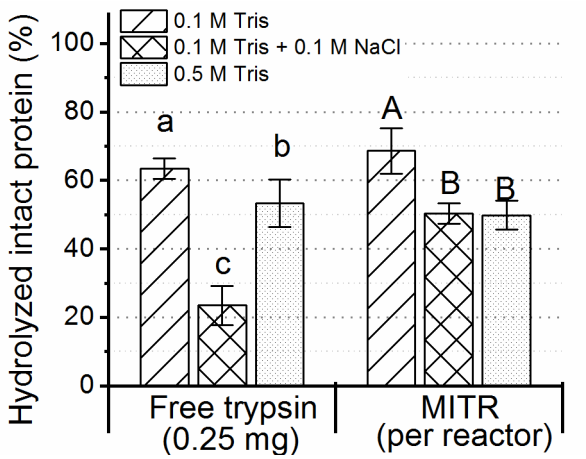

Figure 3.3-2. Effects of Tris buffer and NaCl on the hydrolysis of intact β-lactoglobulin. Hollow bars, bars with crossed lines and dots represent the hydrolysis of β-Lg in 0.1 M Tris, 0.1 M Tris + 0.1 M NaCl, and 0.5 M Tris, respectively. Data values represent mean values of three replicates with a 95% confidence interval. Values with the same

lowercase letter (for free trypsin) or with the same uppercase letter (for monolith-based immobilized trypsin reactor) are not statistically different ($P \geq 0.05$).

3.3.3.2 The influence of Tris buffer

Both 10 mg mL^{-1} β-Lg in 0 (1.05 mS cm^{-1}) and 0.1 M (3.82 mS cm^{-1}) Tris buffers were hydrolyzed by free trypsin or MITR for 3 h. Because of the buffering capacity of Tris, the DH measured by a pH drop does not represent the actual extent of the reaction. Thus, the amount of intact protein hydrolyzed was used to follow the reaction progress. For free trypsin, 65.67% (without Tris) and 63.46% (with Tris) of the β-Lg were hydrolyzed after 1 h, while MITR required 3 hours to hydrolyze similar amounts of β-Lg (64.42% without Tris; 66.63% with Tris). The peptide profiles of these four samples were analyzed by HPLC and MALDI-TOF-MS.

The effects of Tris on peptide profiles

As shown in Fig. 3.3-3, peaks which eluted before 45 min contained peptides with a molecular weight below 3000 Da. Most of these peaks were assigned to final peptides based on trypsin specificity (as shown in Table 3.3-1), except the cleavage at Tyr_{20}–Ser_{21}, which is a nonspecific (chymotrypsin-like) cleavage by trypsin, as reported in other studies (Butré, Sforza, Wierenga & Gruppen, 2015; Cheison et al., 2011). Although the HPLC profiles of these four samples before 45 min were quite similar, the amounts of individual peptides (mainly the final peptides) differed significantly. As illustrated in Fig. 3.3-4, the relative amount of each peptide based on the hydrolyzed protein content (value R_1) is compared, and the theoretically maximum R_1 value should be 100%. The effects of Tris on the release of peptides, as indicated by R_1 values, are summarized in Table 3.3-2. Compared with hydrolysis in water, the presence of 0.1 M Tris contributed to the release of most final peptides for both forms of trypsin, except f(71–75). This peptide is typically released quickly during tryptic hydrolysis because of its external position in the three-dimensional structure of β-Lg (Fernández, Suárez, Zhu, FitzGerald & Riera, 2013). However, its precursor peptide f(70–75) accumulated significantly in Tris buffer, indicating that its further hydrolysis was prevented. Other intermediate peptides f(41–60), f(92–101) and f(76–91) also accumulated more in 0.1 M Tris than in water for both forms of trypsin, e.g., 6-fold (for free trypsin) and 7-fold (for MITR) increases in f(41–60) were observed. f(41–60) possesses one missed cleavage site Lys_{47}, which links to a proline residue and is resistant to trypsinolysis, as observed by Olsen et al. (2004). Particularly for MITR, the amount of f(125–138) increased greatly. Regarding peptides eluted after 45 min, peaks representing f(102–138)b and f(15–141)a showed increasing area in the presence of Tris for both forms of trypsin.

Table 3.3-1 Identification of peptides generated from the hydrolysis of β-lactoglobulin by free and immobilized trypsin

Peaks	Calculated mass [a]	Observed mass [b]	Assigned Sequence [c]
	1180.2	1180.5	f(61–69)a
1	1122.2	1122.5	f(61–69)b
	1308.4	1307.4	f(61–70)a
	1250.4	1249.3	f(61–70)b
2	595.4 Na	595.4	f(71–75)
3	739.4 K	739.3	f(70–75)
4	938.5	938.5	f(84–91)
5	695.4 Na	695.4	f(9–14)
6	825.0 Na	825.0	f(71–77)
7	1245.6	1245.8	f(125–135)
8	696.8	696.9	f(15–20)
9	955.5 Na	955.5	f(1–8)
10	837.5	837.5	f(142–148)
11	1194.4	1193.5	f(92–101)
12	674.4	674.5	f(78–83)
13	904.1	904.1	f(76–83)
14	1658.7 Na	1659.0	f(125–138)
15	2092.4	2092.3	f(84–101)
16	1949.1	1949.3	f(125–141)
17	1802.1	1802.2	f(76–91)
18	1754.893 K	1753.6	f(149–162)
19	/	2189.1	/
20	/	1658.0 / 3315.1	/
21	2069.3 k	2069.2	f(21–40)
22	2313.3	2313.2	f(41– 60)
23	2820.2	2820.2	f(102–124)b
	2848.3	2848.2	f(102–124)a
	4075.6	4075.8	f(102–135)b
A	4203.7	4203.5	f(101–135)a
	4213.7 K	4215.2	f(101–135)b
B	4437.9	4437.0	f(102–138)b
	14480.5	7240.1 *	f(15–141)b
	3546.0	3544.4	f(41–70)b
C	7195.2	3597.8 *	f(78–138)a
	7167.1	7167.9	f(78–138)b
	3626.0 Na	3624.7	f(41–70)a
	4466.0	4466.5	f(102–138)a
D	5613.3	5614.1	f(92–138)b
	14480.5	7239.9 *	f(15–141)b

Table 3.3-1 con't

Peaks	Calculated mass [a]	Observed mass [b]	Assigned Sequence [c]
	6989.0	3494.0 *	f(41–100)a
	7034.0	3519.3 *	f(76–135)a
E	7006.0	3504.7 *	f(76–135)b
	7295.3	3649.4 *	f(102–162)a
	7267.3	3633.7 *	f(102–162)b
	5597.4	5598.1	f(102–148)a
F	5569.4	5569.9	f(102–148)b
	5641.4	5642.1	f(92–138)a
	5613.3	5614.6	f(92–138)b
G	/	/	/
H	11190.9	5595.5 *	f(1–100)b
	10808.4	5403.5 *	f(71–162)a
	5488.2	5487.5	f(21–69)a
I	5430.1	5430.9	f(21–69)b
	11249.0	5624.5 *	f(1–100)a

[a] Monoisotopic mass with single charge, calculated from amino acid sequence. Na and K represent sodium and potassium adduct, respectively.

[b] Observed mass with single charge except for those marked with *, * means double charged mass.

[c] a represents this sequence particularly from β-lactoglobulin A, and b is from β-lactoglobulin B.

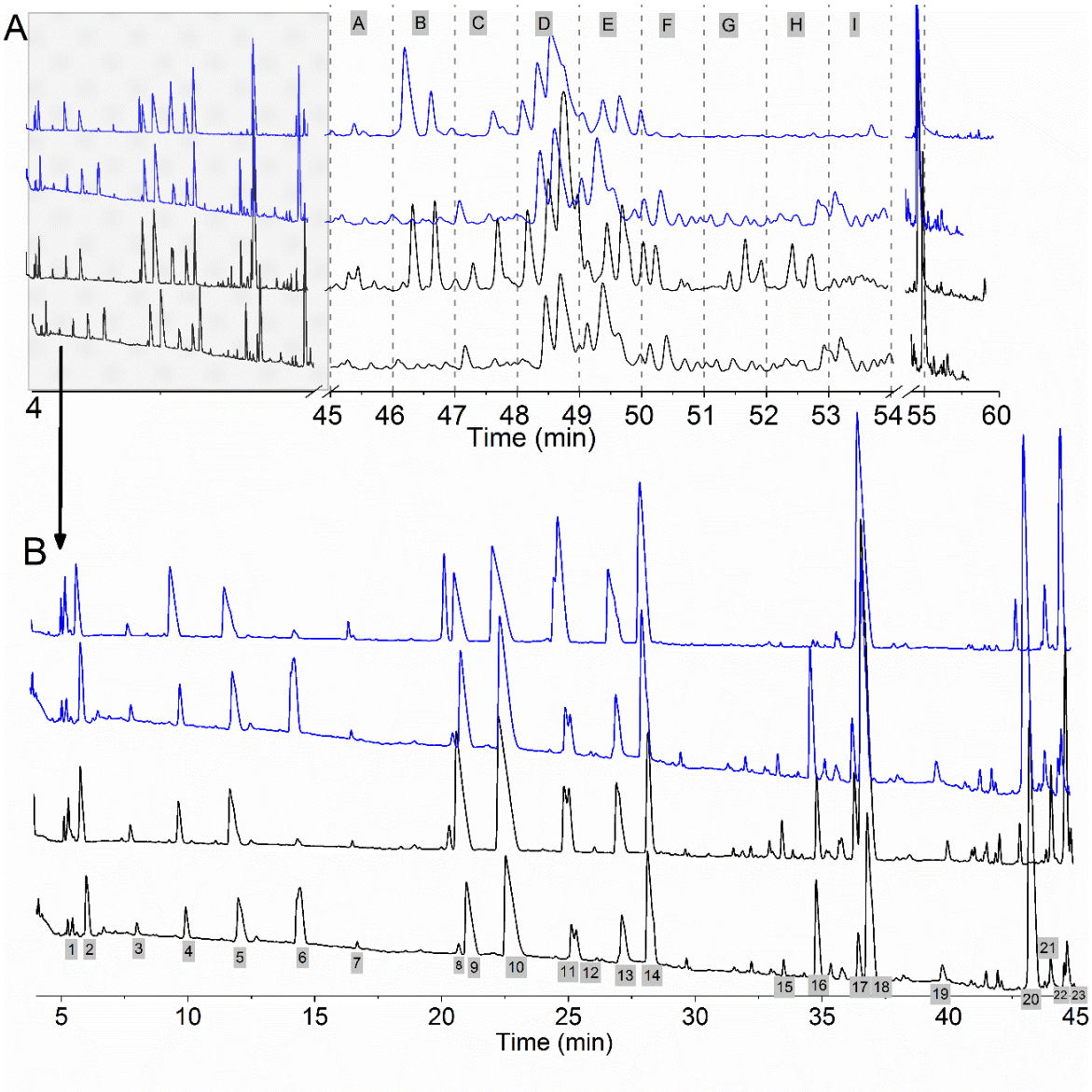

Figure 3.3-3. HPLC profiles of β-lactoglobulin hydrolysates generated from free or immobilized trypsin in the presence or absence of Tris buffer. The peaks eluted after 45 min are clearly illustrated in A, and the peaks eluted before 45 min are highlighted in B. Samples from top to bottom are hydrolysates produced in 0.1 M Tris by immobilized trypsin, in water by immobilized trypsin, in 0.1 M Tris by free trypsin and in water by free trypsin, respectively. Those peaks marked with number or letter are identified and reported in Table 3.3-1.

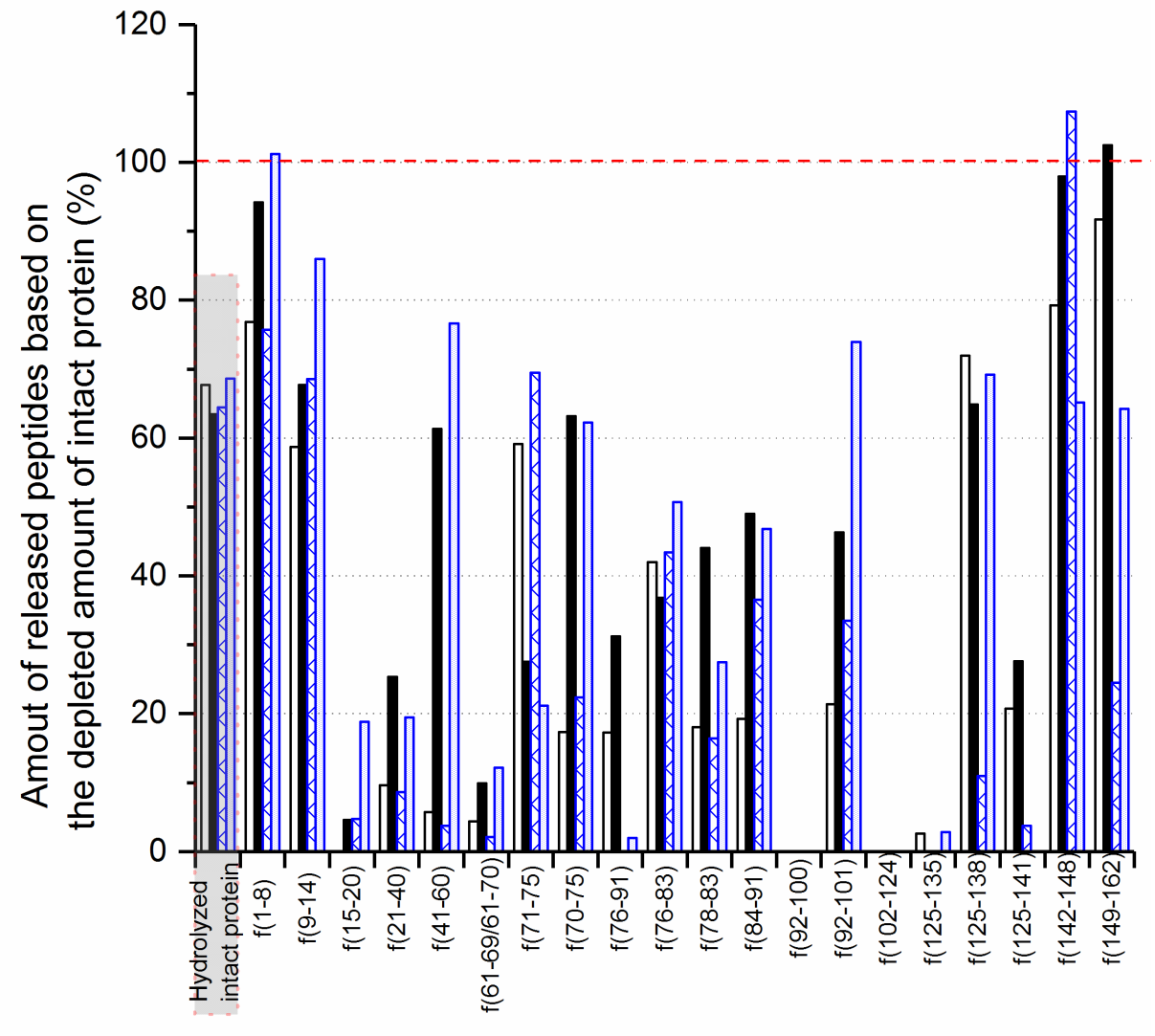

Figure 3.3-4. Effects of Tris buffer on the release of specific peptides. Hollow and black bars represent the cases hydrolysed by free trypsin with and without Tris buffer, respectively. Bars with crossed lines and dots represent the cases hydrolyzed by immobilized trypsin with and without Tris buffer, respectively.

The mechanism underlying the observed influence of Tris

Compared with the hydrolysis without Tris, the addition of 0.1 M Tris did not reduce the hydrolysis of intact β-Lg, while contributed to the release of most final peptides. Taha and Lee (2010) reported that Tris preferentially interacted with the peptide backbone by virtue of its –OH and amine groups through hydrogen bonding. Quan et al. (2008) found that Tris molecules formed hydrogen bonds with Asp_{52}, Glu_{35}, and Ala_{107} residues in lysozyme. Hence, it is speculated that Tris molecules mainly interact with certain intermediate peptides (the precursors of final peptides) and trypsin molecules through hydrogen bonds simultaneously, enhancing their interactions and then improving their hydrolysis. To determine whether Tris molecules preferentially interact with certain polypeptides, the characteristics of intermediate peptides are summarized in Table 3.3-S1 (Supplementary Material), including isoelectric point (PI), hydrophilicity, and the ratio of hydrophilic residues to total number of residues (%).

However, there is no clear correlation between the influence of Tris and the peptide characteristics.

3.3.3.3 Influence of NaCl

Samples with 10 mg mL-1 β-Lg in 0 (1.05 mS cm-1), 0.02 (3.25 mS cm-1), 0.1 (10.25 mS cm-1) and 0.5 M (46.55 mS cm-1) NaCl were hydrolyzed by free trypsin or MITR for 3 h.

The effects of NaCl on DH and amounts of residual intact β-Lg

The DH as a function of time is presented in Fig. 3.3-5A1 for free trypsin and in B1 for immobilized trypsin. The hydrolysis of β-Lg in water by free trypsin reached a DH of 5.87 ± 0.79% after 3 h, which was significantly higher than that by MITR (3.93 ± 0.74%). In both cases, the fastest increase in DH was observed with the addition of 0.02 M NaCl, where DH values reached 7.18 ± 0.76% (free trypsin) and 6.37 ± 0.95% (MITR), respectively. Interestingly, increasing NaCl concentration from 0 to 0.1 M significantly promoted the hydrolysis efficiency by MITR, reaching DH 5.67 ± 0.75%, but it decreased DH from 5.87 ± 0.79% to 5.14 ± 0.82% for free trypsin. The addition of 0.5 M NaCl seriously hindered the hydrolysis, irrespective free or immobilized trypsin applied, i.e., the DH values were only 3.83 ± 0.82% and 2.74 ± 0.81%, respectively.

Regarding the hydrolysis of intact protein, the Linderstrøm-Lang theory presents two models: “zipper” and “one-by-one” (Adler-Nissen, 1976). In a “one-by-one” model, intact protein will slowly break down and no appreciable amounts of intermediate peptides will be accumulated, while a much faster degradation of intact protein at the initial stage of hydrolysis will be observed in a “zipper” model. In fact, most proteins show an intermediate behavior between these two models, and their behaviors depend not only on the nature of substrate and enzyme, but also on hydrolytic conditions. For immobilized trypsin, although linear decreases in intact protein dependent on DH were observed at all explored concentrations of NaCl, close to the “one-by-one” model (Fig. 3.3-5 B2), increasing NaCl concentrations led to a clear decrease in the depletion of intact β-Lg. Specifically, around 18–26% intact protein was hydrolyzed in 0 or 0.02 M NaCl at DH ≈1%, while it was only 7–10% in 0.1 or 0.5 M NaCl. For free trypsin, a sharp increase in the depletion rate was noted at the initial stage of hydrolysis with 0 or 0.02 M NaCl, during which the increase in DH from 0 to 1% corresponded to a depletion of 30–40% of the intact protein content (Fig. 3.3-5 A2). This is more in agreement with the “zipper” model, while it seems to at the “one-by-one” model, when NaCl concentration increased from 0.02 to 0.1 or 0.5 M.

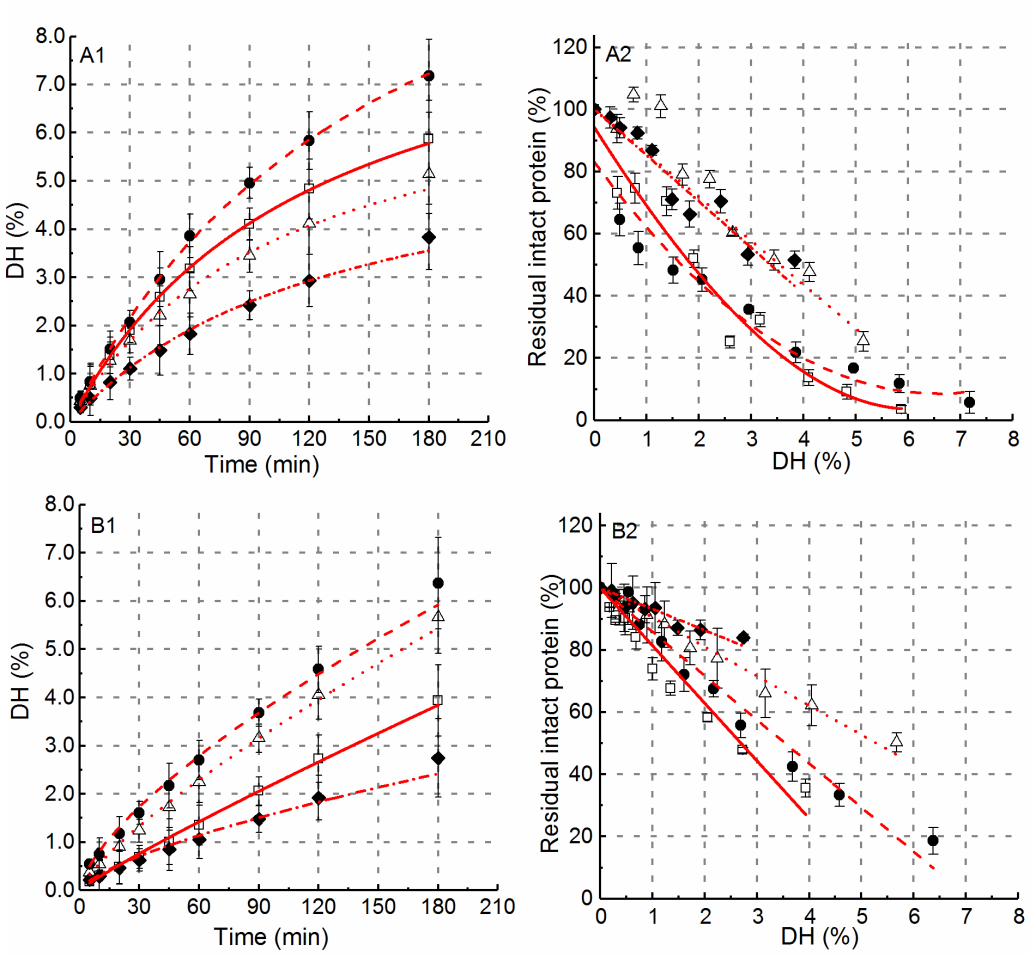

Figure 3.3-5. Effects of 0 M (□), 0.02 M (●), 0.1 M (Δ), and 0.5 M (♦) NaCl on DH (A1&B1) and the amount of residual native β-lactoglobulin (A2 and B2). A, hydrolysis by free trypsin; B, hydrolysis by MITR. Data values represent mean values of three replicates with a 95% confidence interval.

The effects of NaCl on peptide profiles

As illustrated in Fig. 3.3-6 and Table 3.3-1, peaks located in the range of 45–60 min correspond to intermediate peptides. The accumulation of these peptides was primarily due to the fast breakdown of intact β-Lg and secondarily due to the insufficient subsequent hydrolysis. For both forms of trypsin, 0.1 and 0.5 M NaCl significantly diminished the peaks of intermediate peptides, partly due to the slow hydrolysis of intact β-Lg (Fig. 3.3-5 A2 & B2). These results are in accordance with the findings of Butré, Wierenga and Gruppen (2012), who reported that in 0.5 M NaCl, the hydrolysate composition of 1%−5% WPI (w/w) showed increasing levels in hydrophilic peptides and decreasing amount of hydrophobic peptides, compared to the hydrolysis without NaCl.

Regarding peaks eluted before 45 min, most of them were assigned to the final peptides as previously discussed for Fig. 3.3-3, thus, these peaks in Fig. 3.3-6 are not repeatedly highlighted. The DH-dependent release of these identified peptides is illustrated in Fig. 3.3-S1 for free trypsin and in Fig. 3.3-S2 for MITR (Supplementary

Material). Furthermore, Fig. 3.3-7 shows the relative amounts of individual peptides based on the relative DH (value R_2). A higher R_2 value of a peptide indicates that this peptide is preferred to be released than other peptides during the hydrolysis. If all final peptides released at the same rate, all R values would be 100%. The effects of NaCl on the release of peptides, as indicated by R2 values, are summarized in Table 2. For free trypsin, peptides f(61−69/61−70), f(84−91), f(125−125), f(92−101) and f(41−60) were released significantly faster at 0.1 or 0.5 M NaCl. Specifically, at DH 3%, 3-fold higher amount of f(61−69/61−70) and 2-fold higher amounts of f(92−101) and f(41−60) were released with the addition of 0.5 M NaCl, compared to those in 0 and 0.02 M NaCl. Also, f(15−20), f(21−40) and f(125−135) were released much earlier in 0.1 and 0.5 M NaCl. For immobilized trypsin, the addition of 0.1 or 0.5 M NaCl significantly increased f(61−69/61−70) and f(125−135). In addition, levels of f(71−75) and its precursor f(70−75) decreased significantly with the addition of 0.1 and 0.5 M NaCl for immobilized trypsin, while no significant difference in these peptides was observed for free trypsin. In general, the final peptides directly associated with the breakdown of intact protein diminished with increasing NaCl concentrations.

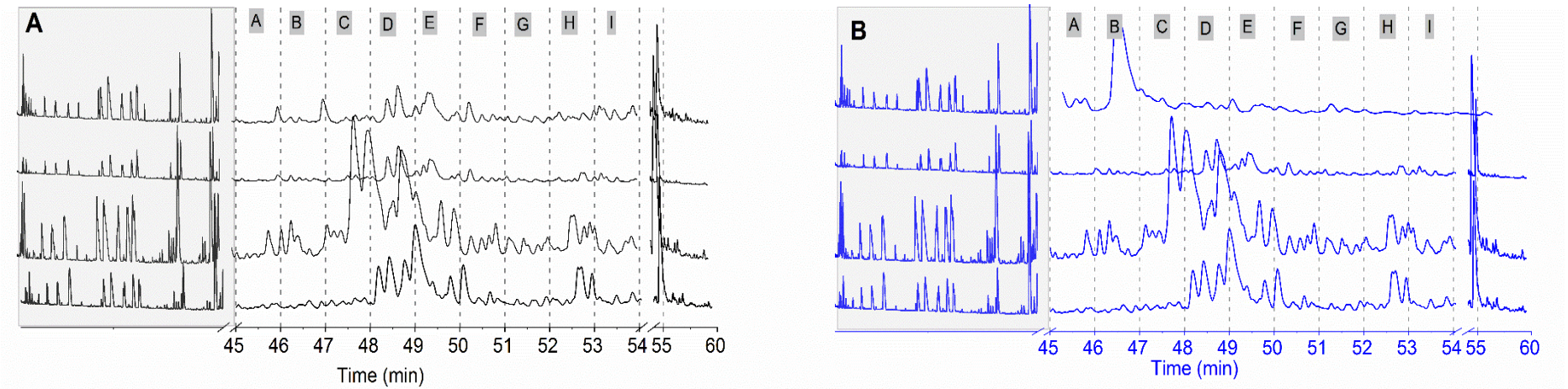

Figure 3.3-6. HPLC profiles of β-lactoglobulin hydrolysates generated from free (A) or immobilized trypsin (B) with increasing NaCl. Samples from top to bottom are hydrolysates produced in 0.5 M, 0.1 M, 0.02 M and 0 M NaCl, respectively.

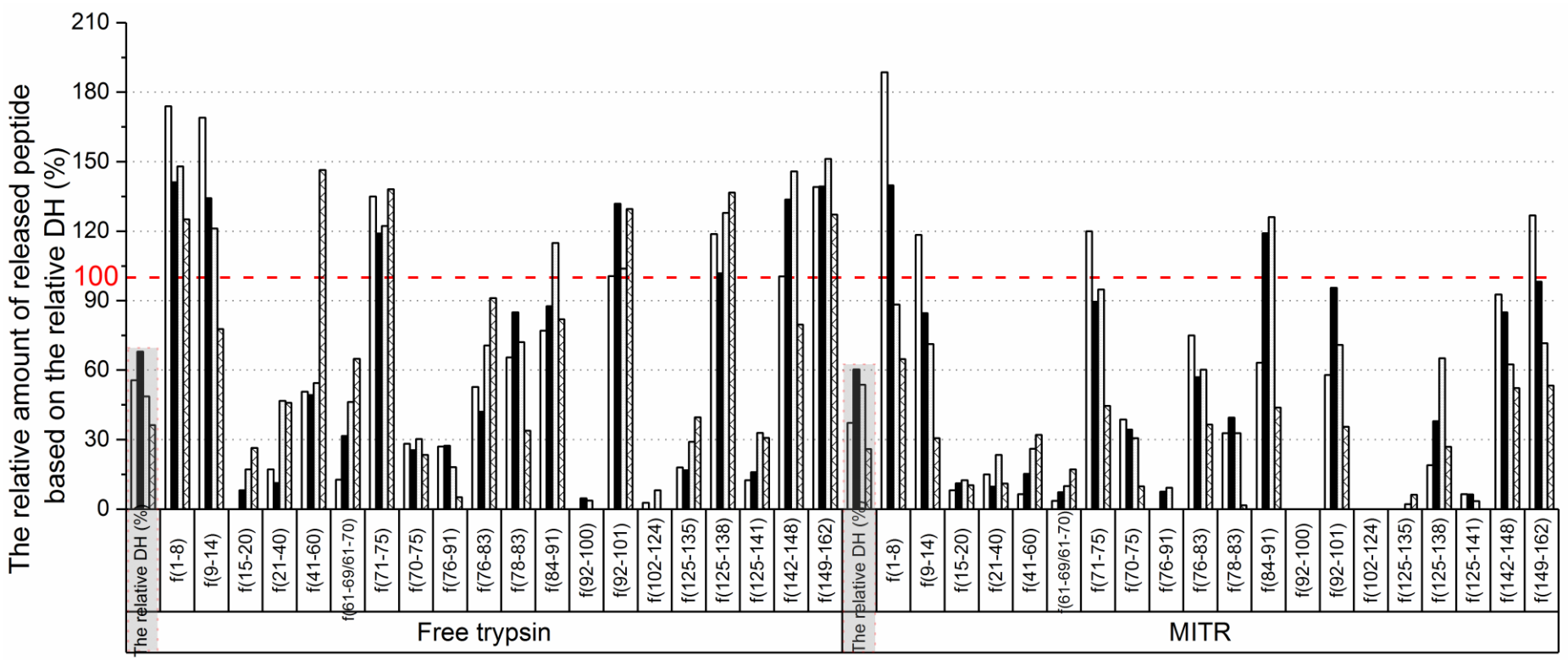

Figure 3.3-7. Effects of NaCl on the release of specific peptides. Hollow bars, black bars, bars with dots, and bars with crossed lines represent the hydrolysis of β-lactoglobulin in 0, 0.02, 0.1 and 0.5 M NaCl, respectively.

Table 3.3-2. The effects of salts on the release of peptides

Effects	Free trypsin	MITR
	Effects of Tris [a]	
Increase	f(1–8); f(9–14); f(15–20); f(21–40); f(41–60); f(61–69/61–70); f(78–83); f(84–91); f(92–101)*; f(142–148); f(149–162)	f(1–8); f(9–14); f(15–20); f(21–40) ;f(41–60); f(61–69/61–70); f(78–83); f(84–91); f(92–101)*; f(125–138)*; f(125–135); f(149–162)
Decrease	f(71–75)	f(71–75); f(142–148)
No significant effect	f(92–100); f(125–138)*; f(125–135)	f(92–100)
	Effects of NaCl [b]	
Monotonic decrease	f(1–8); f(9–14)	f(1–8); f(9–14); f(71–75); f(142–148); f(149–162)
Monotonic increase	f(15–20); f(21–40); f(41–60)*; f(61–69/61–70); f(92–101)*; f(125–135); f(125–138)*	f(41–60)*; f(61–69/61–70); f(125–135)
Increase then decrease	f(78–83); f(84–91); f(92–100); f(101–124)*; f(142–148); f(149–162)	f(78–83); f(84–91); f(92–101)*; f(125–138)*
No significant effect	f(71–75)	f(15–20); f(21–40); f(92–100); f(101–124)*

[a] based on the R_1 value; [b] based on the R_2 value; * peptides with one missed cleavage site and a negligible amount of the final derivative peptide.

The mechanism underlying the observed influence of NaCl

In contrast to Tris, NaCl is a strong electrolyte and is reported to show quasi-neutral behavior, as both its anion and cation are located in the middle of the Hofmeister series (Salis et al., 2007). Sedlak, Stagg and Wittung-Stafshede (2008) concluded that at low ion concentrations (< 100–200 mM), ions specifically interacted with protein molecules in the manner of Langmuir binding isotherm (specific binding or pairing of ions with proteins), while at ion concentrations > 200 mM, Hofmeister effects dominated (salting out or salting in of proteins). The study exploring ion-pairing effects of NaCl on β-Lg indicates that Na+ ions pair with carboxylate groups, while Cl^- ions are not significantly enriched near positively charged residues, such as Lys and Arg (Beierlein et al., 2015). At pH 8.7, the overall surface charge of trypsin molecules is theoretically positive, as its PI is 10.1–10.5 (Buck, Vithayathil, Bier & Nord, 1962). As the electrostatic interactions between free enzyme and substrate molecules dominate (Endo et al., 2016), the pairing effect of Na+ ions with the carboxylic groups of β-Lg at low NaCl concentrations could protect intact protein molecules from hydrolysis by free trypsin. The addition of high concentration of NaCl significantly increased the ionic strength of the reaction media, which might hinder enzyme–substrate interactions through charge shielding. In addition, due to Hofmeister effects, the interactions between molecules of β-Lg increase with increasing concentrations of NaCl, toward dimer formation. This further decreases the depletion of intact protein significantly by both forms of trypsin. Beierlein et al. (2015) provided models on the formation of β-Lg dimmers, including the “Lock-and –key”, corresponding well to our results. The residues involved in interactions in this model are mainly in termini, and the release of final peptides located in termini decreased significantly at high concentrations of NaCl in this study.

3.3.3.4 The mechanism underlying the different influences on free and immobilized trypsin exerted by salts

As previously discussed, Tris and NaCl exerted different influences on free and immobilized trypsin. These differences are probably due to (i) the unconventional flow-through hydrolysis mode; (ii) the surface characteristics of the support used to immobilize trypsin. In this flow-through approach, shear force is a decisive force, driving substrate molecules to immobilized trypsin, since a higher flow rate contributes to a higher hydrolysis efficiency in our previous work (Mao et al., 2017; Mao & Kulozik, 2018). Further, immobilized trypsin attracts substrate molecules at a short distance, depending on the interactions of substrate-enzyme and/or substrate-support surface. In this study, aldehyde-activated columns without a spacer linker were used as the immobilization support, and the surface was preferentially neutral (Naldi, Černigoj, Štrancar & Bartolini, 2017). In addition, the surface coverage ratio by trypsin molecules was high, about 65 ± 10% (Mao et al., 2017). Thus, the surface charge and hydrophobicity of the support is considered to be same as that of the formed layer of immobilized trypsin molecules. Trypsin was immobilized at pH 5.6 (Mao et al., 2017), where the overall surface charge of trypsin molecules is, in theory, highly positive. Based on the principles of electrostatic interactions, each trypsin molecule probably regulates its position to reach a charge balance with other trypsin molecules during the

immobilization. Hence, the attractive force between substrate molecules and immobilized trypsin is probably different from that for free trypsin, which is mainly dependent on electrostatic interactions (Evnin et al., 1990). Our results corroborate this prediction. For instance, negatively-charged precursor peptides f(125–141), f(125–138) and f(102–138) were much less attracted to immobilized trypsin than for free trypsin. Alternatively, the hydrophobic precursor peptides were generally preferred over hydrophilic peptides for immobilized trypsin. Therefore, hydrophobic interactions are implicated as the attracting forces at a short distance, determining the interactions between substrate molecules and immobilized trypsin. With the addition of salts, ions may provide charge shielding/electrical double layer or stoichiometric ion binding on the support surface in MITR, which is used for column chromatography to suppress nonspecific adsorption of proteins to the column surface (Tsumoto et al., 2007). Thus, due to the ions binding on the surface of immobilization support, this support may exerts an additional repulsive force on intact protein and/or an attractive force on certain peptides.

3.3.4 Conclusion

In this study, the influence of salts was explored comparatively between free and immobilized trypsin for the hydrolysis of β-Lg. Compared with the hydrolysis without additional NaCl, DH increased faster for both forms of trypsin with the presence of 0.02 NaCl, especially for immobilized trypsin, DH increased in 0.1 M NaCl as well. Regarding the hydrolysis of intact protein, increasing NaCl concentrations significantly reduced the depletion rate for both forms of trypsin, while 0.1 M Tris had no significant influence on hydrolyzing intact protein. In addition, both forms of trypsin preferentially hydrolyzed certain intermediate peptides in the presence of salts, depending on the type and concentration of salts as well as on the form of trypsin. This study followed the change in peptide profiles at the early stage of hydrolysis, and provided the possibility of a partial hydrolysis of β-Lg with desired peptide compositions, for example, a hydrolysate with a maximum accumulation of certain functional intermediate peptides.

Generally, the hydrolysis efficiency and hydrolysate profiles can be regulated by adding different salts at varied concentrations, since salts significantly influence the interactions between proteins/peptides and enzymes. This study may provide some hints on the choices of buffers or salts to regulate the hydrolysis process, improve the hydrolysis efficiency or obtain desired product profiles. In future studies, the investigation of a hydrolysis medium with more complex salt compositions, such as milk salts, could be quite interesting. Milk salts contain calcium, magnesium, sodium, and potassium as the main cations and inorganic phosphate, citrate, and chloride as the main anions. The hydrolysis of milk proteins without the removal or with the addition of these salts could provide consumers with extra benefits, as these minerals are essential for bone growth and development. However, it is necessary to clarify whether these minerals will considerably influence the hydrolysis efficiency and/or the resulting hydrolysate profiles.

Financial support
This research did not receive any specific grant from funding agencies in the public, commercial, or not-for-profit sectors.

Acknowledgements
The first author thanks China Scholarship Council (China) for the support of her personal costs. The authors would like to thank Urh Černigoj from BIA Separations (Ajdovščina, Slovenia) for his te Supporting information chnical help in developing the MITR.

3.3.5 Supporting information

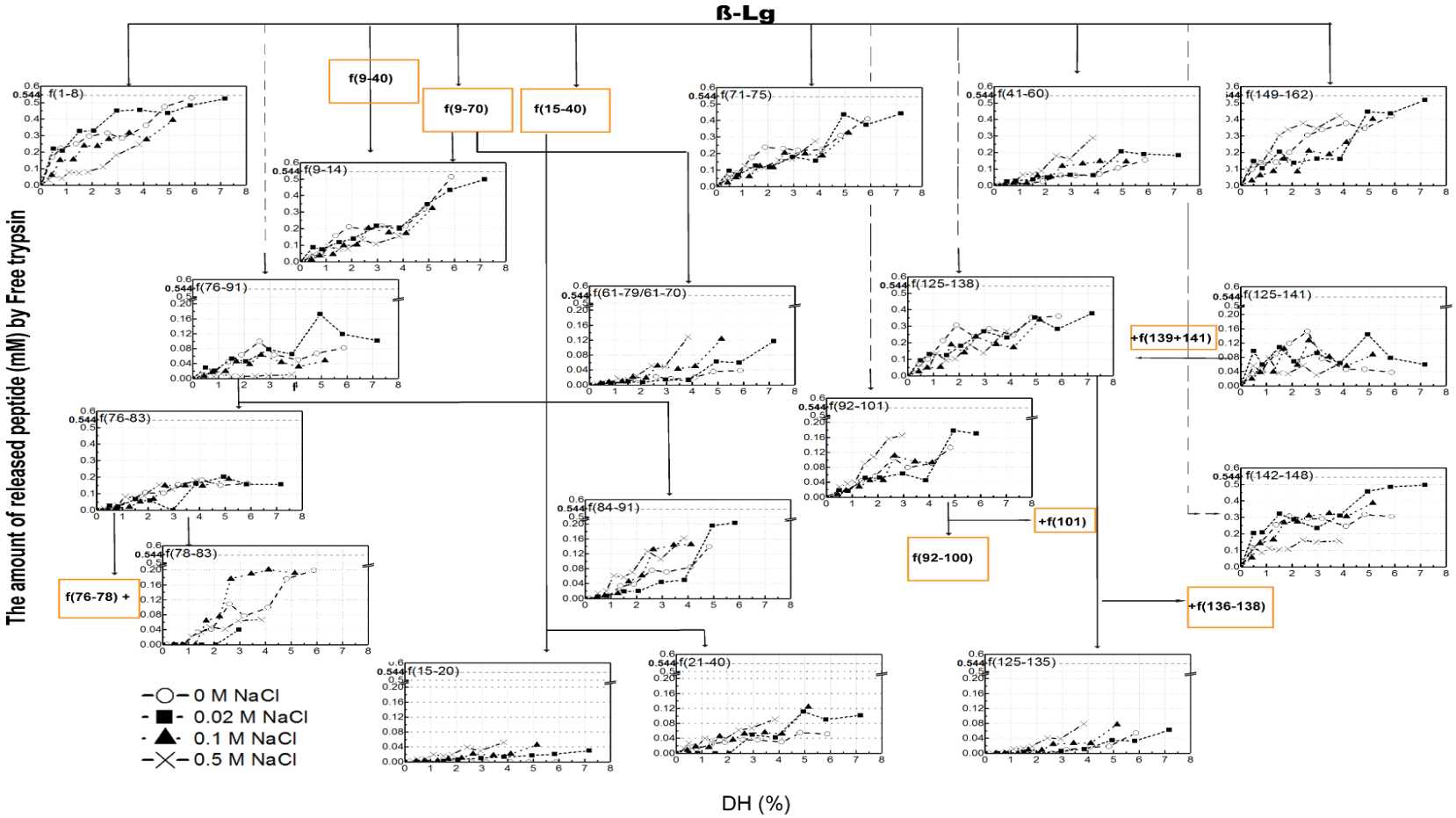

Figure 3.3-S1 The dynamic evolution of peptides generated from β-Lg by free trypsin: the solid arrow indicates that the peptide is released from the intact protein or a confirmed intermediate peptide. If one peptide is generated from an uncertain polypeptide, a dashed arrow is used.

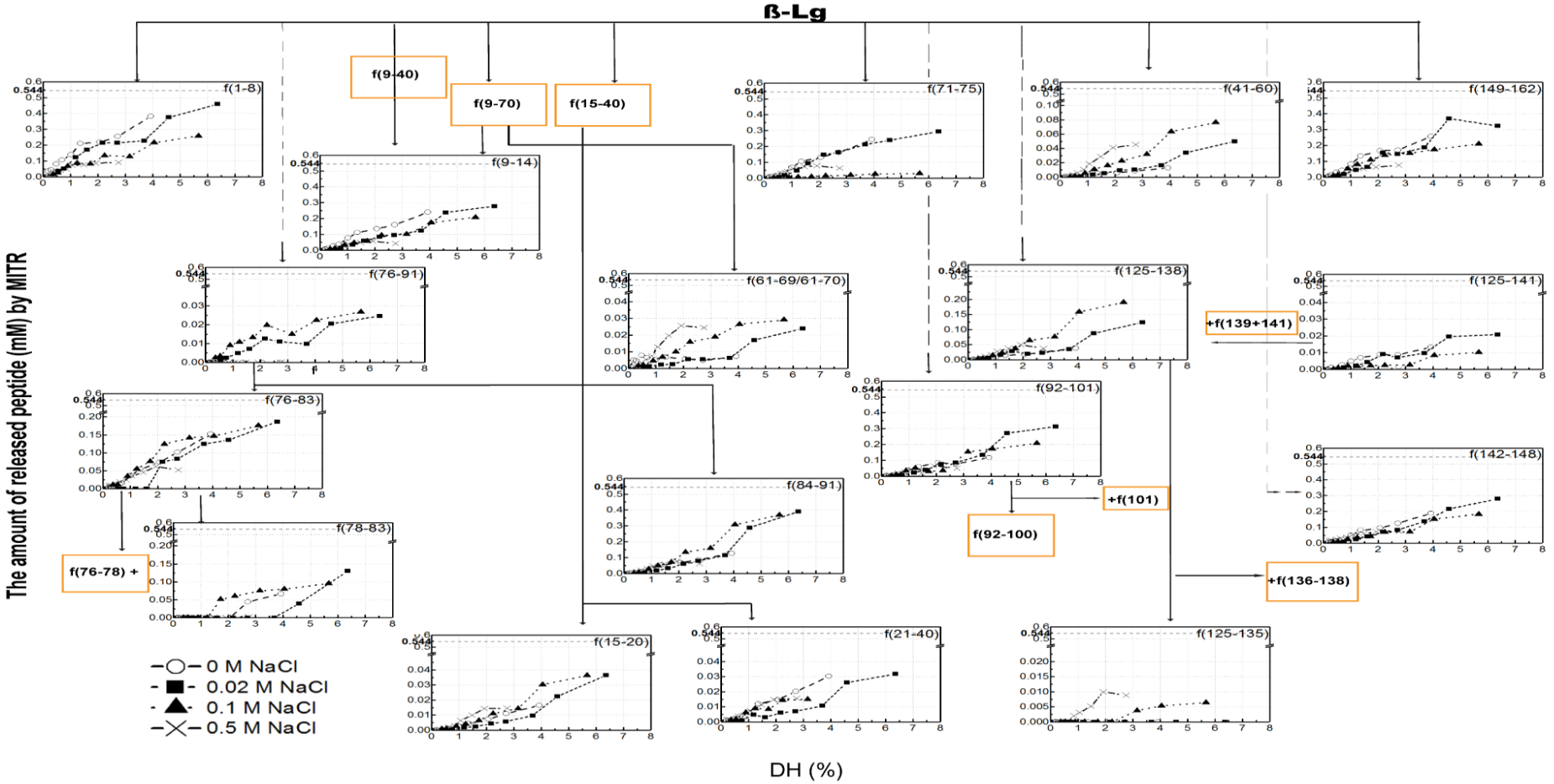

Figure 3.3-S2 The dynamic evolution of peptides generated from β-Lg by MITR: the solid arrow indicates that the peptide is released from the intact protein or a confirmed intermediate peptide. If one peptide is generated from an uncertain polypeptide, a dashed arrow is used.

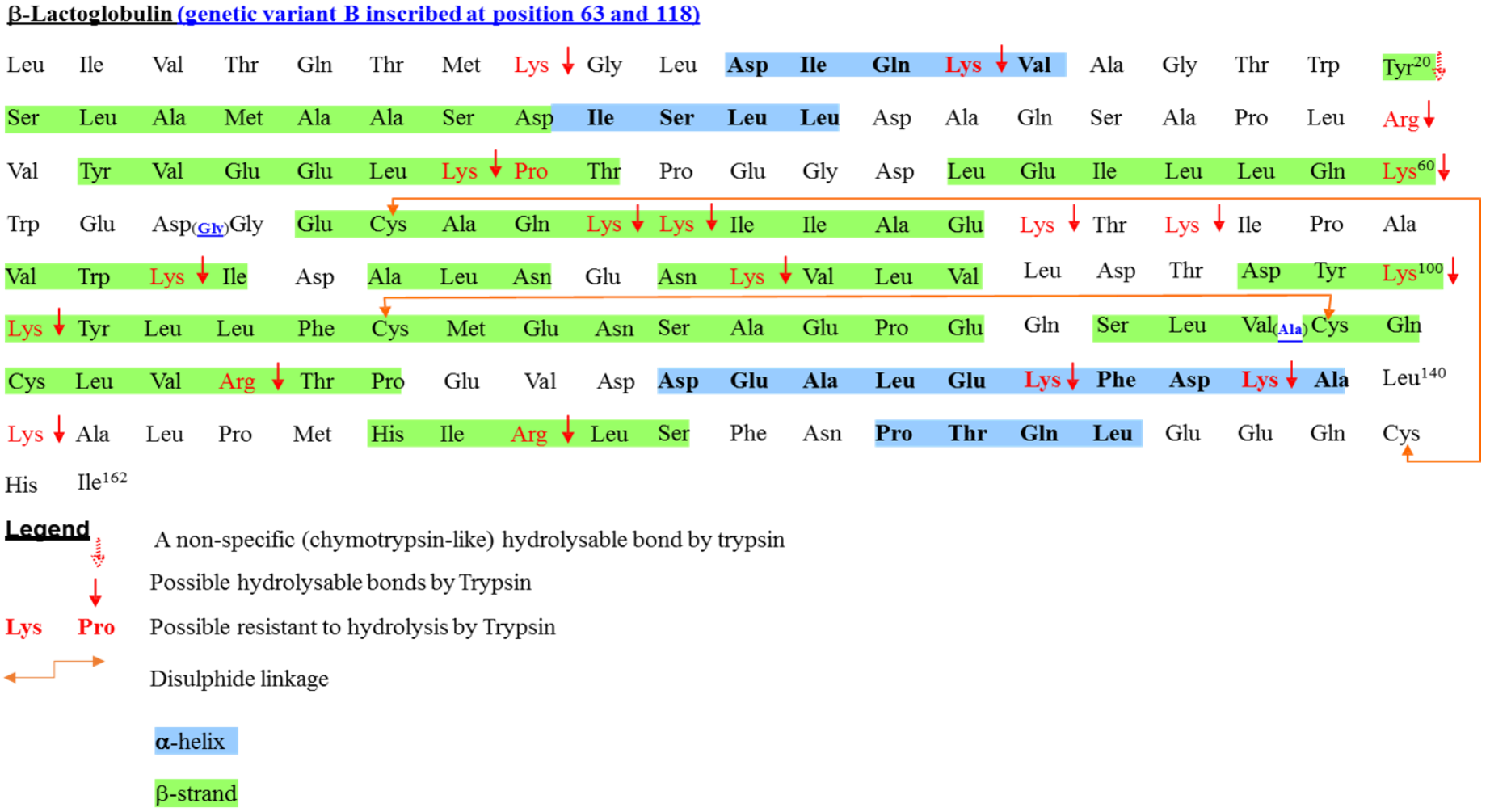

Figure 3.3-S3 Sequence of β-Lg, including the main secondary structures and potential cleavage sites by trypsin, cited from https://www.rcsb.org/structure/1b0o.

Table 3.3-S1 The characteristics of several intermediate peptides*

Polypeptides	Isoelectric point	Average hydrophilicity	Ratio of hydrophilic residues /total number of residues (%)
f(1-14)	9.9	-0.1	36
f(1-20)	9.7	-0.5	25
f(1-40)	6.9	-0.3	33
f(15-40)	3.9	-0.4	31
f(41-70)a	4.2	0.6	50
f(70-75)	9.9	0.8	50
f(71-91)	9.7	0.3	0.3
f(92-124)a	4.3	-0.1	39
f(92-138)a	4	0.3	45
f(92-141)a	4.2	0.3	44
f(102-138)	3.8	0.3	46
f(125-138)	3.8	1.2	57
f(125-141)	4.1	1.1	53
f(142-162)	6	-0.3	33

*Calculated from http://www.bachem.com/service-support/peptide-calculator/

3.4 β-lactoglobulin hydrolysis by a flow-through monolithic immobilized trypsin reactor in ethanol/aqueous solvents

Summary and contribution of the doctoral candidate

This study aims to address: (i) The feasibility of β-Lg hydrolysis by MITR in an ethanol/water solvent mixture; (ii) How the addition of organic solvent will influence the hydrolysis process, on both efficiency (enzymatic activity) and products profiles; (iii) Whether will these potential influences differ due to applying the different forms of trypsin (i.e. free and immobilized)?

In this study, methacrylate monolith based immobilized trypsin reactors (MITRs, pore size 2.1 µm, bed volume 1 mL) were developed using different immobilization protocols. The influence of applied reducing agents were compared. One of the developed MITRs was used to hydrolyse β-Lg by circulating the substrate solution in a flow-through system. The feasibility of β-Lg hydrolysis by MITR in an ethanol/water solvent mixture was evaluated based on the physical properties of β-Lg (e.g., molecular size & viscosity) and the activity of MITR measured using model substrate BAEE. Two solvents at pH 8.7, i.e. aqueous and 20% water/ethanol were used as the reaction media for the hydrolysis of β-Lg. Free trypsin was applied in parallel to comparatively illustrate the influence of ethanol. The hydrolysis process was characterized using three descriptors: (i) degree of hydrolysis (DH); (ii) the amount of residual intact β-Lg as a function of DH; and (iii) quantitative analysis of dynamic evolutions of peptides.

This study reports for the first time on the systematic evaluation of trypsin after its immobilization for the production of protein hydrolysates in the absence and presence of ethanol. Our results can be used as a reference for others when they consider the application of immobilized trypsin and the implementation of an organic solvent in the reaction media.

Most significant contribution to this manuscript was made by the doctoral candidate. This comprised (i) the conception and design of experiments based on preceded critical literature review; (ii) experimental conduction on the characterization or IMTRs, protein hydrolysis, and hydrolysates analysis; (iii) data analysis and data interpretation. In addition, writing and revising of the manuscript was done by the doctoral candidate.

Adapted original manuscript[4]

β-lactoglobulin hydrolysis by a flow-through monolithic immobilized trypsin reactor in ethanol/aqueous solvents

Yuhong Mao[a*], Maria Krischke[a], Claudia Hengst[a], Ulrich Kulozik[a,b]
Technical University of Munich, aChair of Food and Bioprocess Engineering, bInstitute of Food and Health (ZIEL)–Technology Unit,
Weihenstephaner Berg 1, D-85354, Freising-Weihenstephan, Germany

Abstract: Monolith based immobilized trypsin reactors (MITRs) were developed using different immobilization protocols. Compared with the use of reducing agent NaCNBH3, the application of 2-PB led to around 33% decrease in immobilization yield, while improved the specific activity of immobilized trypsin. The developed flow-through MITR was used to hydrolyze β-Lactoglobulin (β-Lg), and the feasibility of integrating ethanol in reaction media was evaluated. Raising ethanol concentrations from 0 to 50% increased the size of β-Lg molecules from 1.74 ± 0.32 nm to 5.67 ± 2.78 nm, and doubled the viscosity of β-Lg solutions. To avoid high backpressure and potential clog on MITR, β-Lg was hydrolyzed with the addition of ethanol up to 20%, where the activity of immobilized trypsin increased by 20% than that in aqueous media. Similar to free trypsin, the addition of ethanol contributed to an increase in DH and a faster depletion of intact protein for MITR. The presence of ethanol decreased the releases of peptides locating on C- termini, i.e., f(149–162) and f(142–148) for free and immobilized trypsin. However, the release of peptides locating inner β-Lg increased, e.g., a 5 times higher amount of f(125–138) was detected for MITR in 20% ethanol.

[4] Adaptions refer to formatting issues: e.g., numbering of sections, figures, tables and equations, abbreviations, manufacturer specifications, axis labeling, figure captions and style of citation.

[4] Originally published in: *Bioprocess Chemistry* (2019), in press. Permission for reuse of this article was granted by Elsevier.

3.4.1 Introduction

Hypoallergenic formulae are frequently manufactured from the whey protein fraction (bovine milk), which contains a high amount of β-Lactoglobulin (β-Lg), a major allergen absent from human milk (Lozano-Ojalvo, Pérez-Rodríguez, Pablos-Tanarro, López-Fandiño & Molina, 2017). Enzymatic hydrolysis of this protein using trypsin (EC 3.4.21.4) not only effectively reduces the allergenicity (Jost, Meister & Monti, 1991; Kim et al., 2007), but also results in the release of various biofunctional peptides (Pellegrini, Dettling, Thomas & Hunziker, 2001; Pihlanto-Leppälä, Rokka & Korhonen, 1998; Silveira, Martinez-Maqueda, Recio & Hernandez-Ledesma, 2013). These findings inspire us to consistently study the tryptic hydrolysis of β-Lg and to further improve its relevance to the industrial implementation. To reduce cost, many enzymes used in food processing are produced from recombinant microorganisms. However, the expression of mammalian trypsin in microbial systems is not easy to achieve in commercially relevant levels. Therefore, trypsin on market is commonly extracted and purified from animal pancreas such as bovine, ovine and porcine, suffering a relatively high cost (Yu & Ahmedna, 2012). Applying trypsin in an immobilized form represents an alternative approach because of the possibility of reusing the enzyme and producing enzyme-free hydrolysates.

Among the different immobilization supports, monolithic columns have been of recent interest, because they generally allow for a higher mass flow at a low backpressure. The mass transfer in monolithic columns is exclusively convective and laminar, which is not diffusion limited (Podgornik, Savnik, Jancar & Krajnc, 2014). Moreover, the surface of most organic monolithic materials can be modified with various functional groups, which makes the covalent bonding of enzyme much easier.

Immobilization protocols, especially by covalent bonding, may significantly influence the immobilization efficiency, i.e., conformational distortion of enzyme and/or physical blockage of its active site could happen (Garcia-Galan, Berenguer-Murcia, Fernandez-Lafuente & Rodrigues, 2011). Furthermore, the coupling chemistry also defines the final surface chemistry, which might lead to the so-called nonspecific interactions. Nicoli et al. (2008) reported that the use of ethylendiamine (EDA), an 8-carbon spacer moiety, could enhance the mobility of trypsin immobilized on EDA-glutaraldehyde (GLA)-CIM disks (compared with the use of epoxy or carbonyldiimidazole). However, after immobilization EDA-GLA exhibits secondary amino groups and these groups are positively charged at the working pH of trypsin (pH 7–9), which might result in nonspecific ionic interactions (Naldi et al., 2017). Alternatively, aldehyde (ALD) activated CIM monolith was used as the immobilization support for the multipoint covalent bonding of trypsin through Schiff base reactions, as the surface of ALD monolith after enzyme immobilization is preferentially neutral (Mao et al., 2017; Marques et al., 2011; Naldi et al., 2017). Our earlier work evaluated the influence of large pore sizes (2.1 µm versus 6 µm) on the performance of immobilized trypsin reactors based on ALD-CIM monolithic columns (MITRs), to meet the crucial requirements for protein hydrolysates production, i.e., processing large amount of

substrate and long continuous digestion time in each cycle. Here, different immobilization protocols were investigated to assess whether the immobilization efficiency could be improved, in terms of immobilization yield and enzyme activity.

In our previous works (Mao et al., 2017, 2018, 2019), the specificity of immobilized trypsin remained unchanged. Regardless of the specificity, not all theoretically cleavable sites are hydrolyzed at the same time. Thus, another criteria “selectivity” is introduced, referring to the rate at which individual cleavage sites in a protein substrate are hydrolyzed relative to other cleavage sites (Butré et al., 2014). According to our earlier investigations (Mao et al., 2017, 2018, 2019), the selectivity of trypsin toward β-Lg changed once it was covalently immobilized, resulting in different kinetics for peptides releases. Furthermore, these changes varied at different pH values (Mao et al., 2018) or with the addition of salts (Mao et al., 2019). Consistent with these findings, here, we aim at clarifying how the change in medium polarity by adding ethanol influences the selectivity of immobilized trypsin toward substrate β-Lg.

The presence of ethanol contributes to stabilizing the hydrolysis process by suppressing eventual microbial infections which can become an issue in a continuous enzymatic hydrolysis by immobilized enzymes. Besides, the addition of ethanol leads to the decrease in bulk dielectric constant of the solvent. This significantly shifts the balance of electrostatic charges on the protein and alters the organization of dipolar moments (Dufour, Bertrand-Harb & Haertlé, 1993). Furthermore, ethanol molecules can compete with the protein hydrogen bond system, and perturb its hydration, whereby the protein refolding is pushed toward the reorganization of hydrogen bonds, hydrophobic interactions, and salt bridges (Nikolaidis & Moschakis, 2018). Thus, structural changes and a subsequent exposure of the hydrophobic core for proteins might happen. The compact globular structure of β-Lg contains a β-barrel, consisting of eight antiparallel β-strands forming a central hydrophobic core (Leeb et al., 2015). Nine of eighteen peptide bonds after amino acids Lys and Arg, which are theoretically cleavable for trypsin, locate in this hydrophobic core. Consequently, an ethanolic aqueous media is expected to assist the hydrolysis of intact β-Lg. However, aggregation or gelation due to the increasing hydrophobic interactions among β-Lg molecules might subsequently take place as well (Renard, Lefebvre, Robert, Llamas & Dufour, 1999). This would seriously impair the hydrolysis process, especially for the hydrolysis by a flow-through MITR, as high backpressure and blockage could occur. Therefore, particular attention should be paid to the physical characteristics of β-Lg in ethanol/water solutions. In addition, enzymes might undergo structural distortion with the addition of ethanol, leading to decreased activity even inactivation (Tchorbanov & Iliev, 1993). Covalent immobilization is reported to stabilize enzymes against certain denaturing conditions (Mozhaev, Melik-nubarov, Sergeeva, Šikšnis & Martinek, 1990). Thus, we expect that immobilized trypsin can be functioning in the presence of ethanol up to certain concentrations.

This study evaluated different protocols for the immobilization of trypsin on ALD-CIM monolithic columns. The developed MITR was used for the hydrolysis of β-Lg, and the

feasibility inclusive ethanol in the reaction media was investigated. To comprehensively clarify the influence of medium polarity (ethanol) on the hydrolysis of β-Lg by immobilized trypsin, the hydrolysis efficiency and hydrolysate profiles were compared with those for free trypsin.

3.4.2 Materials and methods

3.4.2.1 Materials

Trypsin (EC 3.4.21.4) from bovine pancreas (Type I, approximately 10,000 BAEE units/mg protein), Nα-Benzoyl-L-arginine ethyl ester hydrochloride (BAEE), trypsin inhibitor from chicken egg white, β-Lg A (99% purity), β-Lg B (99% purity), Tris (hydroxymethyl)-aminomethane, ethanolamine, benzamidine hydrochloride (BAHC), 2-methylpyridine borane complex (2-PB), 2-(N-morpholino) ethanesulfonic acid (MES), sodium chloride (NaCl), sodium borohydride (NaBH4), sodium cyanoborohydride (NaCNBH3), calcium chloride (CaCl2), and sodium hydroxide (NaOH), trifluoroacetic acid (TFA), dithiothreitol (DTT) and chloroacetamide (CAA) were purchased from Sigma–Aldrich (St Louis, USA). α-cyano-4-hydroxycinnamic acid (HCCA), 2,5-dihydroxyacetophenone (DHAP), mass calibration standards (PAS and Protein Calibration Standard I) were from Bruker Daltonics GmbH (Bremen, Germany). Deionized water was acquired using a Milli-Q System (Millipore Corporation, Bedford, USA). Bovine β-Lg powder was fractionated from whey protein isolate (WPI), a product developed by Fonterra Co-operative Group Ltd (Auckland, New Zealand). It has a dry matter content of 91.5% and a protein content of 98.6% relative to the dry matter, the native β-Lg represented >99% of the total protein content.

3.4.2.2 Preparation and characterization of MITRs

Aldehyde activated CIM® radial monolithic columns (outer diameter (D) – 1.86 cm, inner diameter (d) – 0.67 cm, height (h) – 0.42 cm) were provided by BIA Separations d.o.o. (Ajdovščina, Slovenia). Trypsin was immobilized on monolithic columns. Three coupling protocols were investigated, as shown in Fig. 3.4-1. Each protocol was applied in triplicate.

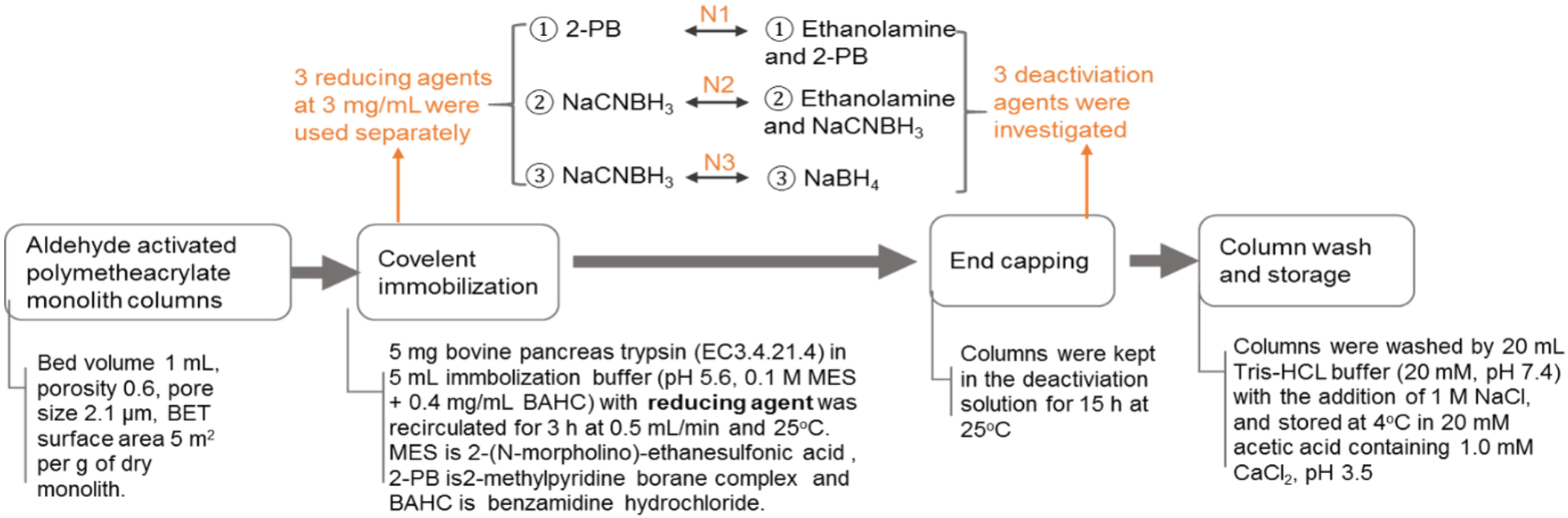

Fig. 3.4-1 Schematic illustration of the trypsin immobilization on aldehyde activated CIM® radial monolithic columns.

The developed MITRs were characterized in terms of the amount of immobilized trypsin and the initial permeability. Briefly, the amount of immobilized trypsin was followed from the trypsin concentrations before, during and after immobilization, which were chromatographically measured as described by Naldi et al. (Naldi et al., 2017). The permeability was measured as described by us previously (Mao et al., 2017). Based on the measured permeability, the theoretical backpressure on MITR with a specific mobile phase (substrate solution) at a given flow rate was calculated according to Eq. (3.4-1) (Podgornik et al., 2014):

$$\Delta P = \frac{F}{B} \times \frac{\eta \times \ln(\frac{D}{d})}{2\pi h} \quad (3.4\text{-}1)$$

Where, ΔP (MPa) is the theoretical pressure drop; η (mPa*s) is the viscosity of mobile phase; B (m^2) is the permeability of monolith; F (m^3/s) is the volumetric flow rate; outer diameter (D) and inner diameter (d) of this MITR are 0.0186 m and 0.0067 m, respectively; its height (h) is 0.0042 m.

3.4.2.3 Trypsin activity measurements

The activity of free trypsin was measured using a continuous spectrophotometric rate determination. 75 µL 0.5 mg/mL trypsin in 1 mM HCl solution (prepared freshly before each measurement at 4°C) or 75 µL 1 mM HCl (as blank) was mixed with 3.125 mL 0.25 mM BAEE in 0.1 M Tris-HCl (pH 7.2–9.2, in water or in ethanol/water solvents, 25°C) at 25°C. After the immediate mix by inversion, the increase in A_{253} was recorded every 3 s for 5 minutes. The activity (U) was expressed as BAEE units/mg free trypsin and calculated using Eq. 3.4-2:

$$U = \frac{S_{trypsin} - S_{blank}}{0.001 \times 0.075 \times c_{trypsin}} \quad (3.4\text{-}2)$$

Where, $S_{trypsin}$ and S_{blank} were obtained by the ΔA_{253}/minute using the maximum linear rate, $C_{trypsin}$ is the concentration of the prepared trypsin solution.

One BAEE unit is defined to produce a ΔA253 of 0.001 per minute in a reaction volume of 3.20 mL at a given pH and 25°C.

The activity of immobilized trypsin toward substrate BAEE was measured at a continuous flow approach (Mao et al., 2017). Briefly, 10 mM BAEE in 0.1 M Tris-HCl (pH 7.2–9.2, in water or in ethanol/water solvents) was continuously pumped through the MITR at 10 mL/min. The activity U* (µmol/min) which is defined as the amount of BAEE one MITR converted to Nα-Benzoyl-L-arginine (BA) in 1 min, was calculated using Eq. 3.4-3 :

$$U^* = \frac{\Delta A \times F \times Di \times 10^3}{L \times \varepsilon} \quad (3.4\text{-}3)$$

ΔA (Au) is the absorbance difference of BAEE solution before and after hydrolysis; Di is dilution factor; L is the light path, here is 1 cm; ε is the molar extinction coefficient, corresponding to the differential molar absorbance of BAEE against BA at 253 nm,

here is 808 mol^{-1} cm^{-1}. U* can be easily converted to BAEE units, using the conversion factor 270, as determined by Bergmeyer et al. (Bergmeyer, 1974).

The apparent specific activity of immobilized trypsin (U**) was calculated using Eq. 3.4-4:

$$U^{**} = \frac{U^*}{m} \tag{3.4-4}$$

Where m (mg) is the amount of immobilized trypsin in each MITR.

3.4.2.4 Characterization of β-Lg

Sample preparation

β-Lg powder was dissolved in deionized water and stirred for 15 ± 1 h at 4°C to allow complete hydration. To remove denatured β-Lg, the pH was adjusted to 4.6 (Dannenberg & Kessler, 1988) at ambient temperature, and then centrifuged at 6,000 g for 10 min. The supernatant was filtered through a cellulose membrane with a cut-off of 0.45 μm. The obtained β-Lg solution was mixed with ethanol/water solution (0, 10, 20, 40, 60, 80, 100%, v/v) at a volume ratio of 1:1, and the pH was adjusted to 8.7. The final β-Lg concentration was 9.5–10.5 mg/mL.

Viscosity measurement

The viscosity was measured at 25°C using a Modular Compact Rheometer MCR 302 (Anton Paar Inc., Austria) coupled with a double gap, as a relatively low viscosity was expected. After the removal of air bubbles, approximately 5 mL protein solution was used. During the measurement, the shear rate increased linearly from 0.1 to 100 s^{-1} and then decreased to 0.1 s^{-1}. 20 measurement points were recorded every 15 s during either the increase or decrease. The viscosity as a function of shear rate was modeled using Newtonian fluid model. Each sample was prepared in duplicate and every one was measured in triplicate.

Molecular size measurement

The sizes of β-Lg molecules in ethanol/water solutions were measured by dynamic light scattering using a Zetasizer NanoSystem (Malvern Instruments Inc., Worcester, UK). The measured dynamic viscosity of each bulk sample, and the dielectric constants of ethanol/water solvents reported by Wyman (1931) were used. The results were calculated as an average of 12 measurements from two individual samples. All measurements were conducted at 25°C.

3.4.2.5 Hydrolysis of β-Lg

Hydrolysis by free trypsin

100 mL β-Lg in 0 or 20% ethanol/water solvent (10 mg/mL) was hydrolyzed by free trypsin. A relatively low enzyme-substrate (E/S) ratio of 0.1% (w/w) was chosen to practically follow the hydrolysate profiles at the initial stage of hydrolysis. A TitroLine alpha plus auto-titrator (Schott AG, Mainz, Germany) was used to keep the pH constant during the hydrolysis process and to record the consumed volumes of 0.25 N NaOH

every three seconds. The detailed calculation of DH is described by us previously (Mao et al., 2017).

Hydrolysis by immobilized trypsin

10 mg/mL β-Lg in 0 or 20% ethanol/water solution was hydrolyzed via MITR which was inserted in a flow-through system (Äkta explorer, GE Healthcare Life Sciences, Freiburg, Germany). After discarding the first 10 mL, 100 mL of the substrate solution was circulated at 10 mL/min for 3 h. The auto-titrator system was used to maintain pH at 8.7 and follow DH.

3.4.2.6 Analysis of hydrolysates

1-mL samples were obtained at different intervals during hydrolysis. 0.5 mL trypsin inhibitor solution (10 mg/mL) was immediately mixed with each sample to stop the hydrolysis, when free trypsin was applied. All samples were stored at −20°C until further analysis.

Quantification of residual intact β-Lg

The quantitative determination of intact β-Lg in samples was done using an Agilent 1100 series HPLC system (Agilent Technologies, California, USA). Each sample was diluted to a protein concentration of 4 mg/mL, then 20–60 µL of diluted sample was injected and eluted through a PLRP-S 300 Å-8 µm Latek column (150 × 4.6 mm) at 1 mL/min and 40ºC. The eluent was detected at 226 nm. The detailed gradient information has been described earlier (Mao et al., 2017). The intact β-Lg concentration was calculated from the detected peak area and a calibration curve.

Identification and quantification of peptides

All the aliquots drawn out were firstly diluted at a ratio of 1:1. 1-mL diluted sample was incubated with 150 µL 80 mM DTT at 37°C and pH 7.5-8.5 for 45 min, and then mixed with 200 µL 400 mM CAA and stored in the dark for 30 min. 60-µL of the pre-treated samples were injected and analyzed by HPLC using a Kinetex_XB-C18-100Å column (100 x 4.6 mm, Phenomenex) at 1.5 mL/min. Solvent A containing 0.1% TFA dissolved in MilliQ water and solvent B (0.0555 mL TFA in 1000 mL 80% acetonitrile/water, v/v) were applied. Table 3.4-1 illustrates the detailed gradient. The elution was monitored at 214 nm and the entire analysis was conducted at 60°C.

Table 3.4- 2 Gradient of solvent B during the elution for the chromatographic analysis of β-Lg hydrolysates.

Time (min)	0	1	3	5	10–11	16–17	19–20	25–26	28–29	34–38	40–41	44	45–46	48	59	60
Solvent B (%)	1	1	9	8	11	15	16	19	22	26	30	33	34	36	45	100

The samples drawn out at 3 h were fractionated. Each peak eluted before 45 min were collected based on the slope and time. Peaks after 45 min were separately collected

every 1 min. The peptide composition of each collected fraction was analyzed by matrix-assisted laser desorption/ionization time-of-flight mass spectrometry (MALDI-TOF-MS, Bruker Daltonics, Bremen, Germany). Two matrixes HCCA (for peptides with a mass from 500 to 4000 Da) and DHAP (for peptides/proteins with a mass up to 20000) were used separately. 1-µl samples (including a blank sample) or standards were mixed with 1 µl matrix directly on the anchor target (stainless steel MTP 384). The detailed mass spectrometry method and peptide identification are described in our previous work (Mao et al., 2017).

The molar concentration of each specific peptide was calculated from the peak area according to Eq. 3.4-5 (Muñoz-Tamayo et al., 2012):

$$X_i = 1 \times 10^6 \left(\frac{A_i}{\varepsilon_i \times l \times v}\right) \times f \times d \quad (3.4\text{-}5)$$

where x_i (µM) is the concentration of peptide i, Ai (AU min) is the peak area, l (0.6 cm) is the path length of the UV cell, v is the injection volume (60 µL), f (1.5 mL/min) is the flow rate, d is the sample dilution factor, and ε_i (AU M^{-1} cm^{-1}) is the molar extinction coefficient of peptide *i* at 214 nm calculated according to Kuipers and Gruppen (2007).

The relative release rate (R_i) of a final peptide i was quantified using Eq. 3.4-6

$$R_i\ (\%) = \frac{x_i^*}{DH^*} = \frac{\frac{x_i}{x_0}}{\frac{DH_t}{DH_{max}}} \quad (3.4\text{-}6)$$

Where, x_i^* (%) and DH* (%) are the relative amount of the peptide i and the relative DH value at a given time t, respectively. x_i (µM) is the amount of peptide i obtained from Eq. 5, x_0 is the initial concentration of substrate β-Lg (µM), DH_t is the reached DH value at a given time t, DH_{max} is the theoretical maximum DH value for the tryptic hydrolysis of β-Lg, here is 11.18% (β-Lg contains 161 peptide bonds, of which 18 peptide bonds after amino acid Lys and Arg are theoretical cleavage sites for trypsin).

3.4.2.7 Statistical analysis

The mean values ± standard deviations are reported. One-way ANOVA and Tukey's test were applied to estimate the differences between the mean values at a confidence level of 95%. Data were plotted using Origin Pro 9.0 or R 3.3.3 (open source software).

3.4.3 Results and discussion

3.4.3.1 Characterization of MITRs

Influence of reducing agents on the immobilization efficiency

Trypsin was immobilized on ALD-CIM columns by a multipoint covalent bonding through Schiff base reactions. For such reactions, reducing agents are necessary to convert enzyme-support linkages (non-protonated amino groups-aldehyde groups) into stable secondary amino groups and convert the remaining aldehyde groups on the support into hydroxy groups (Orrego et al., 2018). The most common strong reducing agent is $NaBH_4$, which however, might adversely affect the structure of certain

enzymes due to its low selectivity (Orrego et al., 2018). 2-PB and $NaCNBH_3$ are suggested as alternatives as they are much milder, especially 2-PB, which is also recommended for green chemistry application. Naldi et al. (2017) found that the immobilization efficiency increased by decreasing the buffer pH from 7.2 to 5.6 for trypsin immobilization on ALD-CIM disks, irrespective 2-PB or $NaCNBH_3$ was applied. Therefore, we investigated three protocols applying varied reducing agents while at the same immobilization pH 5.6.

As shown in Table 3.4-2, around 32% less amount of trypsin was immobilized in MITRs, when 2-PB instead of $NaCNBH_3$ was used as the reducing agent, which is in agreement with the findings of Naldi et al. (Naldi et al., 2017). This is probably due to the fact that 2-PB is much larger than $NaCNBH_3$, which restricts its ability to reduce Schiff bases as it has to go through the region that lies between the enzyme and the support (the width of this region is around 2 nm) (Orrego et al., 2018). Considering BET surface area of monolithic columns used (5 m^2 per g dry monolith) and the molecular dimension of native trypsin (Saha, Saikia & Das, 2015), the highest possible surface density of immobilized trypsin molecules was approximately 65 ± 10% for N2 and N3, and around 45 ± 10% for N1. Therefore, even at the highest immobilized density, trypsin molecules are not overcrowded on the monolith surface and the activity should not be adversely affected by intermolecular steric hindrance

Table 3.4-3 Reducing agents used in the immobilization of trypsin and the characteristics of developed monolith based immobilized trypsin reactors (MITRs)

IMTRs	Agents in immobilization	Agents in deactivation	Immobilized trypsin per column (mg)	Apparent activity per reactor at pH 8.7	Permeability after immobilization (m^2)
N1	2-PB	ethanolamine & 2-PB (pH 5.6)	3.4 ± 0.2	19745.4 ± 682.4	2.44E-12
N2	$NaCNBH_3$	ethanolamine & $NaCNBH_3$ (pH 5.6)	4.8 ± 0.2	20183.2 ± 702.8	2.46E-12
N3	$NaCNBH_3$	$NaBH_4$ (pH 10.5)	4.9 ± 0.1	19180.7 ± 668.7	1.92E-12

The difference in apparent activity among three series of MITRs at pH 8.7 was insignificant. Due to the fact that N1 had 32% less immobilization yield than N2 and N3, actually, it showed a much higher specific activity. Compared with the specific activity of free trypsin at different pH values (Fig. 3.4-2), N2 and N3 decreased by 74–48%, while for N1, only a decrease of 25–54% was observed, indicating that the application of 2-PB instead of $NaCNBH_3$ could better retain the native state of trypsin after immobilization. This contradicts the findings of Naldi et al (2017), who reported that no difference in specific activity of immobilized trypsin was noted, irrespective 2-PB or $NaCNBH_3$ was applied. The reason is unclear. It is noted that different immobilization conditions were used here due to the enlarged pore size (0.6/1.35 µm → 2.1 µm) and the upscaled bed volume (0.1 mL → 1 mL), such as the concentrations of reducing agents (1.3 mg/mL → 3 mg/mL).

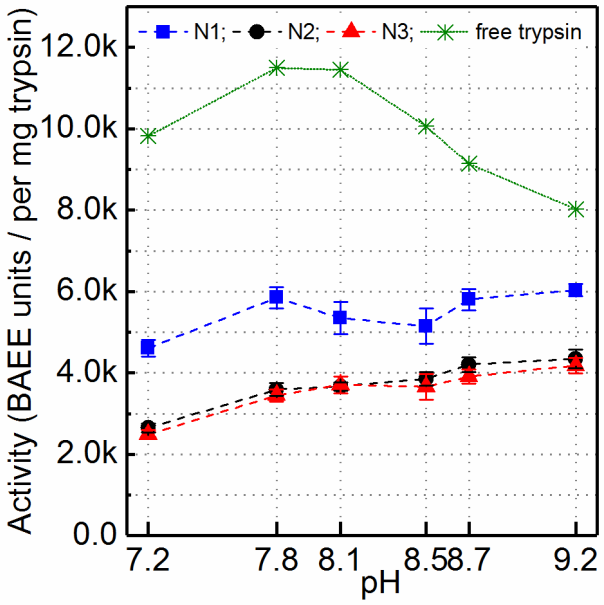

Figure 3.4-2 The apparent specific activity of immobilized trypsin and free trypsin at increasing pH values.

Free trypsin showed the highest activity in the pH range of 7.8–8.1, and its activity gradually decreased above pH 8.1. Covalent immobilization stabilized the trypsin molecules against the pH-induced distortion. In addition, the optimum pH shifted to 8.7–9.2 after the immobilization. This shift might result from the ionization change in acidic and basic amino acid side chain in the microenvironment around the enzyme active site. Interestingly, like free trypsin, pH 7.8 is the optimum working pH for N1 as well.

The permeability of a porous bed depends on the pore size forming the bed, as well as on its porosity (Podgornik et al., 2014). A constant permeability for each MITR at increasing flow rates (up to 15 mL/min) was obtained, confirming the stability of their mechanical properties.

For the further investigation, N2 was chosen due to its highest values in immobilization yield, enzymatic activity and permeability. The long-term use of N2 series were examined and reported in our previous work (Mao et al., 2017), where N2 series were able to be used to hydrolyze β-Lg (10 mg/mL) at least for 18 cycles (each cycle ≥ 3 h). Furthermore, N2 series was completely stable during storage over 30 weeks, in terms of BAEE activity and permeability, monitored over 3 weeks.

Influence of ethanol on the activity of immobilized trypsin

As illustrated in Fig. 3.4-3, the enzymatic activity of free trypsin toward substrate BAEE remained unchanged upon the addition of ethanol up to 20% (v/v). Interestingly, the activity of immobilized trypsin increased by around 20%, when the ethanol concentration increased from 0 to 20%. This is in contrast to a previous report that the BAEE activity of trypsin, which was covalently immobilized on soap-free P(MMA-EA-AA) latex particles, decreased by around 8% with the addition of 20% ethanol (Kang, Kan, Yeung & Liu, 2005). Increasing the ethanol concentration to 30%, the activity decreased for both forms of trypsin. For free trypsin, the decreased activity is probably due to a conformational distortion (25°C & pH 8.7). A study (Simon, Kotorman, Garab & Laczko, 2001) found an increase in α-helix structures and a decrease in β-sheets for free trypsin when ethanol concentrations increased from 0 to 50%. For MITR, where trypsin is covalently immobilized, in theory, the conformational distortion should be reduced. Except for the potential structural distortion, the significantly increased viscosity of 30% ethanol/water solvent (data will be presented later) could be a reason. Kanosue, Kojima, and Ohkata (2004) suggest that the high viscosity of hydrolysis media interferes the “induced-fit” process (the formation of enzyme/substrate complex), causing a decrease in enzymatic reaction rate. This effect might be enhanced in a flow-through hydrolysis system, especially at a high flow rate of 10 mL/min, as the increased viscosity led a raised shear force meanwhile.

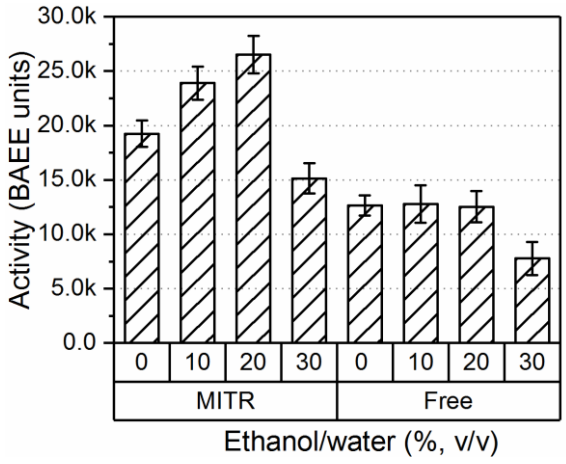

Figure 3.4-3 Enzymatic activity of per mg free trypsin and the apparent activity of the whole monolith based immobilized trypsin reactor (MITR) in 0–30% ethanol/water solvents (v/v).

3.4.3.2 Physical characteristics of β-Lg solution in the presence of ethanol

Viscosity and backpressure

As shown in Fig. 3.4-4 A, the viscosity of 10 mg/mL β-Lg in ethanol/water solvents steadily raised with increasing concentrations of ethanol, so did pure ethanol/water solvents. A study (Mikhail & Kimel, 1961) suggests that the intermolecular forces become stronger for alcoholic aqueous mixtures, which prevents the sliding of molecules past each other and results in a more viscous fluid. A relatively low concentration of β-Lg (10 mg/mL) did not significantly contribute to the increment of viscosity, except those at ethanol concentrations greater than 20%. As structures of β-Lg changed significantly in the presence of ethanol with high concentrations (> 20%) (Dufour et al., 1993; Mousavi, Chobert, Bordbar & Haertlé, 2008; Renard et al., 1999), these changes might enhance the hydrophobic interactions among protein molecules, even leading to protein aggregation (β-Lg aggregates were visibly found at 60% ethanol, figure is not shown here). Assuming that no significant blockage happens for all cases, the calculated backpressure on MITR for each β-Lg solution at 10 mL/min is presented in Fig. 3.4-4 B. A doubling backpressure (1.64 MPa) was noted when ethanol concentration increased from 0 to 40%, and the operational limit of this MITR is 2 MPa.

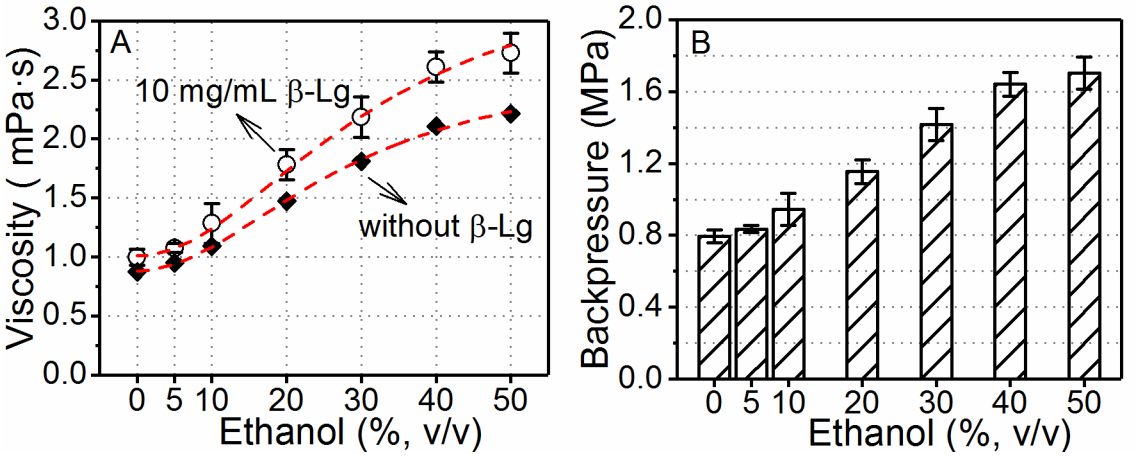

Figure 3.4-4 Viscosities of 0 and 10 mg/mL β-Lg in 0–50% ethanol/water solvents (v/v) (A); the theoretical backpressures on a monolith based immobilized trypsin reactor (MITR) with the recirculation of 10 mg/mL β-Lg in 0–50% ethanol/water solvents (v/v) at a flow rate of 10 mL/min (B).

Molecular size

The molecular sizes of β-Lg in ethanol/water mixtures were measured from its hydrodynamic sizes, including the hydration layer, i.e., a thin electric dipole layer of the solvent adheres to the surface of each molecule (Stetefeld, McKenna & Patel, 2016). β-Lg exists as a dimer under physiological conditions, which will dissociate either by increasing temperature or exceeding pH above 8 (Cheison & Kulozik, 2017). As shown in Fig. 3.4-5, β-Lg in water at pH 8.7 has the mean hydrodynamic diameter of 1.74 ± 0.32 nm. The particle size increased insignificantly with the addition of ethanol with a concentration ≤ 20%. This slight increase is attributed to changes in the protein tertiary

structure or in the hydration layer, rather than to the aggregation of protein molecules. Above 20% ethanol, the distribution of β-Lg size increased considerably, even up to 5.67 ± 2.78 nm at 50% ethanol, indicating the formation of β-Lg dimer, even of small aggregates. In contrast to β-Lg, the hydrodynamic radius of lysozyme decreased continuously upon the addition of ethanol up to 50% (v/v), indicating that ethanol induced a more compact structure for lysozyme (Bonincontro, De Francesco, Matzeu, Onori & Santucci, 1997). This might be due to the ability of β-Lg to bind hydrophobic ligands (Mousavi et al., 2008).

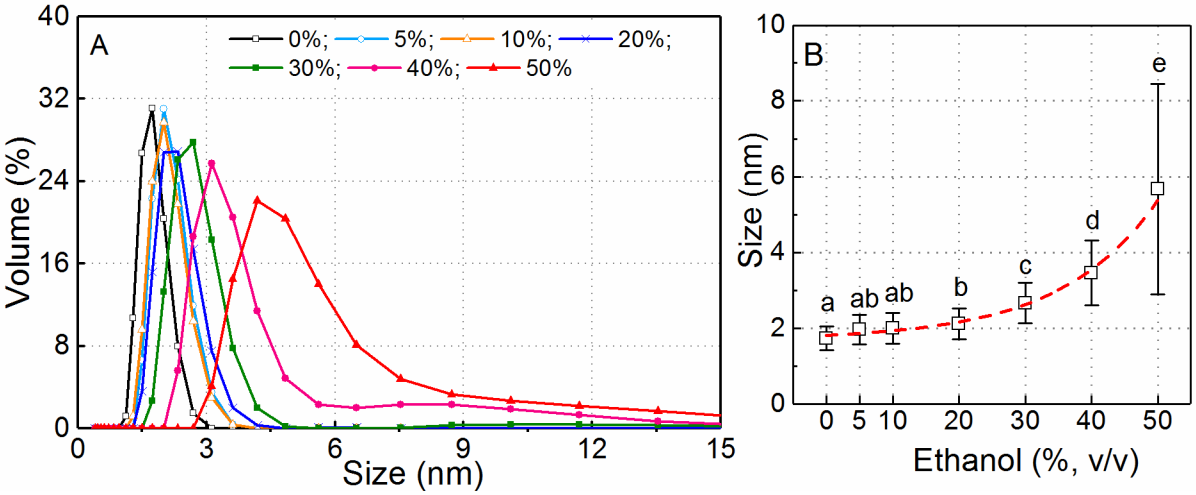

Figure 3.4-5 The volume based particle size distribution of 10 mg/mL β-Lg in 0–50% ethanol/water solvents (v/v) (A); the corresponding mean sizes (B).

3.4.3.3 Comparison between free and immobilized trypsin for the hydrolysis of β-Lg

The greatly increased molecular size of β-Lg in the presence of 40% or 50% ethanol (Fig. 3.4-5) indicated that an aggregation indeed took place because of the enhanced hydrophobic interactions. A study (Leeb et al., 2015) reports that the subsequent aggregation after the heat denaturation of β-Lg decreases the accessibility of trypsin toward the cleavable sites on β-Lg. Thus, a relative low concentration of ethanol is preferred here, whereby the protein is present in an intermediate form and the aggregation does not yet occur. In addition, the highest activity of MITR was detected at 20% ethanol (Fig. 3.4-3). Hence, the hydrolysis of β-Lg was only conducted with or without 20% ethanol.

Hydrolysis efficiency and depletion of intact β-Lg

Previously, we systematically investigated the influence of flow rate on the hydrolysis efficiency for MITRs, and found that at a high flow rate, such as 10 mL/min, the substrate molecules could be sufficiently supplemented at a recirculation approach, thus, a dramatic ratio of enzyme/substrate (the amount of enzyme is much higher than substrate) did not exist (Mao et al., 2017). In this earlier investigation, MITR (N2) showed significant activity toward β-Lg at room temperature, i.e., the final DH reached 9.68% (86.58% of total cleavage sites) within 4 h (25 mL β-Lg at 10 mg/mL and pH

7.8). Besides, at the optimal temperature of free trypsin 37°C, the enzyme selectivity is with little chance to be controlled by other environmental conditions, like pH, as temperature is the dominating influencer (Cheison, Leeb, Toro-Sierra & Kulozik, 2011). We expected to regulate the enzyme selectivity with the addition of ethanol. Hence, all hydrolysis experiments were conducted at 25 ± 1°C, and a flow rate of 10 mL/min was applied for the hydrolysis by MITR.

The hydrolysis efficiency was evaluated based on the evolution of DH depending on hydrolysis time, as shown in Fig. 3.4-6 A1 for free trypsin and in Fig. 3.4-6 B1 for MITR. At the beginning, the increase in DH using free trypsin was much faster than that using MITR, i.e., DH values of 0.35 ± 0.18% and 0.18 ± 0.07% were detected for free and immobilized trypsin after 5 min, respectively. The addition of 20% ethanol significantly accelerated the DH increase for MITR by around 128% at 5 min. A higher enzymatic activity of MITR (Fig. 3.4-3) and an intermediate state of β-Lg in the presence of 20% ethanol are supposed to contribute to the faster increase in DH. However, ethanol did not consistently accelerate the DH increase for MITR, because DH reached 4.43 ± 0.52% after 3 h, which was only 12% higher than that without ethanol. For free trypsin, a faster increase in DH was observed with the addition of 20% ethanol after 1 h hydrolysis, and the DH reached 7.56 ± 0.95% after 3 h, increasing by 20% than that in aqueous media.

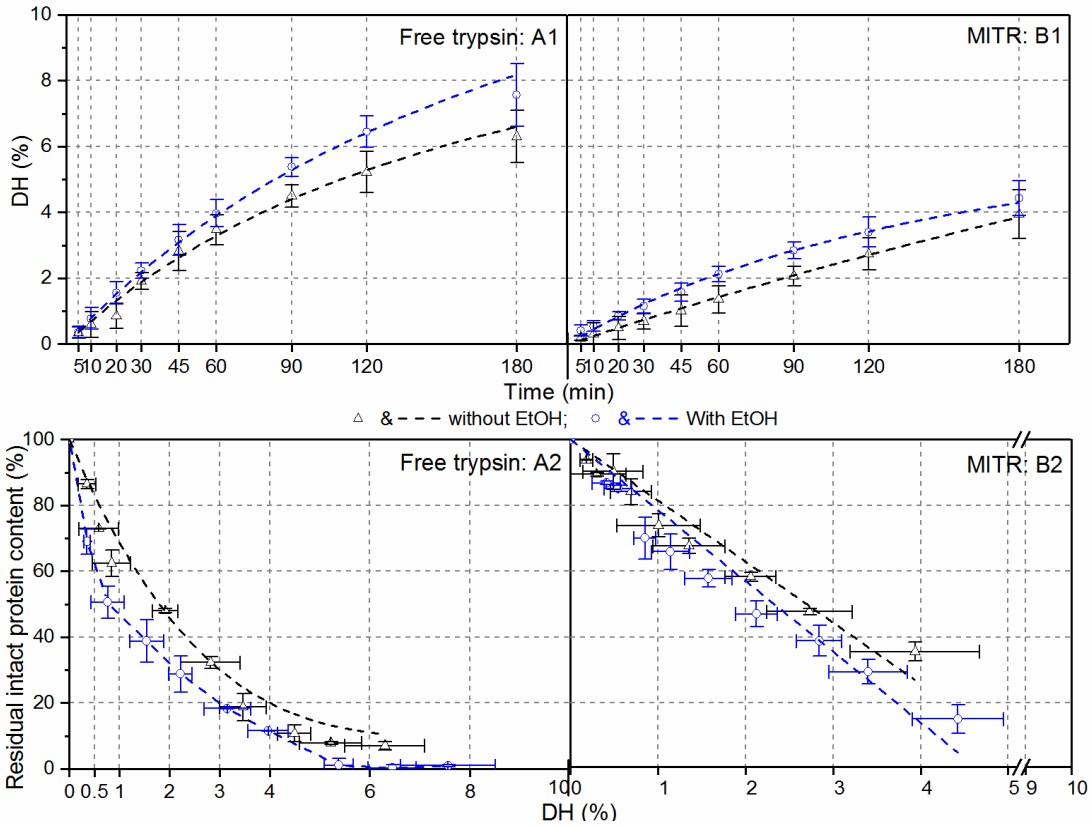

Figure 3.4-6 The evolution of DH as a function of time (A1 & B1), and the depletion rate of intact β-Lg as a function of DH (A2 & B2). (A): the hydrolysis of β-Lg by free trypsin; (B): the hydrolysis of β-Lg by immobilized trypsin.

To describe the hydrolysis of intact β-Lg, Linderstrøm-Lang (1952) suggests two models on protein hydrolysis, i.e., “one-by-one”: enzyme may split all the possible peptide bonds in each substrate molecule before it goes to the next; and “zipper”: enzyme runs from molecule to molecule and breaks one peptide bond in each before it starts to cleave another bond. In fact, all naturally occurring proteolytic reactions show an intermediate behavior between these two models, while might be tendentious to one of them. This tendency depends not only on the nature of substrate and enzyme, but also on hydrolytic conditions. For immobilized trypsin, only a linear decrease in intact protein content as a function of DH was observed, which is close to the “one-by-one” model, while the addition of 20% ethanol generally contributed to a faster depletion rate of intact protein (Fig. 3.4-6 B2). For free trypsin, a sharp increase in the depletion of intact β-Lg was noted at the initial stage of hydrolysis with 0 or 20% ethanol, i.e., the increase in DH from 0 to 1% corresponded to a depletion of 40–50% intact protein content, which is more in agreement with the “zipper” model (Fig. 3.4-6 A2). For free trypsin, intact protein was also depleted faster in the presence of 20% ethanol than in water. Namely, no more intact protein was detected at DH 5.38% in 20% ethanol, while 6.93% of intact β-Lg still remained in aqueous media at DH 6.30%. The different behaviors between free and immobilized trypsin on hydrolyzing intact β-Lg are probably because of the different interacting mechanisms between substrate molecules and free/immobilized trypsin, which will be discussed later inclusive the results on the release of peptides.

Comparison of the peptides release

The chromatographic profiles of hydrolysates generated from β-Lg hydrolysis by free or immobilized trypsin are illustrated in Fig. 3.4-7, including the identified peptides or the detected masses for each peak. The peaks eluted after 45 min, corresponding to polypeptides, are not well separated. A complex mixture of peptides was found in each fraction (A–I), and some detected masses were not able to be assigned to specific peptides, leading to a failure in analyzing the whole set of peptides. As shown in Fig. 3.4-7 A, all samples mainly contained polypeptides f(41–70), f(71–138), f(78–138), f(102–138), f(92–138), etc.. The accumulation of these polypeptides was partly due to the fast breakdown of intact β-Lg. The hydrolysates generated from both forms of trypsin exhibited a greater peak area of polypeptides in the presence of 20% ethanol, corresponding to the faster depletion rate of intact β-Lg in Fig. 3.4-6 A2 & B2. In addition, more abundant peaks were eluted after 45 min for the samples generated from free trypsin than those from MITR, indicating that immobilized trypsin showed more focused attacks toward cleavage sites on β-Lg than free trypsin.

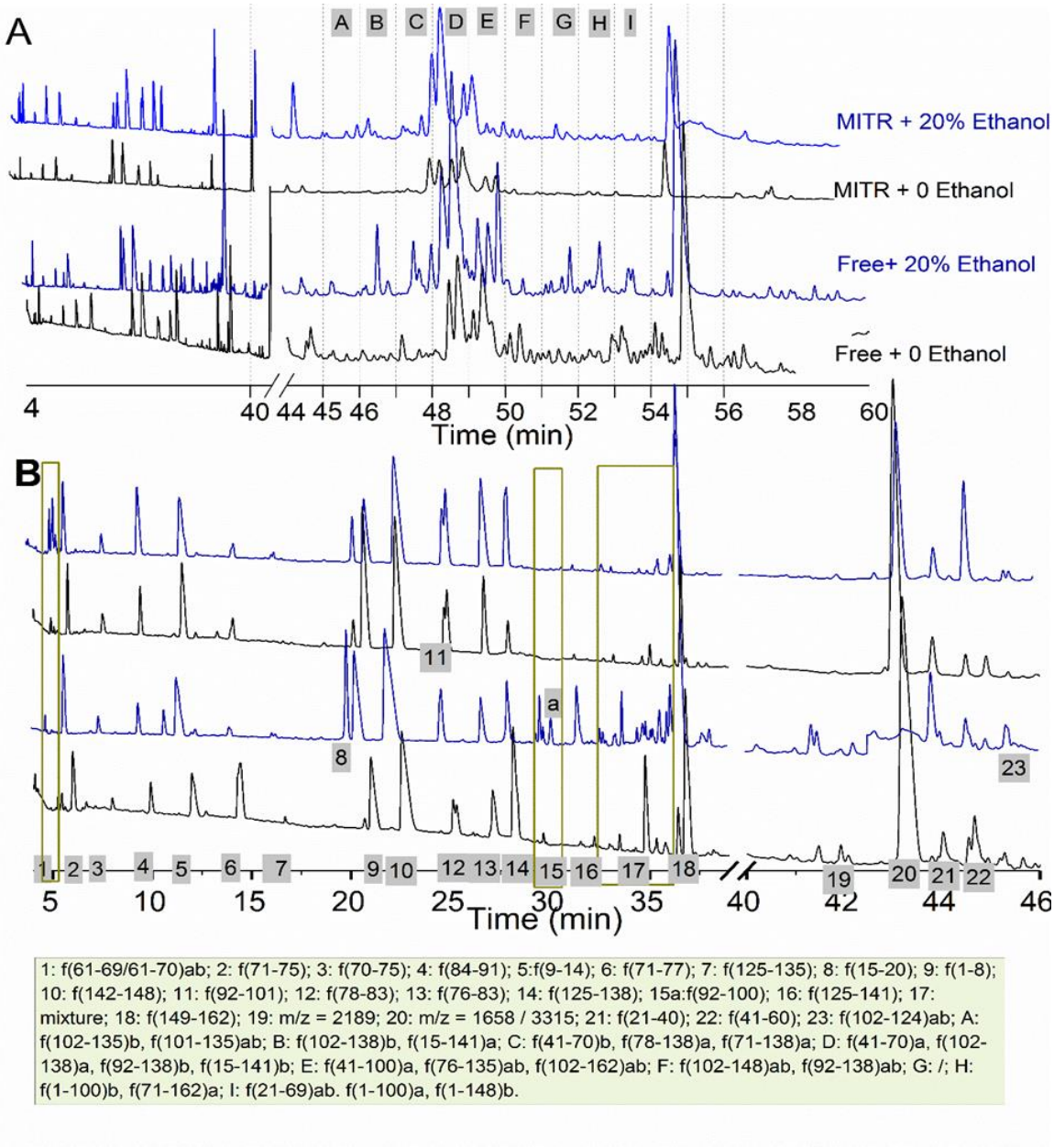

Figure 3.4-7 Chromatographic profiles of hydrolysates generated by free and immobilized trypsin after 3 h in 0 and 20% ethanol/water solvents (A). The chromatogram before 45 min are highlighted in (B).

The DH dependent release of identified peptides eluted before 45 min, is shown in Fig. 3.4-8. For both forms of trypsin in aqueous media, the peptides f(1–8), f(9–14), f(71–75), f(142–148), and f(149–162) increased quickly at the initial stage of hydrolysis. The addition of ethanol significantly decelerated the releases of peptides located on the C-terminal region, irrespective of free or immobilized trypsin was applied. On the contrary, the addition of ethanol showed significantly promoting effects on the release of final peptides f(15–20), f(21–40) and f(61–69/61–70), for both forms of trypsin. Particularly, the amount of peptide f(71–75) greatly increased at the very beginning during the hydrolysis by free trypsin in ethanol/water solvent, corresponding to the extremely fast depletion of intact β-Lg (Fig. 3.4-6 A2). For MITR, the release of peptides

f(71–75) and f(84–91) decreased significantly due to the addition of ethanol, while the released amount of peptide f(125–138) increased by a large extent.

To quantitatively illustrate the influence of ethanol on the release of final peptides, the R values of individual peptides are compared in Table 3. A peptide with a higher R value indicates that this peptide has the priority versus other peptides to be released during the hydrolysis. If all final peptides released at the same rate, R values would be 100% for all. At 5 min, similar final peptides, locating on the N- and C- terminal regions or the outer surface of β-Lg, were observed for free and immobilized trypsin. The final peptides located in the inner core of β-Lg were not detected, except peptides f(84–91) and f(125–135), which were released in 5 min by free trypsin in the presence of ethanol. With the hydrolysis, more and more final peptides were detectable, and the difference in R values tended to be insignificant. The fast consumption of intact β-Lg and the continuous accumulation of certain intermediate peptides resulted in that more cleavage sites in the protein inner core were exposed. This correlates well with a recent study, which reports a bimodal demasking process with a fast part at the beginning and lag-type kinetics of release for peptides during the tryptic hydrolysis of β-Lg (Vorob'ev, 2019). However, peptides f(92–100), f(102–124) and f(125–135) still showed very low R values after 3 h hydrolysis for both forms of trypsin, correlating to the large peak areas of their precursor peptides in fractions from B to E in Fig. 3.4-7 A. In particular, peptide f(125–135) showed negligible amounts during the hydrolysis by MITR. In the conclusion of Deng et al. (2017), trypsin shows low accessibility toward a cleavage site, when both amino acids on neighbor positions of this cleavage site are charged, such as Lys_{100} and Lys_{135}. Thus, the influence of primary structure can explain such low R values for these three peptides.

According to Table 3.4-3, ethanol exerted significant influence on the release of final peptides, especially at the initial stage of hydrolysis. For both forms of trypsin, the R values of peptides locating on C- termini decreased after the addition of ethanol, which is more pronounced for immobilized trypsin, i.e. 9.4 and 4.7 times lower of R values were observed for peptide f(149–162) and f(142–148). Overall, 20% ethanol showed reducing effects on the release of final peptides for immobilized trypsin at the beginning, such as f(71–75) (a negligible amount at 5 min was observed). However, for free trypsin, the addition of ethanol largely promoted the release of several final peptides. For instance, the R values of peptides f(1–8) and f(71–75) increased by 1.8 and 3.3 times. As the hydrolysis by MITR in 20% ethanol showed a faster increase in DH, it is speculated that in 20% ethanol immobilized trypsin prefers to attack certain cleavage sites which is different from those in water, such as Lys_{138}, as a 5 times higher amount of f(125–138) was detected (Fig. 3.4-8).

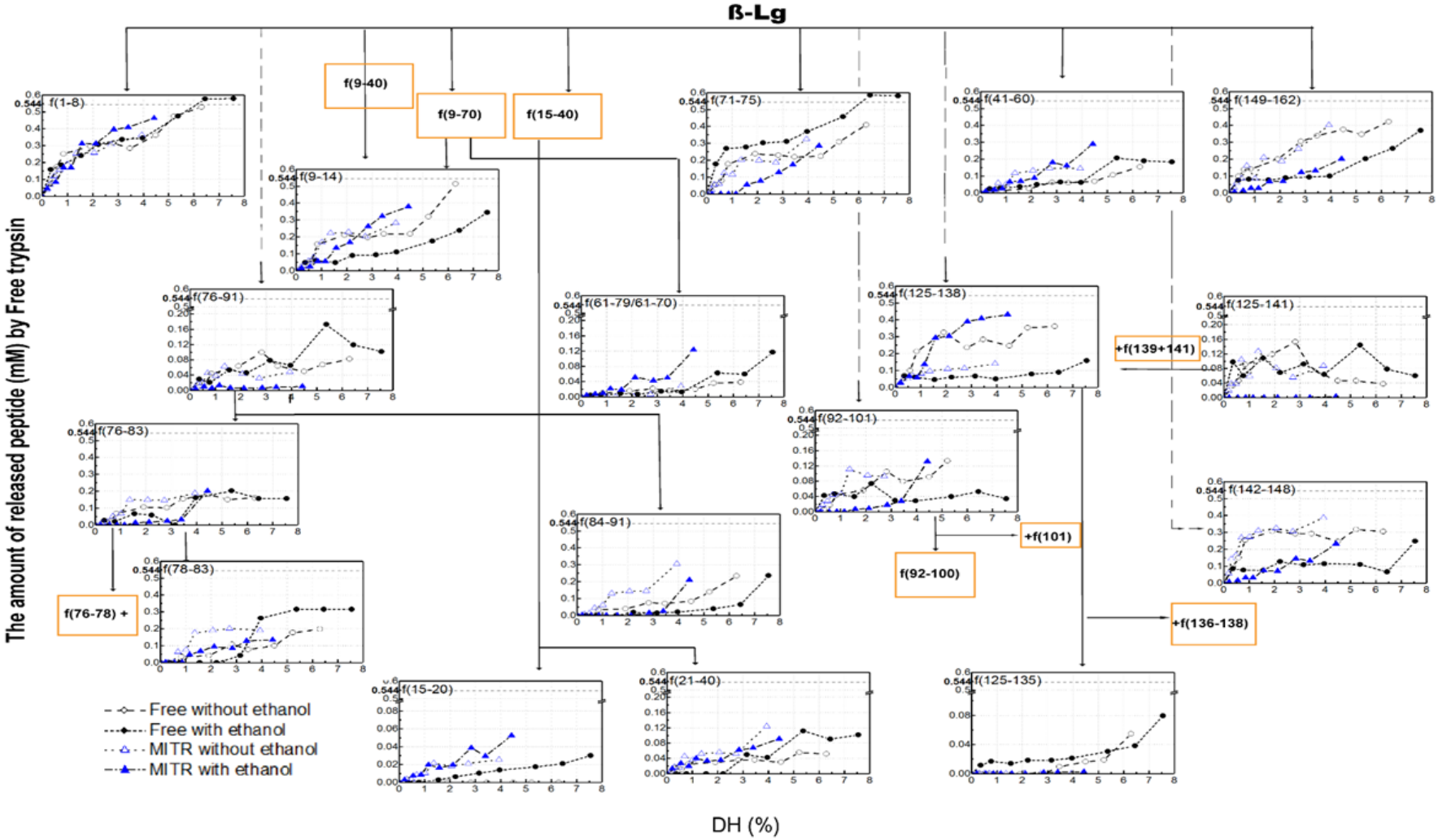

Figure 3.4-8 The evolution of peptides as a function of DH. The solid arrow indicates that the peptide is released from the intact protein or a confirmed intermediate peptide. If one peptide is generated from an uncertain polypeptide, a dashed arrow is used. Free trypsin: ○ (without ethanol), ● (with ethanol); MITR: Δ (without ethanol), ▲ (with ethanol).

Table 3.4-4 The relative amount of the released peptide based on the relative DH (R value) for individual final peptides generated from the β-Lg hydrolysis by free or immobilized trypsin in 0 or 20% ethanol/water solvent at 5, 60 and 180 min.

	5 min				60 min				180 min			
	Free trypsin		MITR		Free trypsin		MITR		Free trypsin		MITR	
Peptide	Water	20% EtOH	Water	20% EthOH	Water	20% EtOH	Water	20% EtOH	Water	20% EtOH	Water	20% EtOH
f(1-8)	551.0	968.7	447.1	458.5	177.0	187.3	406.2	317.5	181.5	165.4	198.9	226.1
f(9-14)	170.9	294.2	251.6	139.1	135.3	60.2	354.7	172.0	176.2	98.7	155.7	184.8
f(41-60)*	51.2	154.5	80.6	83.6	38.1	34.2	186.8	89.6	52.9	52.3	79.6	141.7
f(61-69/61-70)	13.9	29.1	0.0	44.5	10.1	6.8	0.0	52.2	13.3	33.5	15.2	60.1
f(71-75)	328.8	1079.0	274.6	0.0	136.3	201.5	327.1	79.1	140.8	166.4	178.8	138.9
f(78-83)	0.0	0.0	0.0	0.0	48.0	142.9	282.0	96.2	68.3	90.3	105.5	65.7
f(84-91)	0.0	0.0	20.2	0.0	44.3	10.8	210.0	0.0	80.4	67.7	167.9	102.9
f(92-100)	0.0	0.0	0.0	0.0	0.0	0.0	0.0	0.0	0.0	5.0	5.5	2.8
f(102-124)	0.0	0.0	0.0	0.0	2.2	5.0	15.5	0.0	2.8	3.2	11.9	0.0
f(125-135)	0.0	69.0	0.0	0.0	6.0	11.6	0.0	0.0	18.7	22.7	0.0	2.9
f(142-148)	593.1	515.6	356.6	76.8	182.6	62.4	337.2	72.1	104.8	71.0	213.1	113.4
f(149-162)	600.3	463.1	685.5	73.3	211.4	54.2	494.6	71.2	145.1	105.9	221.0	98.1

The mechanism underlying the different influences on free and immobilized trypsin exerted by ethanol

In the case of free trypsin, the contact between substrate and enzyme depends on the fundamentals of Brownian movement, as well as on the intermolecular forces, mainly the electrostatic forces. For immobilized trypsin, as its flexibility is considerably reduced, substrate molecules are driven to the monolith wall largely by shear force firstly and then attracted by immobilized trypsin through intermolecular forces. This process is influenced by the mass transfer properties, as well as by the characteristics of the monolith surface covered by immobilized trypsin molecules.

The mass transfer in monolithic MITRs is exclusively convective and laminar (Podgornik et al., 2014). With laminar flow key solute dispersion comes from laminar dispersion, thus, all solutes flow with the current regardless of their sizes theoretically are transported at the same rate. This first transportation of substrate molecules by shear force can largely reduce the independent selectivity of immobilized trypsin. This might explain that the depletion of intact protein by immobilized trypsin tends to a “one-by-one” model, which is dramatically different from free trypsin. In addition, the monolith surface used as the immobilization support in this study is preferentially neutral (Naldi et al., 2017), and the coverage ratio of trypsin molecules on the surface of MITR (N2) is high, about 65 ± 10%. Thus, the surface charge and hydrophobicity of the monolith surface is considered to be the same as that of the formed layer by immobilized trypsin molecules. The immobilization of trypsin was performed at pH 5.6, where the overall surface charge of trypsin molecules is, in theory, highly positive, as its isoelectric point is 10.1–10.5 (Buck, Vithayathil, Bier & Nord, 1962). Based on the fundamentals of electrostatic interactions, each trypsin molecule probably re-orientated its position to reach a charge balance with other trypsin molecules during the immobilization. Hence, the attractive force between substrate molecules and immobilized trypsin is probably different from that for free trypsin which is mainly dependent on electrostatic interactions (Evnin, Vásquez & Craik, 1990). It is postulated that hydrophobic interactions might significantly contribute to the interactions between substrate and immobilized trypsin. Thus, the addition of ethanol, leading to changes in the surface hydrophobicity of substrate molecules, largely altered the accessibility of immobilized trypsin, but did not shift the preference of free trypsin greatly.

3.4.4 Conclusion

Flow-through MITRs were developed using different immobilization protocols. Compared with the use of NaCNBH3, the application of 2-PB led to a lower immobilization yield, while could improve the specific activity of immobilized trypsin. In addition, the covalent immobilization largely stabilized trypsin molecules against structural distortion induced by ethanol. Interestingly, the addition of ethanol up to a certain concentration (20% here) even improved the activity of immobilized trypsin. Thus, it is feasible to produce protein hydrolysates using MITR with the integration of ethanol.

This study reports, for the first time, the selectivity of trypsin after its immobilization in the absence/presence of ethanol. Different from specificity, selectivity means the differences in the affinity of one enzyme towards the theoretical cleavage sites on a substrate. This is a better indicator to regulate the hydrolysis process. The presence of ethanol assisted the hydrolysis of intact β-Lg, as well as influenced the hydrolysate profiles. For both forms of trypsin, the release of peptides locating on C- termini decreased after the addition of ethanol, which is more pronounced for immobilized trypsin. In the contrast, the release of peptides locating inner β-Lg increased significantly due to the addition of 20% ethanol. Furthermore, immobilized trypsin preferentially attacked certain cleavage sites in ethanol/water solvent, such as Lys_{138}. Hydrophobic interactions might play an important role in the interactions between immobilized trypsin and substrate.

Acknowledgements
This research did not receive any specific grant from funding agencies in the public, commercial, or not-for-profit sectors. The first author thanks China Scholarship Council (China) for the support of her personal cost. The authors would like to thank Urh Černigoj from BIA Separations (Ajdovščina, Slovenia) for his technical help in developing the MITR.

Conflicts of interest: None

3.5 Selective hydrolysis of whey proteins using a flow-through monolithic reactor containing immobilized trypsin

Summary and contribution of the doctoral candidate

Previous studies provide proof of concept for selectively hydrolyzing β-Lg in whey proteins using trypsin. However, the high cost of large-scale trypsin use in solution severely limits this application to industrial implementation. Correspondingly, immobilized trypsin represents an alternative approach due to the possibility of reusing the enzyme and producing enzyme-free hydrolysates. Hence, this study examined the applicability of the MITR for selectively hydrolyzing β-Lg in whey protein isolate (WPI). Specifically, β-Lg was selectively hydrolyzed by the immobilized trypsin in the CIM-MITR-8 mL at ambient temperature, resulting that above 85% α-La remained native in the final hydrolysates. Despite the inaccessibility of the immobilized trypsin to α-La at all explored conditions, its accessibility toward β-Lg was pH and ionic strength dependent. Namely, higher pH (15% residual at pH 9.2 vs 60% at pH 7.8) and lower ionic strength (30% residual at 0 M NaCl vs 70% at 0.1 and 0.25 M NaCl) was preferential. In addition, the increase in flow rate (up to 32 mL/min) contributed to the hydrolysis efficiency of immobilized trypsin and did not affect its ability to deplete β-Lg.

The developed CIM-MITR-8 mL in this study was able to be operated at high flow rates while maintaining low backpressure, which significantly improved its productivity. The 11 mg trypsin immobilized on the CIM monolithic column through a multipoint covalent binding technique remained stable over 30 cycles of intensive uses, thus demonstrating the CIM-MITR to be cost effective, time efficient, and reusable. These above advantages render the CIM-MITR suitable for large-scale operations.

Most significant contribution to this manuscript was made by the doctoral candidate. This comprised (i) the conception and design of experiments based on preceded critical literature review; (ii) experimental conduction on the characterization or IMTRs, protein hydrolysis, and hydrolysates analysis; (iii) data analysis and data interpretation. In addition, writing and revising of the manuscript was done by the doctoral candidate.

Adapted original manuscript[5]

Selective hydrolysis of whey proteins using a flow-through monolithic reactor containing immobilized trypsin

Yuhong Mao[a*] & Ulrich Kulozik[a,b]
[a]Chair of Food and Bioprocess Engineering, [b]Institute of Food and Health (ZIEL)–Technology Unit, Technical University of Munich
Weihenstephaner Berg 1, D-85354, Freising-Weihenstephan, Germany

Abstract: The present study developed a monolith based immobilized trypsin reactor (MITR) with 6.2 µm pore size and 8 mL bed volume. This MITR selectively hydrolyzed β-Lactoglobulin (β-Lg) in whey protein isolate (WPI) at 25 ± 1°C resulting that above 85% α-Lactalbumin (α-La) remained as native in all obtained hydrolysates. In kinetic analysis, the existence of α-La led to a three-fold decrease in Vmax of hydrolyzing β-Lg. Raising flow rate from 0.8 to 32 mL/min, reduced 45% the required time reaching DH 4%, but did not affect the enzymatic preference toward intact β-Lg. Furthermore, immobilized trypsin exhibited greater accessibility to intact β-Lg as the pH increased (7.8–9.2) and as the NaCl concentration decreased (≤ 0.05 M). Only 14.75 ± 10.14% β-Lg at DH 4% was detectable (pH 9.2, without NaCl). This MITR provides high potential for large-scale use to produce a whey product rich in native α-La while hydrolyzed β-Lg.

[5] Adaptions refer to formatting issues: e.g., numbering of sections, figures, tables and equations, abbreviations, manufacturer specifications, axis labeling, figure captions and style of citation.

[5] Originally published in: *International Dairy Journal* (2018), Vol. 85, pp. 96-104. Permission for reuse of this article was granted by Elsevier.

3.5.1 Introduction

Whey is a major co-product from cheese manufacturing. Whey mainly consists of β-lactoglobulin (β-Lg) and α-lactalbumin (α-La), which represents approximately 53% and 20–25% of whey proteins, respectively (Edwards & Jameson, 2014). β-Lg acts as a primary allergen, especially in infant formulae, as it is not present in human milk. On the contrary, the amino acid composition of bovine α-La shows a 72% sequence homology to human α-La, which plays an important role in the lactose synthesis (Lisak et al., 2013). Hence, a whey product rich in native α-La with zero to low allergenicity appears to be very attractive.

Enzymatic hydrolysis is a common approach to reduce the allergenicity of proteins by cleaving the antigenic regions (Lowe, Dharmage, Allen et al., 2013). Along with the reduction in allergenicity of β-Lg by enzymatic hydrolysis, the results of bioactivities (Hernandez-Ledesma, Recio & Amigo, 2008) reported for its peptide fragments are exciting as well. In addition, Schmidt and Poll (1991) indicated that, contrary to native β-Lg, native α-La was resistant to tryptic digestion. This action highly depended on the composition of medium (Ca^{2+}, buffer, pH, etc.), incubation temperature and the degree of denaturation of the protein. Taking advantage of this trypsin selectivity, Konrad and Kleinschmidt (2008) succeeded in isolating α-La with 90-95% purity from whey proteins by applying tryptic hydrolysis (42^{o}C, pH 7.7) and membrane filtration. However, only 15% α-La was recovered mainly due to the high hydrolysis temperature. Actually, increasing the temperature near or above the trypsin optimum of 37 °C resulted in less controlled hydrolysis of whey proteins, with low resistance of α-La to trypsin (Cheison et al., 2011). To improve the yield of α-La, Cheison et al. (2011) optimized the conditions for tryptic hydrolysis of whey protein isolate (WPI), and 67.87% α-La was recovered at pH 8.5 and 25^{o}C. These findings provide proof of concept for selectively hydrolyzing β-Lg in whey proteins using trypsin.

However, the high cost of large-scale trypsin use in solution severely limits this application to industrial implementation. Correspondingly, immobilized trypsin represents an alternative approach due to the possibility of reusing the enzyme and producing enzyme-free hydrolysates. In particular, a flow-through hydrolysis system offers better process control than batch-based methods. To produce protein hydrolysates using immobilized enzymes, some groups (Atacan, Cakiroglu & Ozacar, 2016b; Bassan, de Souza Bezerra, Peixoto et al., 2016) have sought to develop particle based immobilized enzymes systems. These systems still suffer from low capacity in terms of volume throughput, as well as low processing stability due to high backpressure over use. Our previous work (Mao et al., 2017) reported the monolithic columns (bed volume 1 mL, nominal pore sizes 2.1 and 6 µm) based immobilized trypsin reactors (MITRs), which showed significant activity towards β-Lg. In that study, the MITR with 6 µm pore size showed constant backpressure over intensive uses for producing β-Lg hydrolysates, whereas the 2 µm-MITR exhibited increasing backpressure. This was due to the 7.8 times higher permeability when the pore size increased from 2 to 6 µm. However, because of the increase of pores, the surface area

deceased 60% correspondingly 40% less amount of immobilized trypsin. These led to the failure of 1-mL MITRs for hydrolyzing WPI, i.e., clog problem in 2 μm-MITR was too serious (backpressure increased after only 5 uses), and long hydrolysis time (up to 8 h for DH 4%) was required by using 6 μm-MITR. In this study, we scaled up the bed volume of MITR with 6 μm pore size to 8 mL so that its surface area was enough for trypsin immobilization, and simultaneously it was still highly permeable.

Although free trypsin selectively hydrolyzes β-Lg in whey proteins under certain conditions (Cheison et al., 2011; Schmidt & Poll, 1991), this selectivity may change upon its immobilization. Actually, our previous work (Mao et al., 2018) found that immobilization of trypsin led to the changes of its preference to individual cleavage sites in β-Lg. Hence, the main purpose of this study was to examine the applicability of the MITR for selectively hydrolyzing β-Lg in WPI.

As the performance of enzymes strongly depends on environmental conditions, we systematically investigated the influence of flow rate, pH, and ionic strength. As discussed before, much higher resistance to free trypsin by α-La was detected at < 30^{o}C (Cheison et al., 2011). In addition, Rocha, Gonçalves and Teixeira (2011) found that immobilized trypsin (on spent grains) showed similar accessibilities to β-Lg and α-La above 37^{o}C. Hence, we conducted all hydrolysis experiments at ambient temperature, where β-Lg was able to be efficiently hydrolyzed by MITRs-1 mL (Mao et al., 2017). In addition, kinetic studies as functions of flow rate and substrate resource (single or mixture) were undertaken. The long-term stability and reusability of this MITR was monitored throughout the entire study.

3.5.2 Materials and methods

3.5.2.1 Materials

WPI powder (93.84% protein) was a product of Fonterra Co-operative Group Ltd, Auckland, New Zealand and contained 91.87% native whey proteins (18.68% α-La, 32.07% β-Lg B, 41.13% β-Lg A). Trypsin from bovine pancreas (Type I, ~10,000 BAEE units/mg protein), Nα-Benzoyl-L-arginine ethyl ester (BAEE, B4500), tris (hydroxymethil)-aminomethane (Tris), sodium hydroxide, and calcium chloride were purchased from Sigma–Aldrich (St Louis, MO, USA). The reagents used for the immobilization of trypsin were identical to those described in our previous work (Mao et al., 2017). Deionized water was acquired from a MilliQ System (Millipore Corporation, Bedford, USA).

3.5.2.2 Characterization of MITR

An aldehyde activated Convective Interaction Media® (CIM®) radial column (CIM-ALD, tube dimensions: outer diameter (D) – 1.50 cm, inner diameter (d) – 0.65 cm, height (h) – 5.6 cm; bed volume 8.0 mL) with nominal pore size diameter of 6 μm and 60% porosity was provided by BIA Separations d.o.o. (Ajdovščina, Slovenia). Trypsin was covalently immobilized on this CIM-ALD monolithic column using the protocol described by us previously (Mao et al., 2017). The amount of immobilized trypsin was

11 mg in the whole MITR, and 1.4 mg/mL of the bed volume. The MITR was additionally characterized for permeability and enzymatic activity.

Evaluation of permeability

To calculate the permeability, the backpressures without and with MITR were recorded at increasing flow rates, namely 4, 8, 16, 32 and 48 mL/min, by pumping deionized water. The difference between these two values at a defined flow rate was considered to be the pressure drop created by the inserted reactor. According to the study of Podgornik et al. (2014), the permeability of a monolith was calculated according to Eq. 3.5-1:

$$B = \frac{F}{\Delta P} \times \frac{\eta \times \ln(\frac{D}{d})}{2\pi h} \quad (3.5\text{-}1)$$

Where, B (m^2) is the calculated permeability of the monolith; ΔP (MPa) is the pressure drop; η is the viscosity of mobile phase (0.87685 mPa*s for deionized water); F (mL/min) is the volumetric flow rate; D (m) and d (m) are outer and inner tube diameters, and h (m) is monolith height.

Determination of activity units

Using BAEE as a low molecular mass substrate, the enzymatic activity of immobilized trypsin was measured employing zonal approach. The MITR was inserted in an Äkta Explorer system (GE Healthcare Bio Sciences) with 100 mL pump heads. 20 mM Tris-HCl containing 19 mM $CaCl_2$ was used as a buffer to equilibrate the reactor and dissolve BAEE. A loop of 6 mL was used to inject BAEE solution with increasing concentrations at 24 ± 1°C, namely 1, 3, 10, 30, 100 mM. The BAEE solution was injected at 80 mL/min, and 100 or 200 mL eluents were collected. The amounts of the substrate BAEE and its product N-α-benzoyl-D, L-arginine (BA) were chromatographically separated by high-performance liquid chromatography (HPLC) analysis. The Michelis-Menten graph was obtained and the apparent V_{max} value was calculated as described by Naldi et al. (2017).

3.5.2.3 Hydrolysis of WPI by MITR

WPI powder was dissolved in deionized water and stirred for 15 h at 4°C to allow complete hydration. To remove denatured whey proteins, the pH of the obtained WPI solution was adjusted to 4.6 (Dannenberg & Kessler, 1988) at ambient temperature, and then centrifuged at 6 000 g for 10 min, the supernatant was filtered through cellulose membrane with a cut-off of 0.45 µm. The prepared WPI solution was further altered according to the experimental design (changes in pH, ionic strength, and concentration).

The MITR was inserted in an ÄKTA™ pure system (GE Healthcare Bio Sciences) consisting of a sample pump (S9), system pumps, auto-sampler (F9-R) and detectors for UV (U9-M), pH, temperature and conductivity. The system was controlled using Unicorn Software 7. Before each hydrolysis cycle, the reactor was washed using 10 column volumes (CVs) of deionized water, and pre-conditioned with 15 CVs 0.1 M Tris-HCl buffer at the same pH value as the applied substrate solution. The flow rate was

16 mL/min. The hydrolysis was performed using recirculation or single flow-through approach.

Recirculation approach

96 mL WPI solution with the concentration of 20 mg/mL was used. The first 2 CVs (16 mL) was discarded, and then a total 80 mL of substrate solution was recirculated for the hydrolysis. The degree of hydrolysis (DH) was measured by auto-titrator (TitroWiCo, Werner Cornelius, Bochum, Germany) and calculated using Eq. 3.5-2 according to the pH-stat method (Adler-Nissen, 1986).

$$DH = \frac{h}{h_{tot}} \times 100\ \% = \frac{V_b \times N_b}{\alpha \times M_p \times h_{tot}^*} \times 100\% \quad (3.5\text{-}2)$$

where, V_b (mL) is the base consumption; N_b is normality of the base (0.5 M NaOH); α is average degree of dissociation of the NH groups; M_P (g) is the mass of protein; h_{tot}^* is total number of peptide bonds in one gram protein substrate (8.8 meqv/g for WPI).

In addition, the initial depleting rate of β-lg (R) was calculated according to Eq. 3.5-3

$$R = \frac{\Delta C \times V}{t} \quad (3.5\text{-}3)$$

Where, R (μmol/min) is the depleting rate of β-Lg, ΔC (μmol/mL) is concentration difference at DH 0 and 0.5%, V is the volume of substrate solution (80 mL), and t (min) is the time reaching DH 0.5%.

All hydrolysis experiments were conducted at 24 ± 1°C. The recirculation time was set up to 8 h in the software, but it was manually terminated when the DH reaching the final desired values (i.e. DH 4% or 8%). Aliquots (1 mL) were drawn out at different DHs from 0 to 4%. To explore the influence of recirculation flow rate (0.8, 4, 8, 16, 32 mL/min), WPI solution at pH 8.7 without NaCl was used. For pH effects (pH 7.8, 8.3, 8.7 and 9.2), hydrolysis was performed at 32 mL/min without adding NaCl. To evaluate the effect of ionic strength (0, 0.05, 0.1 and 0.25 M NaCl corresponding to increasing conductivity 2.70, 6.46, 10.46 and 24.60 ms/cm), pH was 8.7 and flow rate was 32 mL/min.

Single flow-through approach

To explore the apparent kinetic parameters of depleting β-Lg in WPI, the pre-treated WPI solution was mixed with 0.2 M Tris-HCl buffer (pH 8.7) at a ratio of 1:1 to reach the desired concentrations, i.e. 5, 10, 20 and 30 mg/mL. The MITR was pre-conditioned with 0.1 M Tris-HCl buffer (pH 8.7). 32 mL of the prepared WPI solution was pumped through the MITR and fractionated into 4 tubes by the auto-sampler, 8 mL in each tube. Increasing flow rates from 0.8 to 48 mL/min were investigated. The average native protein content in the last two tubes was used as the protein concentration of the hydrolyzed sample.

The depleting rate of β-Lg was calculated according to Eq. 3.5-4:

$$R = \frac{\Delta C \times v}{t} = \frac{\Delta C \times v}{v_{/F}} = C_d \times F \quad (3.5\text{-}4)$$

where, ΔC (μmol/mL) is the difference of β-Lg concentration in WPI solution before and after hydrolysis, v (mL) is pore volume (6.4 mL), t (min) is the retention time. Retention time is calculated by pore volume V (mL) and F (mL/min).

In addition, the pure β-Lg solution was used under the same conditions to evaluate the effect of other whey proteins, mainly α-La, on the depletion of β-Lg.

3.5.2.4 Washing and storage of MITR

After each hydrolysis experiment, the MITR was washed according to the following procedure: 0% 1 M NaCl (pH 10.5, adjusted by 1 M NaOH) in water linearly increasing to 100% 1 M NaCl over 10 CVs at 16 mL/min, and then 10 CVs of 100% this 1 M NaCl solution. Afterwards, 10 CVs of deionized water was passed through the MITR followed by 20 CVs of the storage solution (19 mM $CaCl_2$ in 5% ethanol/water (v/v), pH 3, adjusted by 1 M HCl). The MITR was stored at 4°C.

3.5.2.5 Determination of the residual protein

The obtained samples were firstly diluted with deionized water to a protein concentration around 2 mg/mL, and then the pH was adjusted to 4.6 before filtering through a 0.45 μm cellulose membrane. The native whey proteins contents (β-Lg A, β-Lg B and α- La) in the pre-treated samples was quantitatively determined by HPLC using an Agilent 1100 series HPLC system (Agilent Technologies) and a PLRP-S 300 A-8 μm Latek column (150 × 4.6 mm). The detailed gradient information was previously described by Leeb et al. (2015). α-La (91% purity, Sigma Aldrich L6010), β-Lg A (99% purity, Sigma Aldrich, L7780) and β-Lg B (98% purity, Sigma Aldrich, L8005) were used as standards to build the calibration curve.

3.5.2.6 Statistical analysis

Considering the potential decline of hydrolysis efficacy of the applied MITR, all hydrolysis experiments were carried out in triplicate and the three repeats under the same condition were conducted in a staggered way to reduce bias. Mean values ± standard deviation are reported. Data were plotted using Origin Pro 9.0.

3.5.3 Results and discussion

3.5.3.1 Characteristics of MITR

The design of the CIM tubular column allows the mobile phase to run in a radial direction from the outer to the inner surface. The scale-up of bed volume from 1 to 8 mL was realized by increasing the height of the column, namely from 4.2 to 56 mm. However, the short separation layer, through which the mobile phase passes, was maintained and even decreased from 6.05 to 4.25 mm in this case. To ensure the quality of this upscaled MITR-8 mL, its basic characteristics were compared with the

MITR-1 mL (pore size 5.80 µm and bed volume 1 mL) reported in our earlier work (Mao et al., 2017).

Basic characteristics

The total immobilized amount of trypsin in the 8 mL column was around 11 mg, resulting in an approximately twice-lower immobilized trypsin coverage density than that in the 1 mL column, as illustrated in Table 3.5-1. Considering Brunauer–Emmett–Teller (BET) surface area (approximately 2 m^2/g dry monolith with pore size 6 µm) and the molar mass of trypsin from bovine pancreas (23.8 kDa), each trypsin molecule in the MITR-8 mL occupied approximately 23 nm^2 of surface area, while only 11 nm^2 for each molecule in the MITR-1 mL, as calculated in Mao et al. (2017). Theoretically, one trypsin molecule would occupy between 10 and 20 nm^2 of surface (Naldi et al., 2017). Hence, the surface coverage of trypsin molecules in MITR-8 mL was still very high, in the range between 50 and 85%.

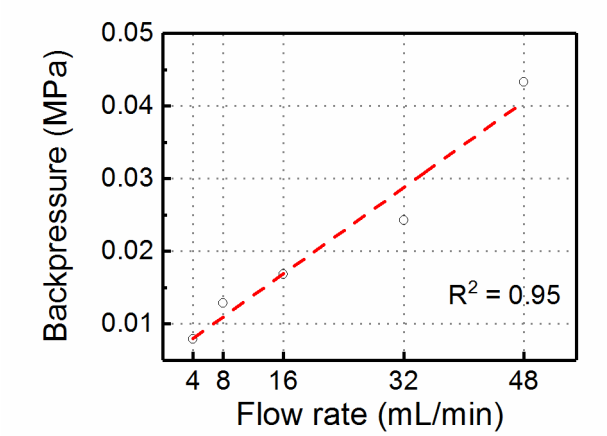

Figure 3.5-1. Initial backpressure of the MITR-8 mL at increasing flow rates

Low backpressure, corresponding to a high permeability, is a crucial requirement to prepare immobilized enzyme reactors capable of processing large amounts of protein. For the MITR-8 mL, a linear increase of pressure drop depending on flow rates was observed, as expected for constant permeability, proving that the porous monolithic structure was stable and no mechanical compression occurred, as illustrated in Fig. 3.5-1. Based on the pressure drop behaviour, the permeability was calculated to be 2.63 x 10^{-11} using Eq. 3.5-1, which was slightly higher than that of the MITR-1 mL (Table 3.5-1). Exact pore sizes of tested MITRs, determined by Hg porosimetry, were 5.8 µm and 6.2 µm for 1 mL and 8 mL MITR, respectively. Assuming the same porosity and structural constant, the permeability of CIM monoliths correlates linearly with a square of pore size (Podgornik et al., 2014), which was confirmed for both tested MITRs.

Enzymatic activity

BAEE, with a small molecular weight of 342.82 Da, was used as the model substrate to evaluate the enzymatic activity. It is important to ensure that the MITR works in steady-state conditions, thus allowing the estimation of maximum enzymatic activity.

Despite the knowledge that zonal approach of the BAEE activity determination is slightly misleading (underestimation of the apparent active units) (Naldi et al., 2017), it was used in our study due to the lower consumption of BAEE substrate compared to the continuous flow approach. The estimated maximum enzymatic activity calculated from Michaelis-Menten curve was 141 µmol/min. Calculating the specific activity in unit per mg trypsin, the two MITRs showed the similar enzymatic activity (Table 3.4-1).

Table 3.5-1 Characteristics of CIM-MITRs based on 8 mL and 1 mL bed volume

CIM-MITRs	Pore size (µm)	Bed volume (mL)	Density of immobilized trypsin (mg per mL monolith)	Permeability in deionized water (m^2)	Activity U* (µmol/min) per mg trypsin
MITR-8 mL	6.2 ± 0.3	8	1.4 ± 0.3	2.63×10^{-11}	12.82
MITR-1 mL*	5.8 ± 0.3	1	3.0 ± 0.3	1.91×10^{-11}	12.19

**The data for MITR-1 mL was reproduced from Mao et al. (2017) with permission.*

3.5.3.2 Influences of operational parameters on the hydrolysis of WPI

In this study, we investigated the influences of operational parameters, i.e., flow rate, pH, and ionic strength, on the hydrolysis of WPI. The hydrolysis was mainly characterized by DH and residual native proteins, including the comparison between α-La and β-Lg, as well as two genetic variants of β-Lg. Specifically, DH was rated based on the time to reach the same value, and the residual native proteins contents were evaluated as the function of DH.

The effect of recirculation flow rate

Flow rate is an important factor affecting the flow-through bioreactor performance. In contrast to conventional porous beads based supports, the only voids in a monolithic unit are the interconnected pores. Consequently, mass transfer is much faster due to the convective flow that becomes the dominant transport mechanism (Vodopivec et al., 2003).

As shown in Fig. 3.5-2 A, raising flow rate up to 32 mL/min, the required time reaching the same DH value was shorter. Especially from 0.8 to 4 mL/min, the time to reach DH 4% was reduced from 277.0 ± 26.8 min to 206.5 ± 34.2 min. This corroborates conclusions from the past investigations (Naldi et al., 2017; Ponomareva, Kartuzova, Vlakh et al., 2010), i.e. higher flow rates contribute to higher enzymatic efficiency. Except for faster mass transfer contribution at higher flow rates, the enhanced diffusivity of substrate molecules from the mobile phase to the monolith surface increased the number of efficient contacts between the molecules of substrate and immobilized trypsin, resulting in improved efficiency. In addition, the difference of efficacy at the initial stage of hydrolysis among the flow rates above 4 mL/min was negligible, while during hydrolysis, the DHs increased faster at 16 and 32 mL/min,

which was due to the decrease of substrate so that a higher flow rate was required to sufficiently replenish substrate. It is notable that the increased flow rate leads to a simultaneous increase in shear stress, which may mechanically degrade the immobilized enzyme (Bencina et al., 2007). For example, Bartolini et al. (2009) found that enhanced flow rates led to decreased hydrolysis efficiency. They speculated that the severe friction at higher flow rates reversibly modified the 3D structure of the immobilized enzyme. In our case, no degradation of immobilized trypsin was found at least up to 32 mL/min thanks to the 6.2 µm pore size of the monolithic support and the multipoint covalent binding technique. Regarding the depletion of native proteins, as shown in Fig. 3.5-2 B, C and D, 90% of the starting α-La remained at DH 4% whereas only 30% β-Lg was residual at all explored flow rates, which confirms the significant preference of immobilized trypsin toward β-Lg over α-La. Furthermore, the ability to deplete native β-Lg A and B as a function of DH was independent of the flow rate, and no significant difference between these two genetic variants was noted.

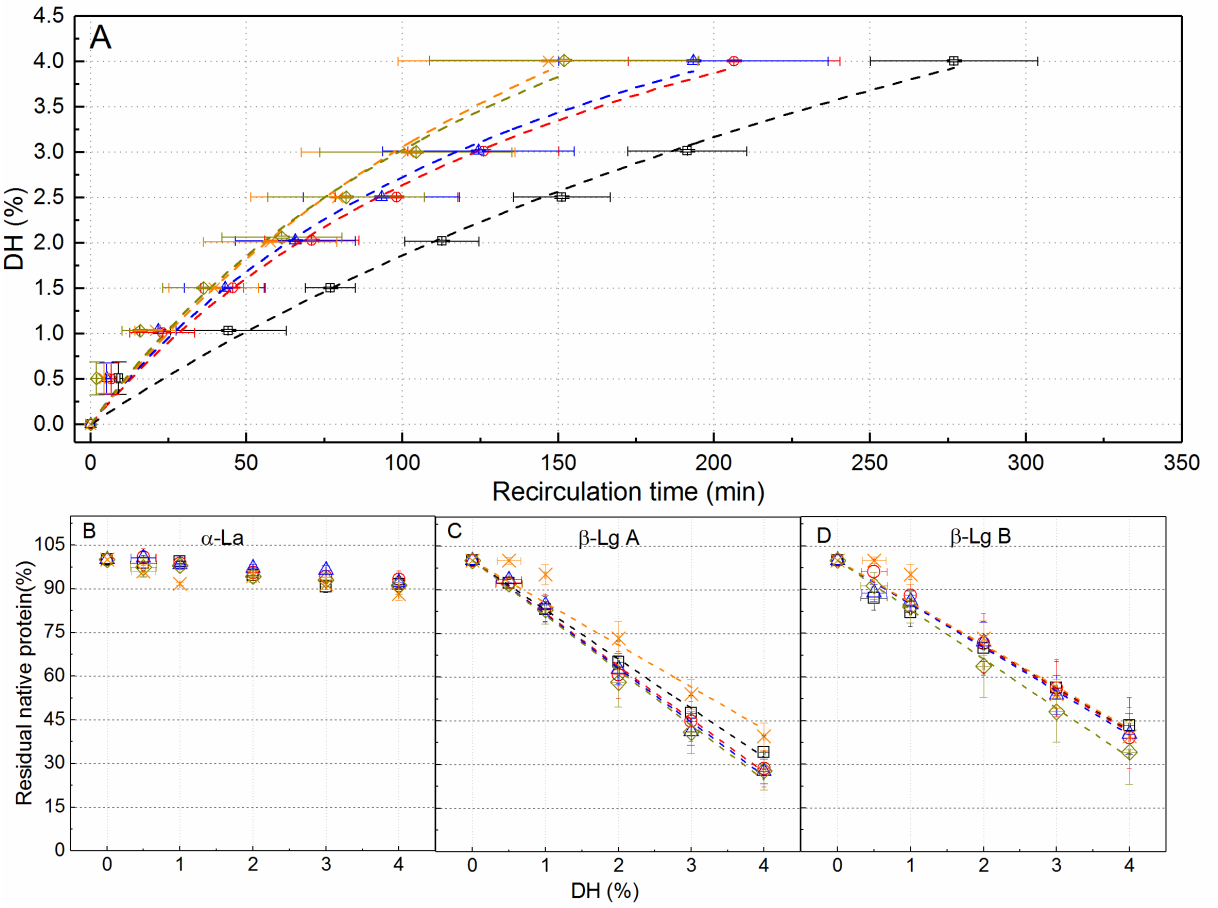

Figure 3.5-2. The hydrolysis of WPI at increasing flow rates 0.8 (□), 4 (○), 8 (Δ), 16 (x), 32 (◊) mL/min, respectively. A): Increase of DH as a function of time; B), C), and D) show the residual protein contents of α-La, β-Lg A and β-Lg B, respectively.

The effect of hydrolysis pH

It is well-known that enzymes are active only in certain pH ranges and each enzyme has a strongly defined pH optimum where its activity reaches a maximum. In our earlier work (Mao et al., 2017), the enzymatic activity of immobilized trypsin (based on

substrate BAEE) increased slightly from pH 7.8 to 9.2. However, as shown in Fig. 3.5-3 A, no significant difference in the efficiency of hydrolyzing WPI was observed, except for that at pH 8.3 where the DH increased faster than the others at the initial stage of hydrolysis. Likewise, Rocha, Gonçalves and Teixeira (2011) used the immobilized trypsin on spent grains for whey protein hydrolysis and suggested an optimal pH interval from pH 8 to 9 where the DH profiles were very similar between each other.

Although the highest hydrolysis efficacy was observed at pH 8.3, the depletion of β-Lg exhibited a clear dependence on the pH. Namely, at DH 4%, 68.20 ± 8.44% β-Lg still remained at pH 7.8, whereas only 14.75 ± 10.14% was detectable at pH 9.2. On the contrary, the increase of pH did not lead to the obvious hydrolysis of α-La, since 90% of the starting α-La remained in the final hydrolysates, especially at pH 7.8. The decrease of residual native β-Lg content as a function of DH indicates a preference for the hydrolysis of intact protein molecules versus the intermediate peptides. Hence, the observed results suggested that the formed intermediate peptides were more favoured at pH 7.8 and 8.3 than that at higher pH values. In the comparison of β-Lg A and B, the former was more accessible than the later at lower pH values, while at pH 8.7 and 9.2, the difference in their accessibility was insignificant. As discussed in our previous work (Mao et al., 2018), the pH-dependent structural characteristics of β-Lg contributed to its improved tryptic accessibility with increasing pH values. Theoretically, β-Lg B displayed a higher resistance to tryptic digestion (Cheison & Kulozik, 2017), while this resistance seems can be eliminated above pH 8.5. We speculated that the increase of pH up to 8.5 converted both β-Lg A and B into molten globule structures, so that their tertiary structures refold and both become more susceptible to tryptic hydrolysis.

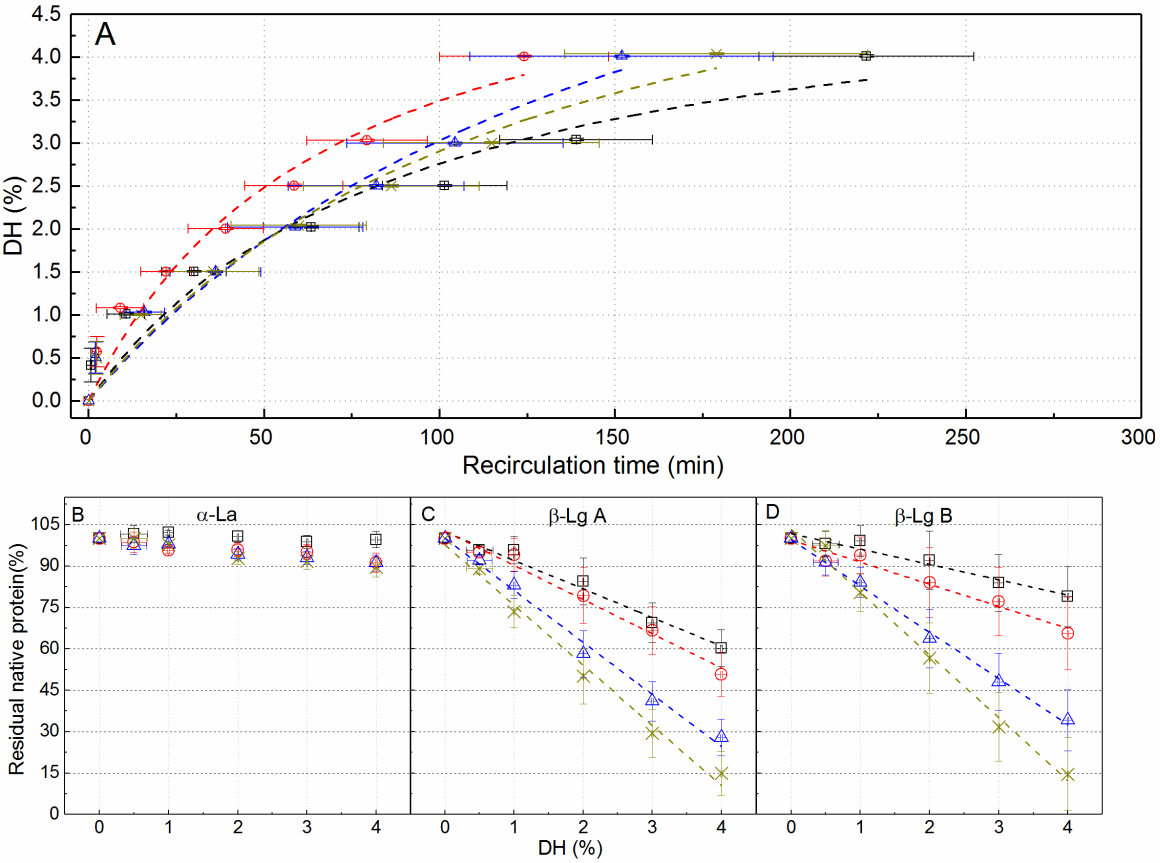

Figure 3.5-3. The hydrolysis of WPI at pH values 7.8 (□), 8.3 (○), 8.7 (Δ), 9.2 (x). A): Increase of DH as a function of time; B), C), and D) show the residual protein contents of α-La, β-Lg A and β-Lg B, respectively.

The effect of ionic strength

The effect of ionic strength, i.e., salts, on the hydrolysis is complex. With the addition of salts (typically NaCl) at low concentrations, the surface charges of proteins become shielded. For the substrate, this may result in decreasing electrostatic free energy of the protein molecules and increasing the activity of the solvent, which in turn, leads to improved solubility (Cheison & Kulozik, 2017). Simultaneously, the catalytic activity of immobilized trypsin could be strongly affected due to changes in surface charge since the negatively charged aspartate residue (Asp_{189}) located in the catalytic pocket of trypsin is responsible for attracting and stabilizing positively charged lysine and/or arginine on the substrate (Salis, Bilanicŏva, Ninham et al., 2007).

As shown in Fig. 3.5-4, the decrease of both hydrolysis rate and depletion of native proteins with the presence of 0.25 M NaCl could be due to the increased structural stability of protein molecules at high ionic strength (Yon, 1958). In addition, the strong electrostatic interaction between mobile phase and monolithic surface at 0.25 M NaCl could prevent contact between substrate molecules and the immobilized trypsin to some extent as well (Luey, McGuire & Sproull, 1991). Albeit, the efficiency at 0.1 M NaCl was slightly higher than those at 0 or 0.05 M NaCl, the depletion of β-Lg was much slower, even close to that at 0.25 M NaCl (67.56 ± 6.03 % and 72.74 ± 5.42% native β-Lg remained at DH 4% with presence of 0.1 and 0.25 M NaCl, respectively).

Speculatively, the addition of NaCl (≤ 0.1 M) negatively affected the depletion of intact β-Lg while it promoted the hydrolysis of the formed intermediate peptides. This can be illustrated by the fact that ionic strength has different effects on the hydrolysis of polypeptides that do not have defined secondary or tertiary structures. Actually, in the work of Fukuda and Kundugi (1989), the increase of ionic strength (0 to 0.9 M NaCl) also resulted in an increased rate of hydrolysis of synthetic peptide substrates by thermolysin.

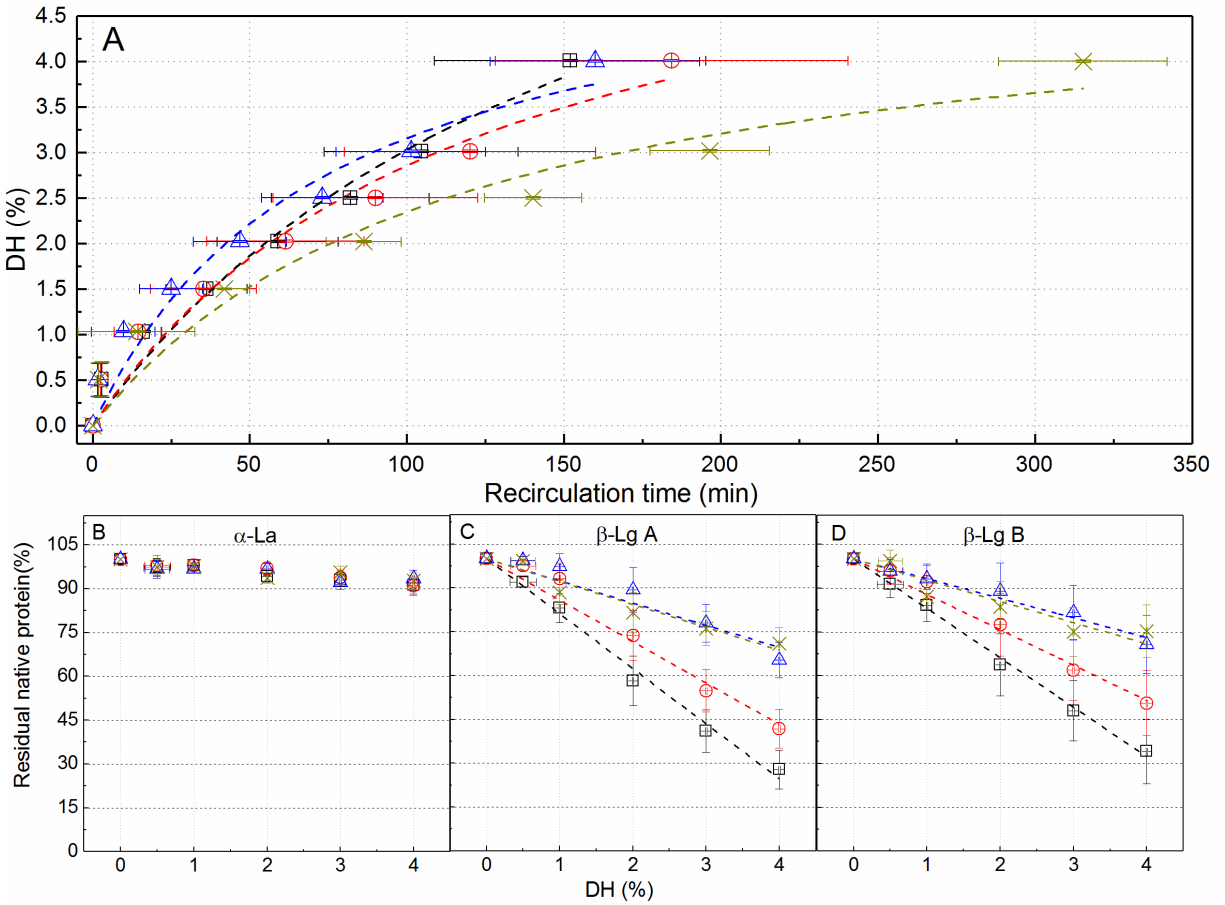

Figure 3.5-4. The hydrolysis of WPI with NaCl concentrations at 0 (□), 0.05 (○), 0.1 (Δ), 0.2 (x) M. A): Increase of DH as a function of time; B), C), and D) show the residual protein contents of α-La, β-Lg A and β-Lg B, respectively.

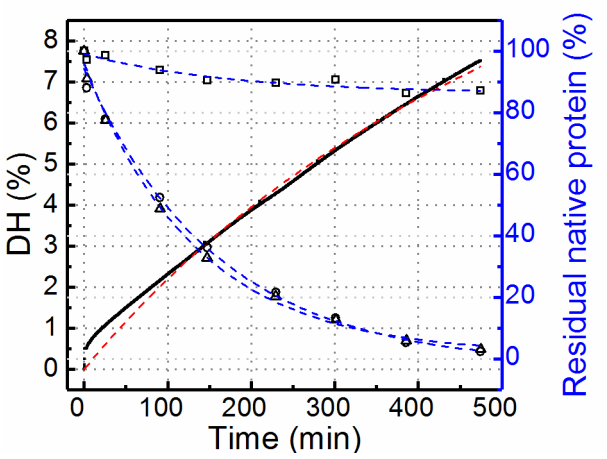

Figure 3.5-5. Hydrolysis of WPI solution. The evolution of DH and the amounts of residual native α-La (□), β-Lg A (Δ), and β-Lg B (○) were described.

In addition, the depletion of α-La was, again, insignificant, irrespective of the ionic strength. Based on the above findings, α-La was almost insusceptible to the immobilized trypsin under all explored conditions. To further confirm this speculation, the hydrolysis of 80 mL 20 mg/mL WPI solution (pH 8.7 without NaCl) was extended. As shown in the Fig. 3.5-5, no more β-Lg was detectable at DH 8% while approximately 85% of the native α-La could still be found in the hydrolysates. Another experiment with pure α-La was conducted, and no significant decrease of protein content was detected after 3 h recirculation through the MITR (data not shown).

3.5.3.3 Kinetic analysis of depleting β-Lg in the MITR

We found that the efficiency of the MITR in hydrolyzing WPI decreased to some extent, compared with the hydrolysis of pure β-Lg (data not shown). To estimate the potential influence introduced by the existence of other whey proteins, mainly α-La, pure β-Lg was used as the substrate as well to explore the kinetic analysis.

Michaelis and Menten (1913) developed the classical model describing kinetic properties of most enzymes. According to this model, the maximal reaction velocity V_{max} (= K_{cat} × [E]; K_{cat} turnover number) and Michaelis–Menten constant (K_m) are typically used to characterize the kinetic properties of an enzyme. In this study, the apparent kinetic parameters, K_M and V_{max}, were estimated based on the overall amount of immobilized trypsin in the MITR. Although, the initial reaction velocity theoretically was evaluated based on the hydrolyzed peptide bonds, in this study, it was obtained by measuring the depleting rate of β-Lg, which was able to be precisely determined by HPLC method, see Eq. 3.5-4. It was practically difficult to measure the exact hydrolyzed peptide bonds (h) in the initial stage of hydrolysis. In our experiments, the consumed volume of NaOH for the calculation of h (irrespective which concentration was used) increased suddenly to a certain value once the recirculation started. This practical problem led to the lack of initial evolution of DH. As the depleting rate of β-Lg was used as the index, single flow-through approach is practically easier and more precisely controlled, comparing with the recirculation approach. Furthermore,

hydrolysis at single flow-through approach maximally prevented from the potential inhibition of products. Thus, the kinetic analysis was explored at increasing flow rates (0.8 to 48 mL/min) by applying the single flow-through approach.

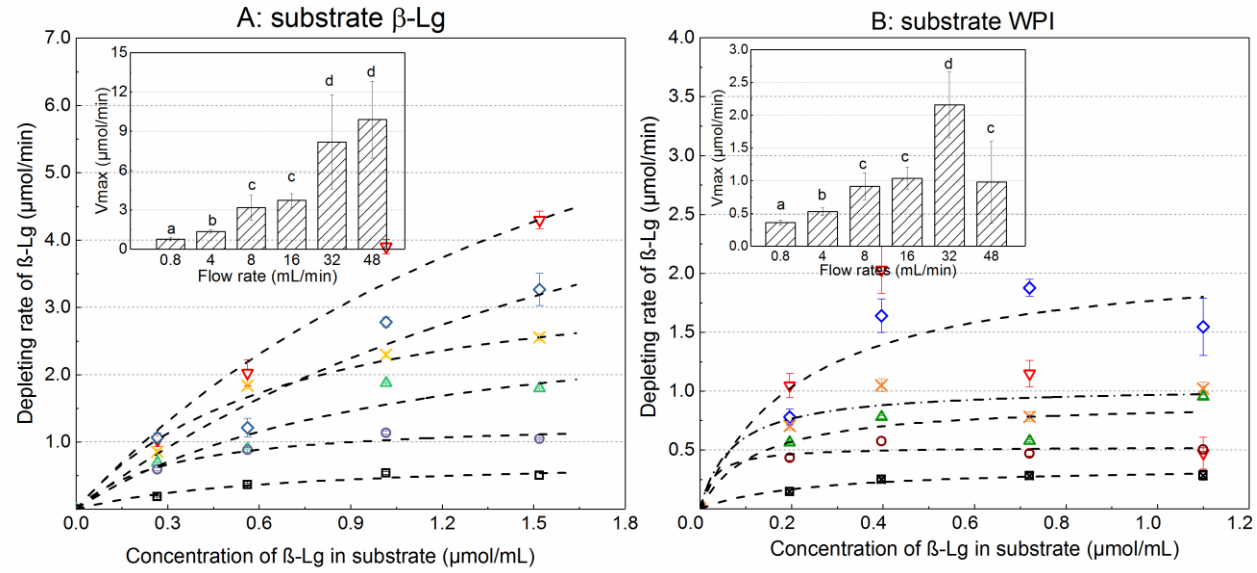

Flow rate (mL/min)		0.8	4	8	16	32	48
β-Lg	R^2	0.97	0.98	0.95	0.98	0.97	0.98
	K_m (µmol/mL)	0.64 ± 0.29	0.30 ± 0.1	1.04 ± 0.63	0.69 ± 0.23	2.38 ± 1.58	1.97 ± 0.94
WPI	R^2	0.98	0.96	0.87	0.92	0.90	0.41
	K_m (µmol/mL)	0.23 ± 0.08	0.03 ± 0.04	0.12 ± 0.13	0.07 ± 0.08	0.22 ± 0.17	/

Fig. 3.5-6. The depleting rates of β-Lg by the MITR at increasing flow rates 0.8 (□), 4 (○), 8 (Δ), 16 (x), 32 (◊), and 48 (∇) mL/min are displayed in A) for pure substrate β-Lg and B) for substrate WPI, respectively. Inset: V_{max} values depending on flow rates are plotted in a bar graph. The R_2 and K_m are illustrated below A) and B).

As discussed previously, the increase of flow rate was followed by the growth of hydrolysis efficiency. As shown in Fig. 3.5-6 A, the efficacy of depleting β-Lg was improved with increasing flow rates (0.8–48 mL/min) at each concentration when pure β-Lg was used, corresponding to a clear flow rate dependent V_{max}. However, the depletion efficiency decreased unexpectedly at 48 mL/min when WPI at a high concentration was applied, leading to a sharp decrease of V_{max} there (Fig. 3.5-6 B). Because of this extraordinary phenomenon, the Michaelis-Menten model could not be used to fit the data obtained during the hydrolysis of WPI at 48 mL/min (R^2 = 0.41). In the range of 0.8 to 32 mL/min, the initial depleting rate of β-Lg at recirculation approach was calculated from Eq. 3.5-3 and compared with the predicted values from the obtained model at single flow-through approach. As illustrated in Fig. 3.5-7, the predicted values were higher at all flow rates, but both showed the same trend.

Regarding K_m, no significant flow rate dependence was found. Specifically, the lowest K_m for β-Lg hydrolysis was noted at 4 mL/min. The same was noted for the hydrolysis of WPI. Comparing the obtained V_{max} values between the hydrolysis of β-Lg and WPI, a three-fold decrease in V_{max} was noted for WPI at all explored flow rates. It is

speculated that, although α-La is resistant to the hydrolysis by the immobilized trypsin, its existence acts as a competitor with β-Lg for the active site of trypsin, and this competition can be enhanced by increasing the flow rate or the α-La amount to some extent.

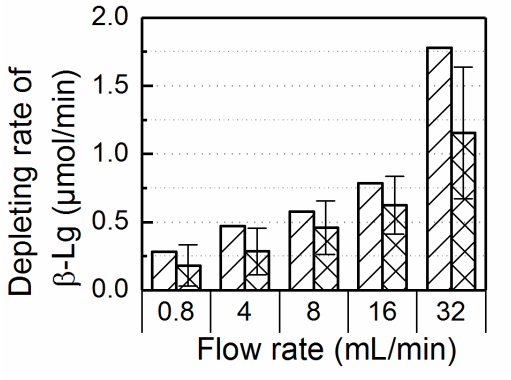

Fig. 3.5-7. The comparison of predicted depleting rates of β-Lg at single flow-through approach (left) and the experimental values at recirculation approach (right).

3.5.3.4 Operational stability of the MITR

Due to the diffusion-limiting step in conventional particle-based immobilized enzyme reactors, these reactors are commonly operated at low flow rates. For instance, in a corn-cob power based packed-bed immobilized trypsin reactor, the flow rate was only 10.1 mL/h due to the high backpressure, and a hydraulic retention time of 78 h was required (Bassan et al., 2016). However, the initial backpressure of the developed MITR in this work was only 0.045 MPa at 48 mL/min, offering the possibility of operating this reactor at an industrial scale.

After over 30 cycles of intensive operation, the initial hydrolysis velocity only decreased 12.1% compared with that of the first run (both hydrolysis experiments were conducted at the exactly same conditions), as illustrated in Fig. 3.4-8A. However, the permeability decreased 70% after 30 cycles, which was probably due to an accumulation of particles on the surface of monolith. This problem was also observed in our previous work (Mao et al., 2017), where the permeability decreased significantly while enzymatic activity still remained at similar levels. Speculatively, due to the 6 μm pore size, the accumulated particles did not block the pores. Rather, we believe they attached to bare monolith surfaces so that trypsin contact with substrate molecules was not inhibited. It is worth nothing that the backpressure of the MITR-8 mL was still below 0.15 MPa at 48 mL/min (6 CVs/min) even when the permeability declined 70%, and its operational limit was up to 2 MPa.

The upscaled MITR showed excellent reusability for WPI hydrolysates production compared to the previously reported reactors. For example, Rocha, Gonçalves and Teixeira (2011) prepared immobilized trypsin on spent grains for whey protein hydrolysis in a 50 mL batch reactor with 5 cycles of guaranteed reuse (each cycle 30 min). In the work of Pessato, Carvalho, Tavano et al. (2016), alcalase enzyme was

immobilized on glyoxyl-agarose beads and used to hydrolyze whey protein in a batch process. However, it lost 15% activity already after the third hydrolysis cycle.

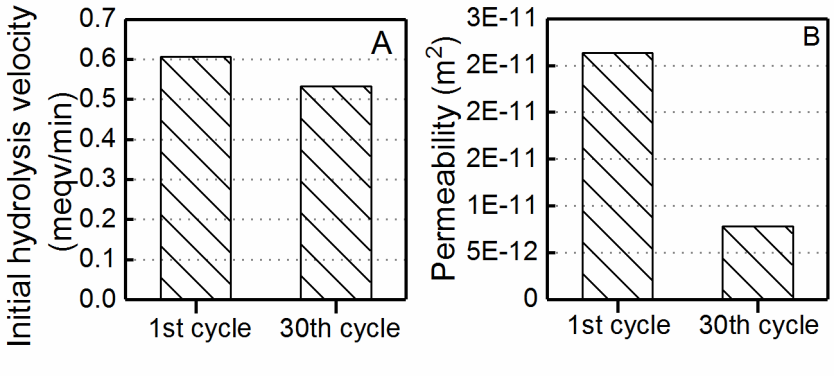

Figure 3.5-8. The comparison of initial hydrolysis velocity A) and permeability B) at the 1st and 30th cycles, respectively.

3.5.4 Conclusion

β-Lg was selectively hydrolyzed by the immobilized trypsin in the CIM-MITR-8 mL at ambient temperature resulting that above 85% α-La remained native in the final hydrolysates. Despite the inaccessibility of the immobilized trypsin to α-La at all explored conditions, its accessibility toward β-Lg was pH and ionic strength dependent. Namely, higher pH (15% residual at pH 9.2 vs 60% at pH 7.8) and lower ionic strength (30% residual at 0 M NaCl vs 70% at 0.1 and 0.25 M NaCl) was preferential. In addition, the increase of flow rate (up to 32 mL/min) contributed to the hydrolysis efficiency of immobilized trypsin and did not affect its ability to deplete β-Lg.

The Michaelis–Menten kinetics of the CIM-MITR-8 mL were explored using a single flow-through approach. The influences of flow rate and substrate composition were evaluated. Although higher flow rates contributed to the improved efficacy, beyond a certain range it might cause an unexpected decline in efficiency, especially for the complex substrate mixtures.

The developed CIM-MITR-8 mL in this study was able to be operated at high flow rates while maintaining low backpressure, which significantly improved the productivity of this reactor. The 11 mg trypsin immobilized on the CIM monolithic column through a multipoint covalent binding technique remained stable over 30 cycles of intensive uses, thus demonstrating the CIM-MITR to be cost effective, time efficient, and reusable. These above advantages render the CIM-MITR suitable for large-scale operations.

Acknowledgements

The first author thanks China Scholarship Council (China) for the support of her personal cost. The authors would like to thank Urh Černigoj from BIA Separations (Ajdovščina, Slovenia) for his technical help in developing the CIM-MITR, as well as for his revision work.

4 Overall Discussion

In this chapter, the obtained results will be integrally discussed mainly from three respects, i.e., (i) the development of CIM-IMTRs; (ii) kinetic studies on IMTRs; (iii) the influence of hydrolytic conditions on the performance of IMTRs, particularly focusing on the comparison between free and immobilized trypsin.

4.1 The development of CIM-IMTRs

In the study of Nicoli et al. (2008), trypsin immobilized on ethylendiamine (EDA)-CIM disks derivatized with glutaraldehyde (GLA) showed a better performance than those immobilized on epoxy or carbonyldiimidazole (CDI)-CIM disks. They suggest that the use of EDA, 8-carbon spacer moiety, can enhance the mobility of immobilized trypsin. With the spacer EDA, however, the immobilization of trypsin was performed through EDA-GLA chemistry, after which EDA-GLA exhibits secondary amino groups and these groups are positively charged at the optimal pH for trypsin activity (pH 7–8) (Naldi et al., 2017). Thus, potential nonspecific ionic interactions between monolith surface (EDA-GLA) and charged substrate molecules might induce a serious blockage, leading to the increased backpressure and then to a shortened cycle lifespan. Alternatively, aldehyde (ALD) activated CIM columns are suggested to be suitable for the enzyme immobilization, because ALD columns do not show any spacer linker and the monolith surface after enzyme immobilization is preferentially neutral (Naldi et al., 2017).

Regarding pore size, the development of CIM-IMTRs for proteomic applications clearly demonstrated that decrease of pore size down to 0.6 µm was preferable due to higher immobilized trypsin density on the monolithic surface and consequently higher enzymatic conversion (Naldi et al., 2017). Unfortunately, the decrease of pore size by a factor of 2 results in a 4 times higher pressure drop and a drastic decrease in permeability, which is not an option for protein hydrolysates production. Therefore, an alternative approach was considered, where monoliths were with larger pores (2.1 µm and 6 µm in this thesis) and consequently higher permeability. The monolithic surface area is one of the most important parameters influencing the maximum amount of immobilized enzyme. BET surface areas of CIM monoliths (before trypsin immobilization) were measured to be 5.0 and 2.0 m^2 per g of dry monolith with 2.1 µm and 6 µm pore sizes, respectively.

Immobilization protocols, i.e. reducing agents, pH, temperature, etc., might significantly influence the amount of immobilized trypsin and its activity. Based on the findings of Naldi et al. (2017), three protocols with varied reducing agents were investigated for the immobilization of trypsin on ALD-CIM columns with a bed volume of 1 mL and a normalized pore size of 2.1 or 6 µm, as shown in Table 4-1. Trypsin was immobilized on ALD-CIM columns by a multipoint covalent binding through Schiff base reactions. For such reactions, reducing agents are necessary to convert enzyme-support linkages (amino groups-aldehyde groups) into stable secondary amino groups and convert the remaining aldehyde groups on the support into hydroxy groups (Orrego, Romero-Fernández, Millán-Linares et al., 2018). The most common strong reducing

agent is sodium borohydride ($NaBH_4$), which however, might adversely affect the structural activity of certain immobilized enzymes due to its low selectivity (Orrego et al., 2018). 2-picoline borane (2-PB) and sodium cyanoborohydride ($NaCNBH_3$) are suggested as alternatives as they are much milder, especially 2-PB, which is also recommended for green chemistry application. But these two agents are not able to reduce remaining aldehyde groups into hydroxyl groups after immobilization, a blocking agent ethanolamine was additionally applied at the deactivation stage.

Table 4-1 Protocols for the immobilization of trypsin on ALD-CIM columns. Data on N3 and N4 are from Mao et al. (2017)

CIM-IMTRs		Pore size (μm)	Immobilization conditions	Deactivation agents	Immobilized trypsin per column (mg)	Trypsin surface density (molecules per nm^2)
1	N1	2.1	2-PB (3 mg/mL) as reducing agent, in 0.1 M MES + BAHC (0.4 mg/mL) buffer at pH 5.6	ethanolamine and 2-PB (pH 5.6)	3.4 ± 0.2	8 ± 4
	N2	6			1.5 ± 0.4	9 ± 5
2	N3	2.1	$NaCNBH_3$ (3 mg/mL) as reducing agent, in 0.1 M MES + BAHC (0.4 mg/mL) at pH 5.6	ethanolamine and $NaCNBH_3$ (pH 5.6)	5.0 ± 0.2	11 ± 4
	N4	6			3.0 ± 0.3	17 ± 5
3	N5	2.1	$NaCNBH_3$ (3 mg/mL) as reducing agent, in 0.1 M MES + BAHC (0.4 mg/mL) at pH 5.6	$NaBH_4$ (pH 10.5)	4.9 ± 0.1	11 ± 4
	N6	6			3.2 ± 0.3	18 ± 5

Benzamidine hydrochloride (BAHC), 2-(N-morpholino)-ethanesulfonic acid (MES)

Compared with IMTRs using protocols 2 or 3, much less amounts of immobilized trypsin were determined in IMTRs using immobilization protocol 1, where 2-PB was selected as the reducing agent (Table 4-1). This is probably due to the fact that 2-PB is much larger than other two hydrides, which restricts its ability to reduce Schiff bases as it has to go through the region that lies between the enzyme and the support (the width of this region is around 2 nm) (Orrego et al., 2018). Albeit, $NaCNBH_3$ is a milder reducing agent than $NaBH_4$, there is no significant difference between IMTRs with a pore size of 2.1 μm, in terms of the immobilization yield (Table 4-1) and the enzymatic activity (Fig. 4-1). Specifically, for IMTRs with a pore size of 2.1 μm, no significant difference in their activity was observed, except that N1 exhibited a higher activity than other two IMTRs (N3 & N5) at pH 7.2 and 7.8. On the contrast, the influence of different reducing agents on the activity of IMTRs with a pore size of 6 μm was much more pronounced. N4 using the protocol 2, where $NaCNBH_3$ was used as the reducing agent, showed the highest activity at all explored pH values (Fig. 4-1). N6 showed a

higher immobilization yield while a decreased activity, compared with N4. The amount of immobilized trypsin in N2 was almost reduced by half than those in N4 and N6, accounting for its such low activity. Reducing agents showed distinct influences on IMTRs with different pore sizes, which might be due to the higher trypsin surface density induced by the decreased surface area in IMTRs with larger pores. In addition, the enzymatic activity of each IMTR toward substrate BAEE generally increased at increasing pH up to 9.2, as shown in Fig. 4-1. The measured initial apparent permeability of IMTRs with 6 µm pores showed considerably higher values than those with smaller pores, as illustrated in Fig. 4-2.

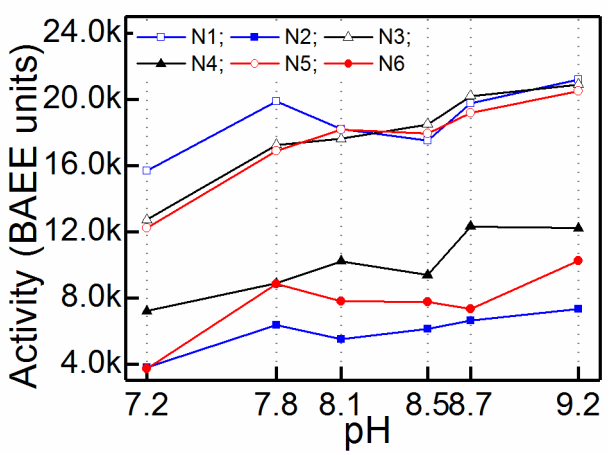

Figure 4-1. Activity of IMTRs with different pore sizes and using different immobilization protocols. Data on N3 and N4 is from Mao et al. (2017)

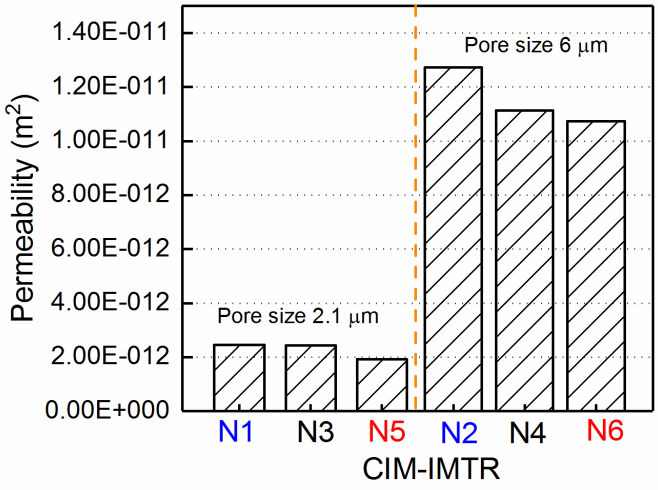

Figure 4-2. Initial permeability values of IMTRs.

To investigate the influence of pore size on the stability and reusability of developed IMTRs, N3 and N4 were chosen for the hydrolysis of β-Lg, as both used the same immobilization protocol and showed relatively higher activity than other IMTRs. 10 mg/mL β-Lg solution was recircualted through N3 and N4 for 6 h, respectively. N3 exhibited an approximate 5 times higher backpressure than N4 due to its smaller pores. Besides, a slight increment in recorded backpressure was noted for N3, namely from

0.30 MPa to 0.33 MPa, whereas the backpressure for N4 completely kept constant. Thus, it seems that the non specific adsorption of β-Lg molecules on the surface of N3 (IMTR–2.1 µm) might happen even only in one cycle (6 h).

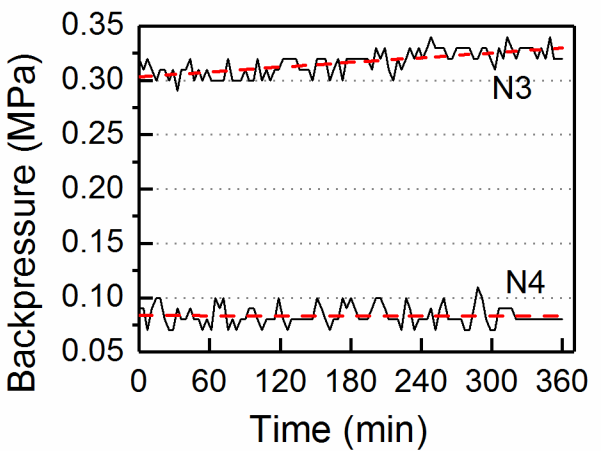

Figure 4-3. Backpressure on N3 and N4 during 6 h recirculation with 10 mg/mL β-lactoglobulin solution (Mao et al., 2017).

On the other hand, cumulative action from each cycle to the next one is a potential issue. N4 was used to hydrolyze β-Lg (10 mg/mL) for 18 cycles (except for 6 h in the first cycle, others were continued for 3 h each time), both enzymatic activity and pressure drop almost remained constant, as shown in Fig. 4-4. For N3, no significant decrease in its permeability was observed in first 8 cycles, indicating that most accumalted protein molecules can be washed out. Hereafter, the permeability of N3 declined gradually while the enzymatic activity was still almost unchanged until the 18th cycle. After these operations, N4 was completely stable during storage over 30 weeks, in terms of BAEE activity and permeability, monitored over 3 weeks. Therefore, IMTRs with a pore size of 6 µm are considered to be more suitable than those with 2 µm for the production of protein hydrolysates, as a much higher reusability can be expected.

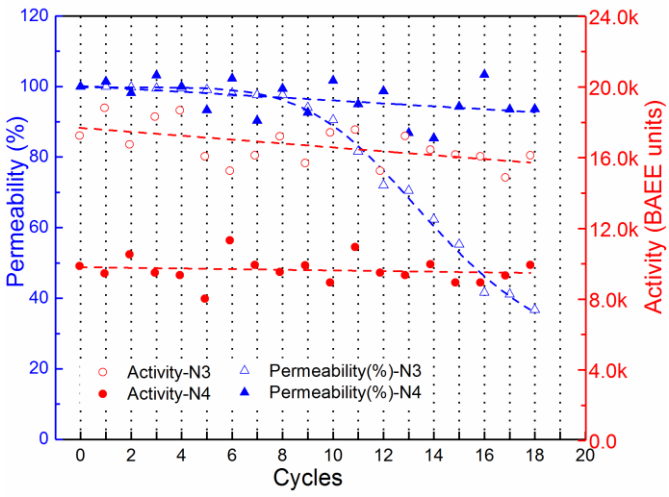

Figure 4-4. Permeability and enzymatic activity of N3 and N4 over 18 cycles. Data is from Mao et al. (2017)

To achieve a long-term investigation on the hydrolysis of WPI by an IMTR, the bed volume of the IMTR with 6 µm pore size was scaled up from 1 mL to 8 mL, so that its surface area was enough for trypsin immobilization, and simultaneously it was still highly permeable. The immobilization protocol applied for this IMTR-8 mL was same as that for N4, except that a larger amount of fee trypsin was used. However a much lower density of immobilized trypsin for IMTR-8 mL than N4 was determined, i.e., 1.4 ± 0.3 mg trypsin per mL monolith for IMTR-8 mL versus 3.0 ± 0.3 mg/mL for N4. The maximum enzymatic activity for IMTR-8 mL calculated from Michaelis-Menten curve was 141 µmol/mi. In terms of the specific activity in unit of per mg immobilized trypsin, IMTR-8 mL showed similar value to that of N4. Therefore, it shows the potential to increase the immobilization yield by optimizing the immobilization protocol, such as immobilization time, flow rate, free trypsin concentration, etc.. Following the objective of this thesis, this IMTR-8 mL was not further optimized, as it was already able to effectively hydrolyze WPI.

With this IMTR-8 mL, the hydrolysis of 20 mg/mL WPI solution was conducted. As shown in Fig. 4-5, the initial hydrolysis velocity only decreased 12.1% in the 30th cycle compared with that of the first run (both hydrolysis experiments were conducted at the exactly same conditions). However, the permeability decreased 70% after 30 cycles, which was probably due to an accumulation of particles on the surface of monolith. Speculatively, due to the 6 µm pore size, the accumulated particles did not block the pores, rather, they attached to bare monolith surfaces so that the contact between trypsin and substrate molecules was not inhibited while the reactor permeability decreased. It is to be noted that the backpressure of the MITR-8 mL was still below 0.15 MPa at 48 mL/min (6 CVs/min) even when the permeability declined 70%, and its operational limit was up to 2 MPa.

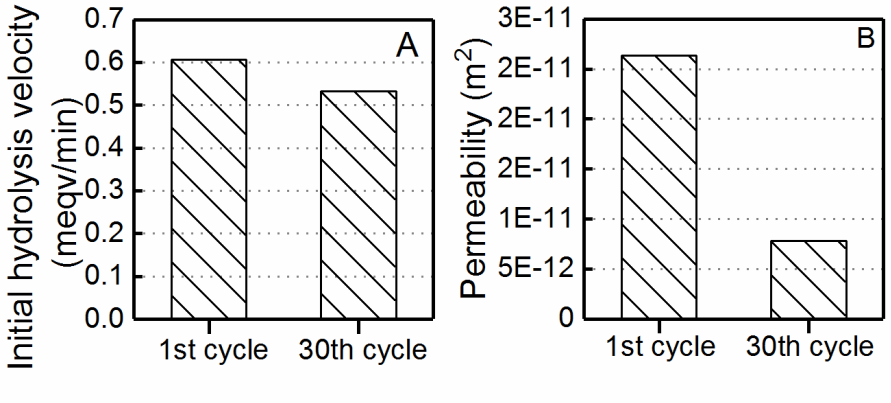

Figure 4-5. The comparison of initial hydrolysis velocity (A) and permeability (B) at the 1st and 30th cycles, respectively (Mao & Kulozik, 2018).

4.2 Kinetic studies on IMTRs

Kinetic studies in this thesis was conducted with both proteins and a model substrate BAEE. An IMTR-8 mL with a pore size of 6 µm was used for kinetic studies with substrate β-Lg or WPI. Alternatively, with the small molecular substrate BAEE, the kinetic properties in CIM-IMTRs with a bed volume of 1 mL and a pore size of 2.1 µm (N3) or 6 µm (N4) were investigated. This is due to the fact that an extremely large amount of BAEE was required for the kinetic studies with the IMTR-8 mL. The simple model describing kinetic properties of the most part of enzymes is developed by Michaelis and Menten (1913). According to this model, the turnover number K_{cat} and Michaelis-Menten constant K_m are typically used to characterize kinetic properties of an enzyme. However, K_{cat} can be determined only when the active enzyme concentration is known, which has to be measured by titrating the active site of the enzyme. In case of IMTRs, the direct estimation of such active enzyme concentration is impossible. As a compromise, measuremnent of the maximal velocity V_{max} (= K_{cat} × [E]) is an alternative. In this study, the apparent kinetic parameters K_M and V_{max} were estimated, based on the total amount of active trypsin immbolized in one reactor.

To explore the influence of flow rate on the aparaent kinetic parameters of immobilized trypsin, BAEE soulutions with increasing concentrations from 0.1 to 50 µmol/mL were continuously pumped through N3 or N4 at increasing flow rates by single flow-through approach. The velocity of BAEE conversion was evaluated by the amonut of produced BA per minute. At flow rates 0.5 and 2 mL/min, the reaction velocity increased linearly even the highest initial substrate concentration applied, indicating that the reactions at 0.5 and 2 ml/min were at first order in the range of applied substrate concentrations. Thus, it is not able to extrapolate K_m and V_{max} values. At flow rates 5, 10 and 15 mL/min, K_m and V_{max} were extrapolated by plotting the velocity of produced BA (µmol/min) to the initial substrate BAEE concentration (µmol/mL) and fitting with the Michaelis–Menten equation (Fig. 4-6), as shown in Table 4-2. For both N3 and N4, a slight increase in V_{max} with increasing flow rates was observed, while K_m showed a decrease when the flow rate increased from 5 to 15 mL/min. An enzyme with a high K_m has a low affinity to this substrate, and requires a greater concentration of substrate to

achieve V_{max}. In a conventional batch based hydrolysis system, K_m is the initial concentration of substrate which permits the enzyme to achieve half V_{max}, while for a flow-through IMTR, it should be evaluated based on the substrate concentration inside the reactor. Although, the same initial substrate concentrations were applied, substrate concentrations in the IMTR varied at different flow rates. At a low flow rate, the substrate is insufficient to be supplemented, leading to a situation that the immobilized enzyme is waiting for the substrate. Thus, a higher initial substrate concentration at a lower flow rate is required to reach the same substrate concentration in the reactor as a higher flow rate is applied. Alternatively, another kinetic paramter K_m", i.e. the amount of substrate required by an IMTR in 1 min to reach its half V_{max}, might better illustrate the affinity of immobilized trypsin to a substrate, which is calcuted according to Eq. 4-1. As shown in Table 4-2, similar K_m" values were obtained in the range of 5–10 mL/min for both N3 and N4.

$$K_m" = K_m \times F \quad (4\text{-}1)$$

Where Km is the Michaelis-Menten constant based on the applied initial substrate concentration and F is the applied flow rate.

Assuming the same ratio of active trypsin amount based on its total amount in N3 (≈ 5 mg) and N4 (≈3 mg), 40% less amount of active trypsin in N4 than N3 can be expected. If per mg active trypsin in both IMTRs would have the same V_{max} and K_m", in theory, 40% less of these values could be observed for N4 than N3. However, N4 showed 60% less in V_{max} values while simliar K_m" values at all explored flow rates, compared with N3. In other words, K_m" increased while V_{max} decreased for per mg active immobilized trypsin when the pore size of an IMTR enlarged from 2.1 to 6 µm. The results of Bencina et al. (2007) also demonstrate that trypsin immobilized inside smaller pores is more effective (pore size 634 nm versus 2900 nm). They provide a possible reason that the number of contacts for BAEE molecules with immobilized trypsin, in smaller pores, is larger due to the shorter path they travel from one pore wall to another, resulting in more efficient digestion. In this thesis, another speculation is provided. As previously discussed, for immobilized trypsin, substrate molecules are driven to the monolith wall largely by shear force firstly and then attracted by immobilized trypsin through intermolecular forces at a relatively short distance, finally forming the complex of enzyme and substrate. This process is influenced by the mass transfer, which are exclusively convective and laminar in a monolithic reactor (Podgornik et al., 2014). For a laminar boundary layer, the length scale associated with the boundary layer thickness (pore size) is inversely proportional to the square root of the Reynolds number. With increasing Reynolds number the wall shear stress in a laminar flow increases monotonously (Germano, Piomelli, Moin et al., 1991). Therefore, a much stronger shear force in N3 than N4 can be expected. The decrease in shear force probably reduces the sufficient contacts between substrate and immobilized enzyme, in turn, a lower V_{max} and a higher K_m".

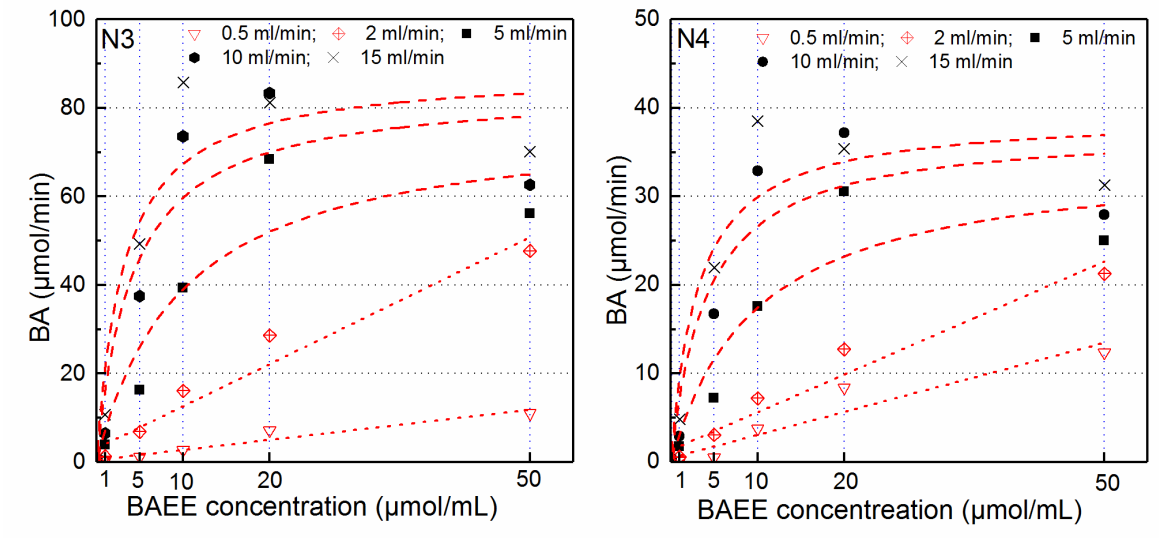

Figure 4-6. Influence of flow rate on the enzymatic activity of N3 and N4 with increasing substrate BAEE concentrations.

Table 4-2. Apparent kinetic parameters of N3 and N4 with the substrate BAEE at increasing flow rates.

IMTRs	N3			N4		
Flow rate (mL/min)	5	10	15	5	10	15
R^2	0.86	0.84	0.87	0.86	0.84	0.87
V_{max} (μmol/min)	77.99 ± 18.63	84.58 ± 15.85	88.58 ± 13.08	34.804 ± 8.31	37.74± 7.07	39.22 ± 5.82
K_m (μmol/mL)	9.97 ± 6.76	4.16 ± 3.06	3.15± 2.01	9.97 ± 6.76	4.17 ± 3.06	3.11 ± 2.01
K_m " (μmol/min)	49.85 ± 33.8	41.6 ± 30.6	47.25 ± 30.15	49.85 ± 33.8	41.6 ± 30.6	47.25 ± 30.15

Regarding the apparent kinetic parameters for substrate proteins, the initial reaction velocity theoretically should be evaluated based on the hydrolyzed peptide bonds. However, it was practically difficult to measure the exact hydrolyzed peptide bonds (h) at the initial stage of hydrolysis, as the consumed volume of NaOH for the calculation of h (irrespective which concentration was used) increased suddenly to a certain value once the recirculation started. In this thesis, the reaction velocity was obtained by measuring the depleting rate of intact β-Lg, which was able to be precisely determined by HPLC method.

As shown in Fig. 4-7 A, the efficacy of depleting β-Lg was improved with increasing flow rates (0.8–48 mL/min) at each concentration when pure β-Lg was used, corresponding to a clear flow rate dependent V_{max} (Table 4-3). However, the depletion efficiency decreased unexpectedly at 48 mL/min when WPI at a high concentration was applied, leading to a sharp decrease of V_{max} there (Fig. 4-7 B). Because of this extraordinary phenomenon, the Michaelis-Menten model could not be used to fit the data obtained during the hydrolysis of WPI at 48 mL/min (R^2 = 0.41). Comparing the obtained V_{max} values between the hydrolysis of β-Lg and WPI, a three-fold decrease in V_{max} was noted for WPI at all explored flow rates. It is speculated that although α-La is resistant to the hydrolysis by the immobilized trypsin (results in 3.4), it still acts as a competitor with β-Lg for the active site of trypsin, and this competition can be enhanced by increasing the flow rate or the α-La amount to some extent.

Regarding K_m, no significant flow rate dependence was found, irrespective pure β-Lg or WPI was applied, while K_m'' values showed a clear increase with increasing flow rates, indicating that more protein molecules are required to be supplemented for immobilized trypsin to achieve its half V_{max}. The observed K_m and K_m'' values for proteins as a function of flow rates differed significantly from those for substrate BAEE. This difference might be due to the fact that there is only one cleavable site on each BAEE molecule, while (at least) 16 potential cleavage sites on each β-Lg molecule. Thus, at a single flow-through approach, immobilized trypsin might catalyze more cleavage sites on one protein molecule at a lower flow rate, compared with that at high flow rates where a much faster mass transfer is achieved.

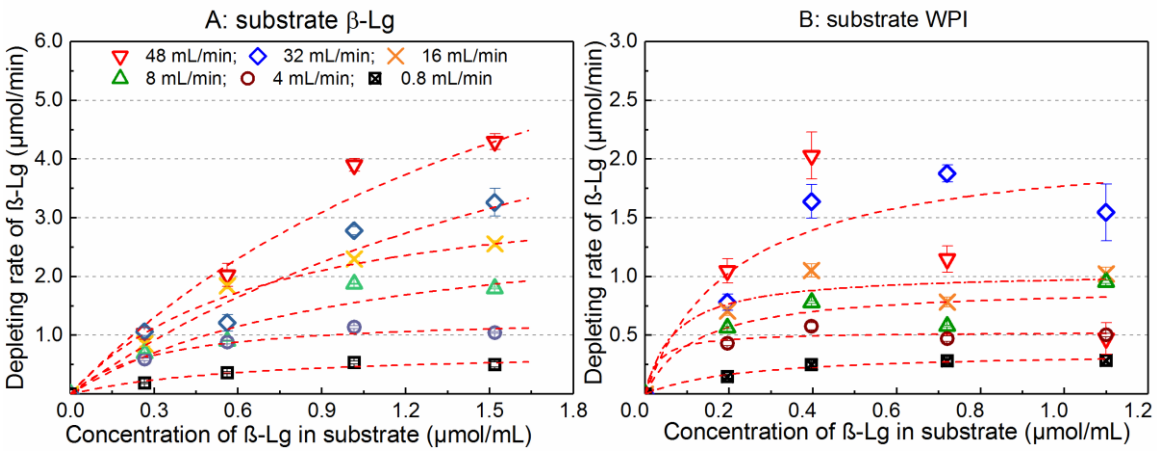

Figure 4-7. Influence of flow rate on the depleting rate of intact β-lactoglobulin by IMTR-8 mL with increasing concentrations of substrate β-Lg (A) or whey protein isolate (B) (Mao & Kulozik, 2018).

Table 4-3. Apparent kinetic parameters of IMTR with the substrate β-Lactoglobulin or whey protein isolate at increasing flow rates.

Flow rate (mL/min)		0.8	4	8	16	32	48
β-Lg	R^2	0.97	0.98	0.95	0.98	0.97	0.98
	V_{max} (µmol/min)	0.76 ± 0.14	1.33 ± 0.13	3.16 ± 0.95	3.72 ± 0.52	8.18 ± 3.6	9.89 ± 2.93
	K_m (µmol/ mL)	0.64 ± 0.29	0.3 ± 0.1	1.04 ± 0.63	0.69 ± 0.23	2.38 ± 1.58	1.97 ± 0.94
	K_m "(µmol/ mL)	0.11 ± 0.05	0.25 ± 0.08	1.73 ± 1.05	2.3 ± 0.77	15.87 ± 10.53	19.7 ± 9.4
WPI	R^2	0.98	0.96	0.87	0.92	0.90	0.41
	V_{max} (µmol/min)	0.64 ± 0.29	0.3 ± 0.1	1.04 ± 0.63	0.69 ± 0.23	2.38 ± 1.58	1.97 ± 0.94
	K_m (µmol/ mL)	0.23 ± 0.08	0.03 ± 0.04	0.12 ± 0.13	0.07 ± 0.08	0.22 ± 0.17	/
	K_m "(µmol/ mL)	0.04 ± 0.01	0.03 ± 0.03	0.2 ± 0.22	0.23 ± 0.27	1.47 ± 1.13	/

4.3 The influence of hydrolytic conditions on the performance of immobilized trypsin

The specificity of a proteolytic enzyme describes the type of amino acid, after which it can hydrolyze a peptide bond, such as Lys and Arg for trypsin. Regardless of the specificity of a protease for individual cleavage sites, not all cleavable sites are hydrolyzed at the same time. Thus, another criteria "selectivity" is introduced, referring to the rate at which individual cleavage sites in a protein substrate are hydrolyzed relative to other cleavage sites. The selectivity of a protease toward a specific substrate depends on the primary structure of this substrate, as well as on the spatial structures of both the substrate and the enzyme. Normally, the protein primary structure is not able to be substantially changed, in addition to certain modifications, such as isomerization and posttranslational modifications (e.g., glycosylation, methylation, hydroxylation, etc.). However, most of such modifications are not applicable to the processing of food proteins. Alternatively, it is much easier to achieve transformations in protein spatial structures, which highly depends on environmental conditions, i.e., temperature, pH, salts, etc..

In this thesis, the influence of temperature is not investigated, due to the fact that with the experimental apparatus, the temperature in IMTRs is not able to be heated up and to remain a desired value at a flow-through hydrolysis approach. In addition, a previous study (Cheison et al., 2011) indicated that at the optimal temperature of free trypsin (37°C), the enzyme selectivity was with little chance to be regulated by other environmental conditions, like pH, as temperature was the dominating influencer. Therefore, the influence of pH, salts and organic solvents on the performance of IMTRs-1 mL (N3 series) is systematically investigated at 25°C, and compared with free trypsin.

Influence on DH

DH, calculated by Eq. 4-2, provides the degree of the hydrolysis process. This is an often-used protein hydrolysis index other than the hydrolysis time. Due to the specificity of trypsin, each substrate protein has its own maximum DH. For instance, a theoretical DH_{max} of 11.18% for substrate β-Lg can be achieved during trypsinolysis, as 18 of the 161 peptide bonds of β-Lg are potential cleavage sites for trypsin.

$$DH = \frac{h}{h_{tot}} \tag{4-2}$$

Where, h is the number of hydrolyzed peptide bonds and h_{tot} is the total number of peptide bonds in a substrate.

DH can be calculated using the pH-stat method, according to the consumed amount of base induced by pH drop during the hydrolysis (Adler-Nissen, 1986). There are other methods used to determine DH, which depend on the NH_2 reaction chemistry to form a chromogenic complex, such as the reactions with trinitrobenzenesulphonic acid (TNBS) (Adler-Nissen, 1979) or β-phthaldialdehyde (OPA) (Church, Porter, Catignani et al., 1985). In the study of Spellman, McEvoy, O'Cuinn et al. (2003), pH-stat, TNBS and OPA

were generally compared well with each other for monitoring the DH values during whey protein hydrolysis by alcalase 2.4L or debitrase HYW20. In this thesis, however, the measured DH values using TNBS or OPA were unreasonable, i.e., a higher amount of chromogenic complex was determined in samples without hydrolysis than certain hydrolyzed samples (data not shown). This is probably due to the relatively low overall DH in tryptic samples (most ≤ DH 5% in this thesis). Comparatively, most samples showed a DH higher than 5% in other studies, where the DH determined by TNBS or OPA worked well (Spellman et al., 2003). Thus, DH was only evaluated by PH-stat method in this thesis.

As shown in Fig. 4-8, the evolutions of DH during β-Lg hydrolysis by free or immobilized trypsin were compared at varied hydrolytic conditions. No significant difference in the evolutions of DH at pH 7.8 and 8.7 was observed, irrespective free or immobilized trypsin applied. NaCl with increasing concentrations or 20% ethanol (v/v) was included in the reaction media at pH 8.7. For both types of trypsin, the presence of 0.02 M NaCl significantly increased DH while 0.5 M NaCl seriously retarded the hydrolysis of β-Lg. Compared with the hydrolysis without additional NaCl, the DH increased for immobilized trypsin while decreased for free trypsin when 0.1 M NaCl was added. Interestingly, DH increased fastest for free trypsin in the 20% ethanol/water among all the explored conditions, while for immobilized trypsin, the DH in the hydrolysis with 20% ethanol only increased slightly, lower than those with the presence of 0.02 or 0.1 M NaCl. To sum up, hydrolytic conditions showed different influences on the behaviors of free and immobilized trypsin. The underlying mechanism will be discussed later, inclusive the results on enzyme selectivity.

In addition, the DH increased generally in a linear model for immobilized trypsin within 180 min, while a much faster increase at the initial stage of hydrolysis was always observed for free trypsin at all explored conditions except for the case with 0.5 M NaCl. Obviously, free trypsin is more flexible in making contact with substrate β-Lg than the immobilized one, contributing to a higher reaction velocity at the initial stage of hydrolysis, which has been discussed in many cases of immobilized catalysts (Duggal & Bucholz, 1982; Mao et al., 2017; Rocha et al., 2011). During hydrolysis by free trypsin, autodigestion of enzyme, reduction of substrate, and potential inhibition by products might slow down the overall hydrolysis. Thereby, DH increased in a logistic model for free trypsin, while the decrease in the reaction velocity for immobilized trypsin was less pronounced, mainly because of the absence of autodigestion, as well as the fast removal of products.

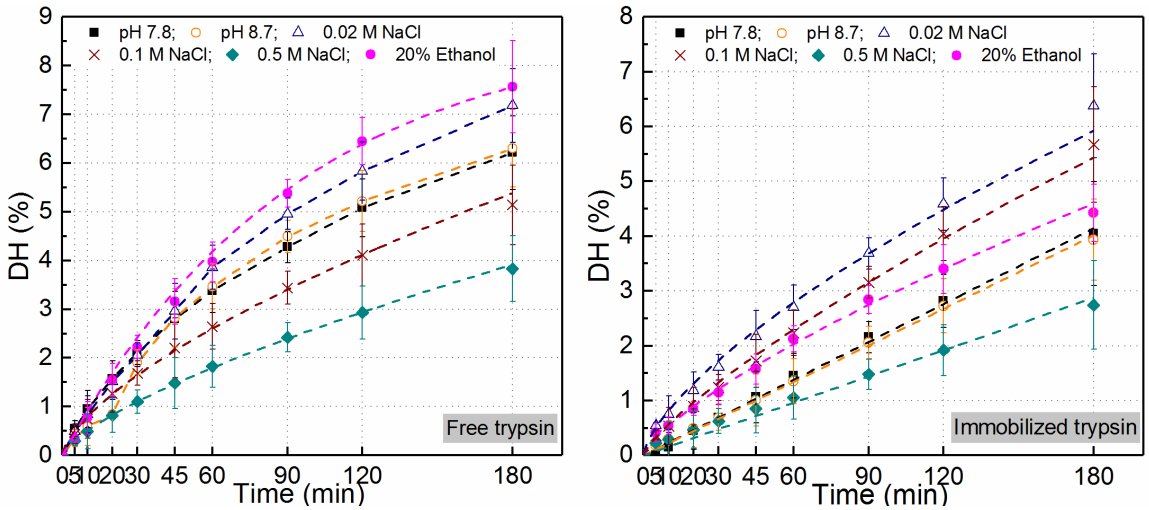

Figure 4-8. Influence of hydrolytic conditions on DH as a function of time. Data is from Mao et al., 2017, 2018.

Influence on hydrolyzing intact β-Lg

The Linderstrøm-Lang theory on protein hydrolysis presents two models: “zipper” and “one-by-one” (Adler-Nissen, 1976). In a “one-by-one” model, intact protein will slowly break down and no appreciable amounts of intermediate peptides will be accumulated, while a much faster degradation of intact protein at the initial stage of hydrolysis will be observed in a “zipper” model. In fact, most proteins show an intermediate behavior between these two models, and their behaviors depend not only on the nature of substrate and enzyme, but also on hydrolytic conditions. As shown in Fig. 4-9, both free and immobilized trypsin exhibited greater accessibility to intact β-Lg at an increasing pH value. The increase in pH from 7.8 to 8.7 even shifted the trend of the depletion in intact β-Lg by free trypsin from “one-by-one” to “zipper,” whereas this influence on the hydrolysis by immobilized trypsin was limited. For immobilized trypsin, linear decreases in intact protein dependent on the DH were observed at all explored concentrations, close to the “one-by-one” model, and the slope continuously decreased with increasing NaCl at pH 8.7. For free trypsin, a sharp increase in the depletion rate was noted at the initial stage of hydrolysis with 0 or 0.02 M NaCl, during which the increase in DH from 0 to 1% corresponded to a depletion of 30–40% of the intact protein content, which is more in agreement with the “zipper” model (Fig. 4-9). However, the depletion of intact protein by free trypsin was more close to “one-by-one”, when the NaCl concentration increased from 0.02 to 0.1 M. Generally, the addition of NaCl prevented intact β-Lg from hydrolysis, irrespective free or immobilized trypsin was applied. Contrast to NaCl, the fastest depletion rate of intact β-Lg was observed in the presence of 20% ethanol for both types of trypsin.

The significant differences in susceptibility of intact β-Lg to tryptic hydrolysis are probably due to its conformational transitions at different hydrolytic conditions. For instance, β-Lg undergoes the transitions from monomer at a natural pH to dimmer at alkaline or at very acidic pH values, even to octamer at pH 3.7–5.1 (Fig. 1-3). Regarding its pH-dependent structural characteristics, the so-called Tanford transition

occurs at the pH near 7.5. The increase in pH to values exceeding 8.0 induces further structural changes because the charge states of the side groups of a protein depend on the pH. Thus the intact protein was generally more accessible with increasing pH values. Similar to the pH increase, the addition of ethanol also rendered the β-Lg more tryptic accessible. In the study of Dufour et al. (1993), the secondary structure transformation of β-Lg from a predominantly β-structure into a α-helical one is influenced by solvent polarity changes, and the mid-points of the observed structural transformation occur at dielectric constant ≈ 60 (30–40% ethanol). Some studies (Dufour, Bertrand-Harb & Haertlé, 1993; Dufour & Haertlé, 1990; Mousavi et al., 2008; Renard et al., 1999) suggest that β-Lg exhibits an intermediate state around 20% ethanol. However, the presence of NaCl generally prevented intact β-Lg from hydrolysis. The addition of high concentration of salts (NaCl) significantly increased the ionic strength of the reaction media, which might hinder enzyme–substrate interactions through charge shielding. In addition, NaCl contributes to the dimerization of β-Lg, which might decrease its depletion rate as well.

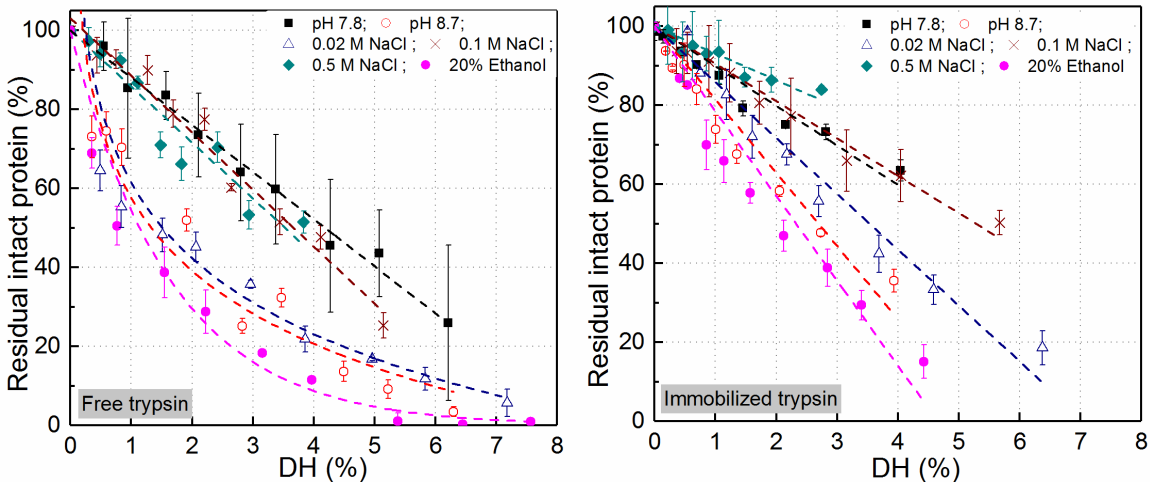

Figure 4-9. The influence of hydrolytic conditions on the depletion of intact β-Lg. Data is from Mao et al., 2017, 2018.

Influence on peptides

Both free and immobilized trypsin showed strong preference to cleavages at the C- and N-termini, e.g., Lys_{8}, Lys_{14}, Arg_{40}, Arg_{141} and Lys_{148}, which are considered the most physically accessible. Another peptide f(71–75) typically presents a quick release during tryptic hydrolysis because of its external position in the three-dimensional structure of β-Lg and its neighbor amino acid compositions. As expected, peptides corresponding to the cleavages at these sites were released in the initial stage of hydrolysis by both free and immobilized trypsin, irrespective of the pH at which the hydrolysis was performed (pH 7.2–8.7). Besides, more peaks were in the range of 4000–10,000 Da with increasing pH, indicating that more intact β-Lg was attacked directly at higher pH values. Regarding the differences between free and immobilized trypsin, free trypsin preferentially attacked the cleavage sites located at the C-terminus at pH 7.8, whereas an opposite preference was observed at pH 8.7. However, for the

immobilized trypsin, no significant preference regarding the C- or N-terminus was noted, only a slight increase in preference for Lys_8 was identified at pH 8.7.

With the addition of salts (Tris & NaCl), both free and immobilized trypsin preferentially hydrolyzed certain intermediate peptides, compared with that in the absence of salts. This preference toward specific peptides depends on the type and concentration of salts, as well as on the form of trypsin. The presence of 0.1 M Tris contributed to the release of most final peptides for both forms of trypsin, i.e., f(1–8), f(9–14), f(15–20), f(21–40), f(61–69/61–70),f(149–162). However, the final peptides directly associated with the breakdown of intact protein diminished with increasing NaCl concentrations. Contrast to aforementioned final peptides, for free trypsin, peptides f(61−69/61−70), f(84−91), f(125−125), f(92−101), and f(41−60) were released significantly faster at a higher concentration of NaCl, and peptides f(15−20), f(21−40), and f(125−135) were released much earlier in samples with the presence of 0.1 or 0.5 M NaCl. Nevertheless, for immobilized trypsin, these effects were less pronounced. The addition of 0.1 and 0.5 M NaCl only significantly increased the peptides f(61−69/61−70) and f(125−135). In addition, Tris did not affect the hydrolysis of intact protein, whereas NaCl generally retarded the depletion of intact protein. Hence, it is speculated that Tris molecules mainly interact with certain intermediate peptides (the precursors of final peptides) and trypsin molecules simultaneously, promoting the interactions between the polypeptides and trypsin through hydrogen bonds. Differently, at high concentrations of NaCl (0.1 & 0.5 M), intact β-Lg was prevented to bind with trypsin, in turn, both forms of trypsin preferentially bind to the intermediate peptides.

The presence of ethanol showed promoting as well as reducing effects on the release of peptides for free and immobilized trypsin. Namely, for both forms of trypsin, the release of peptides locating on C- termini decreased after the addition of ethanol, which is more pronounced for immobilized trypsin. For free trypsin, the addition of ethanol largely promoted the release of most detected final peptides at the initial stage of hydrolysis, such as f(1–8) and f(71–75). However, 20% ethanol showed significant reducing effects on the release of peptide f(71–75) for immobilized trypsin, leading to a negligible amount at 5 min, alternatively, immobilized trypsin seems to preferentially attack certain cleavage sites in 20% ethanol differently from those in aqueous medium, such as Lys_{138}.

Regarding the differences in peptides generated from free or immobilized trypsin, generally, the immobilization of trypsin led to more focused cleavage sites within its specificity at the initial stage of hydrolysis compared with the findings for free trypsin. Salts and pH exerted more pounced influence on free trypsin than its immobilized form, whereas the addition of ethanol led to a more significant influence on the hydrolysis by immobilized trypsin.

Mechanism underlying the observed effects of hydrolytic conditions

The changes in β-Lg structures are not able to interpret the different behaviors of free and immobilized trypsin. The differences in the hydrolysis by free and immobilized trypsin stem from that the interactions between enzyme and substrate might change largely due to the immobilization. As is well known, the critical step for tryptic catalysis is to form the complex of substrate and enzyme. In the case of free trypsin, the contact between substrate and enzyme depends on the fundamentals of Brownian movement, as well as on the intermolecular forces, mainly the electrostatic forces, which further drive substrate and enzyme together. For immobilized trypsin, as its flexibility is considerably reduced, substrate molecules are driven to the monolith wall largely by shear force firstly and then attracted by immobilized trypsin through intermolecular forces at a relatively long distance, finally the complex of enzyme and substrate can form by intermolecular forces at a short distance. This process is influenced by the mass transfer properties, as well as by the characteristics of the monolith surface covered by immobilized trypsin molecules. The mass transfer in monolithic IMTRs is exclusively convective and laminar. With laminar flow key solute dispersion comes from laminar dispersion, thus, all solutes flow with the current regardless of their sizes theoretically are transported at the same rate. Generally, there is no first selection among different substrate molecules during the mass transfer.

As previously mentioned, ALD-CIM columns, used as the immobilization support, do not use a spacer linker, and the surface is preferentially neutral (Naldi et al., 2017). Besides, the surface coverage ratio of IMTRs by trypsin molecules is quite high, in the range of 65–100%. Thus, the surface charge and hydrophobicity of the monolith wall after trypsin immobilization is considered to be the same as the formed layer by immobilized trypsin molecules. In the explored pH range (7.2–9.2), the net charge of free trypsin molecule is theoretically positive, as its isoelectric point is 10.1–10.5. Substrates β-Lg and α-La are negatively charged, as both have a PI around 4.5–5.2. The electrostatic interactions are considered to be the main driving force for the substrate binding to free trypsin. However, the attractive force between substrate molecules and immobilized trypsin might differ from that for free trypsin. The immobilization of trypsin was performed at pH 5.6, where the net surface charge of trypsin molecules is, in theory, highly positive. Based on the fundamentals of electrostatic interactions, each trypsin molecule probably reorientates its position to reach a charge balance with other trypsin molecules during the immobilization. Increasing pH mainly induced changes in the surface charge of protein molecules, affecting the electrostatic interactions between substrate and enzyme, and the addition of ethanol mainly contributed to hydrophobic interactions. Taken results on the influence of various hydrolytic conditions on the release of peptides together, changes in the selectivity of free trypsin were more significant than immobilized due to the pH increase, while for immobilized trypsin the addition of ethanol significantly altered its accessibility toward cleavage sites on intact β-Lg. It is postulated that after the shear

force driving substrate molecules close to immobilized trypsin, the attractive forces between them at a relative long distance might be hydrophobic interactions.

Selective hydrolysis in whey proteins

The selectivity of a protease toward various substrates differs due to the different structural properties of these substrates. Schmidt and Poll (1991) investigated the accessibility of in total 14 types of enzyme toward whey proteins and indicated that, contrary to native β-Lg, native holo α-La was resistant to tryptic digestion. This action highly depended on the composition of medium (Ca^{2+}, buffer, pH, etc.), incubation temperature and the degree of protein denaturation. Taking advantage of this trypsin selectivity, Konrad and Kleinschmidt (2008) succeeded in isolating α-La with 90-95% purity from whey proteins by applying tryptic hydrolysis (42°C, pH 7.7) and membrane filtration. However, only 15% α-La was recovered mainly due to the high hydrolysis temperature. Actually, increasing the temperature near or above the trypsin optimum of 37 °C resulted in less controlled hydrolysis of whey proteins, with low resistance of α-La to trypsin (Cheison et al., 2011). To improve the yield of α-La, Cheison et al. (2011) optimized the conditions for tryptic hydrolysis of WPI, and 67.87% α-La was recovered at pH 8.5 and 25°C. These findings provide proof of concept for selectively hydrolyzing β-Lg in whey proteins using trypsin. In this thesis, the possibility of selective hydrolysis of β-Lg by immobilized trypsin was investigated at various hydrolytic conditions.

As shown in Fig. 4-10, β-Lg was selectively hydrolyzed by the immobilized trypsin in a CIM-MITR-8 mL at ambient temperature, resulting that above 85% α-La remained native in final hydrolysates (without detectable intact β-Lg). Despite the inaccessibility of the immobilized trypsin to α-La at all explored conditions, its accessibility toward β-Lg was pH and ionic strength dependent. Namely, higher pH (15% residual at pH 9.2 vs 60% at pH 7.8) and lower ionic strength (30% residual at 0 M NaCl vs 70% at 0.1 and 0.25 M NaCl) was preferential. In addition, the increase of flow rate (up to 32 mL/min) contributed to the increase in hydrolysis efficiency of immobilized trypsin and did not affect its ability to deplete β-Lg.

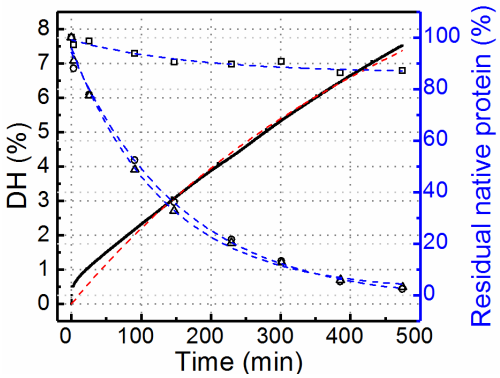

Figure 4-10. Hydrolysis of WPI solution. The evolution of DH and the amounts of residual native α-La (□), β-Lg A (Δ), and β-Lg B (○) were described (Mao & Kulozik, 2018)

5 Conclusion

Despite extensive investigations on the development of IMTRs, no available systems were able to be used for the production of protein hydrolysates with high reusability and processing capacity. Thus, the primary aim of this thesis was to develop IMTRs with improved performances in producing protein hydrolysates. The developed IMTRs-1 mL with a 6 µm pore size, in this thesis, was consecutively used for the hydrolysis of β-Lg over 18 cycles, during which both enzymatic activity and permeability remained constant. In addition to the 6 µm pore size, IMTRs with a pore size of 2 µm were parallel prepared to examine the influence of pore size on the performance of immobilized trypsin. Kinetic studies toward substrate BAEE as a function of flow rate indicate that the increase in the pore size from 2.1 to 6 µm impaired the enzymatic activity of immobilized trypsin. This is probably due to the reduced sufficient contact between the substrate and the immobilized enzyme, as the shear force on the monolith wall simultaneously decreased with increasing pore sizes.

Nevertheless, immobilized trypsin in 6 µm-IMTRs still showed significant activity toward β-Lg. To achieve a long-term investigation of the WPI hydrolysis by an IMTR, the bed volume of the IMTR with 6 µm pore size was scaled up from 1 mL to 8 mL, thereby, compromising with slightly decreased enzymatic efficiency. With respect to hydrolyzing WPI, β-Lg was selectively hydrolyzed by the immobilized trypsin in the IMTR-8 mL at ambient temperature, resulting that above 85% α-La remained native in the final hydrolysates. Despite the inaccessibility of the immobilized trypsin to α-La at all explored conditions, its accessibility toward β-Lg was pH and ionic strength dependent. Namely, higher pH (15% residual at pH 9.2 vs 60% at pH 7.8) and lower ionic strength (30% residual at 0 M NaCl vs 70% at 0.1 and 0.25 M NaCl) was preferential. In addition, the increase of flow rate (up to 32 mL/min) contributed to the hydrolysis efficiency of immobilized trypsin and did not affect its ability to deplete β-Lg. The upscaled IMTR-8 mL in this study was able to be operated at high flow rates while maintaining low backpressure, which significantly improved the productivity of this reactor. The 11 mg trypsin immobilized on the CIM monolithic column through a multipoint covalent binding technique remained stable over 30 cycles of intensive uses, demonstrating the CIM-MITR to be cost effective, time efficient, and reusable. These above advantages render the CIM-IMTRs suitable for large-scale operations.

Another aim of this thesis was to establish a triangular relationship among hydrolytic conditions, DH and hydrolysate profiles for immobilized trypsin, simultaneously to compare with free trypsin. The hydrolysate profiles as a function of DH is determined by the selectivity, which highly depends on hydrolytic conditions. No prior studies discuss in sufficient detail whether these influences will differ once the enzyme is immobilized and an unconventional hydrolysis approach (flow-through) is implemented. In this thesis, the influence of pH, salts and organic solvents on the performance of IMTRs-1 mL (N3 series), particularly on the selectivity of immobilized trypsin, was systematically investigated and compared with free trypsin. Generally, the immobilization of trypsin led to more focused cleavage sites within its specificity at the

initial stage of hydrolysis, compared with the findings for free trypsin. Salts and pH exerted more pounced influence on free trypsin than on its immobilized form, whereas the addition of ethanol led to a more significant influence on the hydrolysis by immobilized trypsin.

Changes in the selectivity of free trypsin were more significant than its immobilized form due to the pH increase, while for immobilized trypsin the addition of ethanol significantly altered its accessibility toward cleavage sites on intact β-Lg. This is probably due to the different mechanisms of interacting with substrate molecules for free and immobilized trypsin. In the case of free trypsin, the contact between substrate and enzyme depends on the fundamentals of Brownian movement, as well as on the intermolecular forces, mainly the electrostatic forces. For immobilized trypsin, as its flexibility is considerably reduced, substrate molecules are driven to the monolith wall largely by shear force firstly, and then the complex of enzyme and substrate can form by intermolecular forces. It is postulated that hydrophobic interactions might contribute significantly to the interactions between free and immobilized trypsin. Thus, the addition of ethanol, leading to changes in the surface hydrophobicity of substrate molecules, largely altered the accessibility of immobilized trypsin, but did not shift the preference of free trypsin significantly, as the dominant attraction force still depends on electrostatic interactions.

6 Summary / Zusammenfassung

6.1 Summary

Whey, a fluid by-product resulting from the precipitation of casein in milk, contains high-quality proteins that not only can benefit consumers from the nutritional perspective, but also are very important to the textural and sensory quality of food products. Among numerous processing techniques, the enzymatic modification of whey proteins represents an attractive way because of its fast reaction rates, mild conditions, and high specificity. Trypsin is one of the most widely used enzymes in food processing, where trypsin or a trypsin preparation (mixed with other enzymes) has been used to improve both the functional and nutritional properties of food proteins. To reduce the cost of large-scale use of trypsin in solution and to improve its industrial application, the enzyme immobilization represents an alternative technique due to the possibility of reusing enzymes and producing enzyme-free hydrolysates.

Due to the exclusive specificity of trypsin, this enzyme is wildly applied in proteomics research. Thus, numerous IMTRs are developed to accelerate the digestion step for proteomics analysis. However, these developed IMTRs do not meet the application for producing protein hydrolysates. The crucial requirements for such an application in each cycle are processing larger amounts of substrate and longer continuous digestion times, and moreover, achieving as many cycles as possible. Aiming at this application, the immobilization of trypsin onto different stationary supports was studied in past decades. Unfortunately, these available systems still suffer from low processing stability and/or low capacity in terms of volume throughput. In addition, no commercialized IMTRs to date have been indicated for the production of food protein hydrolysates. Therefore, an IMTR with improved activity, stability, and reusability compared with available reactors is required for the production of protein hydrolysates. To meet the aforementioned requirements, monolithic materials, consisting of a whole piece material with homogeneously distributed pores, have attracted considerable attention as the support for enzyme immobilization. Monolithic materials generally allow for a high mass flow, and the mass transfer of target molecules toward the enzyme bound to the monolithic channel surfaces is primarily governed by convective flow, contributing to a high volume throughput at a low backpressure. Furthermore, the surface of organic monoliths can be modified with various functional groups, which makes covalent bonding of enzymes much easier. In this thesis, for the first time, trypsin was immobilized on the polymethacrylate monoliths with a pore size of 6 µm, and compared with the 2.1 µm pore size. The immobilization was achieved by multipoint covalent bonding through Schiff base reaction with ALD groups, which were derivatized on the monolith surface.

The developed IMTRs-1 mL with a pore size of 6 or 2.1 µm were extremely stable during storage for 1 year, in terms of enzymatic activity and permeability monitored over 3 weeks. With respect to producing protein hydrolysates, IMTRs with a 6 µm pore size showed a much higher reusability than those with a 2 µm pore size, since a great

decline in the permeability of 2 µm-IMTRs was observed after 10 cycles. In contrast, for 6 µm-IMTRs, both enzymatic activity and permeability remained constant over 18 cycles. Toward substrate BAEE, however, the apparent kinetic parameter K_m" increased and V_{max} decreased for per mg active immobilized trypsin when the pore size of an IMTR enlarged from 2.1 to 6 µm. In other words, the increase in the pore size from 2.1 to 6 µm in an IMTR impaired the enzymatic activity of immobilized trypsin, which is probably due to the reduced sufficient contact between the substrate and the immobilized enzyme as the shear force on the monolith wall simultaneously decreased with increasing pore size. Nevertheless, immobilized trypsin in 6 µm-IMTRs still showed significant activity toward β-Lg. To achieve a long-term investigation of the WPI hydrolysis by an IMTR, the bed volume of the IMTR with 6 µm pore size was scaled up from 1 mL to 8 mL, thereby, compromising with slightly decreased enzymatic efficiency. Eventually, this IMTR-8 mL was able to be consecutively used for the hydrolysis of WPI for at least 30 times, where a constant enzymatic activity while a 70% decline in permeability were observed. It is to be noted that the backpressure of the IMTR-8 mL was still below 0.15 MPa at 48 mL/min (6 CVs/min) even when the permeability declined 70%, and its operational limit is up to 2 MPa.

Based on previous findings that free trypsin has the potential to selectively hydrolyze β-Lg in whey proteins, depending on hydrolytic conditions. For instance, 67.87% α-La remained with the complete depletion of intact β-Lg, when WPI was hydrolyzed by free trypsin at pH 8.5 and 25^{o}C (Cheison et al., 2011). To examine the applicability of this IMTR-8 mL for selectively hydrolyzing β-Lg over α-La, 20 mg/mL WPI was hydrolyzed using a recirculation approach under varied hydrolytic conditions, i.e., pH, salts, flow rate. Interestingly, α-La was almost insusceptible to immobilized trypsin under all explored conditions. At DH 8%, no more intact β-Lg was detectable, while approximately 85% of native α-La remained in the hydrolysates. Although α-La is resistant to the hydrolysis by immobilized trypsin, its existence acts as a competitor with β-Lg for the active site of trypsin. Because a three-fold decrease in V_{max} was noted for WPI, compared with β-Lg at all explored flow rates. Regarding K_m, no significant flow rate dependence was found, irrespective pure β-Lg or WPI was applied, while K_m" values showed a clear increase with increasing flow rates, indicating that more protein molecules were required to achieve V_{max} at higher flow rates in a given time.

The selectivity of a protease toward a specific substrate depends on the primary structure of this substrate as well as on the spatial structures of both the substrate and the enzyme. The hydrolytic conditions, e.g., pH, ionic strength, organic solvents, exert considerable influences on enzyme selectivity. No prior studies discuss in sufficient detail whether these influences will differ once the enzyme is immobilized and an unconventional hydrolysis approach (flow-through) is implemented. In this thesis, the influence of pH, salts and organic solvents on the performance of IMTRs-1 mL (N3 series), particularly on the selectivity of immobilized trypsin, was systematically investigated and compared with free trypsin.

Hydrolytic conditions exerted different influences on the evolutions of DH during the hydrolysis by free and immobilized trypsin. Namely, DH increased fastest for free trypsin in the 20% ethanol/water among all the explored conditions, while for immobilized trypsin, the DH in the hydrolysis with 20% ethanol only increased slightly, lower than those with the addition of 0.02 or 0.1 M NaCl. Besides, with the presence of 0.1 M NaCl, the DH increased for immobilized trypsin while decreased for free trypsin, compared with the hydrolysis without additional NaCl. For both types of trypsin, no significant difference in the evolutions of DH at pH 7.8 and 8.7 was observed. The presence of 0.02 M NaCl significantly increased DH and 0.5 M NaCl seriously retarded the hydrolysis, irrespective free or immobilized trypsin applied.

Regarding the hydrolysis of intact β-Lg, for immobilized trypsin, linear decreases in intact protein dependent on DH were observed at all explored concentrations, close to the “one-by-one” model, and the slope continuously decreased with increasing NaCl at pH 8.7. For free trypsin, a sharp increase in the depletion rate was noted at the initial stage of hydrolysis with 0 or 0.02 M NaCl, which is more in agreement with the “zipper” model. However, the depletion of intact protein by free trypsin was more close to “one-by-one”, when the NaCl concentration increased from 0.02 to 0.1 M. Generally, the addition of NaCl prevented intact β-Lg from hydrolysis, irrespective free or immobilized trypsin was applied. Contrast to NaCl, the fastest depletion rate of intact β-Lg was observed in the presence of 20% ethanol for both types of trypsin. In addition, both free and immobilized trypsin exhibited greater accessibility to intact β-Lg at increasing pH values.

Regarding the differences in peptides generated from free or immobilized trypsin, generally, the immobilization of trypsin led to more focused cleavage sites within its specificity at the initial stage of hydrolysis compared with the findings for free trypsin. Salts and pH exerted more pounced influence on free trypsin than its immobilized form, whereas the addition of ethanol led to a more significant influence on the hydrolysis by immobilized trypsin.

To sum up, the IMTR-6 μm shows high potential to be further upscaled for producing protein hydrolysates. More focused cleavage sites were observed for immobilized trypsin than its free form. A triangular relationship among hydrolytic conditions, DH and hydrolysate profiles is preliminary established. This thesis provides the possibility to precisely control the production of protein hydrolysates with desired profiles.

6.2 Zusammenfassung

Molke ist ein flüssiges Nebenprodukt (der Käseherstellung), welches durch die Ausfällung von Kasein aus der Milch entsteht. Sie enthält hochwertige Proteine, die nicht nur den Verbrauchern aus ernährungsphysiologischer Sicht zugutekommen können, sondern die auch für die Textur und sensorische Qualität von Lebensmittelprodukten von großer Bedeutung sind. Für die Weiterverarbeitung von Molke steht eine Vielzahl an Prozesstechniken zur Verfügung. Von besonderem Interesse ist hierbei die enzymatische Modifikation der Molkenproteine, da es sich um ein sehr schnelles und spezifisches Verfahren handelt, welches zudem unter relativ milden Reaktionsbedingungen abläuft. Das am häufigsten verwendete Enzym in der Lebensmittelverarbeitung ist Trypsin. Trypsin bzw. Trypsin-Präparate (Mischung verschiedener Enzyme) werden eingesetzt, um sowohl die funktionellen als auch die ernährungsphysiologischen Eigenschaften von Lebensmitteln zu verbessern. Im Zusammenhang mit der Entwicklung eines industriell anwendbaren, wirtschaftlichen Verfahrens zur enzymatischen Proteinmodifikation (z. B. Hydrolyse), stellt die Enzymimmobilisierung einen vielversprechenden Ansatz dar. Wesentliche Vorteile einer Immobilisierung bestehen in der Wiederverwendbarkeit der Enzyme sowie der Gewinnung enzymfreier Proteinhydrolysate.

Aufgrund seiner hohen Spezifität ist Trypsin in der Proteomikforschung sehr weit verbreitet. Es wurden auch bereits zahlreiche IMTRs entwickelt, welche es ermöglichen, den Aufschlussschritt der Proteomics-Analyse zu beschleunigen. Die bislang verfügbaren IMTRs sind jedoch nicht zur Herstellung von Proteinhydrolysaten geeignet. Entscheidende Anforderungen für eine solche Anwendung umfassen die Verarbeitbarkeit größerer Substratmengen pro Zyklus, die Ermöglichung längerer kontinuierlicher Aufschlusszeiten sowie die Durchführung möglichst vieler Zyklen. Im Hinblick auf das Ziel, IMTRs für die Proteinhydrolyse einzusetzen, wurde in den letzten Jahrzehnten verstärkt an der Immobilisierung von Trypsin auf verschiedenen stationären Trägermaterialien geforscht. Leider weisen die bislang verfügbaren Systeme eine zu geringe Verarbeitungsstabilität und/oder zu geringe Kapazität hinsichtlich des Volumendurchsatzes auf. Darüber hinaus gibt es bisher keine kommerziell erhältlichen IMTRs, die zur Gewinnung von Proteinhydrolysaten gedacht sind. Um die Herstellung von Proteinhydrolysaten zu realisieren ist es notwendig, IMTRs mit verbesserter Aktivität, Stabilität und Wiederverwendbarkeit im Vergleich zu den bereits verfügbaren Reaktoren zu entwickeln. In diesem Zusammenhang haben monolithische Materialien als Träger für immobilisierte Enzyme bereits beträchtliche Aufmerksamkeit auf sich gezogen. Monolithen werden aus einem Stück gefertigt und besitzen homogene, gleichmäßig verteilte Poren. Sie ermöglichen im Allgemeinen einen hohen Massenfluss sowie einen hohen Volumendurchsatz bei geringem Gegendruck. Letzteres ist dadurch bedingt, dass der Massentransfer der Zielmoleküle zu den an die Porenoberflächen des Monolithen gebundenen Enzyme hauptsächlich durch konvektiven Fluss gesteuert wird. Zudem kann die Oberfläche von organischen Monolithen mit verschiedenen funktionellen Gruppen modifiziert werden, wodurch die kovalente Bindung der Enzyme wesentlich erleichtert wird.

In dieser Arbeit wurde Trypsin zum ersten Mal auf einem Polymethacrylate-Monolithen (Bettvolumen: 1 mL) mit Porengrößen von 6 µm im Vergleich zu 2,1 µm immobilisiert. Die Immobilisierung wurde durch kovalente Mehrpunktbindung durch Schiffsherr Base-Reaktion mit ALD-Gruppen erreicht, die auf der Monolithoberfläche derivatisiert wurden. Die entwickelten IMTRs waren während der Lagerung von mindestens 1 Jahr extrem stabil, was ihre enzymatische Aktivität und Permeabilität über einen Zeitraum von 3 Wochen anbelangt. In Bezug auf die Herstellung von Proteinhydrolysaten zeigten IMTRs mit einer Porengröße von 6 µm eine deutlich höhere Wiederverwendbarkeit als solche mit einer Porengröße von 2,1 µm. Für die 2,1 µm-IMTRs war nach 10 Zyklen eine starke Abnahme der Permeabilität zu beobachten. Im Gegensatz dazu blieb für die 6 µm-IMTRs sowohl die enzymatische Aktivität als auch die Permeabilität über 18 Zyklen konstant. Im Hinblick auf das Substrat BAEE kam es durch die Erhöhung der Porengröße der IMTRs von 2,1 auf 6 µm jedoch zu einer Zunahme des scheinbaren kinetischen Parameters K_m“ während V_{max} pro mg aktivem Trypsin abnahm. Das bedeutet, dass die enzymatische Aktivität des immobilisierten Trypsins durch die Erhöhung der Porengröße von 2,1 auf 6 µm beeinträchtigt wurde. Ursache hierfür könnte ein unzureichender Kontakt zwischen Substrat und immobilisiertem Enzym sein. Dies lässt sich damit erklären, dass die Scherkraft auf der Oberfläche der Monolithen mit zunehmender Porengröße sinkt. Trotzdem zeigte das immobilisierte Trypsin in den 6 µm-IMTRs eine signifikante Aktivität gegenüber (dem Hauptmolkenprotein) β-Lg. Um eine Langzeitstudie zur WPI-Hydrolyse mittels IMTR durchführen zu können, wurde das Bettvolumen des 6 µm-IMTR von 1 mL auf 8 mL hochskaliert. Dies führte einerseits zu einer leichten Reduktion der enzymatischen Effizienz, andererseits konnte dieser 6 µm-IMTR-8 mL für 30 aufeinanderfolgende WPI-Hydrolysen wiederverwendet werden. Die Enzymaktivität blieb über die gesamte Betriebsdauer konstant, wobei eine 70%ige Abnahme der Permeabilität festgestellt werden konnte. Trotzdem blieb der Gegendruck des 6 µm-IMTR-8 mL sogar noch bei einer Flussrate von 48 mL/min (6 CVs/min) unter 0.15 MPa und dementsprechend unterhalb der Betriebsgrenze von 2 MPa.

Es ist bekannt, dass freies Trypsin in Abhängigkeit von den Hydrolysebedingungen in der Lage ist, β-Lg in Molkenproteinen selektiv zu hydrolysieren. Beispielsweise konnte gezeigt werden, dass es bei der Hydrolyse von WPI durch freies Trypsin (pH 8,5, 25°C) zu einem vollständigen Abbau von intaktem β-Lg kam, während α-La zu 67,8 % erhalten blieb (Cheison et al., 2011). Um nun zu untersuchen, inwiefern sich die selektive Hydrolyse β-Lg mit dem 6 µm-IMTR-8 mL realisieren lässt, wurden 20 mg/mL WPI unter Verwendung eines Rezirkulationsverfahrens und in Abhängigkeit verschiedener Hydrolysebedingungen (d. h. pH-Wert, Salze, Flussraten) hydrolysiert. Interessanterweise war α-La bei allen untersuchten Bedingungen nahezu unempfindlich gegenüber dem immobilisierten Trypsin. Bei einem DH von 8 % war zum Beispiel kein intaktes β-Lg mehr nachweisbar, während die Hydrolysate etwa 85 % natives α-La enthielten. Auch wenn α-La gegen die Hydrolyse durch immobilisiertes Trypsin resistent ist, konkurriert es durch seine Existenz mit β-Lg um das aktive Zentrum des Trypsins. Diese Schlussfolgerung basiert darauf, dass bei der

Verwendung von WPI anstatt von β-Lg als Ausgangssubstrat für die Hydrolyse bei allen untersuchten Bedingungen, eine dreimal so starke Abnahme von V_{max} festgestellt wurde. Für K_m wurde keine signifikante Flussratenabhängigkeit bestimmt. Auch das Ausgangssubstrat spielte hierbei keine Rolle. Die Werte für K_m" hingegen stiegen mit zunehmender Flussrate, was darauf hinweist, dass mehr Proteinmoleküle erforderlich waren, um V_{max} bei geringeren Flussraten in einem bestimmten Zeitraum zu erreichen.

Die Selektivität einer Protease gegenüber einem spezifischen Substrat ist abhängig von der Primärstruktur des Substrats sowie der räumlichen Struktur sowohl des Substrats als auch des Enzyms. Zudem spielen die Hydrolysebedingungen wie z. B. der pH-Wert, die Ionenstärke oder organische Lösungsmittel eine wesentliche Rolle in Bezug auf die Enzymselektivität. In bisherigen Studien wurde allerdings nicht untersucht, inwiefern diese Erkenntnisse auch für immobilisierte Enzyme sowie einen eher unkonventionellen Hydrolyseansatz (d. h. Durchfluss) gelten. In dieser Arbeit wurde daher der Einfluss des pH-Werts sowie von Salzen und organischen Lösungsmitteln auf die Leistung und insbesondere die Selektivität von immobilisiertem Trypsin anhand von IMTRs mit einem Bettvolumen von 1 mL (N3-Serie) systematisch untersucht. Die erzielten Ergebnisse wurden mit freiem Trypsin verglichen. In Abhängigkeit der Hydrolysebedingungen wurden für immobilisiertes und freies Trypsin unterschiedliche DH-Verläufe festgestellt. Insgesamt konnte der schnellste DH-Anstieg für freies Trypsin in einer 20 % Ethanol/Wasser-Mischung beobachtet werden. Im Fall des immobilisierten Trypsins kam es durch den Zusatz von 20 % Ethanol nur zu einer leichten Erhöhung des DH. Zudem wurden für Proben mit 0,02 oder 0,1 M NaCl höhere DH-Werte erreicht. Im Vergleich zur Hydrolyse ohne NaCl konnte bei Zugabe von 0,1 M NaCl für immobilisiertes Trypsin eine Zunahme des DH gemessen werden, während der DH für freies Trypsin abnahm. Sowohl für freies als auch immobilisiertes Trypsin konnte kein signifikanter Einfluss einer pH-Änderung (pH 7,8 und 8,7) auf den DH festgestellt werden. In Bezug auf die Ionenstärke wurde für beide Trypsinarten für 0,02 M NaCl eine signifikante Erhöhung des DH beobachtet, während es durch 0,5 M NaCl zu einer Verzögerung der Hydrolyse kam.

Bei der Hydrolyse von β–Lg mit immobilisiertem Trypsin wurde in Abhängigkeit des DH eine lineare Abnahme an intaktem Protein für alle untersuchten Konzentrationen festgestellt, was relativ gut dem „one-by-one"-Modell entspricht. Bei pH 8,7 reduzierte sich die Steigung kontinuierlich mit zunehmender Konzentration an NaCl. Für freies Trypsin wurde ein steiler Anstieg in der Abbaurate in der initialen Phase der Hydrolyse in Anwesenheit von 0 oder 0,02 M NaCl beobachtet, was eher dem „Reißverschluss"-Modell entspricht. Für eine Erhöhung der NaCl-Konzentration von 0,02 bis 0,1 M kam für die Abnahme an intaktem Protein durch freies Trypsin jedoch wieder das „one-by-one"-Modell in Frage. Allgemein führte die Zugabe von NaCl eher zu einer Verhinderung der Hydrolyse von intaktem β-Lg. Dies gilt sowohl für freies als auch immobilisiertes Trypsin. Im Gegensatz dazu konnte für beide Trypsinarten jeweils die höchste Abbaurate von intaktem β-Lg in Anwesenheit von 20 % Ethanol gemessen

werden. Außerdem zeigten sowohl freies als auch immobilisiertes Trypsin mit ansteigendem pH-Wert eine bessere Zugänglichkeit für intaktes β-Lg.

In Bezug auf die Unterschiede der resultierenden Peptide, welche mittels freiem oder immobilisiertem Trypsin erzeugt wurden, führte die Enzymimmobilisierung im Anfangsstadium der Hydrolyse allgemein zu einer stärkeren Fokussierung von Spaltstellen innerhalb der Spezifität. Die Anwesenheit von Salz sowie der pH-Wert zeigten einen stärkeren Einfluss auf die Hydrolyse mittels freiem Trypsin, wohingegen die Zugabe von Ethanol einen deutlicheren Einfluss auf die Hydrolyse mittels immobilisiertem Trypsin hatte.

Zusammenfassend lässt sich sagen, dass der 6 µm-IMTR ein großes Potenzial für die Herstellung von Proteinhydrolysaten in größerem Maßstab besitzt. Im Vergleich zu frei vorliegendem Trypsin wurde für das immobilisierte Enzym eine stärkere Fokussierung von Spaltstellen beobachtet. Die Aufstellung einer Dreiecksbeziehung zwischen Hydrolysebedingungen, DH- und Hydrolysat-Profilen liefert zudem eine fundierte Kenntnisbasis für die zielgerichtete Herstellung von Proteinhydrolysaten mit spezifischen Profilen.

7 Reference

Abramowitz, N., Schechter, I. & Berger, A. (1967). On the size of the active site in proteases II. Carboxypeptidase-A. *Biochemical and Biophysical Research Communications*, 29(6), 862–867.

Adjonu, R., Doran, G., Torley, P. & Agboola, S. (2013). Screening of whey protein isolate hydrolysates for their dual functionality: influence of heat pre-treatment and enzyme specificity. *Food Chemistry*, 136(3–4), 1435–1443.

Adjonu, R., Doran, G., Torley, P. & Agboola, S. (2014). Whey protein peptides as components of nanoemulsions: A review of emulsifying and biological functionalities. *Journal of Food Engineering*, 122, 15–27.

Adler-Nissen, J. (1976). Enzymic hydrolysis of proteins for increased solubility. *Journal of Agricultural and Food Chemistry*, 24(6), 1090–1093.

Adler-Nissen, J. (1979). Determination of the degree of hydrolysis of food protein hydrolysates by trinitrobenzenesulfonic acid. *Journal of Agricultural and Food Chemistry*, 27(6), 1256–1262.

Adler-Nissen, J. (1986). Enzymatic hydrolysis of food proteins: Elsevier Applied Science Publishers, ISBN : 0853343861

Aguero, R., Bringas, E., Román, M. F. S., Ortiz, I. & Ibañez, R. (2017). Membrane Processes for Whey Proteins Separation and Purification. A Review. *Current Organic Chemistry*, 21(17).

Alpay, P. & Uygun, D. A. (2015). Usage of immobilized papain for enzymatic hydrolysis of proteins. *Journal of Molecular Catalysis B*: *Enzymatic*, 111, 56–63.

Alptekin, Ö., Tükel, S. S., Yıldırım, D. & Alagöz, D. (2010). Immobilization of catalase onto Eupergit C and its characterization. *Journal of Molecular Catalysis B*: *Enzymatic*, 64(3–4), 177–183.

Arrutia, F., Rubio, R. & Riera, F. A. (2016). Production and membrane fractionation of bioactive peptides from a whey protein concentrate. *Journal of Food Engineering, 184*, 1–9.

Asao, T., Tsuji, I., Tashiro, M., Iwami, K. & Ibuki, F. (1992). Trypsin hydrolysis of the Tyr (42)–Ser (43) bond, the chymotrypsin reactive–site peptide bond, of faba bean Bowman–Birk type inhibitor. *Bioscience, Biotechnology, and Biochemistry*, 56(3), 521–522.

Atacan, K., Cakiroglu, B. & Ozacar, M. (2016). Improvement of the stability and activity of immobilized trypsin on modified Fe3O4 magnetic nanoparticles for hydrolysis of bovine serum albumin and its application in the bovine milk. *Food Chemistry*, 212, 460–468.

Banach, J. C., Lin, Z. & Lamsal, B. P. (2013). Enzymatic modification of milk protein concentrate and characterization of resulting functional properties*. LWT-Food Science and Technology*, 54(2), 397–403.

Barbosa, O., Torres, R., Ortiz, C. & Fernandez-Lafuente, R. (2012). Versatility of glutaraldehyde to immobilize lipases: Effect of the immobilization protocol on the properties of lipase B from Candida antarctica. *Process Biochemistry*, 47(8), 1220–1227.

Bartolini, M., Cavrini, V. & Andrisano, V. (2005). Choosing the right chromatographic support in making a new acetylcholinesterase-micro-immobilised enzyme reactor for drug discovery. *Journal of Chromatography A*, 1065(1), 135–144.

Bartolini, M., Cavrini, V. & Andrisano, V. (2007). Characterization of reversible and pseudo-irreversible acetylcholinesterase inhibitors by means of an immobilized enzyme reactor. *Journal of Chromatography A*, 1144(1), 102–110.

Bartolini, M., Greig, N. H., Yu, Q. S. & Andrisano, V. (2009). Immobilized butyryl-cholinesterase in the characterization of new inhibitors that could ease Alzheimer's disease. *Journal of Chromatography A*, 1216(13), 2730–2738.

Bassan, J., de Souza Bezerra, T., Peixoto, G., da Cruz, C., Galán, J., Vaz, A., Garrido, S., Filice, M. & Monti, R. (2016). Immobilization of Trypsin in Lignocellulosic Waste Material to Produce Peptides with Bioactive Potential from Whey Protein. *Materials*, 9(5), 357–376.

Baussay, K., Bon, C. L., Nicolai, T., Durand, D. & Busnel, J. P. (2004). Influence of the ionic strength on the heat-induced aggregation of the globular protein beta-lactoglobulin at pH 7. *International Journal of Biological Macromolecules*, 34(12), 21–28.

Beierlein, F. R., Clark, T., Braunschweig, B. R., Engelhardt, K., Glas, L. & Peukert, W. (2015). Carboxylate ion pairing with alkali-metal ions for β-Lactoglobulin and its role on aggregation and interfacial adsorption. *The Journal of Physical Chemistry B*, 119(17), 5505–5517.

Bencina, K., Bencina, M., Podgornik, A. & Strancar, A. (2007). Influence of the meth-acrylate monolith structure on genomic DNA mechanical degradation, enzymes activity and clogging. *Journal of Chromatography A*, 1160(12), 176–183.

Benčina, K., Podgornik, A., Štrancar, A. & Benčina, M. (2004). Enzyme immobilization on epoxy- and 1,1′-carbonyldiimidazole-activated methacrylate-based monoliths. *Journal of Separation Science*, 27(10), 811–818.

Benčina, M., Benčina, K., Štrancar, A. & Podgornik, A. (2005). Immobilization of desoxy-ribonuclease via epoxy groups of methacrylate monoliths. *Journal of Chromatography A*, 1065(1), 83–91.

Bender, M. L. & Kezdy, F. J. (1965). Mechanism of action of proteolytic enzymes. *Annual Review of Biochemistry*, 34(1), 49–76.

Bergmeyer, H. U. (1974). Methods of enzymatic analysis: *Verlag Chemie.*

Bernal, C., Sierra, L. & Mesa, M. (2014). Design of β-galactosidase/silica biocatalysts: Impact of the enzyme properties and immobilization pathways on their catalytic performance. *Engineering in Life Sciences*, 14(1), 85–94.

Betancor, L., López-Gallego, F., Hidalgo, A., Alonso-Morales, N., Mateo, G. D. O. C., Fernández-Lafuente, R. & Guisán, J. M. (2006). Different mechanisms of protein immobilization on glutaraldehyde activated supports: Effect of support activation and immobilization conditions. *Enzyme and Microbial Technology*, 39(4), 877–882.

Bolibok, P., Wiśniewski, M., Roszek, K. & Terzyk, A. P. (2017). Controlling enzymatic activity by immobilization on graphene oxide. *The Science of Nature*, 104(3–4), 36.

Bonincontro, A., De Francesco, A., Matzeu, M., Onori, G. & Santucci, A. (1997). Conformational changes of lysozyme in water-ethanol mixtures. *Colloids and Surfaces B*: *Biointerfaces*, 10(2), 105–111.

Bouaouina, H., Desrumaux, A., Loisel, C. & Legrand, J. (2006). Functional properties of whey proteins as affected by dynamic high-pressure treatment. *International Dairy Journal*, 16(4), 275–284.

Brownlow, S., Cabral, J. H. M., Cooper, R., Flower, D. R., Yewdall, S. J., Polikarpov, I., North, A. C. & Sawyer, L. (1997). Bovine β-lactoglobulin at 1.8 Å resolution-still an enigmatic lipocalin. *Structure*, 5(4), 481–495.

Buchholz, K. & Klein, J. (1987). Characterization of immobilized biocatalysts. *Methods in Enzymology*, 135, 3-30.

Buck, F., Vithayathil, A., Bier, M. & Nord, F. (1962). On the mechanism of enzyme action. LXXIII. Studies on trypsins from beef, sheep and pig pancreas. *Archives of Biochemistry and Biophysics*, 97(2), 417–424.

Butré, C. I., Buhler, S., Sforza, S., Gruppen, H. & Wierenga, P. A. (2015). Spontaneous, non-enzymatic breakdown of peptides during enzymatic protein hydrolysis. *Biochimica et Biophysica Acta*, 1854(8), 987–994.

Butré, C. I., Sforza, S., Gruppen, H. & Wierenga, P. A. (2014). Introducing enzyme selectivity: a quantitative parameter to describe enzymatic protein hydrolysis. *Analytical and Bioanalytical Chemistry*, 406(24), 5827–5841.

Butré, C. I., Sforza, S., Wierenga, P. A. & Gruppen, H. (2015). Determination of the influence of the pH of hydrolysis on enzyme selectivity of Bacillus licheniformis protease towards whey protein isolate. *International Dairy Journal*, 44, 44–53.

Butré, C. I., Wierenga, P. A. & Gruppen, H. (2012). Effects of ionic strength on the enzymatic hydrolysis of diluted and concentrated whey protein isolate. *Journal of Agricultural and Food Chemistry*, 60(22), 5644–5651.

Calleri, E., Temporini, C., Perani, E., Stella, C., Rudaz, S., Lubda, D., Mellerio, G., Veuthey, J. L., Caccialanza, G. & Massolini, G. (2004). Development of a bio-reactor based on trypsin immobilized on monolithic support for the on-line digestion and identification of proteins. *Journal of Chromatography A*, 1045(12), 99–109.

Cao, M., Li, Z., Wang, J., Ge, W., Yue, T., Li, R., Colvin, V. L. & Yu, W. W. (2012). Food related applications of magnetic iron oxide nanoparticles: Enzyme immobilization, protein purification, and food analysis. *Trends in Food Science & Technology*, 27(1), 47–56.

Carrea, G., Bovara, R., Pasta, P. & Cremonesi, P. (1982). The effect of Hofmeister anions and protein concentration on the activity and stability of some immobilized NAD-dependent dehydrogenases. *Biotechnology and Bioengineering*, 24(1), 1–7.

Casal, H. L., Kohler, U. & Mantsch, H. H. (1988). Structural and conformational changes of beta-lactoglobulin B: an infrared spectroscopic study of the effect of pH and temperature. *Biochimica et Biophysica Acta*, 957(1), 11–20.

Castillo-Yanez, F. J., Pacheco-Aguilar, R., Garcia-Carreno, F. L. & Navarrete-Del Toro Mde, L. (2005). Isolation and characterization of trypsin from pyloric caeca of Monterey sardine Sardinops sagax caerulea. Comparative *Biochemistry and Physiology. Part B: Biochemistry and Molecular Biology,* 140(1), 91–98.

Causon, T. J. & Nischang, I. (2014). Critical differences in chromatographic properties of silica- and polymer-based monoliths. *Journal of Chromatography A*, 1358, 165–171.

Chaplin, M. F. & Bucke, C. (1990). The preparation and kinetics of immobilized enzymes. *In Enzyme technology (pp. 141–146),* Cambridge University Press: Cambridge, ISBN: 9780521348843.

Cheison, S. C., Brand, J., Leeb, E. & Kulozik, U. (2011). Analysis of the effect of temperature changes combined with different alkaline pH on the β-lactoglobulin trypsin hydrolysis pattern using MALDI-TOF-MS/MS. *Journal of Agricultural and Food Chemistry*, 59(5), 1572–1581.

Cheison, S. C. & Kulozik, U. (2017). Impact of the environmental conditions and substrate pre-treatment on whey protein hydrolysis: A review. *Critical Reviews in Food Science and Nutrition*, 57(2), 418–453.

Cheison, S. C., Leeb, E., Letzel, T. & Kulozik, U. (2011). Influence of buffer type and concentration on the peptide composition of trypsin hydrolysates of β-lactoglobulin. *Food Chemistry*, 125(1), 121–127.

Cheison, S. C., Leeb, E., Toro-Sierra, J. & Kulozik, U. (2011). Influence of hydrolysis temperature and pH on the selective hydrolysis of whey proteins by trypsin and potential recovery of native alpha-lactalbumin. *International Dairy Journal*, 21(3), 166–171.

Cheison, S. C., Wang, Z. & Xu, S. Y. (2007). Use of response surface methodology to optimise the hydrolysis of whey protein isolate in a tangential flow filter membrane reactor. *Journal of Food Engineering*, 80(4), 1134 –1145.

Cheison, S. C., Zhang, S. B., Wang, Z. & Xu, S. Y. (2009). Comparison of a modified spectrophotometric and the pH-stat methods for determination of the degree of hydrolysis of whey proteins hydrolysed in a tangential-flow filter membrane reactor. *Food Research International*, 42(1), 91–97.

Chen, S. X., Swaisgood, H. E. & Foegeding, E. A. (1994). Gelation of. beta.-lactoglobulin treated with limited proteolysis by immobilized trypsin. *Journal of Agricultural and Food Chemistry*, 42(2), 234–239.

Chizoba-Ekezie, F. G., Cheng, J. H. & Sun, D. W. (2018). Effects of nonthermal food processing technologies on food allergens: A review of recent research advances. *Trends in Food Science & Technology*, 74, 12–25.

Chrysina, E. D., Brew, K. & Acharya, K. R. (2000). Crystal structures of apo- and holo-bovine alpha-lactalbumin at 2. 2-Á resolution reveal an effect of calcium on interlobe interactions. *Journal of Biological Chemistry*, 275(47), 37021–37029.

Church, F. C., Porter, D. H., Catignani, G. L. & Swaisgood, H. E. (1985). An o-phthal-aldehyde spectrophotometric assay for proteinases. *Analytical Biochemistry*, 146(2), 343–348.

Contreras, M. D. M., Hernández-Ledesma, B., Amigo, L., Martín-Álvarez, P. J. & Recio, I. (2011). Production of antioxidant hydrolyzates from a whey protein concentrate with thermolysin: Optimization by response surface methodology. *LWT-Food Science and Technology*, 44(1), 9–15.

Creamer, L., Nilsson, H., Paulsson, M., Coker, C., Hill, J. & Jimenez-Flores, R. (2004). Effect of genetic variation on the tryptic hydrolysis of bovine β-lactoglobulin A, B, and C. *Journal of Dairy Science*, 87(12), 4023–4032.

Dannenberg, F. & Kessler, H. G. (1988). Reaction kinetics of the denaturation of whey proteins in milk. *Journal of Food Science*, 53(1), 258–263.

Delattre, C., Michaud, P. & Vijayalakshmi, M. A. (2008). New monolithic enzymatic micro-reactor for the fast production and purification of oligogalacturonides. *Journal of Chromatography. B: Analytical Technologies in the Biomedical and Life Sciences*, 861(2), 203–208.

Delavari, B., Saboury, A. A., Atri, M. S., Ghasemi, A., Bigdeli, B., Khammari, A., Maghami, P., Moosavi-Movahedi, A. A., Haertlé, T. & Goliaei, B. (2015). α-lactalbumin: A new carrier for vitamin D3 food enrichment. *Food Hydrocolloids*, 45, 124–131.

Deng, Y., van der Veer, F., Sforza, S., Gruppen, H. & Wierenga, P. A. (2017). Towards predicting protein hydrolysis by bovine trypsin. *Process Biochemistry*, 65, 81–92.

Dufour, E., Bertrand-Harb, C. & Haertlé, T. (1993). Reversible effects of medium dielectric constant on structural transformation of β-lactoglobulin and its retinol binding. Biopolymers: *Original Research on Biomolecules*, 33(4), 589–598.

Dufour, E. & Haertlé, T. (1990). Alcohol-induced changes of β-lactoglobulin retinol binding stoichiometry. *Protein Engineering, Design and Selection*, 4(2), 185–190.

Dufour, E., Robert, P., Bertrand, D. & Haertlé, T. (1994). Conformation changes of β-lactoglobulin: An ATR infrared spectroscopic study of the effect of pH and ethanol. *Journal of Protein Chemistry*, 13(2), 143–149.

Duggal, S. & Bucholz, K. (1982). Effects of immobilization on intrinsic kinetics and selectivity of trypsin. *Applied Microbiology and Biotechnology*, 16(2), 81–87.

Dullius, A., Goettert, M. I. & de Souza, C. F. V. (2018). Whey protein hydrolysates as a source of bioactive peptides for functional foods – Biotechnological facilitation of industrial scale-up. *Journal of Functional Foods*, 42, 58–74.

Dwevedi, A. (2016). Basics of Enzyme Immobilization. In *Enzyme Immobilization* (pp. 21–44), Springer, Cham, ISBN 9783319414188.

Edwards, P. B., Creamer, L. K., & Jameson, G. B. (2009). Structure and stability of whey proteins. In A. Thompson, M. Boland, H. Singh (Eds.), *Milk proteins: From Expression to Food* (pp. 163–203), Academic Press, ISBN 978-0123740397.

Endo, A., Kurinomaru, T. & Shiraki, K. (2016). Hyperactivation of α-chymotrypsin by the Hofmeister effect. *Journal of Molecular Catalysis B: Enzymatic*, 133, 432–438.

Endo, A., Kurinomaru, T. & Shiraki, K. (2018). Hyperactivation of serine proteases by the Hofmeister effect. *Molecular Catalysis*, 455, 32–37.

Engasser, J. M. & Horvath, C. (1976). Diffusion and kinetics with immobilized enzymes. *Applied Biochemistry and Bioengineering*, 1,127–220.

Essa, H., Magner, E., Cooney, J. & Hodnett, B. K. (2007). Influence of pH and ionic strength on the adsorption, leaching and activity of myoglobin immobilized onto ordered mesoporous silicates. *Journal of Molecular Catalysis B*: *Enzymatic*, 49(1–4), 61–68.

Evnin, L. B., Vásquez, J. R. & Craik, C. S. (1990). Substrate specificity of trypsin investigated by using a genetic selection. *Proceedings of the National Academy of Sciences*, 87(17), 6659–6663.

Exl, B.M. (2001). A review of recent developments in the use of moderately hydrolyzed whey formulae in infant nutrition. *Nutrition Research*, 21(1–2), 355–379.

Fang, Y. & Dalgleish, D. G. (1997). Conformation of β-lactoglobulin studied by FTIR: effect of pH, temperature, and adsorption to the oil–water interface. *Journal of Colloid and Interface Science*, 196(2), 292–298.

Feng, W. & Ji, P. (2011). Enzymes immobilized on carbon nanotubes. *Biotechnology Advances*, 29(6), 889–895.

Fernandez-Lafuente, R., Rosell, C., Rodriguez, V. & Guisan, J. (1995). Strategies for enzyme stabilization by intramolecular crosslinking with bifunctional reagents. *Enzyme and Microbial Technology*, 17(6), 517–523.

Fernández, A. & Riera, F. (2013). β-Lactoglobulin tryptic digestion: A model approach for peptide release. *Biochemical Engineering Journal*, 70, 88–96.

Fernández, A., Suárez, A., Zhu, Y., FitzGerald, R. J. & Riera, F. A. (2013). Membrane fractionation of a β-lactoglobulin tryptic digest: Effect of the pH. *Journal of Food Engineering*, 114(1), 83–89.

Fiat, A. M., Migliore-Samour, D., Jolles, P., Drouet, L., Bal dit Sollier, C. & Caen, J. (1993). Biologically active peptides from milk proteins with emphasis on two examples concerning antithrombotic and immunomodulating activities. *Journal of Dairy Science*, 76(1), 301–310.

Fukuda, M. & Kundugi, S. (1989). The mechanism of salt activation of thermolysin: Relation with pressure activation and implications of hydration change coupled with rate process. *Biocatalysis*, 2(3), 225–233.

Garajova, K., Balogova, A., Dusekova, E., Sedlakova, D., Sedlak, E. & Varhac, R. (2017). Correlation of lysozyme activity and stability in the presence of Hofmeister series anions. *Biochimica et Biophysica Acta*, 1865(3), 281–288.

Geng, X. L., Tolkach, A., Otte, J. & Ipsen, R. (2015). Pilot-scale purification of α-lact-albumin from enriched whey protein concentrate by anion-exchange chromato-graphy and ultrafiltration. *Dairy Science & Technology*, 95(3), 353–368.

Germano, M., Piomelli, U., Moin, P. & Cabot, W. H. (1991). A dynamic subgrid-scale eddy viscosity model. *Physics of Fluids A*: Fluid Dynamics, 3(7), 1760–1765.

Giorno, L., Drioli, E., Carvoli, G., Cassano, A. & Donato, L. (2001). Study of an enzyme membrane reactor with immobilized fumarase for production of L-malic acid. *Biotechnology and Bioengineering*, 72(1), 77–84.

Grano, V., Diano, N., Rossi, S., Portaccio, M., Attanasio, A., Cermola, M., Spiezie, R., Citton, C. & Mita, D. G. (2004). Production of low-lactose milk by means of non-isothermal bioreactors. *Biotechnology Progress*, 20(5), 1393–1401.

Gupta, M. N. (1992). Enzyme function in organic solvents. *European Journal of Biochemistry*, 203(1-2), 25–32.

Orrego, A., Romero-Fernández, M., Millán-Linares, M., Yust, M., Guisán, J. & Rocha-Martin, J. (2018). Stabilization of Enzymes by Multipoint Covalent Attachment on Aldehyde-Supports: 2-Picoline Borane as an Alternative Reducing Agent. *Catalysts*, 8(8), 333.

Han, W., Xin, Y., Hasegawa, U. & Uyama, H. (2014). Enzyme immobilization on polymethacrylate-based monolith fabricated via thermally induced phase separation. *Polymer Degradation and Stability*, 109, 362–366.

Hartmann, M. (2005). Ordered Mesoporous Materials for Bioadsorption and Biocata-lysis. *Chemistry of Materials*, 17(18), 4577–4593.

Haug, I. J., Skar, H. M., Vegarud, G. E., Langsrud, T. & Draget, K. I. (2009). Electrostatic effects on β-lactoglobulin transitions during heat denaturation as studied by differential scanning calorimetry. *Food Hydrocolloids*, 23(8), 2287–2293.

Heidebrecht, H. J., Kainz, B., Schopf, R., Godl, K., Karcier, Z., Kulozik, U. & Forster, B. (2018). Isolation of biofunctional bovine immunoglobulin G from milk and colostral whey with mixed-mode chromatography at lab and pilot scale. *Journal of Chromatography A*, 1562, 59–68.

Hernandez-Ledesma, B., Recio, I. & Amigo, L. (2008). β-lactoglobulin as source of bioactive peptides. *Amino Acids*, 35(2), 257–265.

Hernandez, K., Garcia-Galan, C. & Fernandez-Lafuente, R. (2011). Simple and efficient immobilization of lipase B from Candida antarctica on porous styrene-divinyl-benzene beads. *Enzyme and Microbial Technology*, 49(1), 72–78.

Hofmeister, F. (1888). Zur Lehre von der Wirkung der Salze. *Archiv für experimentelle Pathologie und Pharmakologie*, 25(1), 1–30.

Homaei, A. (2015). Enzyme Immobilization and its Application in the Food Industry. *Advances in Food Biotechnology*, 12, 145–164.

Hormann, K., Mullner, T., Bruns, S., Holtzel, A. & Tallarek, U. (2012). Morphology and separation efficiency of a new generation of analytical silica monoliths. *Journal of Chromatography A*, 1222, 46–58.

Huang, X. L., Catignani, G. L. & Swaisgood, H. E. (1994). Comparison of the size and rate of formation of peptides released by limited proteolysis of beta-lactoglobulin-a and beta-lactoglobulin-b with immobilized trypsin. *Journal of Agricultural and Food Chemistry*, 42(6), 1281–1284.

Janolino, V. G. & Swaisgood, H. E. (2002). Trypsin imobilization on derivatized cellulose beads by biospecific avidin-biotin interaction and characterization of the immobilized activity. *Journal of Food Biochemistry*, 26(2), 119–129.

Jaziri, M., Migliore-Samour, D., Casabianca-Pignede, M. R., Keddad, K., Morgat, J. L. & Jolles, P. (1992). Specific binding sites on human phagocytic blood cells for Gly-Leu-Phe and Val-Glu-Pro-Ile-Pro-Tyr, immunostimulating peptides from human milk proteins. *Biochimica et Biophysica Acta*, 1160(3), 251-261.

Jochems, P., Satyawali, Y., Diels, L. & Dejonghe, W. (2011). Enzyme immobilization on/in polymeric membranes: status, challenges and perspectives in biocatalytic membrane reactors (BMRs). *Green Chemistry*, 13(7), 1609.

Jost, R., Meister, N. & Monti, J. C. (1991). Preparation of a hypoallergenic whey protein hydrolyzate and food. U.S. Patent No. 5,039,532. Washington, DC: U.S.

Jungreuthmayer, C., Steppert, P., Sekot, G., Zankel, A., Reingruber, H., Zanghellini, J. & Jungbauer, A. (2015). The 3D pore structure and fluid dynamics simulation of macroporous monoliths: High permeability due to alternating channel width. *Journal of Chromatography A*, 1425, 141–149.

Kamau, S. M., Cheison, S. C., Chen, W., Liu, X. M. & Lu, R. R. (2010). α-lactalbumin: its production technologies and bioactive peptides. *Comprehensive Reviews in Food Science and Food Safety*, 9(2), 197–212.

Kang, K., Kan, C., Yeung, A. & Liu, D. (2005). The properties of covalently immobilized trypsin on soap-free P(MMA-EA-AA) latex particles. *Macromolecular Bioscience*, 5(4), 344–351.

Kanosue, Y., Kojima, S. & Ohkata, K. (2004). Influence of solvent viscosity on the rate of hydrolysis of dipeptides by carboxypeptidase Y. *Journal of Physical Organic Chemistry*, 17(5), 448–457.

Karimi, M. (2016). Immobilization of lipase onto mesoporous magnetic nanoparticles for enzymatic synthesis of biodiesel. *Biocatalysis and Agricultural Biotechnology*, 8, 182–188.

Katchalski-Katzir, E. & Kraemer, D. M. (2000). Eupergit® C, a carrier for immobilization of enzymes of industrial potential. *Journal of Molecular Catalysis B: Enzymatic*, 10(1–3), 157–176.

Kawakami, K., Sera, Y., Sakai, S., Ono, T. & Ijima, H. (2005). Development and Characterization of a Silica Monolith Immobilized Enzyme Micro-bioreactor. *Industrial & Engineering Chemistry Research*, 44(1), 236–240.

Kelleher, C. M., O'Mahony, J. A., Kelly, A. L., O'Callaghan, D. J., Kilcawley, K. N. & McCarthy, N. A. (2018). The effect of direct and indirect heat treatment on the attributes of whey protein beverages. *International Dairy Journal*, 85, 144–152.

Khattab, I. S., Bandarkar, F., Fakhree, M. A. A. & Jouyban, A. (2012). Density, viscosity, and surface tension of water+ethanol mixtures from 293 to 323K. *Korean Journal of Chemical Engineering*, 29(6), 812–817.

Kilara, A. & Vaghela, M. N. (2018). 4 - Whey proteins. In Y. Rickey (Ed.), *Proteins in Food Processing* (pp. 93–126), Woodhead Publishing, ISBN 9780081007228.

Kim, S., Ki, K., Khan, M., Lee, W., Lee, H., Ahn, B. & Kim, H. (2007). Peptic and tryptic hydrolysis of native and heated whey protein to reduce its antigenicity. *Journal of Dairy Science*, 90(9), 4043–4050.

Kim, S. E., Kim, H. H., Kim, J. Y., Kang, Y. I., Woo, H. J. & Lee, H. J. (2000). Anticancer activity of hydrophobic peptides from soy proteins. *Biofactors*, 12(1–4), 151–155.

Kishimura, H., Hayashi, K., Miyashita, Y. & Nonami, Y. (2006). Characteristics of trypsins from the viscera of true sardine (Sardinops melanostictus) and the pyloric ceca of arabesque greenling (Pleuroprammus azonus). *Food Chemistry*, 97(1), 65–70.

Klarenbeek, G. (1984). Effects of various heat treatments on structure and solubility of whey proteins. *Journal of Dairy Science*, 67(11), 2701–2710.

Klomklao, S., Benjakul, S., Visessanguan, W., Kishimura, H. & Simpson, B. K. (2007). Purification and characterisation of trypsins from the spleen of skipjack tuna (*Katsuwonus pelamis*). *Food Chemistry*, 100(4), 1580–1589.

Klomklao, S., Benjakul, S., Visessanguan, W., Kishimura, H., Simpson, B. K. & Saeki, H. (2006). Trypsins from yellowfin tuna (*Thunnus albacores*) spleen: purification and characterization. *Comparative Biochemistry and Physiology. Part B: Biochemistry and Molecular Biology*, 144(1), 47–56.

Konrad, G. & Kleinschmidt, T. (2008). A new method for isolation of native α-lactalbumin from sweet whey. *International Dairy Journal*, 18(1), 47–54.

Korhonen, H. & Pihlanto, A. (2003). Food-derived bioactive peptides-opportunities for designing future foods. *Current Pharmaceutical Design*, 9(16), 1297–1308.

Kotal, M., Srivastava, S. K. & Maiti, T. K. (2011). Fabrication of gold nanoparticle assembled polyurethane microsphere template in trypsin immobilization. *Journal of Nanoscience and Nanotechnology*, 11(11), 10149–10157.

Kotormán, M., Laczkó, I., Szabó, A. & Simon, L. M. (2003). Effects of Ca^{2+} on catalytic activity and conformation of trypsin and α-chymotrypsin in aqueous ethanol. *Biochemical and Biophysical Research Communications*, 304(1), 18–21.

Krenkova, J. & Svec, F. (2009). Less common applications of monoliths: IV. Recent developments in immobilized enzyme reactors for proteomics and biotechnology. *Journal of Separation Science*, 32(5–6), 706–718.

Kühne, W. (1877). Zur Photochemie der Netzhaut. Retrived from https://archive.org/details/zurphotochemiede00kh/page/n4

Kuipers, B. J. & Gruppen, H. (2007). Prediction of molar extinction coefficients of proteins and peptides using UV absorption of the constituent amino acids at 214 nm to enable quantitative reverse phase high-performance liquid chromatography mass spectrometry analysis. *Journal of Agricultural and Food Chemistry*, 55(14), 5445–5451.

Kundu, S., Aswal, V. K. & Kohlbrecher, J. (2017). Effect of ethanol on structures and interactions among globular proteins. *Chemical Physics Letters*, 670, 71–76.

Lakshman, P. L. N., Toyokawa, Y., Tachibana, S., Toyama, H., Taira, T. & Yasuda, M. (2011). Reducing the antigenicity of milk whey protein using acid proteinases from Monascus pilosus. *Process Biochemistry*, 46(3), 806–810.

Lee, E. C., Senyk, G. F. & Shipe, W. F. (1975). Performance of an immobilized trypsin system for improving oxidative stability of milk. *Journal of Dairy Science*, 58(4), 473–476.

Leeb, E., Gotz, A., Letzel, T., Cheison, S. C. & Kulozik, U. (2015). Influence of denaturation and aggregation of β-lactoglobulin on its tryptic hydrolysis and the release of functional peptides. *Food Chemistry*, 187, 545–554.

Leeb, E., Holder, A., Letzel, T., Cheison, S. C., Kulozik, U. & Hinrichs, J. (2014). Fractionation of dairy based functional peptides using ion-exchange membrane adsorption chromatography and cross-flow electro membrane filtration. *International Dairy Journal*, 38(2), 116–123.

Lendero, N., Vidic, J., Brne, P., Frankovic, V., Strancar, A. & Podgornik, A. (2008). Characterization of ion exchange stationary phases via pH transition profiles. *Journal of Chromatography A*, 1185(1), 59–70.

Liang, Y., Tao, D., Ma, J., Sun, L., Liang, Z., Zhang, L. & Zhang, Y. (2011). Hydrophilic monolith based immobilized enzyme reactors in capillary and on microchip for high-throughput proteomic analysis. *Journal of Chromatography A*, 1218(20), 2898–2905.

Linderstrøm-Lang, K. U. (1952). Proteins and Enzymes in Lane Medical Lectures. 6, . Stanford University Press.

Linenberger, K. J. & Bretz, S. L. (2015). Biochemistry students' ideas about how an enzyme interacts with a substrate. *Biochemistry and Molecular Biology Education*, 43(4), 213–222.

Lisak, K., Toro-Sierra, J., Kulozik, U., Bozanic, R. & Cheison, S. C. (2013). Chymotrypsin selectively digests beta-lactoglobulin in whey protein isolate away from enzyme optimal conditions: potential for native α-lactalbumin purification. *Journal of Dairy Research*, 80(1), 14–20.

Lonnerdal, B. & Lien, E. L. (2003). Nutritional and physiologic significance of α-lactal-bumin in infants. *Nutrition Reviews*, 61(9), 295–305.

da Costa, E. L., da Rocha Gontijo, J. A. & Netto, F. M. (2007). Effect of heat and enzymatic treatment on the antihypertensive activity of whey protein hydrolysates. *International Dairy Journal*, 17(6), 632–640.

Lowe, A. J., Dharmage, S. C., Allen, K. J., Tang, M. L. & Hill, D. J. (2013). The role of partially hydrolyzed whey formula for the prevention of allergic disease: evidence and gaps. *Expert Review of Clinical Immunology*, 9(1), 31–41.

Lozano-Ojalvo, D., Pérez-Rodríguez, L., Pablos-Tanarro, A., López-Fandiño, R. & Molina, E. (2017). Pepsin treatment of whey proteins under high pressure produces hypoallergenic hydrolysates. *Innovative Food Science & Emerging Technologies*, 43, 154–162.

Luey, J. K., McGuire, J. & Sproull, R. D. (1991). The effect of pH and NaCl concentration on adsorption of β-lactoglobulin at hydrophilic and hydrophobic silicon surfaces. *Journal of Colloid and Interface Science*, 143(2), 489–500.

Luo, Y., Pan, K. & Zhong, Q. (2014). Physical, chemical and biochemical properties of casein hydrolyzed by three proteases: partial characterizations. *Food Chemistry*, 155, 146–154.

Ma, J., Zhang, L., Liang, Z., Zhang, W. & Zhang, Y. (2007). Monolith-based immobilized enzyme reactors: recent developments and applications for proteome analysis. *Journal of Separation Science*, 30(17), 3050–3059.

Mancini, F., Naldi, M., Cavrini, V. & Andrisano, V. (2007). Development and characterization of beta-secretase monolithic micro-immobilized enzyme reactor for on-line high-performance liquid chromatography studies. *Journal of Chromatography A*, 1175(2), 217–226.

Mao, Y., Černigoj, U., Zalokar, V., Štrancar, A. & Kulozik, U. (2017). Production of beta-Lactoglobulin hydrolysates by monolith based immobilized trypsin reactors. *Electrophoresis*, 38(22–23), 2947–2956.

Mao, Y., Krischke, M., Hengst, C. & Kulozik, U. (2018). Comparison of the influence of pH on the selectivity of free and immobilized trypsin for beta-lactoglobulin hydrolysis. *Food Chemistry*, 253, 194–202.

Mao, Y. & Kulozik, U. (2018). Selective hydrolysis of whey proteins using a flow-through monolithic reactor with large pore size and immobilised trypsin. *International Dairy Journal*, 85, 96–104.

Mao, Y., Krischke, M., Hengst, C. & Kulozik, U.. (2019). Influence of salts on β-lactoglobulin hydrolysis by free and immobilized trypsin. *International Dairy Journal*, 93, 106–115.

Markiton, M., Boncel, S., Janas, D. & Chrobok, A. (2017). Highly Active Nanobiocatalyst from Lipase Noncovalently Immobilized on Multiwalled Carbon Nanotubes for Baeyer–Villiger Synthesis of Lactones. *ACS Sustainable Chemistry & Engineering*, 5(2), 1685–1691.

Marques, D., Pessela, B. C., Betancor, L., Monti, R., Carrascosa, A. V., Rocha-Martin, J., Guisan, J. M. & Fernandez-Lorente, G. (2011). Protein Hydrolysis by Immobilized and Stabilized Trypsin. *Biotechnology Progress*, 27(3), 677–683.

Meller, K., Pomastowski, P., Szumski, M. & Buszewski, B. (2017). Preparation of an improved hydrophilic monolith to make trypsin-immobilized microreactors. *Journal of Chromatography. B: Analytical Technologies in the Biomedical and Life Sciences*, 1043, 128–137.

Michaelis, L. & Menten, M. (1913). Die Kinetik der Inwertin-Wirkung. *Biochemische Zeitschrift* (49), 333–369.

Migliore-Samour, D. & Jolles, P. (1988). Casein, a prohormone with an immunomodulating role for the newborn? *Experientia*, 44(3), 188–193.

Mikhail, S. & Kimel, W. (1961). Densities and Viscosities of Methanol-Water Mixtures. *Journal of Chemical and Engineering Data*, 6(4), 533–537.

Mousavi, S. H. A., Chobert, J.-M., Bordbar, A. K. & Haertlé, T. (2008). Ethanol effect on the structure of β-lactoglobulin b and its ligand binding. *Journal of Agricultural and Food Chemistry*, 56(18), 8680–8684.

Mozhaev, V. V., Melik-nubarov, N. S., Sergeeva, M. V., Šikšnis, V. & Martinek, K. (1990). Strategy for Stabilizing Enzymes Part One: Increasing Stability of Enzymes via their Multi-Point Interaction with a Support. *Biocatalysis and Biotransformation*, 3(3), 179–187.

Mullally, M. M., Meisel, H. & FitzGerald, R. J. (1997). Identification of a novel angiotensin-I-converting enzyme inhibitory peptide corresponding to a tryptic fragment of bovine β-lactoglobulin. *FEBS Letters*, 402(23), 99–101.

Mullally, M. M., O'Callaghan, D. M., FitzGerald, R. J., Donnelly, W. & Dalton, J. P. (1994). Proteolytic and peptidolytic activities in commercial pancreatic protease preparations and their relationship to some whey protein hydrolyzate characteristics. *Journal of Agricultural and Food Chemistry*, 42(12), 2973–2981.

Mullner, T., Zankel, A., Holtzel, A., Svec, F. & Tallarek, U. (2017). Morphological Properties of Methacrylate-Based Polymer Monoliths: From Gel Porosity to Macroscopic Inhomogeneities. *Langmuir*, 33(9), 2205–2214.

Muñoz-Tamayo, R., de Groot, J., Wierenga, P. A., Gruppen, H., Zwietering, M. H. & Sijtsma, L. (2012). Modeling peptide formation during the hydrolysis of β-casein by Lactococcus lactis. *Process Biochemistry*, 47(1), 83–93.

Muzzarelli, R. A., Barontini, G. & Rocchetti, R. (1976). Immobilized enzymes on chitosan columns: alpha-chymotrypsin and acid phosphatase. *Biotechnology and Bioengineering,* 18(10), 1445–1454.

Nagaoka, S., Futamura, Y., Miwa, K., Awano, T., Yamauchi, K., Kanamaru, Y., Tadashi, K. & Kuwata, T. (2001). Identification of novel hypocholesterolemic peptides derived from bovine milk beta-lactoglobulin. *Biochemical and Biophysical Research Communications*, 281(1), 11–17.

Nakane, K., Ogihara, T., Ogata, N. & Kurokawa, Y. (2001). Entrap-immobilization of invertase on composite gel fiber of cellulose acetate and zirconium alkoxide by sol-gel process. *Journal of Applied Polymer Science*, 81(9), 2084–2088.

Naldi, M., Černigoj, U., Štrancar, A. & Bartolini, M. (2017). Towards automation in protein digestion: Development of a monolithic trypsin immobilized reactor for highly efficient on-line digestion and analysis. *Talanta*, 167, 143–157.

Naldi, M., Tramarin, A. & Bartolini, M. (2018). Immobilized enzyme-based analytical tools in the -omics era: Recent advances. *Journal of Pharmaceutical and Biomedical Analysis*, 160, 222–237.

Nelson, J. M. & Griffin, E. G. (1916). Adsorption of Invertase. *Journal of the American Chemical Society*, 38(5), 1109–1115.

Nicoli, R., Gaud, N., Stella, C., Rudaz, S. & Veuthey, J. L. (2008). Trypsin immobilization on three monolithic disks for on-line protein digestion. *Journal of Pharmaceutical and Biomedical Analysis*, 48(2), 398–407.

Nikolaidis, A & Moschakis, T. (2018). On the reversibility of ethanol-induced whey protein denaturation. *Food Hydrocolloids*, 84, 389–395.

Okamoto, M., Rikimaru, H., Enomoto, A., Kaminogawa, S. & Yamauchi, K. (2014). High-pressure Proteolytic Digestion of Food Proteins: Selective Elimination of β-Lactoglobulin in Bovine Milk Whey Concentrate. *Agricultural and Biological Chemistry*, 55(5), 1253–1257.

Olsen, J. V., Ong, S. E. & Mann, M. (2004). Trypsin cleaves exclusively C-terminal to arginine and lysine residues. *Molecular & Cellular Proteomics*, 3(6), 608–614.

Papiz, M. & Sawyer, L. (1986). The structure of β-lactoglobulin and its similarity to plasma retinol-binding protein. *Nature*, 324(6095), 383–385.

Park, O., Swaisgood, H. E. & Allen, J. C. (1998). Calcium binding of phosphopeptides derived from hydrolysis of α(s)-Casein or β-Casein using immobilized trypsin. *Journal of Dairy Science*, 81(11), 2850–2857.

Patocka, G. & Jelen, P. (1991). Calcium association with isolated whey proteins. *Canadian Institute of Food Science and Technology Journal*, 24(5), 218–223.

Pellegrini, A., Dettling, C., Thomas, U. & Hunziker, P. (2001). Isolation and characterization of four bactericidal domains in the bovine beta-lactoglobulin. *Biochimica et Biophysica Acta*, 1526(2), 131–140.

Pellegrini, A., Thomas, U., Bramaz, N., Hunziker, P. & von Fellenberg, R. (1999). Isolation and identification of three bactericidal domains in the bovine α-lactalbumin molecule. *Biochimica et Biophysica Acta*, 1426(3), 439–448.

Peng, X., Kong, B., Xia, X. & Liu, Q. (2010). Reducing and radical-scavenging activities of whey protein hydrolysates prepared with Alcalase. *International Dairy Journal*, 20(5), 360–365.

Permyakov, E. A. & Berliner, L. J. (2000). α-Lactalbumin: structure and function. *FEBS Letters*, 473(3), 269-274.

Pessato, T. B., de Carvalho, N. C., Tavano, O. L., Fernandes, L. G. R., Zollner, R. d. L. & Netto, F. M. (2016). Whey protein isolate hydrolysates obtained with free and immobilized Alcalase: Characterization and detection of residual allergens. *Food Research International*, 83, 112–120.

Pessato, T. B. & Tavano, O. L. (2015). Hydrolysis of casein and beta-lactoglobulin by immobilized papain after pre-treatment with immobilized trypsin. *Acta Alimentaria*, 44(4), 570–577.

Pessen, H., Purcell, J. M. & Farrell Jr, H. M. (1985). Proton relaxation rates of water in dilute solutions of β-lactoglobulin. Determination of cross relaxation and correlation with structural changes by the use of two genetic variants of a self-associating globular protein. *Biochimica et Biophysica Acta (BBA)-Protein Structure and Molecular Enzymology*, 828(1), 1–12.

Petro, M., Svec, F. & Fréchet, J. M. J. (2000). Immobilization of trypsin onto “molded” macroporous poly(glycidyl methacrylate-co-ethylene dimethacrylate) rods and use of the conjugates as bioreactors and for affinity chromatography. *Biotechnology and Bioengineering*, 49(4), 355–363.

Pihlanto-Leppälä, A., Rokka, T. & Korhonen, H. (1998). Angiotensin I converting enzyme inhibitory peptides derived from bovine milk proteins. *International Dairy Journal*, 8(4), 325–331.

Podgornik, A., Savnik, A., Jancar, J. & Krajnc, N. L. (2014). Design of monoliths through their mechanical properties. *Journal of Chromatography A*, 1333, 9–17.

Polgar, L. (2005). The catalytic triad of serine peptidases. *Cellular and Molecular Life Sciences*, 62(19–20), 2161–2172.

Ponomareva, E. A., Kartuzova, V. E., Vlakh, E. G. & Tennikova, T. B. (2010). Monolithic bioreactors: effect of chymotrypsin immobilization on its biocatalytic properties. *Journal of Chromatography. B: Analytical Technologies in the Biomedical and Life Sciences*, 878(5–6), 567–574.

Prata-Vidal, M., Bouhallab, S., Henry, G. & Aimar, P. (2001). An experimental study of caseinomacropeptide hydrolysis by trypsin in a continuous membrane reactor. *Biochemical Engineering Journal*, 8(3), 195–202.

Prieto, C. A., Guadix, E. M. & Guadix, A. (2010). Optimal operation of a protein hydrolysis reactor with enzyme recycle. *Journal of Food Engineering*, 97(1), 24–30.

Qin, B. Y., Bewley, M. C., Creamer, L. K., Baker, E. N. & Jameson, G. B. (1999). Functional implications of structural differences between variants A and B of bovine β-lactoglobulin. *Protein Science*, 8(1), 75–83.

Qin, B. Y., Bewley, M. C., Creamer, L. K., Baker, H. M., Baker, E. N. & Jameson, G. B. (1998). Structural basis of the Tanford transition of bovine β-lactoglobulin. *Biochemistry*, 37(40), 14014–14023.

Quan, L., Wei, D., Jiang, X., Liu, Y., Li, Z., Li, N., Li, K., Liu, F. & Lai, L. (2008). Resurveying the Tris buffer solution: the specific interaction between tris(hydroxymethyl)aminomethane and lysozyme. *Analytical Biochemistry*, 378(2), 144–150.

Quintieri, L., Monaci, L., Baruzzi, F., Giuffrida, M. G., de Candia, S. & Caputo, L. (2017). Reduction of whey protein concentrate antigenicity by using a combined enzymatic digestion and ultrafiltration approach. *Journal of Food Science and Technology*, 54(7), 1910–1916.

Rawlings, N. D. & Barrett, A. J. (1994). Families of serine peptidases. *In Methods in Enzymology*, 244 ,19–61.

Reimerdes, E. H. (1979). Model proteolysis of beta-casein by immobilized trypsin. *Journal of Dairy Research*, 46(2), 223–226.

Renard, D., Lefebvre, J., Griffin, M. C. & Griffin, W. G. (1998). Effects of pH and salt environment on the association of beta-lactoglobulin revealed by intrinsic fluorescence studies. *International Journal of Biological Macromolecules*, 22(1), 41–49.

Renard, D., Lefebvre, J., Robert, P., Llamas, G. & Dufour, E. (1999). Structural investigation of β-lactoglobulin gelation in ethanol/water solutions. *International Journal of Biological Macromolecules*, 26(1), 35–44.

Rocha, C., Gonçalves, M. P. & Teixeira, J. A. (2011). Immobilization of trypsin on spent grains for whey protein hydrolysis. *Process Biochemistry*, 46(2), 505–511.

Rodrigues, R. C., Ortiz, C., Berenguer-Murcia, A., Torres, R. & Fernandez-Lafuente, R. (2013). Modifying enzyme activity and selectivity by immobilization. *Chemical Society Reviews*, 42(15), 6290–6307.

Roy, I. & Gupta, M. N. (2003). Lactose hydrolysis by Lactozym™ immobilized on cellulose beads in batch and fluidized bed modes. *Process Biochemistry*, 39(3), 325–332.

Saha, B., Saikia, J. & Das, G. (2015). Correlating enzyme density, conformation and activity on nanoparticle surfaces in highly functional bio-nanocomposites. *Analyst*, 140(2), 532–542.

Salis, A., Bilaničova, D., Ninham, B. W. & Monduzzi, M. (2007). Hofmeister effects in enzymatic activity: weak and strong electrolyte influences on the activity of Candida rugosa lipase. *The Journal of Physical Chemistry B*, 111(5), 1149–1156.

Sanjay, G. & Sugunan, S. (2006). Enhanced pH and thermal stabilities of invertase immobilized on montmorillonite K-10. *Food Chemistry*, 94(4), 573–579.

Sawyer, L. (2003). β-Lactoglobulin. In P. F. FoxP. L. H. McSweeney (Eds.), *Advanced Dairy Chemistry—1 Proteins* (pp. 319–386), Boston: Springer,ISBN 9780306472718.

Sawyer, W. (1969). Complex between β-lactoglobulin and κ-casein. A review. *Journal of Dairy Science*, 52(9), 1347–1355.

Schmidt, D. & Poll, J. (1991). Enzymatic hydrolysis of whey proteins. Hydrolysis of α-lactalbumin and β-lactoglobulin in buffer solutions by proteolytic enzymes. *Nederlands melk en Zuiveltijdschrift*, 45(4), 225–240.

Sedlak, E., Stagg, L. & Wittung-Stafshede, P. (2008). Effect of Hofmeister ions on protein thermal stability: roles of ion hydration and peptide groups? *Archives of Biochemistry and Biophysics*, 479(1), 69–73.

Selo, I., Clement, G., Bernard, H., Chatel, J., Creminon, C., Peltre, G. & Wal, J. (1999). Allergy to bovine β-lactoglobulin: specificity of human IgE to tryptic peptides. *Clinical and Experimental Allergy*, 29(8), 1055–1063.

Sharifi, M., Robatjazi, S. M., Sadri, M. & Mosaabadi, J. M. (2018). Immobilization of organophosphorus hydrolase enzyme by covalent attachment on modified cellulose microfibers using different chemical activation strategies: Characterization and stability studies. *Chinese Journal of Chemical Engineering,* 27(1), 191-199.

Shen, X., Fang, T., Gao, F. & Guo, M. (2017). Effects of ultrasound treatment on physicochemical and emulsifying properties of whey proteins pre- and post-thermal aggregation. *Food Hydrocolloids*, 63, 668–676.

Silveira, S. T., Martinez-Maqueda, D., Recio, I. & Hernandez-Ledesma, B. (2013). Dipeptidyl peptidase-IV inhibitory peptides generated by tryptic hydrolysis of a whey protein concentrate rich in beta-lactoglobulin. *Food Chemistry*, 141(2), 1072–1077.

Simon, L. M., Kotorman, M., Garab, G. & Laczko, I. (2001). Structure and activity of alpha-chymotrypsin and trypsin in aqueous organic media. *Biochemical and Biophysical Research Communications*, 280(5), 1367–1371.

Sipos, T. & Merkel, J. R. (1970). An effect of calcium ions on the activity, heat stability, and structure of trypsin. *Biochemistry*, 9(14), 2766–2775.

Spellman, D., McEvoy, E., O'Cuinn, G. & FitzGerald, R. J. (2003). Proteinase and exopeptidase hydrolysis of whey protein: Comparison of the TNBS, OPA and pH stat methods for quantification of degree of hydrolysis. *International Dairy Journal*, 13(6), 447–453.

Stanciuc, N. & Râpeanu, G. (2010). An overview of bovine [alpha]-lactalbumin structure and functionality. *The Annals of the University of Dunarea de Jos of Galati. Fascicle VI. Food Technology*, 34(2), 82.

Stetefeld, J., McKenna, S. A. & Patel, T. R. (2016). Dynamic light scattering: a practical guide and applications in biomedical sciences. *Biophysical reviews*, 8(4), 409–427.

Subramanian, A., Kennel, S. J., Oden, P. I., Jacobson, K. B., Woodward, J. & Doktycz, M. J. (1999). Comparison of techniques for enzyme immobilization on silicon supports. *Enzyme and Microbial Technology*, 24(1–2), 26–34.

Svec, F. (2006). Less common applications of monoliths: I. Microscale protein mapping with proteolytic enzymes immobilized on monolithic supports. *Electrophoresis*, 27(5–6), 947–961.

Svec, F. & Fréchet, J. M. J. (1999). Molded Rigid Monolithic Porous Polymers: An Inexpensive, Efficient, and Versatile Alternative to Beads for the Design of Materials for Numerous Applications*. Industrial & Engineering Chemistry Research*, 38(1), 34–48.

Taha, M. & Lee, M. J. (2010). Interactions of TRIS [tris (hydroxymethyl) aminomethane] and related buffers with peptide backbone: thermodynamic characterization. *Physical Chemistry Chemical Physics*, 12(39), 12840–12850.

Takahashi, M., Moriguchi, S., Ikeno, M., Kono, S., Ohata, K., Usui, H., Kurahashi, K., Sasaki, R. & Yoshikawa, M. (1996). Studies on the ileum-contracting mechanisms and identification as a complement C3a receptor agonist of oryzatensin, a bioactive peptide derived from rice albumin. *Peptides*, 17(1), 5–12.

Tanford, C., Bunville, L. G. & Nozaki, Y. (1959). The reversible transformation of β-lactoglobulin at pH 7.51. *Journal of the American Chemical Society*, 81(15), 4032–4036.

Tauzin, J., Miclo, L., Roth, S., Mollé, D. & Gaillard, J. L. (2003). Tryptic hydrolysis of bovine α_{S2}-casein: Identification and release kinetics of peptides. *International Dairy Journal*, 13(1), 15–27.

Tchorbanov, B. & Iliev, I. (1993). Limited enzymic hydrolysis of casein in the presence of ethanol. *Enzyme and Microbial Technology*, 15(11), 974–978.

Toro-Sierra, J., Tolkach, A. & Kulozik, U. (2011). Fractionation of α-lactalbumin and β-lactoglobulin from whey protein isolate using selective thermal aggregation, an optimized membrane separation procedure and resolubilization techniques at pilot plant scale. *Food and Bioprocess Technology*, 6(4), 1032–1043.

Tougu, V., Tiivel, T., Talts, P., Siksnis, V., Poyarkova, S., Kesvatera, T. & Aaviksaar, A. (1994). Electrostatic effects in trypsin reactions. Influence of salts. *European Journal of Biochemistry*, 222(2), 475–481.

Tsumoto, K., Ejima, D., Senczuk, A. M., Kita, Y. & Arakawa, T. (2007). Effects of salts on protein-surface interactions: applications for column chromatography. *Journal of Pharmaceutical Sciences*, 96(7), 1677–1690.

Uygun, M., Uygun, D. A., Ozcaliskan, E., Akgol, S. & Denizli, A. (2012). Concanavalin A immobilized poly(ethylene glycol dimethacrylate) based affinity cryogel matrix and usability of invertase immobilization. *Journal of Chromatography. B: Analytical Technologies in the Biomedical and Life Sciences*, 887–888, 73–78.

van den Biggelaar, L., Soumillion, P. & Debecker, D. P. (2017). Enantioselective Transamination in Continuous Flow Mode with Transaminase Immobilized in a Macrocellular Silica Monolith. *Catalysts*, 7(12), 54–66.

Veerman, C., Baptist, H., Sagis, L. M. & van der Linden, E. (2003). A new multistep Ca^{2+}-induced cold gelation process for β-lactoglobulin. *Journal of Agricultural and Food Chemistry*, 51(13), 3880–3885.

Vlakh, E. G. & Tennikova, T. B. (2013a). Flow-through immobilized enzyme reactors based on monoliths: I. Preparation of heterogeneous biocatalysts. *Journal of Separation Science*, 36(1), 110–127.

Vlakh, E. G. & Tennikova, T. B. (2013b). Flow-through immobilized enzyme reactors based on monoliths: II. Kinetics study and application. *Journal of Separation Science*, 36(6), 1149–1167.

Vodopivec, M., Podgornik, A., Berovič, M. & Štrancar, A. (2003). Characterization of CIM monoliths as enzyme reactors. *Journal of Chromatography B*, 795(1), 105–113.

Walsh, K. A. (1970). Trypsinogens and trypsins of various species. *Methods in enzymology*, 19, 41–63.

Wang, H., Jiao, F., Gao, F., Zhao, X., Zhao, Y., Shen, Y., Zhang, Y. & Qian, X. (2017). Covalent organic framework-coated magnetic graphene as a novel support for trypsin immobilization. *Analytical and Bioanalytical Chemistry*, 409(8), 2179–2187.

Welinder, K. G. (1988). Generation of peptides suitable for sequence analysis by proteolytic cleavage in reversed-phase high-performance liquid chromatography solvents. *Analytical Biochemistry*, 174(1), 54–64.

Wesolowska, O., Krokoszynska, I., Krowarsch, D. & Otlewski, J. (2001). Enhancement of chymotrypsin-inhibitor/substrate interactions by 3 M NaCl. *Biochimica et Biophysica Acta*, 1545(1–2), 78–85.

Wijesinha-Bettoni, R., Dobson, C. M. & Redfield, C. (2001). Comparison of the structural and dynamical properties of holo and apo bovine alpha-lactalbumin by NMR spectroscopy. *Journal of Molecular Biology*, 307(3), 885–898.

Wolz, M. & Kulozik, U. (2017). System parameters in a high moisture extrusion process for microparticulation of whey proteins. *Journal of Food Engineering*, 209, 12–17.

Wright, H. T. (1977). Secondary and conformational specificities of trypsin and chymotrypsin. *European Journal of Biochemistry*, 73(2), 567–578.

Wyman, J. (1931). The dielectric constant of mixtures of ethyl alcohol and water from 5 to 40. *Journal of the American Chemical Society*, 53(9), 3292–3301.

Xie, S., Svec, F. & Fréchet, J. M. J. (1999). Design of reactive porous polymer supports for high throughput bioreactors: Poly(2-vinyl-4,4-dimethylazlactone-co-acrylamide-co-ethylene dimethacrylate) monoliths. *Biotechnology and Bioengineering*, 62(1), 30–35.

Yamaguchi, H., Miyazaki, M., Honda, T., Briones-Nagata, M. P., Arima, K. & Maeda, H. (2009). Rapid and efficient proteolysis for proteomic analysis by protease immobilized microreactor. *Electrophoresis*, 30(18), 3257–3264.

Yamamoto, S., Imamura, A., Susanti, I., Hori, K., Tanji, Y. & Unno, H. (2005). Effect of spacer length on β-lactoglobulin hydrolysis by trypsin covalently immobilized on a cellulosic support. *Food and Bioproducts Processing*, 83(C1), 61–67.

Yang, H., Yang, S., Kong, J., Dong, A. & Yu, S. (2015). Obtaining information about protein secondary structures in aqueous solution using Fourier transform IR spectroscopy. *Nature Protocols*, 10(3), 382–396.

Yao, C., Qi, L., Hu, W., Wang, F. & Yang, G. (2011). Immobilization of trypsin on sub-micron skeletal polymer monolith. *Analytica Chimica Acta*, 692(1–2), 131–137.

Yiu, H. H. P., Wright, P. A. & Botting, N. P. (2001). Enzyme immobilisation using siliceous mesoporous molecular sieves. *Microporous and Mesoporous Materials*, 44–45, 763–768.

Yon, J. (1958). Influence des chlorures alcalins sur l'hydrolyse trypsique de la lactoglobuline native et dénaturée par la chaleur. *Biochimica et Biophysica Acta*, 27, 111–121.

Yu, J. & Ahmedna, M. (2012). Functions/applications of trypsin in food processing and food science research. In Nova Science Publishers, Inc.

Zdarta, J., Meyer, A., Jesionowski, T. & Pinelo, M. (2018). A general overview of support materials for enzyme immobilization: characteristics, properties, practical utility. *Catalysts*, 8(2), 92–118.

Zhang, B., Zhang, L., Wang, D. F. & Sun, J. P. (2011). Improvement of purification of trypsin inhibitor from wild soybean (glycine soja sieb. & zucc.) using chitosan resin-immobilized trypsin. *Journal of Food Biochemistry*, 35(6), 1660–1670.

Zhang, L., Zhang, B., Lin, H., Liu, P. P., Yu, L. N. & Wang, D. F. (2008). Preparation of trypsin-immobilised chitosan beads and their application to the purification of soybean trypsin inhibitor. *Journal of the Science of Food and Agriculture*, 88(13), 2332–2339.

Zhang, Z., Zhang, R., Chen, L. & McClements, D. J. (2016). Encapsulation of lactase (beta-galactosidase) into kappa-carrageenan-based hydrogel beads: Impact of environmental conditions on enzyme activity. *Food Chemistry*, 200, 69–75.

Zhao, Z., Li, H. & Li, Q. (2017). Isolation of β-lactoglobulin from buffalo milk and characterization of its structure changes as a function of pH and ionic strength. *Journal of Food Measurement and Characterization*, 11(3), 948–955.

Zhong, Q., Li, X. L., Hu, W. D., Zeng, B., Liang, R. M., Liu, H., Li, Z. X. & Zhang, Z. (2016). Phosvitin phosphopeptide preparation using immobilised trypsin and enhancing calcium absorption in growing rats. *Czech Journal of Food Sciences*, 34(4), 325–331.

Zhou, Q. W., Ding, H. C., Li, D. F., Zhang, Y. P., Dai, Z. Y. & Zhou, T. (2016). Antioxidant activity of enzymatic hydrolysate derived from hairtail surimi wash water using an immobilized chymotrypsin-trypsin column reactor. *Journal of Food Biochemistry*, 40(1), 39–46.

Zhou, Z. & Hartmann, M. (2013). Progress in enzyme immobilization in ordered mesoporous materials and related applications. *Chemical Society Reviews*, 42(9), 3894–3912.

Žoldák, G., Sprinzl, M. & Sedlák, E. (2004). Modulation of activity of NADH oxidase from *Thermus thermophilus* through change in flexibility in the enzyme active site induced by Hofmeister series anions. *European Journal of Biochemistry*, 271(1), 48–57.

8 Appendix

The following publications and presentations were generated in the period of this work. They are shown in chronological order. Publications being part of this thesis are marked in bold.

8.1 Peer reviewed publications

Mao, Y., Černigoj, U., Zalokar, V., Štrancar, A. & Kulozik, U. (2017). **Production of β-Lactoglobulin hydrolysates by monolith based immobilized trypsin reactors**. *Electrophoresis*, 38(22–23), 2947–2956.

Mao, Y., Krischke, M., Hengst, C. & Kulozik, U.. (2018). **Comparison of the influence of pH on the selectivity of free and immobilized trypsin for β-lactoglobulin hydrolysis**. *Food chemistry*, 253: 194–202.

Mao, Y. & Kulozik, U. (2018). **Selective hydrolysis of whey proteins using a flow-through monolithic reactor with large pore size and immobilised trypsin**. *International Dairy Journal*, 85: 96–104.

Mao, Y., Krischke, M., Hengst, C. & Kulozik, U.. (2019). **Influence of salts on β-lactoglobulin hydrolysis by free and immobilized trypsin**. *International Dairy Journal,* 93: 106–115.

Mao, Y., Krischke, M., Hengst, C. & Kulozik, U.. (2019). **β-Lactoglobulin hydrolysis by a flow-through monolithic immobilized trypsin reactor in ethanol/aqueous solvents**. *Bioprocess Chemistry*, in press (accepted).

Yuhong Mao[1]
Urh Černigoj[3]
Viktor Zalokar[3]
Aleš Štrancar[3]
Ulrich Kulozik[1,2]

[1]Technical University of Munich, Chair for Food and Bioprocess Engineering, Freising-Weihenstephan, Germany
[2]Institute for Food and Health (ZIEL) – Technology Unit, Freising-Weihenstephan, Germany
[3]BIA Separations d.o.o., Ajdovščina, Slovenia

Received May 3, 2017
Revised June 25, 2017
Accepted July 3, 2017

Research Article

Production of β-Lactoglobulin hydrolysates by monolith based immobilized trypsin reactors

Tryptic hydrolysis of β-Lactoglobulin (β-Lg) is attracting more and more attention due to the reduced allergenicity and the functionality of resulting hydrolysates. To produce hydrolysates in an economically viable way, immobilized trypsin reactors (IMTRs), based on polymethacrylate monolith with pore size 2.1 μm (N1) and 6 μm (N2), were developed and used in a flow-through system. IMTRs were characterized in terms of permeability and enzymatic activity during extensive usage. N1 showed twice the activity compared with N2, correlating well with its almost two times higher amount of immobilized trypsin. N2 showed high stability over 18 cycles, as well as over more than 30 weeks during storage. The efficiency of IMTRs on hydrolyzing β-Lg was compared with free trypsin, and the resulting hydrolysates were analyzed by MALDI-TOF/MS. The final hydrolysis degree by N1 reached 9.68% (86.58% cleavage sites) within 4 h, while only around 6% (53.67% cleavage sites) by 1.5 mg of free trypsin. Peptides analysis showed the different preference between immobilized trypsin and free trypsin. Under the experimental conditions used in this study, the potential cleavage site Lys^{135}-Phe^{136} was resistant against the immobilized trypsin in N1.

Keywords:
B-Lactoglobulin / Immobilized enzyme reactor / Monolith / Trypsin
DOI 10.1002/elps.201700188

Additional supporting information may be found in the online version of this article at the publisher's web-site

1 Introduction

Among the major whey proteins β-Lactoglobulin (β-Lg) is the main antigen. Enzymatic hydrolysis of this protein is a common approach to reduce allergenicity. The use of the serine protease Trypsin (EC 3.4.21.4), which preferably cleaves the C-terminal peptide bonds of Arginine (Arg/R) and Lysine (Lys/K), not only can significantly reduce its allergenicity [1], but also leads to the release of five biofunctional peptides [2]. In addition, Schmidt and Poll [3] showed that native α-Lactalbumin (α-La) was highly resistant to tryptic digestion while native β-Lg was not. Indeed, Konrad and Kleinschmidt [4], taking advantage of this selective susceptibility of β-Lg, used a combination of membrane technology and trypsin hydrolysis to obtain a yield of α-La of 90 ~ 95% in purity. However, the cost of large-scale use of trypsin in solution is very high, which severely limits its industrial application. Correspondingly, immobilized trypsin represents an alternative approach due to the possibility of reusing the enzyme and producing enzyme-free hydrolysates.

During the past few decades, the immobilization of trypsin onto different stationary supports has been studied resulting in the development of various immobilized trypsin reactors (IMTRs). These IMTRs can generally be divided into three groups: (i) trypsin is immobilized on nano- or microparticles [5–7]; (ii) trypsin is retained by membrane [8]; or (iii) trypsin is immobilized onto surface of monolithic materials [9–13]. However, available systems still suffer from low processing stability, i.e. high pressure drop over time [14], enzyme leakage due to non-covalent bonding [7, 14], and low capacity in terms of volume throughput [15].

Correspondence: Ms. Yuhong Mao, Technical University of Munich, Chair for Food and Bioprocess Engineering, Weihenstephaner Berg 1, D-85354, Freising-Weihenstephan, Germany
Fax: +49-8161-714384
E-mail: yuhong.mao@tum.de

Abbreviations: α-La, α-Lactalbumin; **β-Lg**, β-lactoglobulin; **BAEE**, Nα-Benzoyl-L-arginine ethyl ester; **BET**, Brunauer–Emmett–Teller; **CIM®**, Convective Interaction Media®; **DH**, degree of hydrolysis; **DHAP**, 2,5-Dihydroxyacetophenone; **HCCA**, α-Cyano-4-hydroxycinnamic Acid; **IMTRs**, immobilized trypsin reactors; **N1**, immobilized trypsin reactor based on monolith with pore size 2 μm; **N2**, immobilized trypsin reactor based on monolith with pore size 6 μm

Colour Online: See the article online to view Figs. 2, 3 and 4 in colour.

Among the different immobilization supports, monoliths have been of recent interest, because they generally allow for a higher mass flow, and mass transfer of target molecules with the enzyme bound to the monolithic channel surfaces is primarily governed by the mobile phase convective flow. Furthermore, the surface of monoliths can be modified with various functional groups, which makes covalent bonding of enzyme much easier. However, most of the developed monolithic IMTRs are designed to accelerate the digestion step for proteomics analysis, which differs from the application of producing protein hydrolysates. Besides high enzymatic efficiency, to reach a higher space-time yield (the amount of substrate converted per biocatalyst reactor), the crucial requirements for enzymatic hydrolysates production are a need for processing larger amount of substrate and longer continuous digestion time in each cycle. These requirements may cause a blockage problem. Theoretically, monoliths with very large pores can minimize this issue [16], but at the expense of the decreased surface area, resulting in significant reduction of the amount of immobilized trypsin.

Based on these considerations, for the first time, we immobilized trypsin on monolith with pore size 6 μm (N2), which is less prone to pore blockage, and compared its efficiency with that with pore size 2.1 μm (N1). This allows us to conclude on the effect of convective flow through the pores at longer operation times in a continuous mode. Short polymethacrylate monolithic columns, commercialized under the trademark Convective Interaction Media® (CIM®), were used as the stationary supports. The immobilized trypsin yield was compared in these two IMTR systems and correlated with their digestion activities. The efficiencies of these two CIM-IMTRs in hydrolyzing β-Lg were compared with each other, as well as with free trypsin. Furthermore, long-term stability of these two IMTRs was monitored throughout the whole study.

In addition, differences in the hydrolysates may arise from the use of an immobilized enzyme instead of the free one. In fact, immobilization can change, e.g., the accessibility of the enzyme to the substrate or even the affinity of the enzyme towards a specific substrate. In this study, we also explored the peptides compositions in the hydrolysates resulting from immobilized and free trypsin, separately.

2 Materials and methods

2.1 Materials

Bovine β-Lg was fractionated from WPI, a product from Fonterra Co-operative Group Ltd (Auckland, New Zealand) as described by Toro-Sierra, Tolkach, et al. [17]. Trypsin from bovine pancreas (Type I, ~10 000 BAEE units/mg protein), Nα-Benzoyl-L-arginine ethyl ester (BAEE, B4500), Tris (hydroxymethil)-aminomethane (TRIS), sodium cianoborohydride ($NaCNBH_3$), ethanolamine, sodium chloride (NaCl), benzamidine hydrochloride (BAHC), 2-(N-morpholino)-ethanesulfonic acid (MES), sodium hydroxide, sulphuric(VI) acid, calcium chloride and sodium eriodate were purchased from Sigma–Aldrich (St. Louis, MO, USA). Deionized water was from MilliQ System (Millipore Corporation, Bedford, USA).

2.2 Preparation of CIM-IMTRs and frame of flow-through system

2.2.1 CIM-IMTRs preparation

Aldehyde activated CIM® radial columns (CIM-ALD, tube dimensions: outer diameter (D) –1.86 cm, inner diameter (d) –0.67 cm, height (h) –0.42 cm; volume 1.0 mL) with nominal pore size diameter of 2.1 and 6 μm were provided by BIA Separations d.o.o. (Ajdovščina, Slovenia).

The specific surface area of the monoliths before trypsin immobilization was measured via nitrogen adsorption by TriStar II 3020 (Micromeritics Instrument Corporation, Norcross, GA, USA). Nitrogen of 99.999% purity was used. Before analysis the monolith samples were dried in nitrogen flow at 70°C for 1 h.

Pore size distribution was measured by a Pascal 440 (Thermo-Quest Italia, Rodano, Italy) mercury porosimeter within a range of 15–10 000 nm. Approximately 0.1 g of dried monolith sample was measured before immobilization.

Trypsin was covalently immobilized on CIM-ALD monolithic columns using the following coupling protocol. The immobilization was done in duplicate. A 5.0 mg of trypsin was dissolved in 5 mL of immobilization buffer, composed of 0.1 M MES, pH 5.6, $NaCNBH_3$ (3.0 mg/mL) and BAHC (0.4 mg/mL). The CIM-ALD column was washed with 20 mL of 0.1 M MES buffer at pH 5.6, followed by 10 mL of immobilization buffer. Then the trypsin solution was continuously recirculated for 3 h at a flow rate of 0.5 mL/min. Aliquots of trypsin solution were collected at the beginning, during and at the end of the immobilization procedure for subsequent trypsin mass balance analysis. The residual aldehyde groups were deactivated by treating the columns with ethanolamine and $NaCNBH_3$ solution as it is described in Naldi et al. [9]. Afterward, the column was washed with 20 mL of Tris-HCl buffer (20 mM pH 7.4 containing 1 M NaCl). Before use the prepared CIM-IMTRs were stored at 4°C in aqueous solution of 20 mM acetic acid, pH 3.5 containing 1.0 mM $CaCl_2$.

2.2.2 Determination of immobilized trypsin density

The amount (mg) of immobilized trypsin was calculated according to Eq. (1).

$$m_{\text{immobilized}}(trypsin) = \gamma_{\text{load}}(trypsin) \times V_{\text{load}} - \sum \gamma_{\text{n}}(trypsin) \times V_{\text{n}} \quad (1)$$

Where, γ_{load}(trypsin) is the concentration of trypsin in the loading solution; γ_{n}(trypsin) are concentrations (mg/mL) of trypsin in washing and deactivation fractions after the immobilization; V_{load} is the volume of trypsin solution applied to

the column and V_n is the sum of the washing and deactivation fraction volumes, in mL. The determination of trypsin concentration was performed chromatographically as described by Naldi et al. [9].

2.2.3 Frame of the flow-through system

IMTR was inserted in ÄKTA system (GE Healthcare Bio Sciences) consisting of sample pump (P-960), system pump, auto-sampler and detectors for UV, pH, temperature and conductivity. The whole system was controlled by Unicorn Software 5.31.

2.3 Pressure drop and permeability calculation

The backpressure without and with IMTR was recorded at increasing flow rates, namely 0.5, 2.0, 5.0, 10 and 15 mL/min, by pumping deionized water. The difference between these two values at a defined flow rate was considered to be the pressure drop created by the inserted reactor. According to the study of Podgornik, et al. [18], the permeability of monolith was calculated according to Eq. (2):

$$B = \frac{F}{\Delta P} \times \frac{\eta \times \ln\left(\frac{D}{d}\right)}{2\pi h} \quad (2)$$

Where, ΔP (MPa) is the pressure drop; η is the viscosity of mobile phase (0.87685 MPa*s for deionized water); B (m^2) is the calculated permeability of monolith; F (mL/min) is the volumetric flow rate; D (m) and d (m) are outer and inner tube diameters, and h (m) is monolith height.

2.4 Activity measurements of free and immobilized trypsin

The activity measurement is a spectrophotometric rate determination (A_{253nm}, Light path = 1 cm) in buffer solution based on the following reaction:

$$BAEE + H2O \xrightarrow{Trypsin} N\alpha - Benzoyl - L - arginine\ (BA) + ethanol$$

All the measurements were conducted at 25 ± 1°C. 0.1 M Tris-HCl buffer was used, and its pH was adjusted to different values, namely 7.2, 7.8, 8.1, 8.5, and 9.2, to assess the effect of pH.

2.4.1 Free trypsin activity measurement

For measuring free trypsin activity, a continuous spectrophotometric rate determination was performed following the protocol given by the manufacturer (Sigma-Aldrich, 2016). The activity of free trypsin was expressed as BAEE units. One BAEE unit is defined to produce a Δ A253 of 0.001 per minute in a reaction volume of 3.20 mL.

2.4.2 Immobilized trypsin activity measurement

Inserted IMTR was washed by deionized water firstly and then equilibrated by 0.1 M Tris-HCl buffer (varied pHs) at 5 mL/min. 10 mM BAEE in 0.1 M Tris-HCl buffer was continuously pumped through this IMTR at 10 mL/min. The first 4 mL of sample was discarded because of the dead volume of Äkta system and following 2 mL was collected by the auto-sampler. The collected samples were diluted and further measured by spectrophotometer at 253 nm. The activity unit U* (μmol/min), defined as the amounts of BAEE one CIM-IMTR converted to BA in 1 min at specific conditions, was calculated using Eq. (3):

$$U^* = \frac{\Delta A \times F \times Di \times 10^3}{L \times \varepsilon} \quad (3)$$

ΔA (Au) is the absorbance difference of BAEE solution before and after hydrolysis; Di is dilution factor; L is the light path, here is 1 cm; ε is the molar extinction coefficient, corresponding to the differential molar absorbance of BAEE against BA at 253 nm, here is 808 mol^{-1} cm^{-1} determined by Kedzy et al [19]. U* can be easily converted to BAEE units, using the conversion factor 270 determined by Bergmeyer et al. [20].

2.5 Hydrolysis of β-Lg

Between experiments IMTRs were stored at 4°C in storage solution (19 mM $CaCl_2$ in 10% ethanol/water solution, pH 3 adjusted by 0.1 M HCl). This solution was required to be washed out prior to starting the next cycle. Therefore, before each hydrolysis experiment, the CIM-IMTR was washed by deionized water. The washing step was also used to characterize the IMTR in terms of the pressure drop as described in 2.3. If the pressure drop would be higher than base line, this would have been an indication of pore blockage. Afterward, it was equilibrated by 0.1 M Tris-HCl buffer at pH 7.8 (this step was excluded when pH-stat method was applied). After each hydrolysis of β-Lg, a cleaning step using an alkaline solution (0.5 mM NaOH + 5 mM NaCl, pH 10.8) was used, and deionized water was applied to remove the alkaline prior to filling the system with storage solution. All the hydrolysis experiments were conducted at 25 ± 1°C.

2.5.1 Single flow-through approach

Native β-Lg in 0.1 M Tris-HCl buffer (1.5, 3 and 6 mg/mL) at pH 7.8 was continuously pumped through the IMTR (N1 or N2) at different flow rates, ranging from 0.5 to 10 mL/min. The first 4 mL of hydrolysates were discarded. The following 6 mL were collected by the auto-sampler for the native protein content measurement. The amount of native β-Lg was determined using RP-HPLC as described by Toro-Sierra,

Tolkach, et al. [17]. The depleting rate of β-Lg was calculated according to Eq. (4):

$$R = \frac{C_d \times v}{v/F} = C_d \times F \quad (4)$$

Where, R (mg/min) is the depleting rate of β-Lg, C_d (mg/mL) is the difference of β-Lg concentration before and after hydrolysis, v (mL) is the collected volume, and F (mL/min) is the flow rate.

2.5.2 Recirculation flow approach

50 mL of native β-Lg in 0.1 M Tris-HCl buffer (3 mg/mL) at pH 7.8 was recirculated through N1 for 2 h at 0.5, 5, 10 and 15 mL/min, respectively. Samples at different time intervals (0, 10, 20, 30, 60, 90, 120 min) were drawn for native protein content analysis [17].

2.5.3 Comparison of IMTRs and free trypsin on hydrolyzing β-Lg

Native β-Lg dissolved in deionized water (25 mL, 10 mg/mL, pH was adjusted to 7.8 using 1 M NaOH) was hydrolyzed by free trypsin or IMTRs. For the hydrolysis by IMTRs, the recirculation flow approach at 10 mL/min was applied.

TitroLine alpha plus autotitrator (Schott AG, Mainz, Germany) measured the change of pH every 3 s during the hydrolysis process and kept pH constant by addition of 0.1 M NaOH. The data was acquired by the TitriSoft 2.5 software. The degree of hydrolysis (DH) is defined as the percentage of peptide bonds cleaved (h) compared to the total available peptide bonds (h_{tot}) in the protein substrate (Eq. (5)). Instantaneous DH at any given time was calculated using Eq. (4) according to the pH-stat method [21].

$$DH = \frac{h}{h_{tot}} \times 100\% = \frac{V_b \times N_b}{\alpha \times M_p \times h^*_{tot}} \times 100\% \quad (5)$$

where, V_b (mL), base consumption; N_b, normality of the base; α, average degree of dissociation of the NH groups; M_P (g), mass of protein; h^*_{tot}, total number of peptide bonds in one gram protein substrate, in this work we calculated this value to be 7.63 meqv/g for β-Lg.

From Eq. (5), h was derived directly, and the velocity of reaction was calculated by Eq. (6).

$$V = \frac{dh}{dt} \quad (6)$$

Where, V (meqv/min) is the rate of reaction; h (meqv) is the amount of peptide bonds cleaved; t (min) is the hydrolyzing time.

2.6 Peptides composition analysis using MALDI-TOF mass spectrometry

Collected samples were analyzed for mass composition using MALDI-TOF/ MS system (ultrafleXtreme MALDI-TOF/TOF, Bruker Daltonics, Bremen, Germany) with two matrices separately, α-Cyano-4-hydroxycinnamic Acid (HCCA, Bruker Part-No. #201344) and 2,5-Dihydroxyacetophenone (DHAP, Bruker Part no. #201346). Generally, HCCA is used for the measurement of peptides and proteins in the low mass range (≤4000 Da), whereas DHAP is mainly used for proteins in the higher mass range. The detailed method is described in supporting information.

3 Results and discussion

3.1 IMTRs characterization

3.1.1 Yield of immobilized trypsin in IMTRs

Development of CIM-IMTR for proteomic applications clearly demonstrated that decrease of pore size down to 0.6 μm was preferable due to higher immobilized trypsin density on the monolithic surface and consequently higher enzymatic conversion [9]. Unfortunately, the decrease of pore size by a factor of two results in a 4 times higher pressure drop and a drastic decrease of permeability, which is not an option for hydrolysates production. Therefore, an alternative approach was considered, where monoliths were with larger pores and consequently higher permeabilities. The monolithic surface area is one of the most important parameters influencing the maximum amount of immobilized protein. BET surface areas of CIM monoliths (before trypsin immobilization) were measured to be 5.0 and 2.0 m^2 per g of dry monolith for 2.1 μm (N1) and 6 μm (N2) pore sizes, respectively. In our immobilization protocol, 5 mg of trypsin was available for binding to a monolith with volume of 1 mL. Mass balance calculations showed a complete depletion of trypsin from the immobilization solution for N1, while 2 mg of trypsin remained unbound with the N2. Correlating BET surface area and amount of immobilized trypsin, at least 2 mg more trypsin could be additionally bound to the monolithic surface in case of N1 to obtain the maximum possible ligand density.

Considering BET surface areas and the molar mass of trypsin from bovine pancreas (23.8 kDa), each trypsin molecule in N1 and N2 occupies approximately 17 and 11 nm^2 of surface, respectively. Based on Saha et al. [22] the molecular dimension of native trypsin from porcine pancreas is 4.8 nm x 3.7 nm x 3.2 nm. Assuming that the spatial dimensions of bovine-derived trypsin are similar and that enzyme molecules are surrounded by a hydration layer of approximately 0.2 nm, one trypsin molecule would occupy between 10 and 20 nm^2 surface. It is concluded that the highest possible surface density of immobilized trypsin was achieved with

N2 (100 ± 15%), while approximately 65 ± 10% coverage was obtained for N1.

3.1.2 Initial pressure drop and permeability

The pressure drop created by freshly prepared N1 and N2 at different flow rates was recorded in Supporting Information Fig. 1. A linear increase of pressure drop depending on flow rates for both reactors was observed as expected for constant permeability, proving that porous monolithic structure is stable and no compression occured even when the flow rate was up to 15 mL/min. According to Eq. (2), the calculated initial permeabilities of N1 and N2 were 2.45×10^{-12} m^2 and 1.91×10^{-11} m^2, respectively. Due to the same porosity of N1 and N2 (60%), 7.80 times higher permeability of N2 could be attributed mainly to the pore size difference. According to the Blake–Kozeny equation, the permeability of a porous bed depends on the particle size forming the bed, as well as on its porosity. Instead of particle diameter a pore size (d_v) is used, and then the expression is showed as Eq. (7) [18]:

$$B = K_v \times \varepsilon \times d_V^2 \tag{7}$$

Where, K_v is a structural constant of particular bed. As suming same porosity and structural constant for N1 and N2, an Eq. (8) is derived:

$$\frac{B_{N1}}{B_{N2}} = \frac{d_{V1}^2}{d_{V2}^2} \tag{8}$$

The exact pore sizes of both monoliths were determined by mercury porosimetry before the immobilization (2.15 μm for N1 and 5.80 μm for N2) as described above. The measured permeability ratio (N1/N2 = 7.80) fits very well with the squares of the experimentally determined d_v ratio, thus confirming that N1 and N2 were structurally similar materials.

3.1.3 Activity measurements at increasing pH values

BAEE was dissolved in 0.1 M Tris-HCl buffer and used as substrate to assess the activity of immobilized and free trypsin at increasing pH values. As shown in Fig. 1, N1 showed almost twice the activity compared with N2, which correlates well with the almost two times higher amount of immobilized trypsin in N1. With increasing pH up to 9.2, the activity of both IMTRs was quite stable and even exhibited a slight increment. Actually, the immobilized trypsin could survive without any decrease of activity at pH 10.8, which was decided to be the pH of washing solution applied in this study. On the contrary, the activity of free trypsin started to decrease above pH 8.1.

Not surprisingly, such stabilization of immobilized trypsin with pH increase was attributed to the applied multipoint covalent immobilization, which has been claimed by Fernandez-Lafuente [23]. However, immobilization often results in a decrease of enzymatic activity due to steric

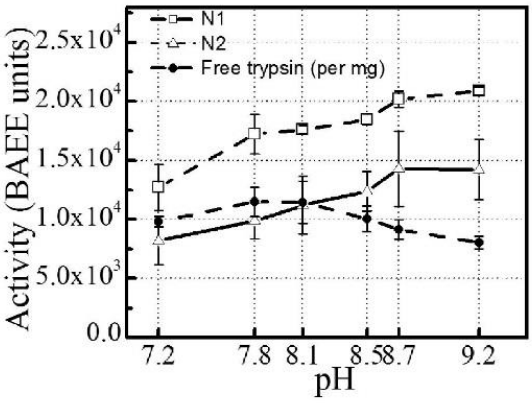

Figure 1. Activity profiles for IMTRs and free trypsin at increasing pH values and 10 mL/min. The activity measurements at each pH value was repeated at least for three times.

hindrance and reduced accessibility to the trypsin active site. Comparing the specific activity of per mg immobilized trypsin in IMTRs with per mg free one, a decrease of 74~ 48% for N1 and 73~41% for N2 at varied pH values was observed.

Based on these results, the characteristics of CIM-ALD columns and corresponding IMTRs are summarized in Table 1.

3.2 Hydrolysis of β-Lg

3.2.1 Efficiency evaluation of IMTRs at different flow rates

The flow rate is one of the most important factors influencing the flow-through bioreactor performance. To evaluate the performance of IMTRs in depleting β-Lg at different flow rates, both single flow-through approach and recirculation flow approach were applied, which are more practical to improve the hydrolysates yield compared with a classical zonal approach (with injection volume only up to microliter or milliliter).

For the immobilized trypsin, the optimal pH is 8.7 or even higher, while activities of the free one started to decrease when the pH value was above 8.1 (see Fig. 1). To compare the efficiencies between the free and the immobilized trypsin, we decided to perform the hydrolysis at pH 7.8.

In a single flow-through approach, β-Lg solutions (in 0.1 M Tris-HCl buffer, pH 7.8) with stepwise increased concentrations were used to avoid underestimation of IMTRs' performance due to the insufficient replenishment of substrate. As shown in Fig. 2A and B, 3 mg/mL native β-Lg was found already to be a saturating concentration for all explored flow rates, since no more β-Lg was depleted when the substrate concentration further raised to 6 mg/mL. As expected, for both N1 and N2 more native β-Lg was depleted at lower flow rates because of the corresponding longer contact time between immobilized trypsin and substrate. However, regarding to the efficiency (i.e. the depleting rate of β-Lg) at

Table 1. Characteristics of CIM-ALD columns (column volume 1 mL) and corresponding IMTRs

Column	Pore size (μm)	BET surface (m^2/g)	Permeability in di-water (m^2)	Amount of immobilized trypsin (mg per mL)	Trypsin surface density (molecules per nm^2)	Activity U* (μmol/min) (substrate BAEE) at pH 7.8 and 10 mL/min
N1	2.15 ± 0.1	5.0 ± 0.4	2.45×10^{-12}	5.0 ± 0.2	11 ± 4	63.86 ± 6.08
N2	5.80 ± 0.3	2.0 ± 0.2	1.91×10^{-11}	3.0 ± 0.3	17 ± 5	36.56 ± 5.56

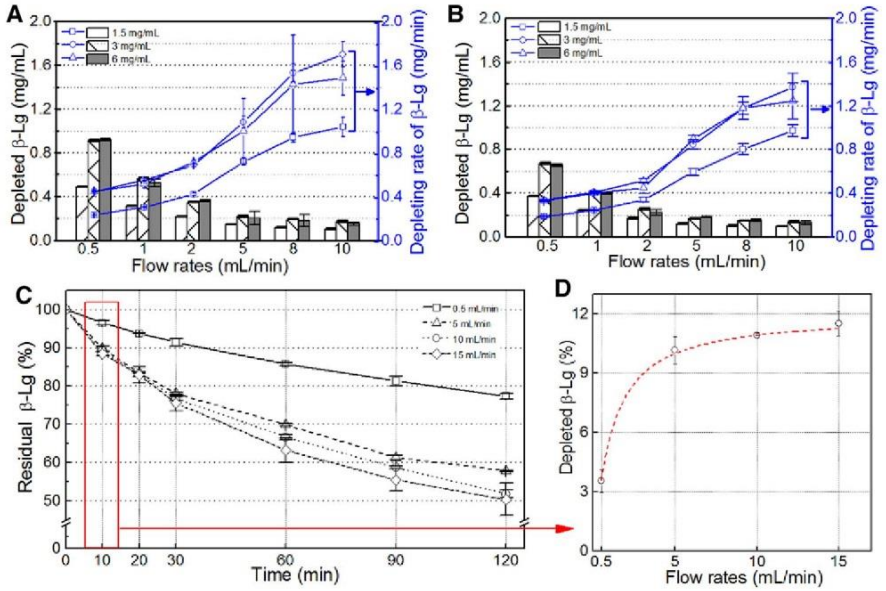

Figure 2. Efficiency of IMTRs in depleting β-Lg: (A) & (B) the depleted amount of β-Lg by N1 and N2 depending on flow rates in single flow-through approach; (C) the residual amount of β-Lg during recirculation at different flow rates by N1; (D) The depleted amount of β-Lg by N1 in first 10 min during recirculation at different flow rates.

each flow rate, a clear increasing dependence on flow rate was found, as can be seen from the curves in Fig. 2A and B. As compared to IMTRs used in proteomic applications, in continuous operation we rate the performance of IMTR technology from a different perspective. A higher depleting rate would be a decisive criteria regarding processing efficiency. To further assess the effects of flow rates on IMTR's efficiency, a recirculation flow approach within a long given time is preferred, which provides the possibility to compare the depleted β-Lg limited to the same given time while at different flow rates. According to the results in Fig. 2A and B, the efficiency values at 5 mL/min seem to be in the middle range. Hence, 50 mL of β-Lg solution (in 0.1 M Tris-HCl buffer, pH 7.8) at 3 mg/mL were recirculated through N1 at 0.5, 5, 10, and 15 mL/min for 2 h, respectively. The residual native β-Lg in substrate solution at different time intervals, as shown in Fig. 2C, decreased significantly faster when flow rates were at or above 5 mL/min during recirculation, compared with that at 0.5 mL/min. The growth of depleting efficiency with increasing flow rates is presumably attributed to the increased mass transfer of β-Lg molecules towards the immobilized trypsin [24]. In addition, the work of Jungreuthmayer et al. [25] demonstrated that the flow in monolith showed a lateral velocity component, which may contribute to the transport of molecules to the monolith wall. This confirmed lateral velocity can be speculated to promote the contact between substrate and fixed trypsin. From this result, it is assumed that the fluctuating flow behavior in monolith may be more severe at higher flow rates, since the efficiency in depleting β-Lg was higher at increased flow rates. However, this increase of efficiency depending on flow rates can reach a plateau, as shown in Fig. 2C, no increment was found when the flow rate further raised to 15 mL/min from 10 mL/min. Actually, a clear plateau was observed in Fig. 2D, where the depleted β-Lg in first 10 min was plotted versus applied flow rates. This dependence of efficiency on flow rates is quite different from that in the single flow-through approach (Fig. 2A and B), where the efficiency improved significantly with increasing flow rates. It was noted that the substrate concentration was assumed constant in the calculation by single flow-through approach, while it declined continuously in a recirculation flow approach. Hence, for further experiments, the recirculation flow rate was fixed at 10 mL/min.

3.2.2 Comparison of the hydrolysis efficiency by IMTRs and free trypsin

The efficiencies of IMTRs in producing β-Lg hydrolysates at recirculation flow approach were compared with each other,

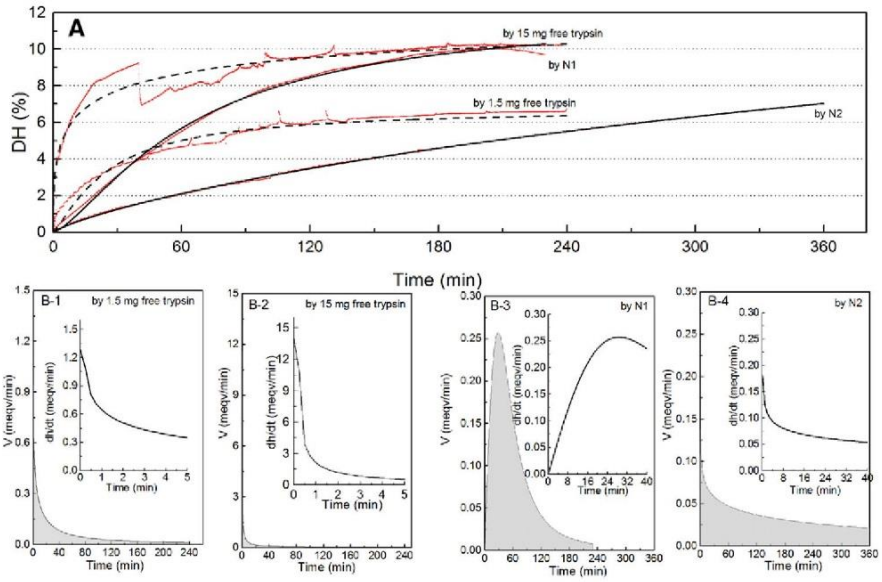

Figure 3. (A): the evolution of DHs depending on time for four hydrolysis experiments; (B): the velocities of these four hydrolysis processes, B-1 ~ B-4 regards to the hydrolysis by 1.5 free trypsin, 15 mg free trypsin, N1 and N2, respectively, in addition, the first 5 min for free trypsin and 40 min for IMTRs were highlighted.

as well as with free trypsin (1.5 and 15 mg) in a stirred solution. The same amount of substrate (25 mL, 10 mg/mL β-Lg in water, pH 7.8) was used. Additionally, it was noted that the activity of 1.5 mg free trypsin equals the activity of N1 in term of BAEE units (Fig. 1).

As shown in Fig. 3A, the DH using 1.5 mg free trypsin increased much faster at the beginning than that using N1 or N2. From the curves of velocity versus time in Figs. 3B-1, B-3 and B-4, the maximum reaction velocity (V) by free trypsin at the given conditions in this study reached around 1.28 meqv/min, 5-fold of that by N1 and 7-fold of that by N2, respectively. Obviously, free trypsin is more flexible to contact with β-Lg compared with immobilized trypsin in IMTRs, forming enzyme-substrate complex, and then contributed to a significantly higher reaction velocity. On the other hand, the steric effects that are involved by non-oriented immobilization can also lead to a lower velocity.

Normally, the maximum velocity at given conditions is determined by measuring the initial reaction velocity in a catalyst system, because it requires a high concentration of substrate. As shown in Fig. 3B-1, in a system with free trypsin, the maximum velocity was achieved immediately once the reaction started. However, it took around 30 min to reach the maximum velocity for N1 (Fig. 3B-3). Since the measurements of DH depended on consumed volumes of NaOH, it is assumed that the initial delay of calculated DH in N1 case is not because of a slower enzymatic reaction, rather because of the residual charge on monolithic surface. The surface of N1 has properties of a weak base (secondary amine) due to ethanolamine deactivation of residual aldehyde groups after trypsin immobilization [26]. The DH experiments were performed in water, therefore the monolith charge was not shielded by the buffer and obviously it served as the neutralizing agent or as a buffering agent in the beginning of the reaction, thus decreasing the consumption of NaOH. In Fig. 2C, where β-Lg was dissolved in 0.1 M Tris-HCl buffer, no delay of β-Lg depletion was observed with N1 in the beginning of the reaction, indirectly confirming the interpretation of DH experiment in Fig. 3C. We also developed two IMTRs using another approach, where ethanolamine was excluded during deactivation, and no delay of initial reaction velocity was observed (data not shown here). One would expect similar observations with N2 as well, but the amount of ethanolamine groups on the N2 surface was considerably lower, which almost eliminated this delay. The reasons are: (i) higher surface coverage by trypsin (see Section 3.1.1.) leading to lower amount of residual aldehyde avaliable for the reaction with ethanolamine; (ii) 2.5 times lower surface area of N2 leading to at least 2.5 times lower amount of charged functional groups.

Along the hydrolysis process, the reaction velocity continuously decreased, especially using free trypsin. The final DH within 4 h by 1.5 mg free trypsin was only around 6%, while its theoretical DH_{max} is 11.18% [2]. The effects of autodigestion, reduction of substrate and potential inhibition of products can account for this result. Correspondingly, the decrease of reaction velocity by immobilized trypsin was much slower mainly because of the absence of autodigestion. Since autodigestion of enzyme is a time-dependent process, more trypsin provided, longer effective hydrolyzing time can be achieved. Hence, 10-fold amount of free trypsin was used to hydrolyze the same amount of substrate. A sharp increase of maximum reaction velocity was observed (Fig. 3B-2) and DH increased extremely fast in a short time, close to the theoretical DH_{max}. The DHs by 15 mg free trypsin and N1 finally reached plateaus so that they were considered as the

practical maximum DHs. Accordingly, the hydrolysates were collected for further analysis. In N2, the DH gradually increased, reaching 7% after 6 h. Presumably, this hydrolysis process can reach its maximum DH when enough time is provided.

3.2.3 Peptides compositions analysis

The peptides compositions in collected samples were analyzed using MALDI-TOF/MS, as shown in Fig. 4. (the mass spectrum exported directly from flex analysis software is shown in Supporting Information Fig. 2). Mass signals in the range between 500 and 8000 Da were clearly observed in the sample from N1, even intact β-Lg peaks around 18 000 Da were still visible (Fig. 4A). On the contrary, most peaks were below 4000 Da in the sample hydrolyzed by free trypsin. Correlating to the practical DH_{max}, the final DH by N1 (9.68%) was indeed lower than that by free trypsin (11.07%).

β-Lg contains 161 peptide bonds, of which 18 peptide bonds are theoretically cleavable by trypsin, leading to the release of 19 peptides after complete trypsinlysis, as shown in Supporting Information Fig. 3. However, the masses below 500 Da are not possible to be detected by our method in this study. Regarding other detectable peptides, only f(48-60) was missing in both samples, f(125-135) and f(61-69) only missed in the sample hydrolyzed by N1. By searching polypeptides in the hydrolysates from N1, no matched peptide starting from Phe^{136} or end at Lys^{135} was found. Hence, it is speculated that the potential cleavage site Lys^{135}-Phe^{136} was resistant against the immobilized trypsin in N1 under our experimental conditions.

Along the hydrolysis process, it is important to point out the competition for the active site between the original protein substrate and the released polypeptides. Analysis of these polypeptides in the final hydrolysates provides information on the preference between immobilized and free trypsin. From the mass spectrum in Fig. 4, f(41-60), f(71-100) and f(70-75) remained in final hydrolysates by free trypsin, as well as by N1. The existence of f(125-138) and f(92-138) further confirms Lys^{135}-Phe^{136} was indigestible by N1. Other polypeptides with quite high intensity, such as f(41-70), f(41-69), f(101-124), and f(92-101), only existed in the hydrolysates from N1. By calculating the content of hydrophobic amino acids, these four polypeptides contain 39.9, 41.38, 41.7, and 60.0%, respectively. These high contents of hydrophobic amino acids may account for the non-digestion. Because the hydrolysis by immobilized trypsin in methacrylate monolith requires a transportation of the substrate to the monolith wall, these hydrophobic peptides seem less prone to be transported and then are hard to contact with the active site of immobilized trypsin.

3.3 Operational stability

During operation of IMTRs, pressure drop and activity were monitored through the whole study. To confirm the durability

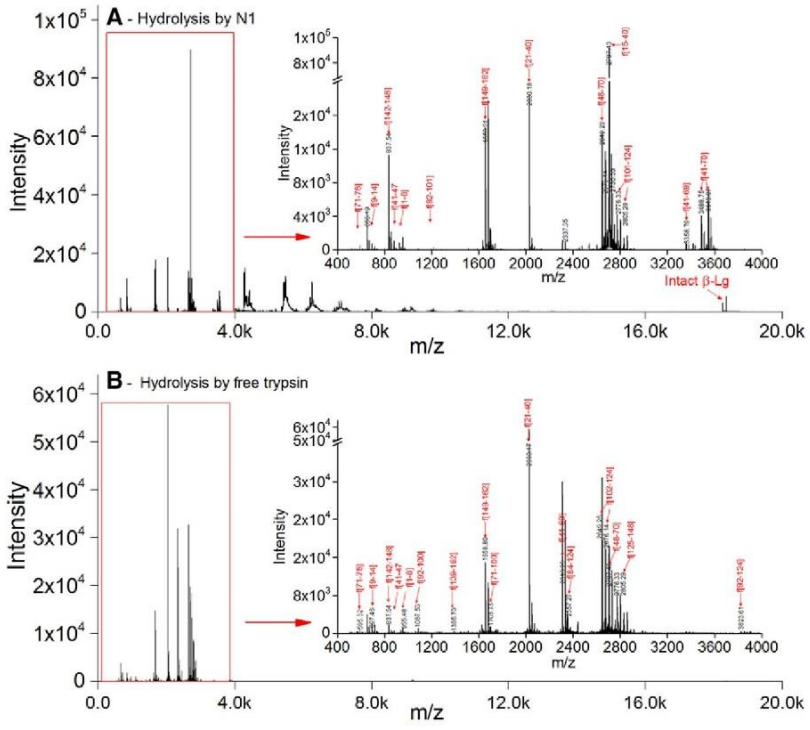

Figure 4. Mass spectra of samples analyzed using the α-Cyano-4-hydroxycinnamic Acid (HCCA) and 2,5-Dihydroxyacetophenone (DHAP) matrix: (A) sample hydrolyzed by N1; (B) sample hydrolyzed by 15 mg free trypsin

of IMTRs in one cycle, 10 mg/mL β-Lg solution was continuously recirculated through N1 or N2 at 10 mL/min for 6 h, respectively. As shown in Supporting Information Fig. 4, a slight increment of recorded pressure drop was noted for N1, namely from 0.30 MPa to 0.33 MPa, whereas the pressure drop by N2 completely kept constant. The adsorption of β-Lg molecules on the surface of monolith should be responsible for this slight increase of N1.

On the other hand, cumulative action from each cycle to the next one is a potential issue. N2 was used to hydrolyze β-Lg (10 mg/mL) for 18 cycles (except for 6 h in the first cycle, others were continued for 3 h each time), both enzymatic activity and pressure drop remained constant (the monitored permeability and activity was recorded in Supporting Information Fig. 5). Regarding to N1, the same substrate solution and recirculation time in each cycle were applied. Supporting Information Fig. 6 records the pressure drop, calculated permeability and activity over 18 cycles. No decrease was observed of either permeability or activity in the first ten cycles. Hereafter, the permeability declined gradually while the enzymatic activity was still unchanged until the 18th cycle. Because of the continuous increase of pressure drop, 20 mL of 0.05 M NaOH solution was used to flash N1 at 5 mL/min after the 18th cycle, which resulted in an increase of permeability, while accompanied by a complete loss of activity. After the application of 1 M NaOH, the permeability nearly returned to its initial value. This result confirms the blockage problem in N1 due to the cumulative action. It should be noted that the cycles were not always conducted over consequent days, and IMTRs were stored at 4°C in storage solution between cycles. After these operations, N2 was completely stable during storage over 30 weeks, in terms of BAEE activity and pressure drop, monitored over 3 weeks.

4 Concluding remarks

Trypsin immobilized on CIM monolith columns showed significant activity toward β-Lg. Different from hydrolysis by free trypsin in stirred solution, the efficient contact time between immobilized trypsin and substrate is much shorter than the recirculation time due to 0.6 mL pore volume of IMTRs. Nevertheless, the hydrolysis by N1 reached a much higher DH (9.68%) than that by 1.5 mg free trypsin (6.02%) in 4 h, mainly due to the autodigestion of free trypsin. To avoid this problem, a higher amount of enzyme is necessary to achieve DH_{max}, leading to higher costs. Furthermore, monoliths with large pores and consequently higher permeabilities make long-term use of IMTRs possible. At least 18 times' reuse of N1 significantly reduces costs in total. In order to additionally improve the operational stability, IMTR based on CIM monolith with pore size of 6 μm (N2) was developed and characterised as highly permeable alternative.

It is noted that hydrolysis conditions, such as pH, ionic strength, temperature, etc., are not optimized in this study. The efficiency of these IMTRs in production of β-Lg hydrolysates is highly potential to be improved after the optimization of processing parameters. Furthermore, these parameters play great roles not only in the effectiveness, but also in the selectivity. For example, Cheison's work [27] confirms that trypsin hydrolysis in solution at pH 8.5 and 25°C offers the complete removal of β-Lg while the retention of 67.87% native α-La. Hence, optimization of these parameters for IMTRs could allow a better process control such that the desired hydrolysis of the target β-Lg would preferably take place, while α-La remained largely unaffected, at lower levels of denaturation.

The first author thanks China Scholarship Council (CSC) for the support of her personal cost. This work was partially supported by Slovenian Research Agency within the research program P4-0369. The authors would like to thank Claudia Hengst and Heidi Wohlschläger for their friendly support with the HPLC analysis. Lev Matoh and Alenka Stopar from BIA Separations are also acknowledged for their technical help in laboratory.

The authors have declared no conflict of interest.

5 References

[1] Jost, R., Meister, N., Monti, J. C., U.S. Patent No. 5,039,532, Washington, DC, 1991.

[2] Leeb, E., Gotz, A., Letzel, T., Cheison, S. C., Kulozik, U., *Food Chem.* 2015, *187*, 545–554.

[3] Schmidt, D., Poll, J., *Nederlands melk en Zuiveltijdschrift* 1991, *45*, 225–240.

[4] Konrad, G., Kleinschmidt, T., *International Dairy J.* 2008, *18*, 47–54.

[5] Wang, H., Jiao, F., Gao, F., Zhao, X., Zhao, Y., Shen, Y., Zhang, Y., Qian, X., *Analyt. Bioanalyt. Chem.* 2017, *409*, 2179–2187.

[6] Yamaguchi, H., Miyazaki, M., Honda, T., Briones-Nagata, M. P., Arima, K., Maeda, H., *Electrophoresis* 2009, *30*, 3257–3264.

[7] Atacan, K., Cakiroglu, B., Ozacar, M., *Food Chem.* 2016, *212*, 460–468.

[8] Prieto, C. A., Guadix, E. M., Guadix, A., *J. Food Engin.* 2010, *97*, 24–30.

[9] Naldi, M., Černigoj, U., Štrancar, A., Bartolini, M., *Talanta* 2017, *167*, 143–157.

[10] Meller, K., Pomastowski, P., Szumski, M., Buszewski, B., *J. Chromatogr. B* 2017, *1043*, 128–137.

[11] Svec, F., *Electrophoresis* 2006, *27*, 947–961.

[12] Liang, Y., Tao, D., Ma, J., Sun, L., Liang, Z., Zhang, L., Zhang, Y., *J. Chromatogr. A* 2011, *1218*, 2898–2905.

[13] Nicoli, R., Gaud, N., Stella, C., Rudaz, S., Veuthey, J. L., *J. Pharmaceut. Biomed. Analysis* 2008, *48*, 398–407.

[14] Cheison, S. C., Zhang, S.-B., Wang, Z., Xu, S.-Y., *Food Res. Internat.* 2009, *42*, 91–97.

[15] Bassan, J., de Souza Bezerra, T., Peixoto, G., da Cruz, C., Galán, J., Vaz, A., Garrido, S., Filice, M., Monti, R., *Materials* 2016, *9*, 357.

[16] Bencina, K., Bencina, M., Podgornik, A., Strancar, A., *J. Chromatogr. A* 2007, *1160*, 176–183.

[17] Toro-Sierra, J., Tolkach, A., Kulozik, U., *Food Bioprocess Technol.* 2011, *6*, 1032–1043.

[18] Podgornik, A., Savnik, A., Jancar, J., Krajnc, N. L., *J. Chromatogr. A* 2014, *1333*, 9–17.

[19] Bender, M. L., Kezdy, F. J., *Ann. Rev. Biochem.* 1965, *34*, 49–76.

[20] Bergmeyer, H. U., *Methods of Enzymatic Analysis*, Elsevier, Amsterdam 2012.

[21] Adler-Nissen, J., *Enzymic Hydrolysis of Food Proteins*, Elsevier Applied Science Publishers, London 1986.

[22] Saha, B., Saikia, J., Das, G., *Analyst* 2015, *140*, 532–542.

[23] Fernandez-Lafuente, R., Rosell, C., Rodriguez, V., Guisan, J., *Enzyme Microbial Technol.* 1995, *17*, 517–523.

[24] Vlakh, E. G., Tennikova, T. B., *J. Sep. Sci.* 2013, *36*, 1149–1167.

[25] Jungreuthmayer, C., Steppert, P., Sekot, G., Zankel, A., Reingruber, H., Zanghellini, J., Jungbauer, A., *J. Chromatogr. A* 2015, *1425*, 141–149.

[26] Lendero, N., Vidic, J., Brne, P., Frankovic, V., Strancar, A., Podgornik, A., *J. Chromatogr. A* 2008, *1185*, 59–70.

[27] Cheison, S. C., Leeb, E., Toro-Sierra, J., Kulozik, U., *Internat. Dairy J.* 2011, *21*, 166–171.

Food Chemistry 253 (2018) 194–202

Contents lists available at ScienceDirect

Food Chemistry

journal homepage: www.elsevier.com/locate/foodchem

Comparison of the influence of pH on the selectivity of free and immobilized trypsin for β-lactoglobulin hydrolysis

Yuhong Mao[a,*], Maria Krischke[a], Claudia Hengst[a], Ulrich Kulozik[a,b]

[a] Chair of Food and Bioprocess Engineering, Technical University of Munich, Weihenstephaner Berg 1, D-85354 Freising-Weihenstephan, Germany
[b] Institute of Food & Health (ZIEL) – Technology Unit, Technical University of Munich, Weihenstephaner Berg 1, D-85354 Freising-Weihenstephan, Germany

ARTICLE INFO

Keywords:
β-lactoglobulin
Tryptic hydrolysis
Immobilization
pH
Selectivity

ABSTRACT

Although immobilized trypsin is a viable alternative to the free one in solution for producing protein hydrolysates, the change of selectivity introduced by immobilization is unclear. In this study, we compared the selectivity of free and immobilized trypsin towards different cleavage sites of β-lactoglobulin (β-Lg) with a focus on the impact of environmental pH. Both free and immobilized trypsin exhibited greater accessibility to native β-Lg at elevated pH (from pH 7.2 to 8.7). Additionally, free trypsin preferred to attack cleavage sites located at the C-terminus at pH 7.8, whereas an opposite preference for the N-terminus was observed at pH 8.7. Regarding the immobilized trypsin, the pH did not significantly influence its preference for the C- or N-terminus. Generally, immobilization of trypsin resulted in more focused cleavage within its specificity during the initial stage of hydrolysis, and some peptides were formed more rapidly by the immobilized trypsin.

1. Introduction

Enzymatic hydrolysis of β-lactoglobulin (β-Lg) produces peptides with reduced allergenicity (Selo et al., 1999) and improved functionality (Leeb, Gotz, Letzel, Cheison, & Kulozik, 2015). However, the cost of the large-scale use of enzymes in solution is very high, which severely limits their implementation at industrial scale. Correspondingly, immobilized enzymes represent an alternative approach due to the possibility of reusing enzymes and producing enzyme-free hydrolysates.

Enzyme immobilization has been exploited over the last four decades to enhance enzymatic activity and stability, which strongly depend on support properties, binding orientation, the number of formed bonds, the microenvironment of the enzyme, and other variables. Aside from measuring stability and activity, some researchers (Atacan, Cakiroglu, & Ozacar, 2016; Naldi, Černigoj, Štrancar, & Bartolini, 2017) analyzed the peptide profiles of the resulting hydrolysates to assess the enzyme specificity after immobilization. The specificity of a proteolytic enzyme describes the type of amino acid, after which it can hydrolyze a peptide bond (e.g., Lys and Arg for trypsin). Regardless of the specificity of the enzyme for individual cleavage sites, not all cleavable sites are hydrolyzed at the same time. Cheison, Brand, Leeb, and Kulozik (2011) followed the release of peptides as a function of hydrolysis time from β-Lg hydrolyzed by free trypsin during the first 10 min. They found that the N- and C-termini (Lys_8-Gly_9, Lys_{141}-Ala_{142}, and Arg_{148}-Leu_{149}) of β-Lg was cleaved early (15 s), implying the ease of trypsinolysis at the exposed termini. The results of Fernández and Riera (2013) also show the existence of areas within the intact β-Lg with different susceptibility to tryptic attack. To describe this preference in protein hydrolysis, Butre, Sforza, Gruppen, and Wierenga (2014) introduced the criteria "selectivity", referring to the rate at which individual cleavage sites in a protein substrate are hydrolyzed relative to other cleavage sites. The ability to discriminate the selectivity of an enzyme is considered essential for understanding enzymatic protein hydrolysis, especially in terms of obtaining hydrolysates consisting of preferred properties.

Upon immobilization of an enzyme, its conformation may change, thus affecting its intrinsic properties (V_{max}, k_{cat}, or K_m), especially when the enzyme is firmly fixed by multipoint covalent immobilization (Duggal & Bucholz, 1982). In addition, the properties of the supports used for immobilization, such as the charge of the stationary phase, hydrophobicity/hydrophilicity, may influence the intrinsic properties of the immobilized enzyme, particularly when charged substrates or products molecules are involved in the enzymatic process. Duggal and Bucholz (1982) presented clear evidence for significant shifts in the association constants for substrates and inhibitors due to the covalent binding of trypsin to a rigid support. Changes of the intrinsic properties of immobilized enzymes may lead to changes in selectivity.

Abbreviations: β-Lg, β-lactoglobulin; α-La, α-lactalbumin; MITR, monolith-based immobilized trypsin reactor; HCCA, α-cyano-4-hydroxycinnamic acid; DHAP, 2,5-dihydroxyacetophenone; BAEE, Nα-benzoyl-L-arginine ethyl ester; DH, degree of hydrolysis

* Corresponding author.
E-mail address: yuhong.mao@tum.de (Y. Mao).

https://doi.org/10.1016/j.foodchem.2018.01.151
Received 29 September 2017; Received in revised form 29 November 2017; Accepted 23 January 2018
Available online 31 January 2018
0308-8146/

Furthermore, the mass transfer properties of an immobilized biocatalyst may affect the competition for the active site of the enzyme between the original protein substrate and released polypeptides, which influences the selectivity to some extent, especially in a diffusion-limited step. Thus, more attention should be devoted to comparing selectivity between free and immobilized enzymes. Rocha, Gonçalves, and Teixeira (2011) compared peptide profiles of whey protein hydrolysates from free and immobilized trypsin by reversed-phase high-performance liquid chromatography (RP-HPLC) and concluded that no significant difference was observable. However, the sensitivity of HPLC, in our eyes, is not sufficient to make this statement. Mass spectroscopy would be required to identify and quantify the resulting peptides not only in the final hydrolysates, but also during the hydrolysis. Hence, many important aspects remain uncharacterized or not well understood, especially the evolutions of peptides, which should be affected by alterations in the selectivity of an enzyme after immobilization.

Additionally, the process of hydrolysis should be performed with a focus on the holistic influence of the hydrolytic environment, including pH, ionic strength, and temperature, et al., as these parameters play important roles regarding effectiveness and selectivity of enzymes. To exert more control over the process, it is important to elucidate the influence of the hydrolytic environment on peptide composition, i.e., the selectivity of the enzyme, allowing hydrolysis to be driven by both the "speed" and the desired peptide profiles obtained at various stages along the hydrolysis process.

Among these parameters, pH is easy to adjust while dramatically affecting the process. The effect of pH on enzymes varies, but it is prominently represented by the fact that each enzyme has an optimal pH range (e.g., pH 7.8–8.1 for free trypsin) in which the highest activity is observed. Meanwhile, changes in pH disrupt hydrogen bonding and affect salt bridges, leading to changes of the secondary and tertiary structures of the substrate as well as the enzyme. In fact, evidence of the influence of pH on enzyme selectivity was revealed in a study of the hydrolysis of whey protein isolate (WPI) by *Bacillus licheniformis* (Butré, Sforza, Wierenga, & Gruppen, 2015), in which large differences in enzyme selectivity for different cleavage sites of β-Lg were observed at pH 7.0, 8.0, and 9.0 (optimal pH for *Bacillus licheniformis* is 8.0).

Our previous work (Mao, Černigoj, Zalokar, Štrancar, & Kulozik, 2017) developed a monolith-based immobilized trypsin reactor (MITR), which has been confirmed as an effective alternative tool for producing β-Lg hydrolysates. This previous work also evaluated the effects of pH on the activity of both immobilized and free trypsin using a model substrate Nα-benzoyl-L-arginine ethyl ester (BAEE). Specifically, the free trypsin showed the highest activity at pH 7.8–8.1, and remained around 80% and 60% activity at pH 7.2 and pH 8.7, respectively. The MITR exhibited 70% activity at pH 7.2 compared with that at its optimal pH range (pH 8.5–8.7). In the present study, we aimed at clarifying the selectivity of the immobilized trypsin for β-Lg hyrolysis in comparison with free trypsin. The influence of pH ranging from pH 7.2 to pH 8.7, was investigated, i.e. somewhat broader than the optimum for free trypsin, in order to also include the pH range optimal for the immobilized one. The hydrolysis was characterized using three descriptors: (i) degree of hydrolysis (DH); (ii) the amount of depleted or remaining intact β-Lg as a function of DH (two genetic variants, β-Lg A and B, were compared); and (iii) the peptide profiles and molecular mass distribution depending on DH. Peptides with a mass of less than 4000 Da were assigned to specific sequences, and the selected peptides were further quantified to follow their dynamic evolutions.

2. Materials and methods

2.1. Materials

Bovine β-Lg was fractionated from WPI, a product developed by Fonterra Co-operative Group Ltd (Auckland, New Zealand), as described by Toro-Sierra, Tolkach, and Kulozik (2011). The obtained β-Lg powder had a protein content of 98.6% relative to the dry matter, and native β-Lg represented > 99% of the total protein content. Trypsin from bovine pancreas (Type I, approximately 10,000 BAEE units/mg protein), BAEE (B4500), Tris (hydroxymethyl)-aminomethane (TRIS), NaCl, $CaCl_2$, and NaOH were purchased from Sigma–Aldrich (St Louis, MO, USA). Deionized water was acquired using the Milli-Q System (Millipore Corporation, Bedford, USA).

The MITR was prepared as described in our earlier work (Mao et al., 2017). Aldehyde-activated Convective Interaction Media® radial column (outer diameter (D), 1.86 cm; inner diameter (d), 0.67 cm; height (h), 0.42 cm; volume, 1.0 mL) with a nominal pore size diameter of 2.1 μm was used as the immobilization support. The amount of immobilized trypsin was 5.0 ± 0.2 mg/mL monolith. After immobilization, the permeability of the MITR was 2.45×10^{-12} m^2 measured using deionized water.

2.2. Hydrolysis of β-Lg

2.2.1. Hydrolysis by free trypsin

β-Lg solution (50 mg/mL) was hydrolyzed by free trypsin with an enzyme-substrate ratio (E/S) of 0.1% (w/w) at 25 ± 1 °C. An additional experiment was conducted at E/S of 1% and pH 7.8 to reach the maximum DH. The pH of substrate solution was adjusted to 7.2, 7.8, 8.1, 8.5, and 8.7. A TitroLine alpha plus auto-titrator (Schott AG, Mainz, Germany) was used for the pH-stat hydrolysis. The detailed calculation of DH and reaction velocity was described in our published work (Mao et al., 2017).

2.2.2. Hydrolysis by immobilized trypsin

The MITR was integrated into an ÄKTA system (GE Healthcare Bio Sciences). In the single flow-through approach, a native β-Lg solution with a concentration of 3 mg/mL was pumped through the MITR at a flow rate of 0.5 or 10 mL/min. The pH of the applied solution was adjusted to 7.2, 7.8, 8.1, 8.5, and 8.7. Using the recirculation flow approach, 100 mL of a native β-Lg solution (10 mg/mL) were recirculated through the MITR at 10 mL/min, pH 7.8 and 8.7 were investigated. The pH-stat method was used to maintain a constant pH and to follow the evolution of DH.

2.3. Analysis of hydrolysates

1-mL samples were taken at different intervals (0, 5, 10, 20, 30, 45, 60, 90, 120, and 180 min) during the pH-stat process and stored at −20 °C. When free trypsin was used, 0.5 mL of the trypsin inhibitor solution (from soybean, 10 mg/mL) was mixed with each sample immediately to stop the hydrolysis. Samples (5 mL) produced by MITR using the single flow-through approach were stored at −20 °C for further analysis.

2.3.1. Quantification of residual native β-Lg

The native β-Lg content in samples was quantitatively determined via RP-HPLC using an Agilent 1100 series HPLC system (Agilent Technologies) and a PLRP-S 300A-8 μm Latek column (150 × 4.6 mm). The detail on the gradient was previously described by Leeb, Gotz, Letzel, Cheison, and Kulozik (2015). β-Lg A (99% purity, Sigma Aldrich, L7780) and β-Lg B (99% purity, Sigma Aldrich, L8005) were used as standards to build a calibration curve.

2.3.2. Separation and quantification of select peptides

The separation of hydrolysates was performed by RP-HPLC using the system described above. All samples were diluted only with the deionized water to a concentration of 4 mg/mL, excluding the sample with the maximum DH for free trypsin that was initially incubated with dithiothreitol (DTT) for 45 min at 37 °C and then mixed with chloroacetamide in dark for 30 min. A mobile phase of solvent A containing 0.1% (v/v) trifluoroacetic acid (TFA) dissolved in Milli-Q water and

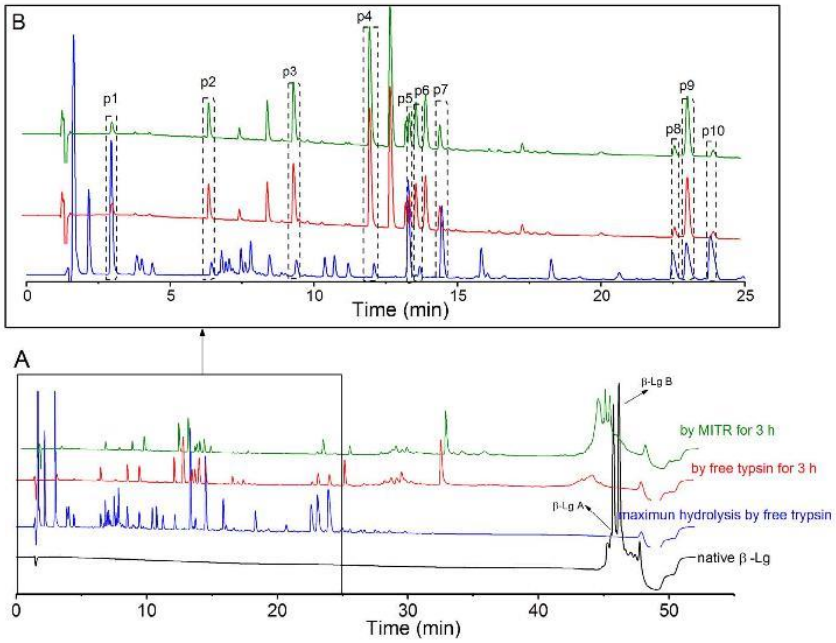

Fig. 1. Chromatographic profiles of intact β-lactoglobulin (β-Lg), the final product of free trypsin hydrolysis, and products generated via intermediate hydrolysis by free trypsin and a monolith-based immobilized trypsin reactor (MITR) (A). The spectra before 25 min for the latter three samples are highlighted in B.

solvent B consisting of 0.0555% (v/v) TFA dissolved in 80% (v/v) acetonitrile (diluted in Milli-Q water) was applied. The entire analysis was conducted at 40 °C and 1 mL/min, and the eluting time was extended to 45.5 min with a gradient from 3% to 57% solvent B. The standard sample injection volume was 20 μL, and the elution was monitored at 214 nm. Selected peaks were collected using a fraction collector for peptide composition analysis. Peaks containing a single peptide were chosen for further quantification, and the molar concentration of each specific peptide was calculated from the peak area according to Eq. (1) (Fernández & Riera, 2013) as follows:

$$X_i = 1 \times 10^6 \left(\frac{A_i}{\varepsilon_i \times l \times v} \right) \times f \times D \quad (1)$$

where x_i (μM) is the concentration of peptide i, A_i (AU min) is the peak area, l (0.6 cm) is the path length of the UV cell, v is the injection volume (20 μL), f is the flow rate (1 mL/min), D is the dilution factor of the sample before injection, and ε_i (AU M^{-1} cm^{-1}) is the molar extinction coefficient of peptide i at 214 nm calculated according to the work of Kuipers and Gruppen (2007).

2.3.3. Identification of peptides using matrix-assisted laser desorption/ionization time-of-flight mass spectrometry (MALDI-TOF-MS)

Mass compositions of collected samples were analyzed using a MALDI-TOF-MS system (ultrafleXtreme MALDI-TOF-TOF, Bruker Daltonics, Bremen, Germany) with two matrices separately, α-cyano-4-hydroxycinnamic acid (HCCA, Bruker Part-No. #201344) and 2,5-dihydroxyacetophenone (DHAP, Bruker Part no. #201346). Generally, HCCA was used to measure peptides in a low mass range (≤ 4000 Da), whereas DHAP was for the higher mass range. The detailed method was described in our previous work (Mao et al., 2017).

2.3.4. Identification of peptides by liquid chromatography-electrospray source ionization-tandem MS (LC-ESI-MS/MS) analysis

To further confirm the peptide composition, the fractions from the maximally hydrolyzed β-Lg, were further analyzed via LC-ESI-MS/MS, which was conducted at BayBioMs (Freising, Germany). The samples were completely dried in the SpeedVaC (Thermo Scientific, Germany) and resuspended in 500 μL 0.1% FA water. 0.1 μg sample was injected and re-chromatographed by an analytical column (75 μm × 40 cm, C18 column, Reprosil Gold, 3 μm, Dr. Maisch, Ammerbuch, Germany) in 60 min. The gradient was 4–32% solvent B (0.1% FA and 5% DMSO in ACN) in A (0.1% FA and 5% DMSO) at a flow rate of 300 nL/min. The MS measurement was performed on the LTQ Orbitrap Velos in a data-dependent mode whereby the ten most prominent precursor ions of the entire MS spectrum were automatically extracted and fragmented at higher energy collisional dissociation (HCD) at 30% collision energy. The dynamic exclusion was set to 30 s. Both survey scans and product ion scans were recorded in the Orbitrap. Inlet capillary temperature was held at 275 °C. A label-free quantification with MaxQuant (version 1.5.3.30) was carried out by the MS data against a Bos taurus UniProt reference database (version 09.07.2016, 24,217 entries, contains both β-Lg A and B).

2.4. Statistical analysis

All hydrolysis experiments were performed in triplicate. Mean values ± 95% confidence levels are reported. Data were plotted using Origin Pro 9.0 or R 3.3.3 (open source software).

3. Results and discussion

3.1. Characterization of the hydrolysates: Chromatographic profile and peptide identification

Some semi-quantitative techniques, i.e. technique based on the peak area of MS-extracted ions (Leeb et al., 2015) or examining the peak area integrated from the chromatography spectrum (Tauzin, Miclo, Roth, Mollé, & Gaillard, 2003), were used to monitor peptide formation. However, these methods do not permit the comparison of the abundance between peptides in terms of the absolute concentration due to differences in the ionization efficiency of different peptides. In this study, the molar extinction coefficient of each identified peptide was calculated and used for the absolute quantification.

Fig. 1 shows typical chromatographic profiles of samples resulting from the hydrolysis by free trypsin and MITR. One profile corresponds to the initial substrate, and the two main genetic variants of β-Lg (A and B) eluted with retention times of 45.71 and 46.13 min, respectively, are

presented. The second profile shows the final step (sample was processed with DTT) in the course of hydrolysis by free trypsin, during which the DH plateaued at 10.02%. As shown in the figure, all peptides present in the final hydrolysates eluted before 25 min. β-Lg contains 161 peptide bonds, of which 18 are theoretically cleavable by trypsin, leading to the release of 19 or 21 (considering the two genetic variants) final peptides after complete trypsinolysis. However, there were 26 peaks observed, indicating the existence of intermediate peptides or nonspecific cleavage. The other two profiles refer to the samples produced via intermediate hydrolysis at pH 7.8 by free trypsin (DH 6.12%) and MITR (DH 4.01%). Different from the maximally hydrolyzed sample, some peaks eluted after 25 min in these samples, and the peaks corresponding to intact β-Lg were still visible in the sample hydrolyzed for 3 h using MITR.

The peaks appearing before 25 min for three samples are highlighted in Fig. 1B. As can be seen, the good resolution allowed to monitor the formations of peptides on the basis of their peak areas, if no co-elution occurred. To assess the composition of individual peaks with identical or similar retention times from different hydrolysates, the peaks resulting from these samples, which were baseline separated, were collected separately. The peak numbers on the chromatogram in Fig. 1B refer to the peptide identification obtained via MALDI-TOF-MS, as reported in Table 1. In addition, the fractions from maximally hydrolyzed β-Lg were further analyzed by ESI-MS/MS (see Table 1) to ensure the correct identification of peptides.

According to previous works (Butré et al., 2015; Cheison et al., 2011) nonspecific cleavage of Tyr_{20}-Ser_{21} (f(21–40)) in β-Lg is a common feature, even when the purest possible trypsin is used. As the proposed fragment was assigned to the detected mass in the MALDI spectrum using a written code in software R 3.3.3 with a built-in database (Mao et al., 2017), peptides f(21–40) and f(15–20) were manually transferred into this database. However, this nonspecific cleavage was not included in the LC-ESI-MS/MS measurement. As shown in Table 1, peptide f(21–40) was detected by MALDI in both peaks P8 and P9 for all three samples. Additionally, peptide f(92–100) co-eluted in P8, which was confirmed by both MALDI and ESI. The polypeptide f(41–60) with one miscleavage site (Lys_{47}) was found in P10. Lys_{47} is linked to a proline amino acid, and it is potentially resistant to trypsinolysis, as observed by Olsen, Ong, and Mann (2004) as well. In addition, P10 from the maximally hydrolyzed sample contained peptide f(21–40), mainly due to the large amount of this peptide in the final hydrolysates.

Regarding peaks *P2–P7*, peptide f(71–75) was detected only by MALDI. It appears that this peptide is not detectable by ESI in this study. Another mass detected by MALDI referring to f(76–83) exhibited extremely strong intensity in the samples produced via intermediate hydrolysis. However, this mass was not observed in the maximally hydrolyzed sample, mainly due to the insufficient amount of this peptide, correlating with the small chromatographic peak shown in Fig. 1, as it is an intermediate peptide with the miscleavage site Lys_{78}. Finally, six peaks (P2–P7) were confidently used for further quantification.

3.2. Comparison of selectivity as a function of pH

Samples with pH values ranging from pH 7.2 to 8.7 were hydrolyzed by free trypsin for 5 min or by MITR at 0.5 and 10 mL/min using single flow-through approach.

3.2.1. Depletion of native β-Lg

The first medium-resolution structure of β-Lg determined by Papiz and Sawyer (1986) illustrates that the molecular structure consists of an antiparallel β-sheet formed by nine strands (A–I) and loops connecting the strands. The work of Qin et al. (1998) indicates that at pH 6.2, the EF loop is closed over the top of the barrel, burying Glu_{89} (the carboxylic acid with the anomalous pK_a) inside the calyx, whereas at pH 7.2, this loop is articulated away from the barrel such that the formerly buried glutamic acid becomes exposed in the carboxylate form. Furthermore, further increases of pH to values exceeding 8.0 induce further structural changes because the charge states of the side groups of a protein depend on the pH. The pH-dependent structural characteristics can explain the observed result, i.e. the fact that the intact protein was generally more accessible with increasing pH values for both free and immobilized trypsin. For free trypsin, a sharp increase in hydrolyzed β-Lg levels was observed when the pH was increased from 7.8 to 8.1 (see Fig. 2), whereas no obvious increment was noted at higher pH values. Concerning the hydrolysis by MITR at 0.5 mL/min, the hydrolyzed β-Lg content significantly increased as the pH was raised from 7.2 to 7.8, as well as from 8.1 to 8.5, as shown in Fig. 2. For the MITR operated at 10 mL/min, a significant increase was observed when the pH exceeded 7.2, while no difference in the levels of the hydrolyzed native protein from pH 7.8 to pH 8.7 was noticeable. It should be noted that the hydrolyzing time (the time for each substrate molecule remained in MITR) at 10 mL/min is extremely short, theoretically corresponding to 0.06 min because of the 0.6-mL pore volume. The enzymatic activity of free trypsin decreased significantly above pH 8.5 (Mao et al., 2017), this can explain why no more protein was hydrolyzed by free trypsin at

Table 1
Peptide identification through MALDI-TOF-MS and ESI-MS/MS analysis.

Peaks	Observed *m/z* by MALDI									Proposed fragment	Maximum hydrolysis by free trypsin detected by ESI	
	Maximum hydrolysis by free trypsin			By free trypsin for 3 h			By MITR for 3 h					
	RT[1] (min)	*m/z*[2]	S/N[3]	RT (min)	*m/z*	S/N	RT (min)	*m/z*	S/N		Sequence	Mass
P1	2.94	/	/	3.02	/	/	3.01	/	/	/	/	nd[4]
P2	6.43	573.18	21.40	6.54	573.18	255.60	6.40	573.20	54.00	f(71–75)	/	nd
P3	9.39	673.27	16.70	9.83	673.27	160.10	9.34	673.31	70.10	f(9–14)	GLDIQK	673.38
P4	12.09	933.49	25.90	11.94	933.53	327.50	12.00	933.49	262.90	f(1–8)	LIVTQTMK	932.54
P5	13.43	837.69	65.30	13.30	837.70	47.90	13.29	837.68	23.20	f(142–148)	ALPMHIR	837.05
P6	13.68	/	/	13.86	903.54	239.60	13.93	903.60	60.30	f(76–83)	/	nd
P7	14.41	1635.72	1001.40	14.41	1635.87	623.30	14.46	1635.88	558.70	f(125–138)	TPE…FDK	1634.77
P8	22.49	2030.12	587.10	22.47	2030.02	196.30	22.55	2030.04	403.30	f(21–40)	/	nd
		1065.57	82.74		1065.59	47.90		1065.59	37.70	f(92–100)	KYL…LVR	1064.58
P9	22.97	2030.07	706.80	22.86	2030.14	154.50	23.08	2030.10	268.90	f(21–40)	/	nd
P10	23.80	2030.93	148.90	23.74	/	/	23.91	/	/	f(21–40)	/	nd
		2313.14	868.80		2313.16	699.60		2313.18	849.60	f(41–60)	VYV…LQK	2312.25

[1] Retention time.
[2] The ration of mass to charge.
[3] The ratio of signal to noise.
[4] Not detected.

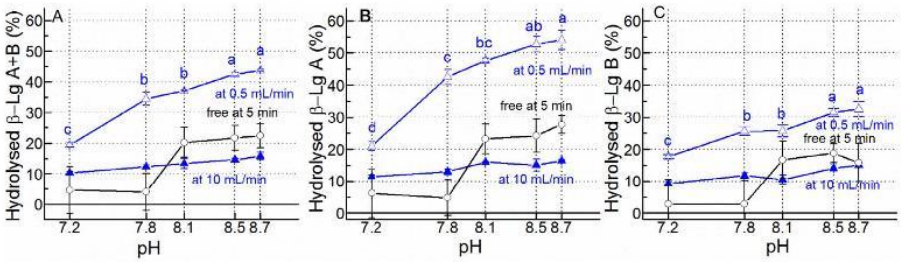

Fig. 2. Hydrolyzed native protein (%) at increasing pH values. A shows the total amount of β-Lg, including the two genetic variants. B and C refer to hydrolyzed β-Lg A (%) and B (%), respectively. A significant difference is presented only for the hydrolysis by MITR at 0.5 mL/min. Data concerning significance for the other two cases are described directly in the text.

pH 8.5 and 8.7 whereas the hydrolytic activity of immobilized trypsin was highest at these pH values. However, it is surprising that no significant difference in the depletion of native protein was observed for free trypsin at pH 7.2 and 7.8, as its activity at pH 7.8 was significantly higher than that at pH 7.2.

The applied β-Lg in this study contains two variants A and B, which differs by two amino acid substitutions, namely Asp64Gly and Val118Ala. The Asp64Gly substitution results in the CD loop adopting a different conformation, whereas the Val118Ala substitution causes no detectable change in the structure (Qin, Bewley, Creamer, Baker, & Jameson, 1999). However, their previous research also suggests that the lower thermal stability of the B variant is mainly due to the substitution of Val118Ala, which results in the hydrophobic core being less well packed. In contrast to the thermal stability, β-Lg B displays a higher resistance to tryptic digestion (Creamer et al., 2004), which is also confirmed in the present study. As shown in Fig. 2B–C, β-Lg A was hydrolyzed faster than the B variant at all applied pH values for both free and immobilized trypsin, and both β-Lg A and β-Lg B were more accessible to trypsin with increasing pH.

3.2.2. Analysis of the composition of hydrolysates

The accessibility of the intact protein is important, but it does not provide information about selectivity among different potential cleavage sites. Hence, the peptide compositions were analyzed by MALDI-TOF-MS, which provides details concerning the mass distribution in a range from 500 Da to the mass of intact β-Lg. As shown in the Venn diagrams (Fig. 3A1, B1, and C1), detected masses smaller than 4000 Da were assigned to specific fragments, and those larger than 4000 Da were directly distributed in Fig. 3A2, B2, and C2.

Peptides lacking miscleavage sites f(1–8), f(9–14), f(15–40), f (142–148), and f(149–162) were detected in all samples. This confirms the strong preference of both free and immobilized trypsin for cleavages at the two C-terminal lysines, N-terminal Lys_{141}, Arg_{148}, and Arg_{40} irrespective of the pH at which the hydrolysis was performed (pH 7.2–8.7). It is already known that arginyl residues are up to 25-fold faster hydrolyzed by trypsin than lysyl residues (Cheison & Kulozik, 2017). There are three arginyl residues among 18 potential cleavable sites in β-Lg. Excluding the aforementioned two cleavable sites, both free and immobilized trypsin preferred Arg_{124}, as peptide f(125–138) with one miscleavage site, Lys_{135}, existed in all samples. Another final peptide, f(71–75), was detectable in the samples from pH 7.8 to 8.7 for free trypsin and for MITR at 0.5 mL/min, whereas this peptide was only found in the sample at pH 8.7 hydrolyzed by the MITR at 10 mL/min. This peptide, located on β-strand D, is exposed to tryptic attacks in the native form of β-Lg, and this attack is considered to be directly associated with enzymatic degradation of the β-Lg molecule (Leeb et al., 2015). Correlating with the depleted intact protein content, it is reasonable to find f(71–75) in the samples hydrolyzed at higher pH values. The last detected peptide without a miscleavage site was f(84–91) in the sample produced by the MITR at 0.5 mL/min and pH 8.7. It is noted that masses smaller than 500 Da cannot be detected by the method applied in this study, leading to the absence of information at least on five final peptides.

Notably, the nonspecific peptide f(21–40) was present in all samples except that produced by the MITR at pH 7.2 and 10 mL/min. An earlier work of Fernández and Riera (2013) indicated that f(21–40) was released from f(15–40); thus, f(15–20) was a companion product. However, f(15–20) was only found in selected samples in this study, specifically in those hydrolyzed by the free trypsin at pH 7.2 and 7.8, as well in those hydrolyzed by the MITR at pH 8.5 (0.5 mL/min) and pH 8.7 (0.5 and 10 mL/min). This finding suggests that f(21–40) can also be directly generated from f(1–40) or f(9–40), as f(9–40) was detected in all samples. A completely different behavior concerning f(15–20) release was observed upon hydrolysis by free trypsin versus the immobilized one. Namely, free trypsin preferentially further hydrolyzed f (15–40) to release f(21–40) at lower pH values, whereas MITR exhibited this preference at pH 8.5 and 8.7. In addition, Lys_{69} and Lys_{70} displayed different accessibilities; e.g., Lys_{70} was cleavable at all experimental pH values, whereas Lys_{69} was preferentially attacked at higher pH values. Because these two lysines have a similar physical accessibility, this difference is mainly due to the modulation by the different residues surrounding the cleavage sites.

Regarding the mass distribution for samples containing peptides larger than 4000 Da, peaks for intact β-Lg were visible in all samples as shown in Fig. 3A2, B2, and C2. In the samples hydrolyzed by the MITR at 0.5 mL/min, more peaks were in the range of 4000–10,000 Da with increasing pH, indicating that more intact β-Lg was attacked directly at higher pH values. Regarding free trypsin, no significant differences in peptide composition were noted between pH 7.2 and 7.8, as well as in the pH range of 8.1–8.7, correlating well with the depleted amounts of native protein as shown in Fig. 2.

3.3. Comparison of selectivity as a function of DH

The comparison in Section 3.2 illustrates that differences in the selectivity between free and immobilized trypsin depend on the pH. To identify the differences in a dynamic hydrolysis process, i.e., which and when peptides were formed, a more detailed analysis based on the evolution of DH was conducted. According to the results in Section 3.2, pH 7.8 and 8.7 were chosen for further experiments.

3.3.1. Analysis of residual native protein as a function of DH

Fig. 4A presents the evolutions of DH as a function of time. As expected, the increase of DH in the initial phase using free trypsin was much faster than that using MITR. As shown in Fig. 4B1 and B2, the maximum reaction velocities for free trypsin reached approximately 7.5 and 4 meqv/min at pH 7.8 and 8.7, respectively, which were much higher than those achieved using MITR. Obviously, free trypsin is more flexible in making contact with substrate β-Lg than the immobilized one, contributing to the higher reaction velocity, which has been discussed in many cases of immobilized catalysts (Duggal & Bucholz, 1982; Mao, et al., 2017; Rocha et al., 2011). During hydrolysis by free trypsin, a sharp decrease of the reaction velocity within 30 min was observed, and after 3 h, the DH reached 6.10% at pH 7.8 and 5.82% at pH 8.7. The effects of autodigestion, reduction of the substrate, and potential inhibition by products can explain this result.

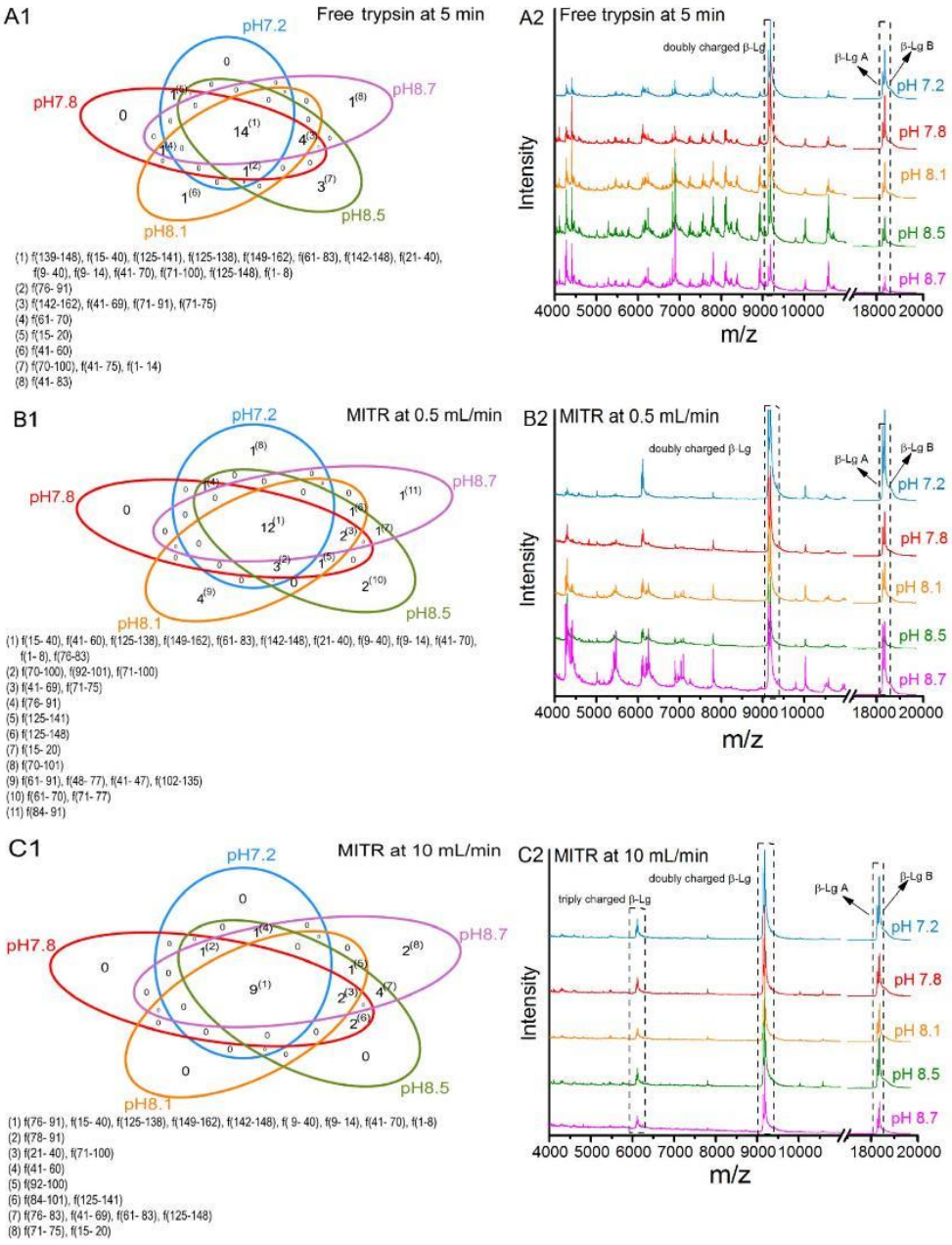

Fig. 3. Comparisons of peptide patterns for masses smaller than 4000 Da at five pH values are shown in A1, B1, and C1, and the mass distributions for larger peptides are presented in A2, B2, and C2. A refers to the samples hydrolyzed by free trypsin for 5 min, and B and C describe samples hydrolyzed by the monolith-based immobilized trypsin reactor (MITR) at 0.5 and 10 mL/min, respectively.

Correspondingly, the decrease of the reaction velocity for immobilized trypsin was less pronounced, mainly because of the absence of auto-digestion, as well as the fast removal of products. It is noted that no significant difference in the DH at pH 7.8 and 8.7 was observed for both free and immobilized trypsin.

The decrease of residual native β-Lg content as a function of DH indicates the preference for the hydrolysis of intact protein molecules versus the intermediate peptides and thereby the selectivity. In the Linderstrøm-Lange theory on protein hydrolysis, two models were distinguished: zipper and one-by-one (Adler-Nissen, 1976). As shown in Fig. 4C1 and C2, for the free and the immobilized trypsin, a similar linear rate of hydrolysis of the intact protein depending on DH was observed at pH 7.8, which met the "one-by-one" model. This rate was faster at pH 8.7 for both forms of trypsin. Especially for the free one, a sharp increase of the depletion rate was noted in the initial stage of hydrolysis, during which the increase in DH from 0 to 1% corresponded to a depletion of 40% of the intact protein content, in agreement with the "zipper" model. For hydrolysis by the MITR at pH 8.7, the intact protein level decreased linearly as a function of DH. As discussed in the 3.2.1, β-Lg exhibits a pH-dependent structure, making it more tryptic accessible at pH 8.7 than that at pH 7.8. In addition, the thermal stability of β-Lg, decreases from 76 °C at pH 7.0 to 58 °C at pH 9.0

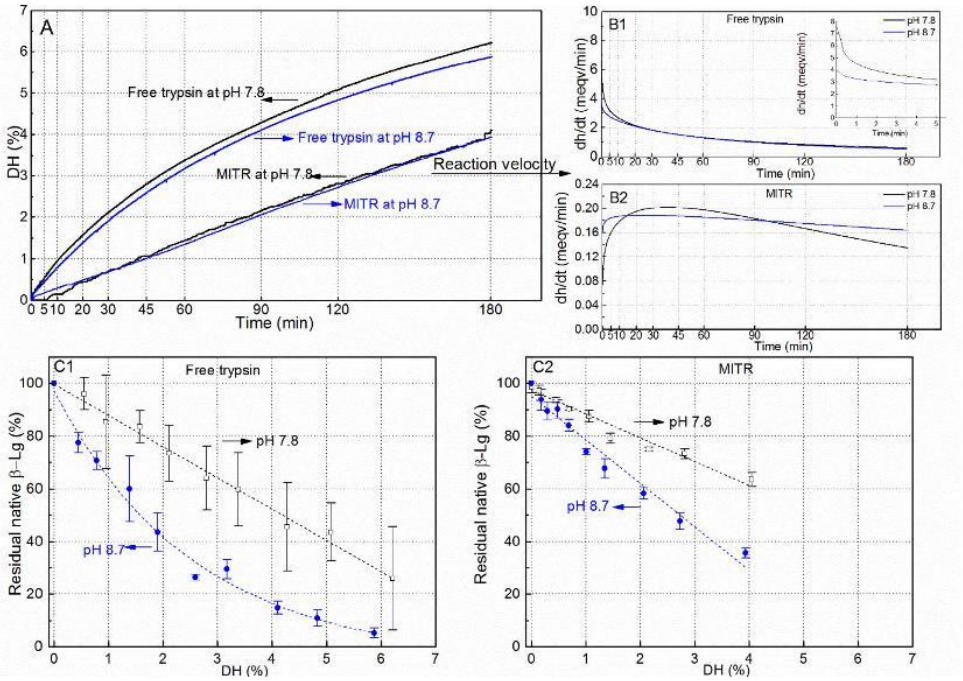

Fig. 4. The evolution of the degree of hydrolysis (DH) depending on time is shown in A. B1 and B2 illustrate the reaction velocities for free and immobilized trypsin, respectively. The inset shows the initial velocity (the first 5 min) of hydrolysis by free trypsin. C1 and C2 show the residual native protein content (%) as a function of DH during hydrolysis by free and immobilized trypsin, respectively.

measured by Haug, Skar, Vegarud, Langsrud, and Draget (2009). This decrease of thermal stability has been suggested to contribute to the increase of hydrolysis rate of the intact protein as well (Cheison et al., 2011).

3.3.2. Peptide formation

As shown in Figs. S1 and S2, the evolution of peptides as a function of DH was compared at pH 7.8 and 8.7 for free (Fig. S1) and immobilized trypsin (Fig. S2). The formed peptides can be classified into three main groups: (i) the final peptides for which their formation is directly linked to the breakdown of intact β-Lg, i.e., normally with high physical accessibility; (ii) some intermediate peptides that are formed rapidly during the first stage of hydrolysis but are then further hydrolyzed, leading to (iii) the smaller or final peptides.

In the first group of peptides, the cleavage sites located at the C- and N-termini, e.g., Lys_8, Lys_{14}, Arg_{40}, Arg_{141} and Lys_{148}, are considered the most physically accessible; as expected, peptides corresponding to the cleavages at these sites were released in the initial stage of hydrolysis by both free and immobilized trypsin. Another peptide f(71–75) typically presents a quick release during tryptic hydrolysis because of its external position in the three-dimensional structure of β-Lg and its amino acid composition, both which favor the action of trypsin (Fernández & Riera, 2013). In this study, it formed during the initial stage of hydrolysis using free trypsin as well, whereas it was only detected in samples with a DH exceeding 2% for the MITR. Regarding the second group, f(125–138) was not further hydrolyzed until the DH reached at least 4% for immobilized trypsin and even 6% for free trypsin, given that f(125–135) was not found. Concerning other intermediate peptides, f(76–91) appeared earlier at pH 7.8 than that at pH 8.7 for both free and immobilized trypsin. The resulting final peptide f (84–91) was also released earlier at pH 7.8 than at pH 8.7, namely at DH values of 0.69% (pH 7.8) and 1.35% (pH 8.7) for immobilized trypsin and 1.84% (pH 7.8) and 5.87% (pH 8.7) for free trypsin. Other studies (Cheison et al., 2011; Fernández & Riera, 2013) indicate that f (76–138) constitutes a resistant core to tryptic attack, which is in accordance with the result using free trypsin in this study, as the cleavage sites within this sequence were less preferred. However, the immobilization of trypsin improved the attack to this area to some extent.

The evolution of polypeptides with high molecular masses, in particular those between 4000 and 10,000 Da, is directly linked to the breakdown of the intact protein. As shown in Figs. S1 and S2, for both free and immobilized trypsin, the number of peaks with masses between 4000 and 10,000 increased much faster at pH 8.7 than that at pH 7.8, correlating well with the depletion rate of the intact protein (see Fig. 4). Regarding hydrolysis by free trypsin at pH 8.7, which was considered to agree with the “zipper” model, hydrolysis of the intact protein was initially rapid, leading to a large number of intermediate peptides, after which the depletion rate of the protein was slower. Likewise, these polypeptides were further hydrolyzed into smaller peptides.

3.3.3. Quantification of selected peptides

The quantification of selected peptides illustrates the dynamics of their formations, in which the concentration of each peptide relative to the theoretical maximum molar concentration is expressed as a function of DH, as shown in Fig. 5.

The peptides located at the C- and N-termini, e.g., f(1–8), f(9–14), and f(142–148), formed more rapidly at pH 8.7 than at pH 7.8 for both forms of trypsin, especially for the free one. As previously discussed, these peptides can be formed from cleavage of the intact protein, being directly linked to the depletion rate of β-Lg. Another peptide, f(71–75), located at the outside of the protein, was released more rapidly at pH 8.7 with free trypsin, whereas no significant difference in its release was noted between pH 7.8 and 8.7 for the immobilized trypsin. Comparing the formation rates of these four peptides, differences in selectivity were identified, and these differences depended on the pH as well as the use of free or immobilized trypsin. For instance, at pH 8.7, the preferred order of formation of these peptides by free trypsin was f(1–8) > f (142–148) > f(9–4) ≈ f(71–75), whereas at pH 7.8, this order was

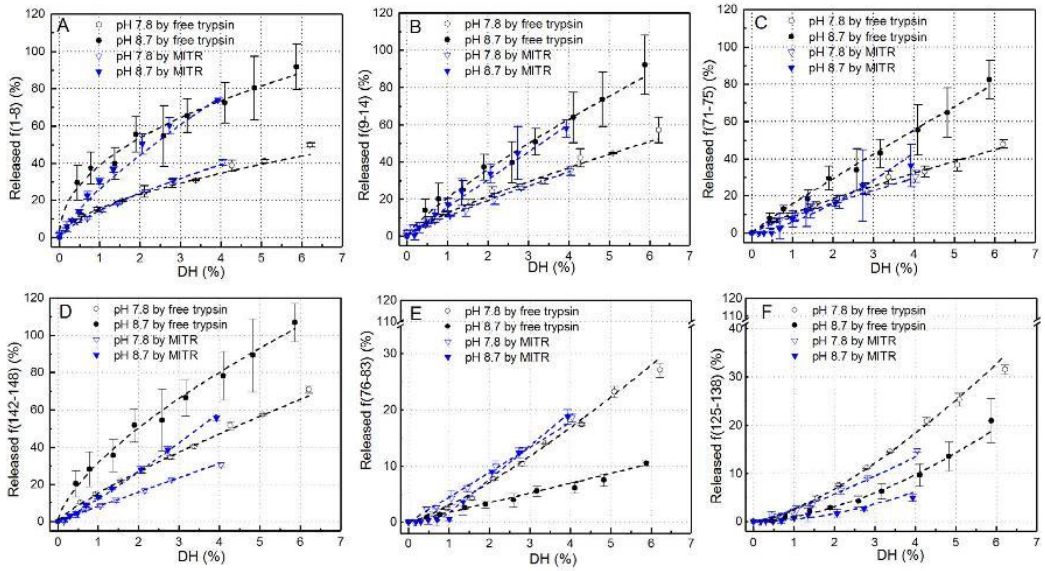

Fig. 5. Formation of six select peptides (%) as a function of the degree of hydrolysis (DH). A, B, C, D, E, and F present data for peptides f(1–8), f(9–14), f(71–75), f(142–148), f(76–83), and f(125–138), respectively.

changed to f(142–148) > f(1–8) ≈ f(9–14) ≈ f(71–75). For the immobilized trypsin, no obviously different preference at pH 7.8 concerning the release of these different peptides was found, and only at pH 8.7, f(1–8) formed significantly faster than the other three peptides.

f(76–83) and f(125–138) are two intermediate peptides, and their relatively slow liberation in the initial stage of hydrolysis is the result of their release from intermediate products opposed to the substrate molecule itself. With the accumulation of intermediate products, the formation rates of these two peptides increased, reaching approximately 30% for the free trypsin at DH 6% and approximately 20% for the immobilized one at DH 4%, which were much lower than the rates for four more physically accessible peptides. An interesting result was that the immobilized trypsin showed the similar trend to form the peptide f (76–83) at pH 7.8 and 8.7, which is faster than that for the free trypsin. Whereas the pH had a great influence on the release of f(76–83) and f (125–138) for free trypsin, both peptides were formed faster at pH 7.8 than at pH 8.7. In addition, there was no decreasing trend observed for these two intermediate peptides, as no final peptide released from these two was detected in any samples (see Fig. S1–2).

Generally, pH exerted more pronounced effects on the selectivity of free trypsin than the immobilized one. In this study, trypsin was rigidified by the multipoint covalent immobilization, which can keep its conformation quite stable when the pH is altered. Whereas, the free trypsin may suffer some structural distortion introduced by the increase of pH values, and this distortion always correlates to the changes of its selectivity (Rodrigues, Ortiz, Berenguer-Murcia, Torres, & Fernandez-Lafuente, 2013).

4. Conclusion

The hydrolysis conditions, e.g., pH, ionic strength, temperature, influence the hydrolysis rate and lead to different product profiles. No prior study discusses in sufficient detail whether these influences will differ once the enzyme is immobilized. In this study, the hydrolysis of β-Lg by free and immobilized trypsin was compared in detail with a focus on the influence of pH. In addition, the performance of the applied MITR, e.g., activity, permeability, remained nearly constant throughout all conducted experiments.

Although no significant difference in the evolution of DH at pH 7.8 and 8.7 was observed, both free and immobilized trypsin exhibited greater accessibility to intact native β-Lg at increasing pH values. The increase of pH from 7.8 to 8.7 even shifted the model of the depletion of native protein by free trypsin from “one-by-one” to “zipper,” whereas this influence on the hydrolysis by immobilized trypsin was limited. Regarding the two genetic variants, β-Lg A was more accessible than variant B under all experimental conditions, and free trypsin exhibited greater differences in this preference than the immobilized one.

The comparison of peptide profiles in the Venn diagrams clearly illustrated the different influences of pH over the range of 7.2–8.7 on the hydrolysis of β-Lg by free and immobilized trypsin. Generally, the immobilization of trypsin led to more focused cleavage sites within its specificity at the initial stage of hydrolysis compared with the findings for free trypsin. The quantification of the selected peptides during the hydrolysis process showed that free trypsin preferentially attacked the cleavage sites located at the C-terminus at pH 7.8, whereas an opposite preference was observed at pH 8.7. However, for the immobilized trypsin, no significant preference regarding the C- or N-terminus was noted, only a slight increase in preference for Lys_8 was identified at pH 8.7.

Based on the findings of this study, obviously, immobilization does lead to the changes of selectivity, which are also affected by pH. However, the influence of pH is hard to predict; thus, particular attention should be paid to hydrolysates compositions when studying the optimal pH of the hydrolysis to obtain the desired products.

Financial support

This research did not receive any specific grant from funding agencies in the public, commercial, or not-for-profit sectors.

Acknowledgements

The first author thanks China Scholarship Council (China) for the support of her personal cost. The authors would like to thank Urh Černigoj from BIA Separations (Ajdovščina, Slovenia) for his technical help in developing the MITR, as well as thank Mr. Bo Zeng from Technical University of Munich for his help for the code writing in R software.

Conflict of interest

None.

Appendix A. Supplementary material

Supplementary data associated with this article can be found, in the online version, at http://dx.doi.org/10.1016/j.foodchem.2018.01.151.

References

Adler-Nissen, J. (1976). Enzymic hydrolysis of proteins for increased solubility. *Journal of Agricultural and Food Chemistry, 24*(6), 1090–1093.

Atacan, K., Cakiroglu, B., & Ozacar, M. (2016). Improvement of the stability and activity of immobilized trypsin on modified Fe3O4 magnetic nanoparticles for hydrolysis of bovine serum albumin and its application in the bovine milk. *Food Chemistry, 212*, 460–468.

Butre, C. I., Sforza, S., Gruppen, H., & Wierenga, P. A. (2014). Introducing enzyme selectivity: A quantitative parameter to describe enzymatic protein hydrolysis. *Analytical and Bioanalytical Chemistry, 406*(24), 5827–5841.

Butré, C. I., Sforza, S., Wierenga, P. A., & Gruppen, H. (2015). Determination of the influence of the pH of hydrolysis on enzyme selectivity of Bacillus licheniformis protease towards whey protein isolate. *International Dairy Journal, 44*, 44–53.

Cheison, S. C., Brand, J., Leeb, E., & Kulozik, U. (2011). Analysis of the effect of temperature changes combined with different alkaline pH on the β-lactoglobulin trypsin hydrolysis pattern using MALDI-TOF-MS/MS. *Journal of Agricultural and Food Chemistry, 59*(5), 1572–1581.

Cheison, S. C., & Kulozik, U. (2017). Impact of the environmental conditions and substrate pre-treatment on whey protein hydrolysis: A review. *Critical Reviews in Food Science and Nutrition, 57*(2), 418–453.

Creamer, L., Nilsson, H., Paulsson, M., Coker, C., Hill, J., & Jimenez-Flores, R. (2004). Effect of genetic variation on the tryptic hydrolysis of bovine β-lactoglobulin A, B, and C. *Journal of Dairy Science, 87*(12), 4023–4032.

Duggal, S., & Bucholz, K. (1982). Effects of immobilization on intrinsic kinetics and selectivity of trypsin. *Applied Microbiology and Biotechnology, 16*(2), 81–87.

Fernández, A., & Riera, F. (2013). β-Lactoglobulin tryptic digestion: A model approach for peptide release. *Biochemical Engineering Journal, 70*, 88–96.

Haug, I. J., Skar, H. M., Vegarud, G. E., Langsrud, T., & Draget, K. I. (2009). Electrostatic effects on β-lactoglobulin transitions during heat denaturation as studied by differential scanning calorimetry. *Food Hydrocolloids, 23*(8), 2287–2293.

Kuipers, B. J., & Gruppen, H. (2007). Prediction of molar extinction coefficients of proteins and peptides using UV absorption of the constituent amino acids at 214 nm to enable quantitative reverse phase high-performance liquid chromatography – mass spectrometry analysis. *Journal of Agricultural and Food Chemistry, 55*(14), 5445–5451.

Leeb, E., Gotz, A., Letzel, T., Cheison, S. C., & Kulozik, U. (2015). Influence of denaturation and aggregation of beta-lactoglobulin on its tryptic hydrolysis and the release of functional peptides. *Food Chemistry, 187*, 545–554.

Mao, Y., Černigoj, U., Zalokar, V., Štrancar, A., & Kulozik, U. (2017). Production of β-lactoglobulin hydrolysates by monolith based immobilized trypsin reactors. *Electrophoresis*.

Naldi, M., Černigoj, U., Štrancar, A., & Bartolini, M. (2017). Towards automation in protein digestion: Development of a monolithic trypsin immobilized reactor for highly efficient on-line digestion and analysis. *Talanta, 167*, 143–157.

Olsen, J. V., Ong, S.-E., & Mann, M. (2004). Trypsin cleaves exclusively C-terminal to arginine and lysine residues. *Molecular & Cellular Proteomics, 3*(6), 608–614.

Papiz, M., & Sawyer, L. (1986). The structure of β-lactoglobulin and its similarity to plasma retinol-binding protein. *Nature, 324*(6095), 383–385.

Qin, B. Y., Bewley, M. C., Creamer, L. K., Baker, E. N., & Jameson, G. B. (1999). Functional implications of structural differences between variants A and B of bovine β-lactoglobulin. *Protein Science, 8*(1), 75–83.

Qin, B. Y., Bewley, M. C., Creamer, L. K., Baker, H. M., Baker, E. N., & Jameson, G. B. (1998). Structural basis of the Tanford transition of bovine β-lactoglobulin. *Biochemistry, 37*(40), 14014–14023.

Rocha, C., Gonçalves, M. P., & Teixeira, J. A. (2011). Immobilization of trypsin on spent grains for whey protein hydrolysis. *Process Biochemistry, 46*(2), 505–511.

Rodrigues, R. C., Ortiz, C., Berenguer-Murcia, A., Torres, R., & Fernandez-Lafuente, R. (2013). Modifying enzyme activity and selectivity by immobilization. *Chemical Society Reviews, 42*(15), 6290–6307.

Selo, I., Clement, G., Bernard, H., Chatel, J., Creminon, C., Peltre, G., & Wal, J. (1999). Allergy to bovine b-lactoglobulin: Specificity of human IgE to tryptic peptides. *Clinical and Experimental Allergy, 29*(8), 1055–1063.

Tauzin, J., Miclo, L., Roth, S., Mollé, D., & Gaillard, J.-L. (2003). Tryptic hydrolysis of bovine α S2-casein: Identification and release kinetics of peptides. *International Dairy Journal, 13*(1), 15–27.

Toro-Sierra, J., Tolkach, A., & Kulozik, U. (2011). Fractionation of α-lactalbumin and β-lactoglobulin from whey protein isolate using selective thermal aggregation, an optimized membrane separation procedure and resolubilization techniques at pilot plant scale. *Food and Bioprocess Technology, 6*(4), 1032–1043.

International Dairy Journal 85 (2018) 96–104

Contents lists available at ScienceDirect

International Dairy Journal

journal homepage: www.elsevier.com/locate/idairyj

Selective hydrolysis of whey proteins using a flow-through monolithic reactor with large pore size and immobilised trypsin

Yuhong Mao [a, *], Ulrich Kulozik [a, b]

[a] Chair of Food and Bioprocess Engineering, Technical University of Munich, Weihenstephaner Berg 1, D-85354, Freising-Weihenstephan, Germany
[b] Institute of Food and Health (ZIEL)-Technology Unit, Technical University of Munich, Weihenstephaner Berg 1, D-85354 Freising-Weihenstephan, Germany

ARTICLE INFO

Article history:
Received 16 March 2018
Received in revised form
4 May 2018
Accepted 22 May 2018
Available online 15 June 2018

ABSTRACT

Immobilised trypsin in a flow-through monolithic reactor was able to selectively hydrolyse β-lactoglobulin (β-Lg) in whey protein isolate (WPI), producing a whey product still rich in native α-lactalbumin (α-La). The monolith, with 6.2 ± 0.3 μm pore size, ensured long-term stability and operation at high flow rates, i.e., low backpressure. Increasing the flow rate from 0.8 to 32 mL min^{-1} reduced the recirculation time by 45% to reach the same degree of hydrolysis (DH) value. The immobilised trypsin showed the greater accessibility to intact β-Lg at increased pH and low ionic strength, i.e., only 14.75 ± 10.14% β-Lg at DH 4% was detectable (pH 9.2, without NaCl). Although α-La was almost inaccessible to the immobilised trypsin (85% of its initial native amount remained in all obtained hydrolysates), its presence significantly influenced the susceptibility of β-Lg, i.e., a three-fold decrease in V_{max} for β-Lg hydrolysis was found in the kinetic analysis.

1. Introduction

Whey is a major co-product from cheese manufacturing. Whey mainly consists of β-lactoglobulin (β-Lg) and α-lactalbumin (α-La), which represents approximately 53% and 20–25% of whey proteins, respectively (Edwards & Jameson, 2014). β-Lg acts as a primary allergen, especially in infant formula, as it is not present in human milk. On the contrary, the amino acid composition of bovine α-La shows a 72% sequence homology to human α-La, which plays an important role in the synthesis of lactose (Lisak, Toro-Sierra, Kulozik, Bozanic, & Cheison, 2013). Hence, a whey product rich in native α-La with zero to low allergenicity appears to be very attractive.

Enzymatic hydrolysis is a common approach to reduce the allergenicity of proteins by cleaving the antigenic regions (Lowe, Dharmage, Allen, Tang, & Hill, 2013). Along with the reduction in allergenicity of β-Lg by enzymatic hydrolysis, the results of bioactivities (Hernandez-Ledesma, Recio, & Amigo, 2008) reported for its peptide fragments are exciting as well. In addition, Schmidt and Poll (1991) indicated that, contrary to native β-Lg, native α-La was resistant to tryptic digestion. This action highly depended on the composition of medium (Ca^{2+}, buffer, pH, etc.), incubation temperature and the degree of denaturation of the protein. Taking advantage of this trypsin selectivity, Konrad and Kleinschmidt (2008) succeeded in isolating α-La with 90–95% purity from whey proteins by applying tryptic hydrolysis (42 °C, pH 7.7) and membrane filtration. However, only 15% α-La was recovered mainly due to the high hydrolysis temperature. Actually, increasing the temperature near or above the trypsin optimum of 37 °C resulted in a less controlled hydrolysis of whey proteins, with low resistance of α-La to trypsin (Cheison, Leeb, Toro-Sierra, & Kulozik, 2011). To improve the yield of α-La, Cheison et al. (2011) optimised the conditions for tryptic hydrolysis of whey protein isolate (WPI), and 67.87% α-La was recovered at pH 8.5 and 25 °C. These findings provide a proof of concept for selectively hydrolysing β-Lg using trypsin in presence of other whey proteins.

However, the high cost of large-scale trypsin use in solution severely limits this application to industrial implementation. Correspondingly, immobilised trypsin represents an alternative approach due to the possibility of reusing the enzyme and producing enzyme-free hydrolysates. In particular, a flow-through hydrolysis system offers better process control than batch-based methods. To produce protein hydrolysates using immobilised enzymes, some groups (Atacan, Cakiroglu, & Ozacar, 2016; Bassan et al., 2016) have sought to develop particle based immobilised enzyme systems. These systems still suffer from low capacity in terms of volume throughput, as well as low processing stability due to the increase of backpressure over use. Our previous work (Mao,

* Corresponding author. Tel.: +49 8161 71 3855.
E-mail address: yuhong.mao@tum.de (Y. Mao).

https://doi.org/10.1016/j.idairyj.2018.05.015
0958-6946/

Cernigoj, Zalokar, Strancar, & Kulozik, 2017) reported the monolithic columns (bed volume 1 mL, nominal pore sizes 2.1 and 6 μm) based immobilised trypsin reactors (MITRs), which showed significant activity towards β-Lg. In that study, the MITR with 6 μm pore size showed constant backpressure along with repetition of cycles, i.e., intensive use for producing β-Lg hydrolysates, whereas the 2 μm MITR exhibited increasing backpressure. This was due to the 7.8 times higher permeability when the pore size increased from 2 to 6 μm. However, because of the increase of pore size, the internal surface area deceased by 60%. Therefore, less trypsin could be immobilised. This led to the failure of 1 mL MITRs for hydrolysing WPI, i.e., clogging of the pores in the 2 μm MITR was too serious (backpressure increased after only 5 uses), and long hydrolysis time (up to 8 h for DH 4%) was required when using the 6 μm-MITR. In this study, we therefore scaled up the bed volume of MITR with 6 μm pore size to 8 mL so that its surface area was large enough for trypsin immobilisation, and simultaneously it was still highly permeable.

Although free trypsin selectively hydrolyses β-Lg in whey proteins under certain conditions (Cheison et al., 2011; Schmidt & Poll, 1991), this selectivity may change upon its immobilisation. Actually, our previous work (Mao, Krischke, Hengst, & Kulozik, 2018) found that immobilisation of trypsin led to changes of its preference to individual cleavage sites of β-Lg in pure solution. Hence, the main purpose of this study was to examine the applicability of the MITR for selectively hydrolysing β-Lg in WPI, i.e., to assess whether the concept of selective hydrolysis of β-Lg in presence of other proteins is affected by the immobilisation of trypsin. The hypothesis was that the immobilisation of trypsin could have an impact on its accessibility to α-La and the presence of α-La might also influence the susceptibility of β-Lg.

As the performance of enzymes strongly depends on environmental conditions, we also systematically investigated the influence of flow rate, pH, and ionic strength. As discussed before, a much higher resistance to free trypsin by α-La was detected at < 30 °C (Cheison et al., 2011). In addition, Rocha, Gonçalves, and Teixeira (2011) found that immobilised trypsin (on spent grains) showed similar accessibilities to β-Lg and α-La above 37 °C. Hence, we conducted all hydrolysis experiments at ambient temperature, where β-Lg was able to be efficiently hydrolysed by 1 mL MITRs (Mao et al., 2017). In addition, kinetic studies as functions of flow rate and substrate resource (single protein or in mixture) were undertaken. The long-term stability and reusability of this MITR was monitored throughout the entire study.

2. Materials and methods

2.1. Materials

WPI powder (93.84% protein) was a product of Fonterra Co-operative Group Ltd, Auckland, New Zealand and contained 91.87% native whey proteins (18.68% α-La, 32.07% β-Lg B, 41.13% β-Lg A). Trypsin from bovine pancreas (Type I, ~10,000 BAEE units mg^{-1} protein), N-α-benzoyl-L-arginine ethyl ester (BAEE, B4500), tris(hydroxymethyl)-aminomethane (Tris), sodium hydroxide, and calcium chloride were purchased from Sigma–Aldrich (St Louis, MO, USA). The reagents used for the immobilisation of trypsin were identical to those described in our previous work (Mao et al., 2017). Deionised water was acquired from a MilliQ System (Millipore Corporation, Bedford, USA).

2.2. Characterisation of MITR

An aldehyde activated Convective Interaction Media® (CIM®) radial column (CIM-ALD, tube dimensions: outer diameter (D), 1.50 cm; inner diameter (d), 0.65 cm; height (h), 5.6 cm; bed volume, 8.0 mL) with nominal pore size diameter of 6 μm and 60% porosity was provided by BIA Separations d.o.o. (Ajdovščina, Slovenia). Trypsin was covalently immobilised on this CIM-ALD monolithic column using the protocol described by us previously (Mao et al., 2017). The amount of immobilised trypsin was 11 mg in the whole MITR, and 1.4 mg mL^{-1} of the bed volume. The MITR was additionally characterised for permeability and enzymatic activity.

2.2.1. Evaluation of permeability

To calculate the permeability, the backpressures without and with MITR were recorded at increasing flow rates, namely 4, 8, 16, 32 and 48 mL min^{-1}, by pumping deionised water. The difference between these two values at a defined flow rate was considered to be the pressure drop created by the inserted reactor. According to the study of Podgornik, Savnik, Jancar, and Krajnc (2014), the permeability of a monolith was calculated according to Eq. (1):

$$B = \frac{F}{\Delta P} \times \frac{\eta \times \ln\left(\frac{D}{d}\right)}{2\pi h} \quad (1)$$

where, B (m^2) is the calculated permeability of the monolith; ΔP (MPa) is the pressure drop; η is the viscosity of mobile phase (0.87685 mPa × s for deionised water); F (mL min^{-1}) is the volumetric flow rate; D (m) and d (m) are outer and inner tube diameters, and h (m) is monolith height.

2.2.2. Determination of activity units

Using BAEE as a low molecular mass substrate, the enzymatic activity of immobilised trypsin was measured employing zonal approach. The MITR was inserted in an Äkta Explorer system (GE Healthcare Bio Sciences) with 100 mL pump heads. 20 mM Tris–HCl containing 19 mM $CaCl_2$ was used as a buffer to equilibrate the reactor and dissolve BAEE. A loop of 6 mL was used to inject BAEE solution with increasing concentrations at 24 ± 1 °C, namely 1, 3, 10, 30, 100 mM. The BAEE solution was injected at 80 mL min^{-1}, and 100 or 200 mL eluents were collected. The amounts of the substrate BAEE and its product N-α-benzoyl-D,L-arginine (BA) were chromatographically separated by high-performance liquid chromatography (HPLC) analysis. The Michelis-Menten graph was obtained and the apparent V_{max} value was calculated as described by Naldi, Cernigoj, Štrancar, and Bartolini (2017).

2.3. Hydrolysis of WPI by MITR

WPI powder was dissolved in deionised water and stirred for 15 h at 4 °C to allow complete hydration. To remove denatured whey proteins, the pH of the obtained WPI solution was adjusted to 4.6 (Dannenberg & Kessler, 1988) at ambient temperature, and then centrifuged at 6000 × g for 10 min, the supernatant was filtered through cellulose membrane with a cut-off of 0.45 μm. The prepared WPI solution was further altered according to the experimental design (changes in pH, ionic strength and concentration).

The MITR was inserted in an ÄKTA™ pure system (GE Healthcare Bio Sciences) consisting of a sample pump (S9), system pumps, auto-sampler (F9-R) and detectors for UV (U9-M), pH, temperature and conductivity. The system was controlled using Unicorn Software 7. Before each hydrolysis cycle, the reactor was washed using 10 column volumes (CVs) of deionised water, and pre-conditioned with 15 CVs 0.1 M Tris–HCl buffer at the same pH value as the applied substrate solution. The flow rate was 16 mL min^{-1}. The hydrolysis was performed using recirculation or single flow-through approach.

2.3.1. Recirculation approach

Ninety-six millilitres of WPI solution at a concentration of 20 mg mL^{-1} were used. The first 2 CVs (16 mL) were discarded, and then a total 80 mL of substrate solution was recirculated for the hydrolysis. The degree of hydrolysis (DH) was measured by an auto-titrator (TitroWiCo, Werner Cornelius, Bochum, Germany) and calculated using Eq. (2) according to the pH-stat method (Adler-Nissen, 1986).

$$DH = \frac{h}{h_{tot}} \times 100\,\% = \frac{V_b \times N_b}{\alpha \times M_p \times h^*_{tot}} \times 100\% \quad (2)$$

where, V_b (mL) is the base consumption; N_b is normality of the base (0.5 M NaOH); α is average degree of dissociation of the NH groups; M_P (g) is the mass of protein; h^*_{tot} is total number of peptide bonds in one gram protein substrate (8.8 meqv g^{-1} for WPI). In addition, the initial depleting rate of β-Lg (R) was calculated according to Eq. (3)

$$R = \frac{\Delta C \times V}{t} \quad (3)$$

where R (μmol min^{-1}) is the depleting rate of β-Lg, ΔC (μmol mL^{-1}) is concentration difference at DH 0 and 0.5%, V is the volume of substrate solution (80 mL), and t (min) is the time reaching DH 0.5%.

All hydrolysis experiments were conducted at 24 ± 1 °C. The recirculation time was set up to 8 h in the software, but it was manually terminated when the DH reaching the final desired values (i.e., DH 4% or 8%). Aliquots (1 mL) were drawn at different DHs from 0 to 4%. To explore the influence of recirculation flow rate (0.8, 4, 8, 16, 32 mL min^{-1}), WPI solution at pH 8.7 without NaCl was used. For pH effects (pH 7.8, 8.3, 8.7 and 9.2), hydrolysis was performed at 32 mL min^{-1} without adding NaCl. To evaluate the effect of ionic strength (0, 0.05, 0.1 and 0.25 M NaCl corresponding to increasing conductivity 2.70, 6.46, 10.46 and 24.60 ms cm^{-1}), pH was 8.7 and flow rate was 32 mL min^{-1}.

2.3.2. Single flow-through approach

To explore the apparent kinetic parameters of depleting β-Lg in WPI, the pre-treated WPI solution was mixed with 0.2 M Tris–HCl buffer (pH 8.7) at a ratio of 1:1 to reach the desired concentrations, i.e., 5, 10, 20 and 30 mg mL^{-1}. The MITR was pre-conditioned with 0.1 M Tris–HCl buffer (pH 8.7). 32 mL of the prepared WPI solution was pumped through the MITR and fractionated into 4 tubes by the auto-sampler, 8 mL in each tube. Increasing flow rates from 0.8 to 48 mL min^{-1} were investigated. The average native protein content in the last two tubes was used as the protein concentration of the hydrolysed sample.

The depleting rate of β-Lg was calculated according to Eq. (4):

$$R = \frac{\Delta C \times v}{t} = \frac{\Delta C \times v}{v/F} = \Delta_C \times F \quad (4)$$

where, ΔC (μmol mL^{-1}) is the difference of β-Lg concentration in WPI solution before and after hydrolysis, v (mL) is pore volume (6.4 mL), t (min) is the theoretical contact time between the enzyme and the substrate, which is calculated from the pore volume V (mL) and F (mL min^{-1}).

In addition, the pure β-Lg solution was used under the same conditions to evaluate the effect of other whey proteins, mainly α-La, on the depletion of β-Lg.

2.4. Washing and storage of MITR

After each hydrolysis experiment, the MITR was washed according to the following procedure: 0% 1 M NaCl (pH 10.5, adjusted by 1 M NaOH) in water linearly increasing to 100% 1 M NaCl over 10 CVs at 16 mL min^{-1}, and then 10 CVs of 100% this 1 M NaCl solution. Afterwards, 10 CVs of deionised water was passed through the MITR followed by 20 CVs of the storage solution (19 mM $CaCl_2$ in 5% ethanol/water (v/v), pH 3, adjusted by 1 M HCl). The MITR was stored at 4 °C.

2.5. Determination of the residual protein

The samples obtained were firstly diluted with deionised water to a protein concentration around 2 mg mL^{-1}, and then the pH was adjusted to 4.6 before filtering through a 0.45 μm cellulose membrane. The native whey proteins contents (β-Lg A, β-Lg B and α-La) in the pre-treated samples was quantitatively determined by HPLC using an Agilent 1100 series HPLC system (Agilent Technologies) and a PLRP-S 300 A-8 μm Latek column (150 × 4.6 mm). The detailed gradient information was previously described by Leeb, Gotz, Letzel, Cheison, and Kulozik (2015). α-La (91% purity, Sigma Aldrich L6010), β-Lg A (99% purity, Sigma Aldrich, L7780) and β-Lg B (98% purity, Sigma Aldrich, L8005) were used as standards to build the calibration curve.

2.6. Statistical analysis

Considering the potential decline of hydrolysis efficacy of the applied MITR, all hydrolysis experiments were carried out in triplicate and the three repeats under the same condition were conducted in a staggered way to reduce bias. Mean values ± standard deviation are reported. Data were plotted using Origin Pro 9.0.

3. Results and discussion

3.1. Characteristics of MITR

The design of the CIM tubular column allows the mobile phase to run in a radial direction from the outer to the inner surface. The scale-up of bed volume from 1 to 8 mL was realised by increasing the height of the column, namely from 4.2 to 56 mm. However, the short separation layer, through which the mobile phase passes, was maintained and even decreased from 6.05 to 4.25 mm in this case. To ensure the quality of this upscaled 8 mL MITR, its basic characteristics were compared with the 1 mL MITR (pore size 5.80 μm and bed volume 1 mL) reported in our earlier work (Mao et al., 2017).

3.1.1. Basic characteristics

The total immobilised amount of trypsin in the 8 mL column was around 11 mg, resulting in an approximately twice-lower immobilised trypsin coverage density than that in the 1 mL column, as illustrated in Table 1. Considering Brunauer–Emmett–Teller (BET) surface area (approximately 2 m^2 g^{-1} dry monolith with pore size 6 μm) and the molar mass of trypsin from bovine pancreas (23.8 kDa), each trypsin molecule in the 8 mL MITR occupied approximately 23 nm^2 of surface area, while only 11 nm^2 for each molecule in the 1 mL MITR, as calculated in Mao et al. (2017). Theoretically, one trypsin molecule would occupy between 10 and 20 nm^2 of surface (Naldi et al., 2017). Hence, the surface coverage of trypsin molecules in the 8 mL MITR was still very high, in the range between 50 and 85%.

Low backpressure, corresponding to a high permeability, is a crucial requirement to prepare immobilised enzyme reactors capable of processing large amounts of protein. For the 8 mL MITR, a linear increase of pressure drop depending on flow rates was observed, as expected for constant permeability, proving that the porous monolithic structure was stable and no mechanical compression occurred, as illustrated in Fig. 1. Based on the pressure

Table 1
Characteristics of CIM-MITRs based on 8 mL and 1 mL bed volume.[a]

CIM-MITR	Pore size (μm)	Bed volume (mL)	Density of immobilised trypsin (mg mL^{-1} monolith)	Permeability in deionised water (m^2)	Activity U (μmol min^{-1} mg $trypsin^{-1}$)
8 mL	6.2 ± 0.3	8	1.4 ± 0.3	2.63×10^{-11}	12.82
1 mL	5.8 ± 0.3	1	3.0 ± 0.3	1.91×10^{-11}	12.19

[a] The data for 1 mL MITR is reproduced from Mao et al. (2017) with permission.

drop behaviour, the permeability was calculated to be 2.63×10^{-11} using Eq. (1), which was slightly higher than that of the 1 mL MITR (Table 1). Exact pore sizes of tested MITRs, determined by Hg porosimetry, were 5.8 μm and 6.2 μm for 1 mL and 8 mL MITRs, respectively. Assuming the same porosity and structural constant, the permeability of CIM monoliths correlates linearly with a square of pore size (Podgornik et al., 2014), which was confirmed for both MITRs tested.

3.1.2. Enzymatic activity

BAEE, with a small molecular mass of 342.82 Da, was used as the model substrate to evaluate the enzymatic activity. It is important to ensure that the MITR works in steady-state conditions, thus allowing the estimation of maximum enzymatic activity. Despite the knowledge that zonal approach of the BAEE activity determination is slightly misleading (underestimation of the apparent active units; Naldi et al., 2017), it was used in our study due to the lower consumption of BAEE substrate compared with the continuous flow approach. The estimated maximum enzymatic activity calculated from Michaelis–Menten curve was 141 μmol min^{-1}. Calculating the specific activity in unit per mg trypsin, the two MITRs showed the similar enzymatic activity (Table 1).

3.2. Influences of operational parameters on the hydrolysis of WPI

In this study, we investigated the influences of operational parameters, i.e., flow rate, pH, and ionic strength, on the selective hydrolysis of β-Lg in WPI. The hydrolysis was mainly characterised by DH and residual native proteins, including the comparison between α-La and β-Lg, as well as two genetic variants of β-Lg. Specifically, the DH was rated based on the time to reach specific values, measured by the pH stat method, and the residual native proteins contents were evaluated as the function of DH.

3.2.1. The effect of recirculation flow rate

Flow rate is an important factor affecting the flow-through bioreactor performance. In contrast to conventional porous beads based supports, the only voids in a monolithic unit are the interconnected pores. Consequently, mass transfer is much faster due to the convective flow that becomes the dominant transport mechanism (Vodopivec, Podgornik, Berovič, & Štrancar, 2003).

As shown in Fig. 2A, when the flow rate was increased up to 32 mL min^{-1}, the required time to reach the same DH value was shorter. Especially from 0.8 to 4 mL min^{-1}, the time to reach DH 4% was reduced from 277.0 ± 26.8 min to 206.5 ± 34.2 min. This corroborates conclusions from the past investigations (Naldi et al., 2017; Ponomareva, Kartuzova, Vlakh, & Tennikova, 2010), i.e., higher flow rates contribute to higher enzymatic efficiency. Except for faster mass transfer contribution at higher flow rates, the enhanced diffusivity of substrate molecules from the mobile phase to the monolith surface increased the number of efficient contacts between the molecules of substrate and immobilised trypsin, resulting in improved efficiency. In addition, the difference of efficacy at the initial stage of hydrolysis among the flow rates above 4 mL min^{-1} was negligible, while during hydrolysis, the DHs increased faster at 16 and 32 mL min^{-1}, which was due to the decrease of substrate so that a higher flow rate was required to sufficiently replenish substrate.

It is notable that the increased flow rate leads to a simultaneous increase in shear stress, which may mechanically degrade the immobilised enzyme (Bencina, Bencina, Podgornik, & Strancar, 2007). For example, Bartolini, Greig, Yu, and Andrisano (2009) found that enhanced flow rates led to decreased hydrolysis efficiency. They speculated that the severe friction at higher flow rates reversibly modified the 3D structure of the immobilised enzyme. In our case, no degradation of immobilised trypsin was found at least up to 32 mL min^{-1} thanks to the 6.2 μm pore size of the monolithic support and the multipoint covalent binding technique. Regarding the depletion of native proteins, as shown in Fig. 2B–D, 90% of the starting α-La remained at DH 4% whereas only 30% β-Lg was residual at all explored flow rates, which confirms the significant preference of immobilised trypsin towards β-Lg over α-La. Furthermore, the ability to deplete native β-Lg A and B as a function of DH was independent of the flow rate, and no significant difference between these two genetic variants was noted.

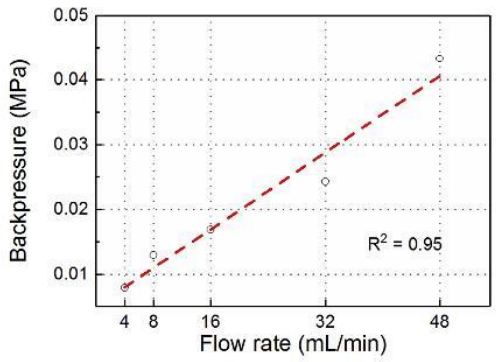

Fig. 1. Initial backpressure of the 8 mL MITR at increasing flow rates.

3.2.2. The effect of hydrolysis pH

It is well-known that enzymes are active only in certain pH ranges and each enzyme has a strongly defined pH optimum where its activity reaches a maximum. In our earlier work (Mao et al., 2017), the enzymatic activity of immobilised trypsin (based on substrate BAEE) increased slightly from pH 7.8 to 9.2. However, as shown in Fig. 3A, no significant difference in the efficiency of hydrolysing WPI was observed, except for that at pH 8.3, where the DH increased faster than the others at the initial stage of hydrolysis. Likewise, Rocha et al. (2011) used the immobilised trypsin on spent grains for whey protein hydrolysis and suggested an optimal pH interval from pH 8 to 9 where the DH profiles were very similar between each other.

Although the highest hydrolysis efficacy was observed at pH 8.3, the depletion of β-Lg exhibited a clear dependence on the pH. Namely, at DH 4%, 68.20 ± 8.44% β-Lg still remained at pH 7.8,

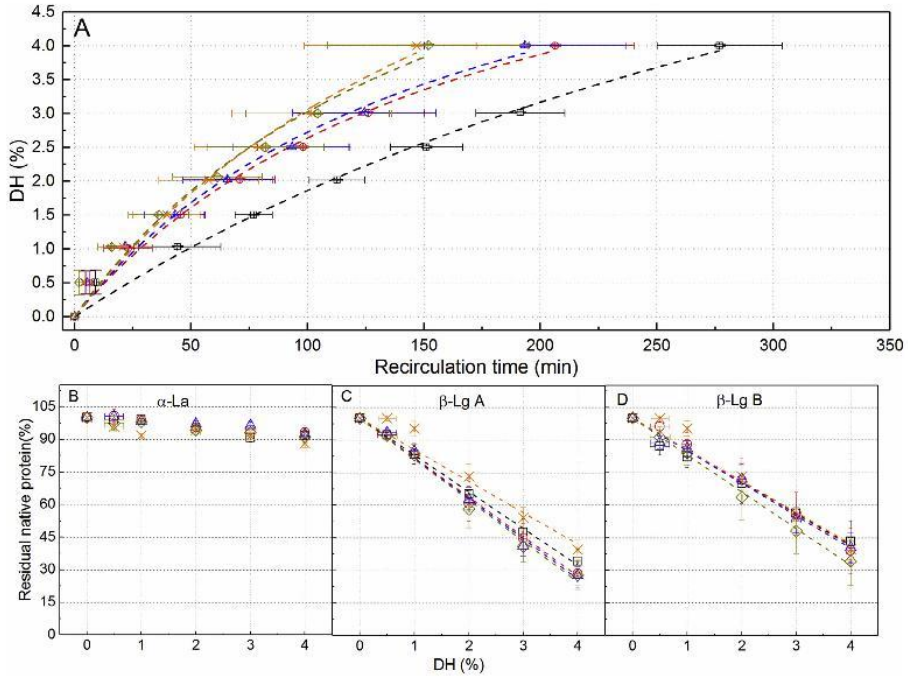

Fig. 2. The hydrolysis of WPI at increasing flow rates 0.8 (□), 4 (○), 8 (△), 16 (×), 32 (◇) mL min^{-1}, respectively. Panel A, increase of DH as a function of time; panels B, C, and D show the residual protein contents of α-La, β-Lg A and β-Lg B, respectively.

whereas only 14.75 ± 10.14% was detectable at pH 9.2. On the contrary, the increase of pH did not lead to a measurable hydrolysis of α-La, since 90% of the starting α-La remained in the final hydrolysates, especially at pH 7.8. The decrease of residual native β-Lg content as a function of DH indicates a preference for the hydrolysis of intact protein molecules versus the intermediate peptides. Hence, the observed results suggested that the formed intermediate peptides were more favoured at pH 7.8 and 8.3 than that at

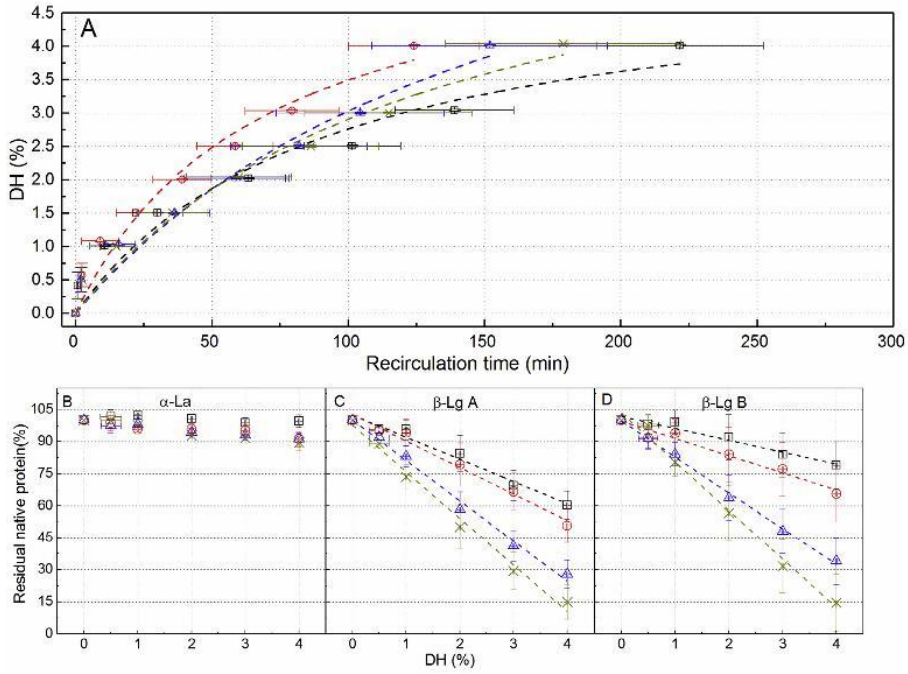

Fig. 3. The hydrolysis of WPI at pH values 7.8 (□), 8.3 (○), 8.7 (△), 9.2 (×). Panel A, increase of DH as a function of time; panels B, C, and D show the residual protein contents of α-La, β-Lg A and β-Lg B, respectively.

higher pH values. In the comparison of β-Lg A and B, the former was more susceptible than the later at lower pH values, while at pH 8.7 and 9.2, the difference in their susceptibility was insignificant.

As discussed in our previous work (Mao et al., 2018), the pH-dependent structural characteristics of β-Lg contributed to its improved tryptic accessibility with increasing pH values. Theoretically, β-Lg B displayed a higher resistance to tryptic digestion (Cheison & Kulozik, 2017), while this resistance seems can be eliminated above pH 8.5. We speculated that the increase of pH up to 8.5 converted both β-Lg A and B into molten globule structures, so that their tertiary structures refold and both become more susceptible to tryptic hydrolysis.

3.2.3. The effect of ionic strength

The effect of ionic strength, i.e., salts, on the hydrolysis is complex. With the addition of salts (typically NaCl) at low concentrations, the surface charges of proteins become shielded. For the substrate, this may result in decreasing electrostatic free energy of the protein molecules and increasing the activity of the solvent, which in turn, leads to improved solubility (Cheison & Kulozik, 2017). Simultaneously, the catalytic activity of immobilised trypsin could be strongly affected due to changes in surface charge since the negatively charged aspartate residue (Asp 189) located in the catalytic pocket of trypsin is responsible for attracting and stabilising positively charged lysine and/or arginine on the substrate (Salis, Bilaničova, Ninham, & Monduzzi, 2007).

As shown in Fig. 4, the decrease of both hydrolysis rate and depletion of native proteins with the presence of 0.25 M NaCl could be due to the increased structural stability of protein molecules at high ionic strength (Yon, 1958). In addition, the strong electrostatic interaction between mobile phase and monolithic surface at 0.25 M NaCl could prevent contact between substrate molecules and the immobilised trypsin to some extent as well (Luey, McGuire, & Sproull, 1991). Albeit the efficiency at 0.1 M NaCl was slightly higher than those at 0 or 0.05 M NaCl, the depletion of β-Lg was much slower, even close to that at 0.25 M NaCl (67.56 ± 6.03% and 72.74 ± 5.42% native β-Lg remained at DH 4% with presence of 0.1 and 0.25 M NaCl, respectively). Speculatively, the addition of NaCl (≤0.1 M) negatively affected the depletion of intact β-Lg while it promoted the hydrolysis of the formed intermediate peptides. This can be illustrated by the fact that the ionic strength has different effects on the hydrolysis of polypeptides that do not have defined secondary or tertiary structures. Actually, in the work of Fukuda and Kundugi (1989), the increase of ionic strength (0–0.9 M NaCl) also resulted in an increased rate of hydrolysis of synthetic peptide substrates by thermolysin.

In addition, the depletion of α-La was, again, insignificant, irrespective of the ionic strength. Based on the above findings, α-La was almost insusceptible to the immobilised trypsin under all explored conditions. To further confirm this speculation, the hydrolysis of 80 mL 20 mg mL^{-1} WPI solution (pH 8.7 without NaCl) was extended. As shown in Fig. 5, no more β-Lg was detectable at DH 8% while approximately 85% of the native α-La could still be found in the hydrolysates. Another experiment with pure α-La was conducted, and no significant decrease of protein content was detected after 3 h recirculation through the MITR (data not shown).

3.3. Kinetic analysis of depleting β-Lg in the MITR

To estimate the potential influence introduced by the existence of other whey proteins, mainly α-La, pure β-Lg was used as the substrate as well to explore the kinetic analysis.

Michaelis and Menten (1913) developed the classical model describing kinetic properties of most enzymes. According to this model, the maximal reaction velocity V_{max} (= K_{cat} × [E]; K_{cat} turnover number) and Michaelis–Menten constant (K_m) are typically used to characterise the kinetic properties of an enzyme.

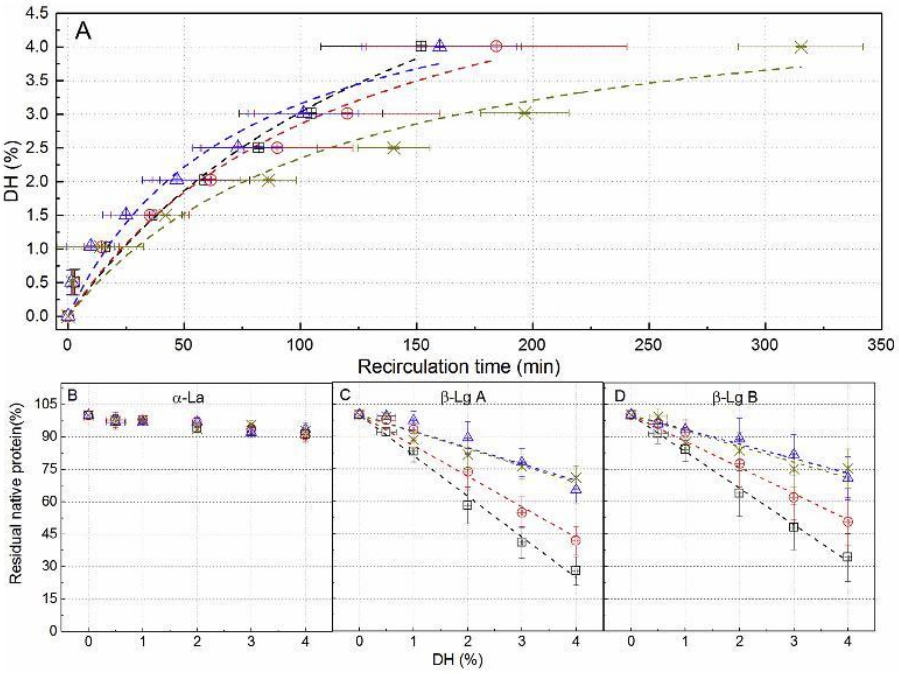

Fig. 4. The hydrolysis of WPI with NaCl concentrations at 0 (□), 0.05 (○), 0.1 (△), 0.2 (×) M. Panels A, increase of DH as a function of time; panels B, C, and D show the residual protein contents of α-La, β-Lg A and β-Lg B, respectively.

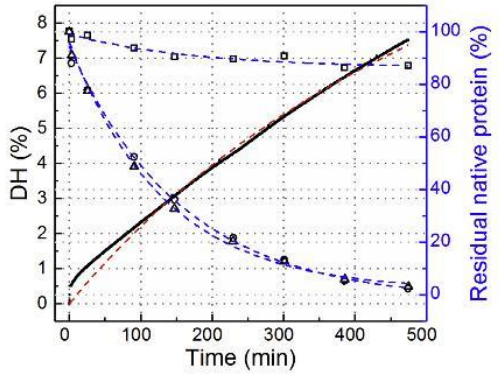

Fig. 5. Hydrolysis of WPI solution. The evolution of DH and the amounts of residual native α-La (□), β-Lg A (△), and β-Lg B (◯) were described.

In this study, the apparent kinetic parameters, K_M and V_{max}, were estimated based on the overall amount of immobilised trypsin in the MITR. Although the initial reaction velocity theoretically was evaluated based on the hydrolysed peptide bonds, in this study, it was obtained by measuring the depleting rate of β-Lg, which was able to be precisely determined by the HPLC method, see Eq. (4). It was practically difficult to measure the exact hydrolysed peptide bonds (h) in the initial stage of hydrolysis. In our experiments, the consumed volume of NaOH for the calculation of h (irrespective which concentration was used) increased suddenly to a certain value once the recirculation started. This practical problem led to the lack of initial evolution of DH. As the depleting rate of β-Lg was used as the index, single flow-through approach is practically easier and more precisely controlled, comparing with the recirculation approach. Furthermore, hydrolysis at single flow-through approach maximally prevented from the potential inhibition of products. Thus, the kinetic analysis was explored at increasing flow rates (0.8–48 mL min^{-1}) by applying the single flow-through approach.

As discussed in section 3.2.1, the increase of flow rate was followed by the growth of hydrolysis efficiency. As shown in Fig. 6A, the efficacy of depleting β-Lg was improved with increasing flow rates (0.8–48 mL min^{-1}) at each concentration when pure β-Lg was used, corresponding to a clear flow rate dependent V_{max}. However, the depletion efficiency decreased unexpectedly at 48 mL min^{-1} when WPI at a high concentration was applied, leading to a sharp decrease of V_{max} there (Fig. 6B; Table 2). Because of this extraordinary phenomenon, the Michaelis–Menten model could not be used to fit the data obtained during the hydrolysis of WPI at 48 mL min^{-1} ($R^2 = 0.41$). In the range of 0.8–32 mL min^{-1}, the initial depleting rate of β-Lg at recirculation approach was calculated from Eq. (3) and compared with the predicted values from the obtained model at single flow-through approach. As illustrated in Fig. 7, the predicted values were higher at all flow rates, but both showed the same trend. However, caution should be paid regarding the prediction on the hydrolysis efficiency of proteins. Proteins, in contrast to model substrates like BAEE, tend to adsorb on surfaces. Therefore, the properties of an enzyme reactor tend to change over time from cycle to cycle, and prediction is, therefore, difficult.

Regarding K_m, no significant flow rate dependence was found. Specifically, the lowest K_m for β-Lg hydrolysis was noted at 4 mL min^{-1}. The same was noted for the hydrolysis of WPI. Comparing the obtained V_{max} values between the hydrolysis of β-Lg and WPI, a three-fold decrease in V_{max} was noted for WPI at all explored flow rates. It is speculated that, although α-La is resistant to the hydrolysis by the immobilised trypsin, its existence acts as a competitor with β-Lg for the active site of trypsin, and this competition can be enhanced by increasing the flow rate or the α-La amount to some extent.

3.4. Operational stability of the MITR

Due to the diffusion-limiting step in conventional particle-based immobilised enzyme reactors, these reactors are commonly operated at low flow rates. For instance, in a corn-cob power based packed-bed immobilised trypsin reactor, the flow rate was only 10.1 mL h^{-1} due to the high backpressure, and a hydraulic retention time of 78 h was required (Bassan et al., 2016). However, the initial backpressure of the developed MITR in this work was only 0.045 MPa at 48 mL min^{-1}, offering the possibility of operating this reactor at an industrial scale.

After over 30 cycles of intensive operation, the initial hydrolysis velocity only decreased 12.1% compared with that of the first run (both hydrolysis experiments were conducted at the exactly same conditions), as illustrated in Fig. 8A. However, the permeability decreased 70% after 30 cycles, which was probably due to

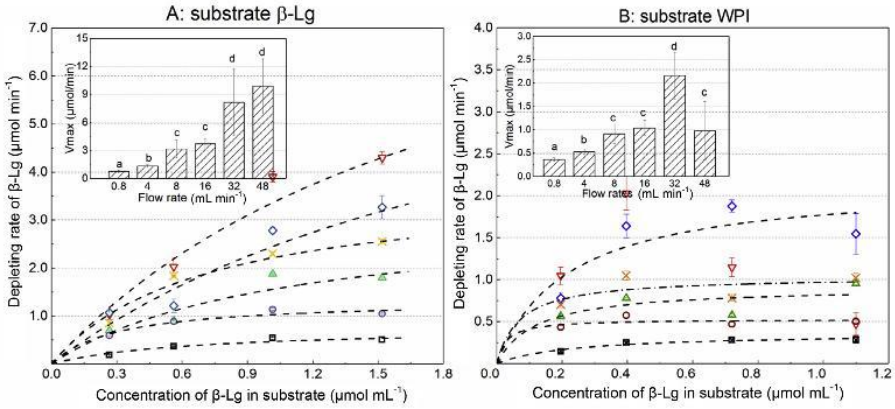

Fig. 6. The depleting rates of β-Lg by the MITR at increasing flow rates 0.8 (□), 4 (◯), 8 (△), 16 (×), 32 (◇), and 48 (▽) mL min^{-1} are displayed in panel A for pure substrate β-Lg and in panel B for substrate WPI, respectively. Inset: V_{max} values depending on flow rates are plotted in a bar graph. The R^2 and K_m are given in Table 2.

Table 2
Kinetic parameters for depleting rates of β-Lg by the MITR with pure β-Lg and with WPI at increasing flow rates.[a]

Parameter	Flow rate (mL min^{-1})					
	0.8	4	8	16	32	48
β-Lg						
R^2	0.97	0.98	0.95	0.98	0.97	0.98
K_m (μmol mL^{-1})	0.64 ± 0.29	0.30 ± 0.1	1.04 ± 0.63	0.69 ± 0.23	2.38 ± 1.58	1.97 ± 0.94
WPI						
R^2	0.98	0.95	0.87	0.92	0.90	0.41
K_m (μmol mL^{-1})	0.23 ± 0.08	0.03 ± 0.04	0.12 ± 0.13	0.07 ± 0.08	0.22 ± 0.17	/

[a] Refer to Fig. 6 for full data set.

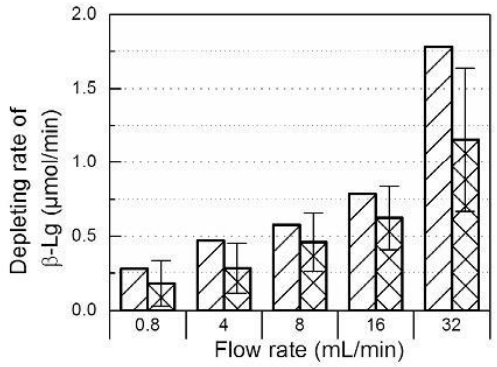

Fig. 7. The comparison of predicted depleting rates of β-Lg at single flow-through approach (left) and the experimental values at recirculation approach (right).

an accumulation of particles on the surface of monolith. This problem was also observed in our previous work (Mao et al., 2017), where the permeability decreased significantly while enzymatic activity still remained at similar levels. Speculatively, due to the 6 μm pore size, the accumulated particles did not block the pores. Rather, we believe they attached to bare monolith surfaces so that trypsin contact with substrate molecules was not inhibited. It is worth nothing that the backpressure of the MITR-8 mL was still below 0.15 MPa at 48 mL min^{-1} (6 CVs min^{-1}) even when the permeability declined 70%, and its operational limit was up to 2 MPa.

The upscaled MITR showed excellent reusability for WPI hydrolysates production compared with the previously reported reactors. For example, Rocha et al. (2011) prepared immobilised trypsin on spent grains for whey protein hydrolysis in a 50 mL batch reactor with 5 cycles of guaranteed reuse (each cycle 30 min). In the work of Pessato et al. (2016), alcalase enzyme was immobilised on glyoxyl-agarose beads and used to hydrolyse whey protein

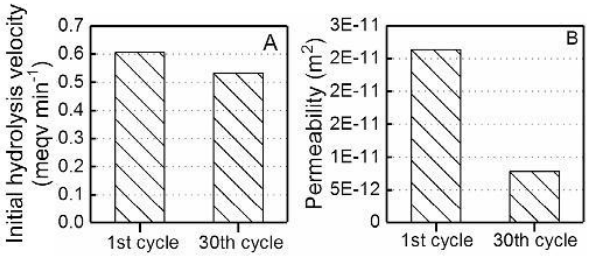

Fig. 8. The comparison of initial hydrolysis velocity (A) and permeability (B) at the 1st and 30th cycles, respectively.

in a batch process. However, it lost 15% activity already after the third hydrolysis cycle.

4. Conclusions

β-Lg was selectively hydrolysed by the immobilised trypsin in the 8 mL CIM-MITR at ambient temperature. The result was that above 85% α-La remained native in the final hydrolysates, while no native β-Lg was detectable. Despite the inaccessibility of the immobilised trypsin to α-La at all explored conditions, its accessibility towards β-Lg was pH and ionic strength dependent. Namely, higher pH (15% residual at pH 9.2 versus 60% at pH 7.8) and lower ionic strength (30% residual at 0 M NaCl versus 70% at 0.1 and 0.25 M NaCl) was preferential. In addition, the increase of flow rate (up to 32 mL min^{-1}) contributed to the hydrolysis efficiency of immobilised trypsin, but did not affect its ability to deplete β-Lg.

The Michaelis–Menten kinetics of the 8 mL CIM-MITR were explored using a single flow-through approach. The influences of flow rate and substrate composition were evaluated. Although higher flow rates contributed to the improved efficacy, beyond a certain range it might cause an unexpected decline in efficiency, especially for the complex substrate mixtures.

The 8 mL CIM-MITR developed in this study was able to be operated at high flow rates while maintaining low backpressure, which significantly improved the productivity of this reactor. The 11 mg trypsin immobilised on the CIM monolithic column through a multipoint covalent binding technique remained stable over 30 cycles of intensive uses, thus demonstrating the CIM-MITR to be cost effective, time efficient, and reusable. These above advantages render the CIM-MITR suitable for large-scale operations.

Acknowledgements

The first author thanks China Scholarship Council (China) for the support of her personal cost. The authors would like to thank Urh Černigoj from BIA Separations (Ajdovščina, Slovenia) for his technical help in developing the CIM-MITR, as well as for his revision work. This research did not receive any specific grant from funding agencies in the public, commercial, or not-for-profit sectors.

References

Adler-Nissen, J. (1986). *Enzymatic hydrolysis of food proteins*. Oxford, UK: Elsevier Applied Science Publishers.

Atacan, K., Cakiroglu, B., & Ozacar, M. (2016). Improvement of the stability and activity of immobilized trypsin on modified Fe_3O_4 magnetic nanoparticles for hydrolysis of bovine serum albumin and its application in the bovine milk. *Food Chemistry, 212*, 460–468.

Bartolini, M., Greig, N. H., Yu, Q. S., & Andrisano, V. (2009). Immobilized butyrylcholinesterase in the characterization of new inhibitors that could ease Alzheimer's disease. *Journal of Chromatography A, 1216*, 2730–2738.

Bassan, J. C., de Souza Bezerra, T. M., Peixoto, G., da Cruz, C. Z. P., Galán, J. P. M., Vaz, A. B. d. S., et al. (2016). Immobilization of trypsin in lignocellulosic waste

material to produce peptides with bioactive potential from whey protein. *Materials, 9*, 357.
Bencina, K., Bencina, M., Podgornik, A., & Strancar, A. (2007). Influence of the methacrylate monolith structure on genomic DNA mechanical degradation, enzymes activity and clogging. *Journal of Chromatography A, 1160*, 176–183.
Cheison, S. C., & Kulozik, U. (2017). Impact of the environmental conditions and substrate pre-treatment on whey protein hydrolysis: A review. *Critical Reviews in Food Science and Nutrition, 57*, 418–453.
Cheison, S. C., Leeb, E., Toro-Sierra, J., & Kulozik, U. (2011). Influence of hydrolysis temperature and pH on the selective hydrolysis of whey proteins by trypsin and potential recovery of native alpha-lactalbumin. *International Dairy Journal, 21*, 166–171.
Dannenberg, F., & Kessler, H. G. (1988). Reaction kinetics of the denaturation of whey proteins in milk. *Journal of Food Science, 53*, 258–263.
Edwards, P. J., & Jameson, G. B. (2014). Structure and stability of whey proteins. In *Milk proteins* (2nd ed., pp. 201–242). Oxford, UK: Elsevier.
Fukuda, M., & Kundugi, S. (1989). The mechanism of salt activation of thermolysin: Relation with pressure activation and implications of hydration change coupled with rate process. *Biocatalysis, 2*, 225–233.
Hernandez-Ledesma, B., Recio, I., & Amigo, L. (2008). Beta-lactoglobulin as source of bioactive peptides. *Amino Acids, 35*, 257–265.
Konrad, G., & Kleinschmidt, T. (2008). A new method for isolation of native α-lactalbumin from sweet whey. *International Dairy Journal, 18*, 47–54.
Leeb, E., Gotz, A., Letzel, T., Cheison, S. C., & Kulozik, U. (2015). Influence of denaturation and aggregation of beta-lactoglobulin on its tryptic hydrolysis and the release of functional peptides. *Food Chemistry, 187*, 545–554.
Lisak, K., Toro-Sierra, J., Kulozik, U., Bozanic, R., & Cheison, S. C. (2013). Chymotrypsin selectively digests beta-lactoglobulin in whey protein isolate away from enzyme optimal conditions: Potential for native alpha-lactalbumin purification. *Journal of Dairy Research, 80*, 14–20.
Lowe, A. J., Dharmage, S. C., Allen, K. J., Tang, M. L., & Hill, D. J. (2013). The role of partially hydrolyzed whey formula for the prevention of allergic disease: Evidence and gaps. *Expert Review of Clinical Immunology, 9*, 31–41.
Luey, J.-K., McGuire, J., & Sproull, R. D. (1991). The effect of pH and NaCl concentration on adsorption of β-lactoglobulin at hydrophilic and hydrophobic silicon surfaces. *Journal of Colloid and Interface Science, 143*, 489–500.
Mao, Y., Cernigoj, U., Zalokar, V., Strancar, A., & Kulozik, U. (2017). Production of beta-Lactoglobulin hydrolysates by monolith based immobilized trypsin reactors. *Electrophoresis, 38*, 2947–2956.
Mao, Y., Krischke, M., Hengst, C., & Kulozik, U. (2018). Comparison of the influence of pH on the selectivity of free and immobilized trypsin for β-lactoglobulin hydrolysis. *Food Chemistry, 253*, 194–202.
Michaelis, L., & Menten, M. (1913). Die kinetik der inwertin wirkung. *Biochemistry, 49*, 333–369.
Naldi, M., Černigoj, U., Štrancar, A., & Bartolini, M. (2017). Towards automation in protein digestion: Development of a monolithic trypsin immobilized reactor for highly efficient on-line digestion and analysis. *Talanta, 167*, 143–157.
Pessato, T. B., de Carvalho, N. C., Tavano, O. L., Fernandes, L. G. R., Zollner, R. d. L., & Netto, F. M. (2016). Whey protein isolate hydrolysates obtained with free and immobilized Alcalase: Characterization and detection of residual allergens. *Food Research International, 83*, 112–120.
Podgornik, A., Savnik, A., Jancar, J., & Krajnc, N. L. (2014). Design of monoliths through their mechanical properties. *Journal of Chromatography A, 1333*, 9–17.
Ponomareva, E. A., Kartuzova, V. E., Vlakh, E. G., & Tennikova, T. B. (2010). Monolithic bioreactors: Effect of chymotrypsin immobilization on its biocatalytic properties. *Journal of Chromatography B: Analytical Technologies in the Biomedical and Life Sciences, 878*, 567–574.
Rocha, C., Gonçalves, M. P., & Teixeira, J. A. (2011). Immobilization of trypsin on spent grains for whey protein hydrolysis. *Process Biochemistry, 46*, 505–511.
Salis, A., Bilaničova, D., Ninham, B. W., & Monduzzi, M. (2007). Hofmeister effects in enzymatic activity: Weak and strong electrolyte influences on the activity of Candida rugosa lipase. *Journal of Physical Chemistry B, 111*, 1149–1156.
Schmidt, D., & Poll, J. (1991). Enzymatic hydrolysis of whey proteins. Hydrolysis of α-lactalbumin and β-lactoglobulin in buffer solutions by proteolytic enzymes. *Nederlands Melk- en Zuiveltijdschrift, 45*, 225–240.
Vodopivec, M., Podgornik, A., Berovič, M., & Štrancar, A. (2003). Characterization of CIM monoliths as enzyme reactors. *Journal of Chromatography B, 795*, 105–113.
Yon, J. (1958). Influence des chlorures alcalins sur l'hydrolyse trypsique de la lactoglobuline native et dénaturée par la chaleur. *Biochimica et Biophysica Acta, 27*, 111–121.

International Dairy Journal 93 (2019) 106–115

Contents lists available at ScienceDirect

International Dairy Journal

journal homepage: www.elsevier.com/locate/idairyj

Influence of salts on hydrolysis of β-lactoglobulin by free and immobilised trypsin

Yuhong Mao [a, *], Maria Krischke [a], Claudia Hengst [a], Ulrich Kulozik [a, b]

[a] Chair of Food and Bioprocess Engineering Technical University of Munich, Weihenstephaner Berg 1, D-85354, Freising-Weihenstephan, Germany
[b] Institute of Food and Health (ZIEL)–Technology Unit, Technical University of Munich, Weihenstephaner Berg 1, D-85354, Freising-Weihenstephan, Germany

ARTICLE INFO

Article history:
Received 6 November 2018
Received in revised form
11 February 2019
Accepted 12 February 2019
Available online 1 March 2019

ABSTRACT

Immobilised trypsin is an alternative to free trypsin for producing protein hydrolysates with increased functionalities. However, the influence of hydrolytic conditions on this process remains unclear. The influence of salts on β-lactoglobulin (β-Lg) hydrolysis by free and immobilised trypsin was compared. For both forms of trypsin, 0.1 M Tris accelerated the release of most final peptides except f (71–75), and had no significant effects on the hydrolysis of intact β-Lg. Increasing NaCl concentrations from 0 to 0.02 M increased the degree of hydrolysis (DH) by 22.4% for free trypsin versus 62.1% for immobilised trypsin. The presence of 0.1 or 0.5 M NaCl hindered the release of peptides associated with the breakdown of intact protein. This led to 2–4 fold decreases in depleting intact β-Lg and DH, except immobilised trypsin at 0.1 M NaCl (DH increased by 44.3% versus without NaCl). Potential mechanisms underlying the effects of salts are discussed.

1. Introduction

In the past several decades, bovine β-lactoglobulin (β-Lg), a major allergen absent from human milk, has been subject to extensive investigations regarding enzymatic processing via various enzymes (Hernández-Ledesma, Recio, & Amigo, 2008). Trypsin (EC 3.4.21.4), a serine protease, is found in the digestive system of humans and many other vertebrates. Tryptic hydrolysis of β-Lg results in reduced allergenicity (Selo et al., 1999) and enhanced nutritional values (Hernández-Ledesma et al., 2008; Leeb, Gotz, Letzel, Cheison, & Kulozik, 2015). However, the costly production and purification of trypsin seriously limits its implementation in the food industry (Yu & Ahmedna, 2012). As an alternative approach, immobilisation of trypsin has attracted more and more attention due to the possibility of reusing the enzyme and producing enzyme-free hydrolysates.

In our previous work (Mao, Černigoj, Zalokar, Štrancar, & Kulozik, 2017), a monolithic column-based immobilised trypsin reactor (MITR) showed significant activity toward β-Lg. The immobilisation of an enzyme can alter its intrinsic properties (V_{max}, k_{cat} or K_m) (Duggal & Bucholz, 1982), leading to changes in enzyme selectivity, i.e., the rate at which individual cleavage sites in a protein substrate are hydrolysed relative to other cleavage sites (Butré, Sforza, Gruppen, & Wierenga, 2014). Consistent with these observations, we compared the selectivity of free and immobilised trypsin for β-Lg hydrolysis focusing on the impact of hydrolytic pH, and found that pH had a greater effect on the selectivity of free trypsin compared with immobilised trypsin (Mao, Krischke, Hengst, & Kulozik, 2018). Except for pH, the influence of salts on hydrolysis process is also important, because the production of food protein hydrolysates is never conducted in a pure aqueous media, but rather in a complex system with various ions.

Salt-effect studies have proven useful for determining the intrinsic properties of enzymes (Endo, Kurinomaru, & Shiraki, 2016, 2018; Garajova et al., 2017; Quan et al., 2008; Salis, Bilanicova, Ninham, & Monduzzi, 2007). Most of these studies interpret the salt-effect data based on ionic properties and ion specificity. Ionic properties refer to the effects of any salt ion, including charge shielding/electrical double layer effects and stoichiometric ion binding to a charged protein (Tsumoto, Ejima, Senczuk, Kita, & Arakawa, 2007). These effects are always independent on the salt type, but dependent on the salt concentration (ionic strength). Ionic properties are important in regulating enzyme–substrate interactions, thereby affecting enzyme activity and selectivity. This factor is particularly important in hydrolysis reactions that depend

* Corresponding author. Tel.: +49 8161 713855.
E-mail address: yuhong.mao@tum.de (Y. Mao).

https://doi.org/10.1016/j.idairyj.2019.02.006
0958-6946/

on the movement of charged molecules relative to each other. In tryptic hydrolysis. Asp_{189}, located in the catalytic pocket of trypsin, attracts and stabilises positively charged Lys and Arg residues on substrates (Evnin, Vásquez, & Craik, 1990). Thus, both the binding of charged substrates to the enzyme and then the movement of charged groups within the catalytic active site will be influenced by the ionic composition of medium (Chaplin & Bucke, 1990).

The ion-specific effect of medium on proteins was first reported in a systematic way by Franz Hofmeister (Hofmeister, 1888), who ranked the ability of ions at a fixed ionic strength to affect the properties of proteins in aqueous solutions. Hofmeister differentiated between chaotropes and kosmotropes, salts that induced either disorder or more order, respectively, in protein conformation. Hofmeister ions are reported to influence the properties of numerous enzymes (Endo et al., 2016; Garajova et al., 2017; Tougu et al., 1994). Mostly, the ion-specific influence on enzyme activity follows the Hofmeister series, with kosmotropes activating enzymes and chaotropes inhibiting enzyme activity (Garajova et al., 2017). Enzyme activation by kosmotropes occurs because these salts increase both the structural stability of the enzyme and the hydrophobic interactions between the enzyme and its substrate (Endo et al., 2016). A bell-shaped dependence of enzyme activity on ions in the Hofmeister series has been observed, indicating that both chaotropic and kosmotropic ions can inactivate enzymes (Žoldák, Sprinzl, & Sedlák, 2004).

Chymotrypsin exhibits increased activity with the addition of 3 M NaCl, but no significant increase in the presence of 3 M LiCl or KCl (Wesolowska, Krokoszynska, Krowarsch, & Otlewski, 2001). Another study observed that with the addition of 0.5 M NaCl, the K_m of chymotrypsin decreased and its K_{cat} increased, while trypsin showed the opposite results (Endo, Kurinomaru, & Shiraki, 2018). In addition, weak electrolytes are widely applied as buffers in enzyme technology. Tris (hydroxymethyl) aminomethane (Tris) solution is one such buffer, which is reported to stabilise BSA molecules (Taha & Lee, 2010) and interact with lysozyme molecules through hydrogen-bonding (Quan et al., 2008).

Previous studies regarding salt effects on enzymes have used primarily low−molecular-mass substrates (Endo et al., 2018, 2016; Tougu et al., 1994). These results may not apply to enzymatic reactions involving proteins as substrates, e.g., β-Lg in this study, as salts may influence β-Lg structure, thus affecting the enzymatic process. For instance, Renard, Lefebvre, Griffin, and Griffin (1998) found that β-Lg favoured dimerisation in the presence of NaCl. Furthermore, ions also affect the tertiary structure of β-Lg, e.g., Trp exposure increases in the presence of NaCl (>0.1 M), indicating that more hydrophobic groups are exposed (Zhao, Li, & Li, 2017). Therefore, the influence of salts on the enzymatic hydrolysis of a specific substrate should be investigated systematically on a case-by-case basis.

There appear to be no studies dealing with the influence of salts on the protein hydrolysis in a flow-through reactor using immobilised trypsin. In the present study, trypsin was covalently immobilised on an aldehyde-activated monolith through multiple attachment points. This covalent immobilisation is the most common approach to stabilise the enzyme against different denaturing conditions (Mozhaev, Melik-nubarov, Sergeeva, Šikšnis, & Martinek, 1990). Hence, compared with free trypsin, the ion-induced conformational effects on immobilised trypsin, in theory, should be significantly reduced. Additionally, substrates are convectively transported to immobilised trypsin in a flow-through MITR. This critical step is largely decided by the mass transfer properties in MITR. It is reasonable to assume that the mass transfer properties in MITR might change with the addition of salts, due to their effects at least on charge-based attraction or repulsion between substrate molecules and the monolith surface.

Therefore, the aim of this study was to determine the influence of salts on immobilised trypsin for β-Lg hydrolysis, and simultaneously to compare with free trypsin. Specifically, the following parameters were investigated: (i) ion-specific effects, i.e., buffer salt (weak organic electrolyte, Tris) versus neutral salt (strong inorganic electrolyte, NaCl); and (ii) ionic strength effects (ionic properties) using different salt concentrations. The influence of these factors was evaluated by measuring the hydrolysis efficiency and analysing the hydrolysates profiles.

2. Materials and methods

2.1. Materials

Bovine β-Lg was fractionated from whey protein isolate (WPI), a product developed by Fonterra Co-operative Group Ltd (Auckland, New Zealand), as described by Toro-Sierra, Tolkach, and Kulozik (2011). The β-Lg powder obtained had a protein content of 98.6% relative to the dry matter. β-Lg powder was dissolved in deionised water at 4 °C overnight. After the removal of denatured β-Lg by adjusting the pH to 4.6 and centrifugation (6000 ×*g* for 10 min), the supernatant was filtered through a cellulose membrane with a cut-off of 0.45 μm (Macherey−Nagel, Düren, Germany). After the pH adjustment to 8.7, β-Lg solution was mixed with pre-dissolved NaCl or Tris buffer solution to reach a final concentration of 10 mg mL^{-1} native protein, and the final pH of the mixed solutions was adjusted to 8.7.

Trypsin from bovine pancreas (Type I, approximately 10,000 Nα-benzoyl-L-arginine ethyl ester [BAEE] units mg^{-1} protein), BAEE (B4500), Tris (hydroxymethyl)-aminomethane (Tris), NaCl, and NaOH were purchased from Sigma Aldrich (St Louis, MO, USA). Deionised water was acquired using the Milli-Q System (Millipore Corporation, Bedford, MA, USA).

An aldehyde (ALD) activated CIMmultus™ column (1 mL-bed volume, BIA Separations, Ajdovščina, Slovenia)-based MITR with 2.15 ± 0.1 μm pore size was developed in our earlier work (Mao et al., 2017). The amount of immobilised trypsin was 5.0 ± 0.2 mg per MITR, and the MITR permeability was approximately 2.45×10^{-12} m^2 using deionised water.

2.2. Trypsin activity toward BAEE substrate

The enzymatic activity of trypsin was measured at pH 8.7 using the model substrate BAEE in three buffers, 0.1 M Tris buffer, 0.1 M Tris + 0.1 M NaCl, 0.5 M Tris buffer. The measurement was a spectrophotometric determination as described previously (Mao et al., 2017). The activity of free trypsin is expressed as BAEE units mg^{-1}. One BAEE unit produces a ΔA_{253} of 0.001 per min in a reaction volume of 3.20 mL. The activity of MITR was calculated as the unit U* (μmol min^{-1}), which is the amount of BAEE converted to BA by the MITR in 1 min. U* can be easily converted to BAEE units, using the conversion factor 270, as determined by Bergmeyer (1974).

2.3. Hydrolysis of β-Lg

A previous study (Cheison, Leeb, Toro-Sierra, & Kulozik, 2011b) indicated that at the optimal temperature of free trypsin, i.e., 37 °C, the enzyme selectivity was little controlled by other environmental conditions, as temperature was the dominating influence. It is expected to regulate the trypsin selectivity with the addition of salts. On the other hand, both free trypsin and MITR already showed significant activity toward β-Lg at ambient temperature (Mao et al., 2017). Hence, all hydrolysis experiments were conducted at 25 ± 1 °C.

To assess the effects of salts, 25 mL β-Lg solution (native protein, 10 mg mL^{-1}) in Tris buffer (0.1 or 0.5 M) or Tris-NaCl buffer (0.1 M Tris + 0.1 M NaCl) was hydrolysed by free trypsin or immobilised trypsin for 1 h. The hydrolysis of β-Lg by free trypsin was conducted at an enzyme/substrate ratio of 0.1% (w/w). Thus, the hydrolysis reaction was ensured to be performed at similar ratios of activity units (BAEE units) to per gram β-Lg for both free trypsin and MITR.

To further explore the effects of salts, 100-mL β-Lg solution (10 mg mL^{-1}) in 0.1 M Tris, or in 0, 0.02, 0.1, or 0.5 M NaCl was hydrolysed by free trypsin or immobilised trypsin for 3 h. During hydrolysis, 1-mL samples were taken out at intervals (0, 5, 10, 20, 30, 45, 60, 90, 120, and 180 min). A TitroLine alpha plus auto-titrator (Schott AG, Mainz, Germany) was used to maintain a constant pH of 8.7 throughout the course of the reaction. The degree of hydrolysis (DH) was calculated according the amount of NaOH consumed, as described previously (Mao et al., 2017). In addition, because 18 of the 161 peptide bonds of β-Lg are potential cleavage sites for trypsin, a theoretical DH_{max} of 11.18% can be achieved during trypsinolysis. The practical DH_{max} values were reached and discussed in our previous work (Mao et al., 2017). In this study, all hydrolysis processes were stopped at intermediate stages to save time. Also, it makes more sense to focus on the release of peptides at the early stage of hydrolysis to explore the enzymatic selectivity.

For the hydrolysis by free trypsin, a constant enzyme–substrate (E/S) ratio of 0.1% (w/w) was applied, and the hydrolysis of 1-mL aliquots was stopped by the addition of 0.5 mL trypsin inhibitor solution (10 mg mL^{-1}, from chicken egg white, Sigma Aldrich). Hydrolysis by MITR was realised in a flow-through system (Äkta explorer, GE Healthcare Europe GmbH, Freiburg, Germany) controlled by Unicorn Software 5.31.

2.4. Analysis of hydrolysates

Hydrolysates profiles were quantitatively analysed for residual native protein content and peptide composition.

2.4.1. Quantification of residual native β-Lg

The native β-Lg content of samples was determined via reversed-phase high-performance liquid chromatography (RP-HPLC) using an Agilent 1100 series HPLC system (Agilent Technologies, CA, USA) and a PLRP-S-300 Å-8 μm column (150 × 4.6 mm, Latek, Eppelheim, Germany). Each sample was diluted with deionised water to ≈4 mg mL^{-1}. After adjusting the pH to 4.6, the sample was filtered through a cellulose membrane with a cut-off of 0.45 μm and 20 μL was injected. Detailed gradient information was previously described by Leeb et al. (2015). The protein concentration was calculated from the detected peak area and a calibration curve using standards β-Lg A (99% purity, Sigma Aldrich) and β-Lg B (99% purity, Sigma Aldrich).

2.4.2. Chromatographic separation and quantification of peptides

All samples were diluted to approximately 4 mg mL^{-1}, and 1-mL aliquots of the diluted solution were firstly incubated with 150 μL 80 mM dithiothreitol (DTT) at pH 8 and 37 °C for 45 min, and then mixed with 200 μL 400 mM chloroacetamide (CAA) and stored in the dark for 30 min. The pre-treated samples were analysed on the Agilent 1100 series HPLC system coupled with a Kinetex_XB-C18-100 Å column (100 × 4.6 mm, Phenomenex, Torrence, CA, USA). The mobile phase of solvent A containing 0.1% (v/v) trifluoroacetic acid (TFA) dissolved in Milli-Q water and solvent B consisting of 0.0555% (v/v) TFA dissolved in 80% (v/v) acetonitrile (diluted in Milli-Q water) was applied. The entire analysis was conducted at 60 °C and 1.5 mL min^{-1}. The gradient was increased multi-linearly from 1 to 45% of solvent B in 60 min. The sample injection volume was 60 μL, and the elution was monitored at 214 nm. The samples with the highest DH at each condition were further fractionated. Peaks eluted before 45 min were automatically collected separately based on the slope, and peaks after 45 min were collected based on time with a unit of 1 min. The collected fractions were analysed by matrix-assisted laser desorption/ionisation time-of-flight mass spectrometry (MALDI-TOF-MS) to determine the peptide composition.

The molar concentration of each specific peptide was calculated from the peak area according to Eq. (1) (Fernández & Riera, 2013) as follows:

$$X_i = 1 \times 10^6 \left(\frac{A_i}{\varepsilon_i \times l \times v} \right) \times f \times D \quad (1)$$

where x_i (μM) is the concentration of peptide i, Ai (AU min) is the peak area, l (0.6 cm) is the path length of the UV cell, v is the injection volume (60 μL), f is the flow rate (1.5 mL min^{-1}), D is the dilution factor of the sample before injection, and ε_i (AU M^{-1} cm^{-1}) is the molar extinction coefficient of peptide i at 214 nm, as calculated according to Kuipers and Gruppen (2007). To quantitatively compare the released peptides, the following indexes were calculated:

$$R_1(\%) = \frac{The\ amount\ of\ released\ peptide(\mu m)}{The\ amount\ of\ hydrolyzed\ protein(\mu m)} \quad (2)$$

$$R_2(\%) = \frac{The\ relative\ amount\ of\ released\ peptide\ (\%)}{The\ relative\ DH(\%)} = \frac{\frac{The\ amount\ of\ the\ released\ peptide(\mu m)}{The\ theoretical\ maximun\ amount\ of\ each\ peptide(\mu m)}}{\frac{The\ reached\ DH\ \ Value(\%)}{The\ theoretical\ maximum\ DH\ value(\%)}} \quad (3)$$

2.4.3. MALDI-TOF-MS

The fractions obtained were analysed for mass composition using a MALDI-TOF-MS system (ultrafleXtreme MALDI-TOF-TOF, Bruker Daltonics GmbH, Bremen, Germany). Matrix α-cyano-4-hydroxycinnamic acid (HCCA) and 2,5-dihydroxyacetophenone (DHAP) were used separately. HCCA is sufficient to measure peptides and proteins in the low mass range from 500 to 4000 Da, and DHAP is commonly used for the high mass range up to 20,000 Da. One microlitre samples (including blank sample) or standards (PAS with HCCA and Protein Calibration Standard I with DHAP, Bruker Daltonics GmbH) were mixed with 1-μL matrices directly on the anchor target (stainless steel MTP 384, Bruker Daltonics GmbH). Each sample was spotted at least three times. The MALDI-TOF-MS was run in a positive reflection mode for mass ranges of 400–4000 Da (sample with HCCA) and 3000–10,000 Da (sample with DHAP), or in a positive linear model for the mass range of 4000–20,000 Da (sample with DHAP). The process was managed using flexControl™ 3.0 Software (Bruker Daltonics GmbH). Peptides were identified by comparing the detected mass/charge (m/z) with the theoretical m/z as described previously (Mao et al., 2017).

2.5. Statistical analysis

All experiments were performed in triplicate and in a staggered manner (for MITR) to reduce bias. Mean values ± standard deviation are reported. Analysis of variance was performed to estimate differences between mean values where the significance level was established as $P < 0.05$. The Tukey-test was used to evaluate the significance of differences. Data were plotted using Origin Pro 9.0 or R 3.3.3 (open-source software).

3. Results and discussion

3.1. General comparison of salt effects on free and immobilised trypsin

The conductivities of the applied buffers were 3.82 mS cm^{-1} (0.1 M Tris), 10.85 mS cm^{-1} (0.1 M Tris + 0.1 M NaCl), and 9.61 mS cm^{-1} (0.5 M Tris), respectively. The enzymatic activity toward BAEE (342.82 Da) and the depletion of intact β-Lg in these buffers were investigated. In all reactions, applied buffers kept pH in 8.6–8.7.

As shown in Fig. 1, either the addition of 0.1 M NaCl or increasing Tris concentration from 0.1 to 0.5 M did not significantly affect the enzymatic activity of free and immobilised trypsin, although the conductivity of the reaction medium increased greatly. Wesolowska et al. (2001) found that the activity of free trypsin toward BAEE was nearly unaffected by the presence of NaCl up to 3 M. Contrastively, the amount of hydrolysed intact β-Lg decreased significantly for both forms of trypsin due to the addition of salts, as shown in Fig. 2. For free trypsin, around 63% of intact protein was hydrolysed in 0.1 M Tris, which decreased by 40% with the addition of 0.1 M NaCl. For immobilised trypsin, the hydrolysed amount of intact β-Lg decreased by 18% with the presence of 0.1 M NaCl or 0.5 M Tris.

The surface charge of β-Lg is much more complex than BAEE. Thus, the influence of salts on electrostatic interactions between substrate and enzyme appears to be greatly strengthened, when β-Lg substituted the substrate BAEE. In addition, salts may stabilise or destabilise β-Lg. For instance, Tris buffer is reported to stabilise macromolecules such as BSA (Taha & Lee, 2010). Increasing concentrations of NaCl (up to 2 M) are reported to increase the thermal stability of β-Lg (Vardhanabhuti & Foegeding, 2008). Stabilisation of substrate molecules may prevent them from hydrolysis.

Although Tris and NaCl did not affect enzymatic activity significantly, they exerted considerable influences on the interactions between β-Lg and trypsin. To interpret the mechanism, Tris and NaCl were introduced to the reaction medium separately, and the hydrolysis without the addition of salts was conducted as well.

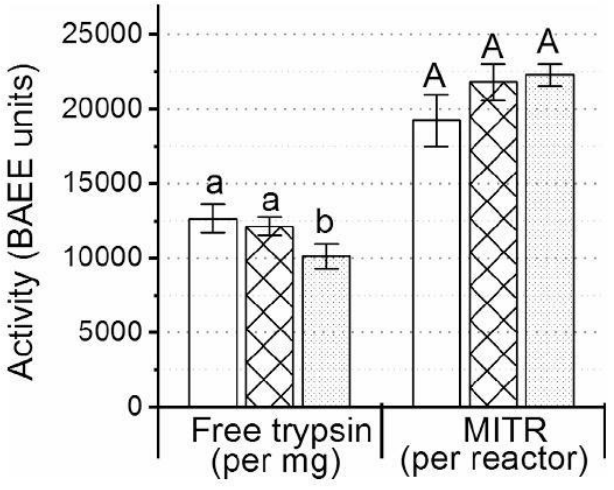

Fig. 1. Effects of Tris buffer and NaCl on trypsin activity. Hollow bars, bars with crossed lines and dots represent the hydrolysis of β-Lg in 0.1 M Tris, 0.1 M Tris + 0.1 M NaCl, and 0.5 M Tris, respectively. Data values represent mean values of three replicates with a 95% confidence interval. Values with the same lowercase letter (for free trypsin) or with the same uppercase letter (for monolith-based immobilised trypsin reactor) are not statistically different ($P \geq 0.05$).

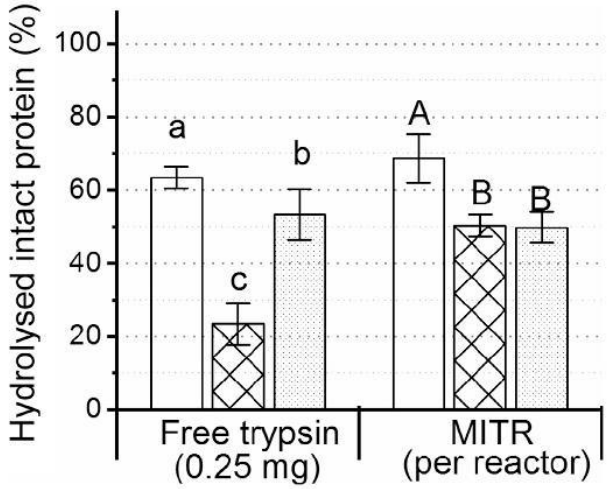

Fig. 2. Effects of Tris buffer and NaCl on the hydrolysis of intact β-lactoglobulin. Hollow bars, bars with crossed lines and dots represent the hydrolysis of β-Lg in 0.1 M Tris, 0.1 M Tris + 0.1 M NaCl, and 0.5 M Tris, respectively. Data values represent mean values of three replicates with a 95% confidence interval. Values with the same lowercase letter (for free trypsin) or with the same uppercase letter (for monolith-based immobilised trypsin reactor) are not statistically different ($P \geq 0.05$).

3.2. Influence of Tris buffer

Both 10 mg mL^{-1} β-Lg in 0 (1.05 mS cm^{-1}) and 0.1 M (3.82 mS cm^{-1}) Tris buffers were hydrolysed by free trypsin or MITR for 3 h. Because of the buffering capacity of Tris, the DH measured by a pH drop does not represent the actual extent of the reaction. Thus, the amount of intact protein hydrolysed was used to follow the reaction progress. For free trypsin, 65.7% (without Tris) and 63.5% (with Tris) of the β-Lg were hydrolysed after 1 h, while MITR required 3 h to hydrolyse similar amounts of β-Lg (64.4% without Tris; 66.6% with Tris). The peptide profiles of these four samples were analysed by HPLC and MALDI-TOF-MS.

3.2.1. The effects of Tris on peptide profiles

As shown in Fig. 3, peaks which eluted before 45 min contained peptides with a molecular weight below 3000 Da. Most of these peaks were assigned to final peptides based on trypsin specificity (as shown in Table 1), except the cleavage at Tyr_{20}–Ser_{21}, which is a nonspecific (chymotrypsin-like) cleavage by trypsin, as reported in other studies (Butré, Sforza, Wierenga, & Gruppen, 2015; Cheison, Leeb, Letzel, & Kulozik, 2011a). Although the HPLC profiles of these four samples before 45 min were quite similar, the amounts of individual peptides (mainly the final peptides) differed significantly. As illustrated in Fig. 4, the relative amount of each peptide based on the hydrolysed protein content (value R_1) is compared, and the theoretically maximum R_1 value should be 100%. The effects of Tris on the release of peptides, as indicated by R_1 values, are summarised in Table 2. Compared with hydrolysis in water, the presence of 0.1 M Tris contributed to the release of most final peptides for both forms of trypsin, except f (71–75). This peptide is typically released quickly during tryptic hydrolysis because of its external position in the three-dimensional structure of β-Lg (Fernández, Suárez, Zhu, FitzGerald, & Riera, 2013). However, its precursor peptide f (70–75) accumulated significantly in Tris buffer, indicating that its further hydrolysis was prevented. Other intermediate peptides f (41–60), f (92–101) and f (76–91) also accumulated more in 0.1 M Tris than in water for both forms of trypsin, e.g., 6-fold (for free trypsin) and 7-fold (for MITR) increases

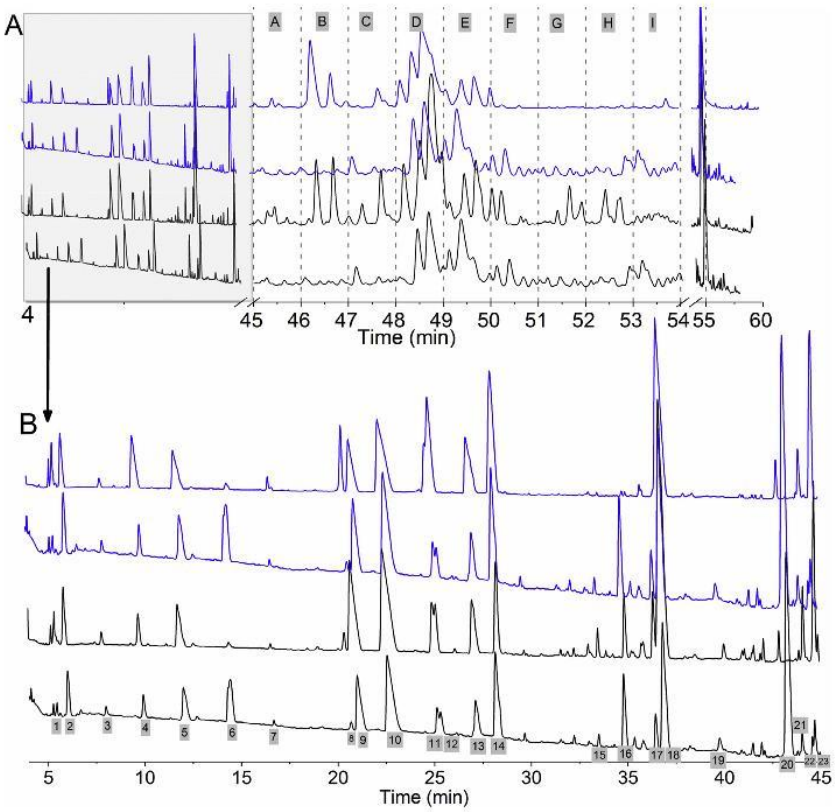

Fig. 3. HPLC profiles of β-lactoglobulin hydrolysates generated from free or immobilized trypsin in the presence or absence of Tris buffer. The peaks eluted after 45 min are illustrated in A, and the peaks eluted before 45 min are highlighted in B. Samples from top to bottom are hydrolysates produced in 0.1 M Tris by immobilised trypsin, in water by immobilised trypsin, in 0.1 M Tris by free trypsin and in water by free trypsin, respectively. Those peaks marked with number or letter are identified and reported in Table 1.

in f (41–60) were observed. The peptide f (41–60) possesses one missed cleavage site Lys_{47}, which links to a proline residue and is resistant to trypsinolysis, as observed by Olsen, Ong, and Mann (2004). Particularly for MITR, the amount of f (125–138) increased greatly. Regarding peptides eluted after 45 min, peaks representing f (102–138)b and f (15–141)a showed increasing area in the presence of Tris for both forms of trypsin.

3.2.2. The mechanism underlying the observed influence of Tris

Compared with the hydrolysis without Tris, the addition of 0.1 M Tris did not reduce the hydrolysis of intact β-Lg, while contributed to the release of most final peptides. Taha and Lee (2010) reported that Tris preferentially interacted with the peptide backbone by virtue of its −OH and amine groups through hydrogen bonding. Quan et al. (2008) found that Tris molecules formed hydrogen bonds with Asp_{52}, Glu_{35}, and Ala_{107} residues in lysozyme. Hence, it is speculated that Tris molecules mainly interact with certain intermediate peptides (the precursors of final peptides) and trypsin molecules through hydrogen bonds simultaneously, enhancing their interactions and then improving their hydrolysis. To determine whether Tris molecules preferentially interact with certain polypeptides, the characteristics of intermediate peptides are summarised in Supplementary material Table S1, including isoelectric point (PI), hydrophilicity, and the ratio of hydrophilic residues to total number of residues (%). However, there is no clear correlation between the influence of Tris and the peptide characteristics.

3.3. Influence of NaCl

Samples with 10 mg mL^{-1} β-Lg in 0 (1.05 mS cm^{-1}), 0.02 (3.25 mS cm^{-1}), 0.1 (10.25 mS cm^{-1}) and 0.5 M (46.55 mS cm^{-1}) NaCl were hydrolysed by free trypsin or MITR for 3 h.

3.3.1. The effects of NaCl on DH and amounts of residual intact β-Lg

The DH as a function of time is presented in Fig. 5A1 for free trypsin and in Fig. 5B1 for immobilised trypsin. The hydrolysis of β-Lg in water by free trypsin reached a DH of 5.87 ± 0.79% after 3 h, which was significantly higher than that by MITR (3.93 ± 0.74%). In both cases, the fastest increase in DH was observed with the addition of 0.02 M NaCl, where DH values reached 7.18 ± 0.76% (free trypsin) and 6.37 ± 0.95% (MITR), respectively. Interestingly, increasing NaCl concentration from 0 to 0.1 M significantly promoted hydrolysis efficiency by MITR, reaching DH 5.67 ± 0.75%, but it decreased DH from 5.87 ± 0.79% to 5.14 ± 0.82% for free trypsin. The addition of 0.5 M NaCl seriously hindered the hydrolysis, irrespective free or immobilised trypsin applied, i.e., the DH values were only 3.83 ± 0.82% and 2.74 ± 0.81%, respectively.

Regarding the hydrolysis of intact protein, the Linderstrøm-Lang theory presents two models: "zipper" and "one-by-one" (Adler-Nissen, 1976). In a "one-by-one" model, intact protein will slowly break down and no appreciable amounts of intermediate peptides will be accumulated, while a much faster degradation of intact protein at the initial stage of hydrolysis will be observed in a "zipper" model. In fact, most proteins show an intermediate

Table 1
Identification of peptides generated from the hydrolysis of β-lactoglobulin (β-Lg) by free and immobilised trypsin.

Peaks	Calculated mass[a]	Observed mass[b]	Assigned sequence[c]
1	1180.2	1180.5	f (61–69)a
	1122.2	1122.5	f (61–69)b
	1308.4	1307.4	f (61–70)a
	1250.4	1249.3	f (61–70)b
2	595.4 ^{Na}	595.4	f (71–75)
3	739.4^{K}	739.3	f (70–75)
4	938.5	938.5	f (84–91)
5	695.4 ^{Na}	695.4	f (9–14)
6	825.0 ^{Na}	825.0	f (71–77)
7	1245.6	1245.8	f (125–135)
8	696.8	696.9	f (15–20)
9	955.5 ^{Na}	955.5	f (1–8)
10	837.5	837.5	f (142–148)
11	1194.4	1193.5	f (92–101)
12	674.4	674.5	f (78–83)
13	904.1	904.1	f (76–83)
14	1658.7 ^{Na}	1659.0	f (125–138)
15	2092.4	2092.3	f (84–101)
16	1949.1	1949.3	f (125–141)
17	1802.1	1802.2	f (76–91)
18	1754.893^{K}	1753.6	f (149–162)
19	/	2189.1	/
20	/	1658.0/3315.1	/
21	2069.3^{k}	2069.2	f (21–40)
22	2313.3	2313.2	f (41–60)
23	2820.2	2820.2	f (102–124)b
	2848.3	2848.2	f (102–124)a
A	4075.6	4075.8	f (102–135)b
	4203.7	4203.5	f (101–135)a
	4213.7^{K}	4215.2	f (101–135)b
B	4437.9	4437.0	f (102–138)b
	14480.5	7240.1 *	f (15–141)b
C	3546.0	3544.4	f (41–70)b
	7195.2	3597.8 *	f (78–138)a
	7167.1	7167.9	f (78–138)b
D	3626.0 ^{Na}	3624.7	f (41–70)a
	4466.0	4466.5	f (102–138)a
	5613.3	5614.1	f (92–138)b
	14480.5	7239.9 *	f (15–141)b
E	6989.0	3494.0 *	f (41–100)a
	7034.0	3519.3 *	f (76–135)a
	7006.0	3504.7 *	f (76–135)b
	7295.3	3649.4 *	f (102–162)a
	7267.3	3633.7 *	f (102–162)b
F	5597.4	5598.1	f (102–148)a
	5569.4	5569.9	f (102–148)b
	5641.4	5642.1	f (92–138)a
	5613.3	5614.6	f (92–138)b
G	/	/	/
H	11190.9	5595.5 *	f (1–100)b
	10808.4	5403.5 *	f (71–162)a
I	5488.2	5487.5	f (21–69)a
	5430.1	5430.9	f (21–69)b
	11249.0	5624.5 *	f (1–100)a

[a] Monoisotopic mass with single charge, calculated from amino acid sequence. Na and K represent sodium and potassium adduct, respectively.
[b] Observed mass with single charge except for those marked with *, * means double charged mass.
[c] a represents this sequence particularly from β-lactoglobulin A, and b is from β-lactoglobulin B.

behavior between these two models, and their behaviors depend not only on the nature of substrate and enzyme, but also on hydrolytic conditions. For immobilised trypsin, although linear decreases in intact protein dependent on DH were observed at all explored concentrations of NaCl, close to the "one-by-one" model (Fig. 5B2), increasing NaCl concentrations led to a clear decrease in the depletion of intact β-Lg. Specifically, around 18–26% intact protein was hydrolysed in 0 or 0.02 M NaCl at DH ≈ 1%, while it was only 7–10% in 0.1 or 0.5 M NaCl. For free trypsin, a sharp increase in the depletion rate was noted at the initial stage of hydrolysis with 0 or 0.02 M NaCl, during which the increase in DH from 0 to 1% corresponded to a depletion of 30–40% of the intact protein content (Fig. 5A2). This is more in agreement with the "zipper" model, while it seems to be at the "one-by-one" model, when NaCl concentration increased from 0.02 to 0.1 or 0.5 M.

3.3.2. The effects of NaCl on peptide profiles

As illustrated in Fig. 6 and Table 1, peaks located in the range of 45–60 min correspond to intermediate peptides. The accumulation of these peptides was primarily due to the fast breakdown of intact β-Lg and secondarily due to the insufficient subsequent hydrolysis. For both forms of trypsin, 0.1 and 0.5 M NaCl significantly diminished the peaks of intermediate peptides, partly due to the slow hydrolysis of intact β-Lg (Fig. 5A2,B2). These results are in accordance with the findings of Butré, Wierenga, and Gruppen (2012), who reported that in 0.5 M NaCl, the hydrolysate composition of 1–5% WPI (w/w) showed increasing levels in hydrophilic peptides and decreasing amount of hydrophobic peptides, compared with hydrolysis without NaCl.

Regarding peaks eluted before 45 min, most of them were assigned to the final peptides as previously discussed for Fig. 3, thus, these peaks in Fig. 6 are not repeatedly highlighted. The DH-dependent release of these identified peptides is illustrated in Supplementary material Fig. S1 for free trypsin and in Fig. S2 for MITR. Furthermore, Fig. 7 shows the relative amounts of individual peptides based on the relative DH (value R_2). A higher R_2 value of a peptide indicates that this peptide is preferred to be released than other peptides during the hydrolysis. If all final peptides released at the same rate, all R values would be 100%. The effects of NaCl on the release of peptides, as indicated by R_2 values, are summarised in Table 2. For free trypsin, peptides f (61–69/61–70), f (84–91), f (125–125), f (92–101) and f (41–60) were released significantly faster at 0.1 or 0.5 M NaCl. Specifically, at DH 3%, 3-fold higher amount of f (61–69/61–70) and 2-fold higher amounts of f (92–101) and f (41–60) were released with the addition of 0.5 M NaCl, compared with those in 0 and 0.02 M NaCl. Also, f (15–20), f (21–40) and f (125–135) were released much earlier in 0.1 and 0.5 M NaCl. For immobilised trypsin, the addition of 0.1 or 0.5 M NaCl significantly increased f (61–69/61–70) and f (125–135). In addition, levels of f (71–75) and its precursor f (70–75) decreased significantly with the addition of 0.1 and 0.5 M NaCl for immobilised trypsin, while no significant difference in these peptides was observed for free trypsin. In general, the final peptides directly associated with the breakdown of intact protein diminished with increasing NaCl concentrations.

3.3.3. The mechanism underlying the observed influence of NaCl

In contrast to Tris, NaCl is a strong electrolyte and is reported to show quasi-neutral behavior, as both its anion and cation are located in the middle of the Hofmeister series (Salis et al., 2007). Sedlak, Stagg, and Wittung-Stafshede (2008) concluded that at low ion concentrations (<100–200 mM), ions specifically interacted with protein molecules in the manner of Langmuir binding isotherm (specific binding or pairing of ions with proteins), while at ion concentrations > 200 mM, Hofmeister effects dominated (salting out or salting in of proteins). The study exploring ion-pairing effects of NaCl on β-Lg indicates that Na^+ ions pair with carboxylate groups, while Cl^- ions are not significantly enriched near positively charged residues, such as Lys and Arg (Beierlein et al., 2015). At pH 8.7, the overall surface charge of trypsin molecules is theoretically positive, as its PI is 10.1–10.5 (Buck, Vithayathil, Bier, & Nord, 1962). As the electrostatic interactions between free enzyme and substrate molecules dominate (Endo et al., 2016), the pairing effect of Na^+ ions with the carboxylic

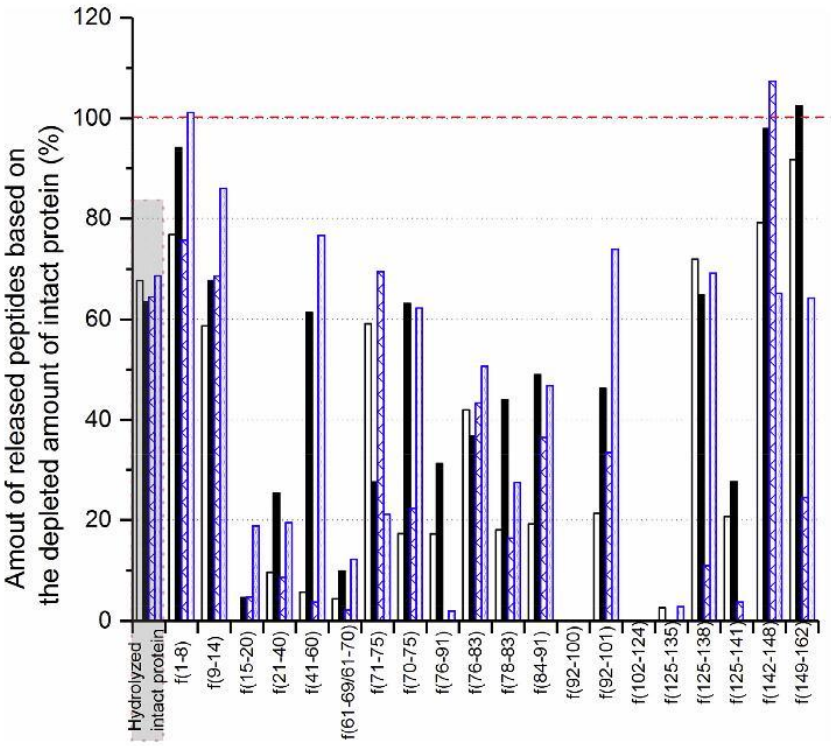

Fig. 4. Effects of Tris buffer on the release of specific peptides. Hollow and black bars represent the cases hydrolysed by free trypsin with and without Tris buffer, respectively. Bars with crossed lines and dots represent the cases hydrolysed by immobilised trypsin with and without Tris buffer, respectively.

Table 2
The effects of salts on the release of peptides.

Effects	Free trypsin	MITR
Effects of Tris[a]		
Increase	f (1–8); f (9–14); f (15–20); f (21–40); f (41–60); f (61–69/61–70); f (78–83); f (84–91); f (92–101)*; f (142–148); f (149–162)	f (1–8); f (9–14); f (15–20); f (21–40); f (41–60); f (61–69/61–70); f (78–83); f (84–91); f (92–101)*; f (125–138)*; f (125–135); f (149–162)
Decrease	f (71–75)	f (71–75); f (142–148)
No significant effect	f (92–100); f (125–138)*; f (125–135)	f (92–100)
Effects of NaCl[b]		
Monotonic decrease	f (1–8); f (9–14)	f (1–8); f (9–14); f (71–75); f (142–148); f (149–162)
Monotonic increase	f (15–20); f (21–40); f (41–60)*; f (61–69/61–70); f (92–101)*; f (125–135); f (125–138)*	f (41–60)*; f (61–69/61–70); f (125–135)
Increase then decrease	f (78–83); f (84–91); f (92–100); f (101–124)*; f (142–148); f (149–162)	f (78–83); f (84–91); f (92–101)*; f (125–138)*
No significant effect	f (71–75)	f (15–20); f (21–40); f (92–100); f (101–124)*

[a] based on the R1 value; [b] based on the R2 value; an asterisk indicates peptides with one missed cleavage site and a negligible amount of the final derivative peptide.

groups of β-Lg at low NaCl concentrations could protect intact protein molecules from hydrolysis by free trypsin. The addition of high concentration of NaCl significantly increased the ionic strength of the reaction media, which might hinder enzyme–substrate interactions through charge shielding. In addition, due to Hofmeister effects, the interactions between molecules of β-Lg increase with increasing concentrations of NaCl, toward dimer formation. This further decreases the depletion of intact protein significantly by both forms of trypsin. Beierlein et al. (2015) provided models on the formation of β-Lg dimmers, including the "lock-and-key", corresponding well to our results. The residues involved in interactions in this model are mainly in termini, and the release of final peptides located in termini decreased significantly at high concentrations of NaCl in this study.

3.4. The mechanism underlying the different influences on free and immobilised trypsin exerted by salts

As previously discussed, Tris and NaCl exerted different influences on free and immobilised trypsin. These differences are probably due to (i) the unconventional flow-through hydrolysis mode and (ii) the surface characteristics of the support used to immobilise trypsin. In this flow-through approach, shear force is a decisive force, driving substrate molecules to immobilised trypsin, since a higher flow rate contributes to a higher hydrolysis efficiency in our previous work (Mao et al., 2017; Mao & Kulozik, 2018). Further, immobilised trypsin attracts substrate molecules at a short distance, depending on the interactions of substrate–enzyme and/or substrate-support surface. In this study, aldehyde-activated

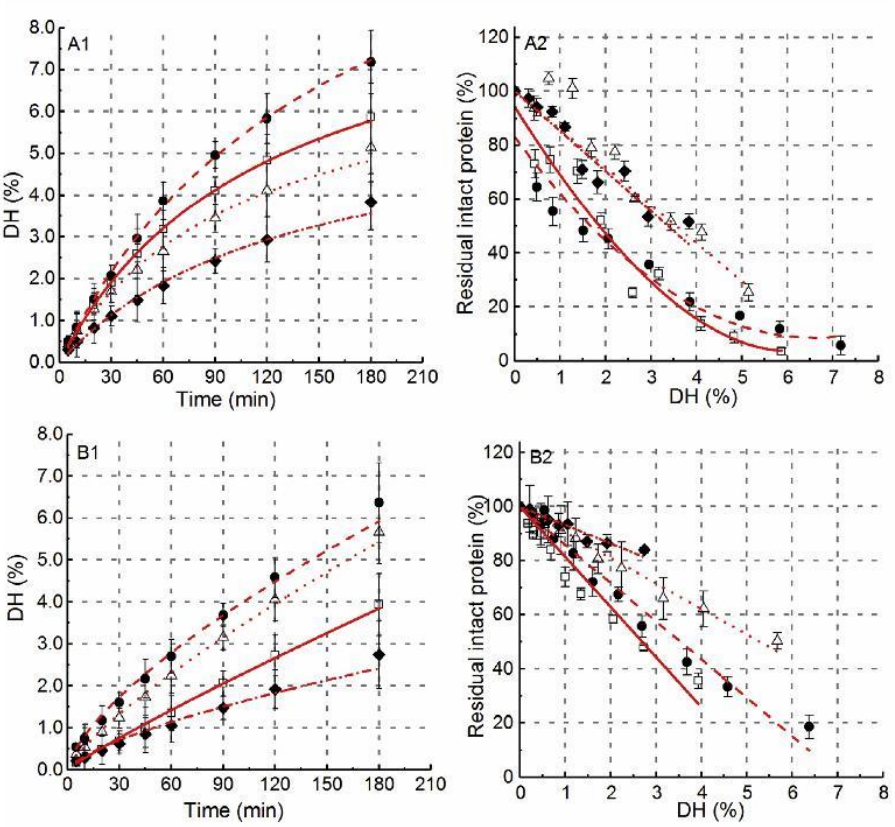

Fig. 5. Effects of 0 M (□), 0.02 M (●), 0.1 M (△), and 0.5 M (◆) NaCl on DH (A1&B1) and the amount of residual native β-lactoglobulin (A2 and B2). A, hydrolysis by free trypsin; B, hydrolysis by MITR. Data values represent mean values of three replicates with a 95% confidence interval.

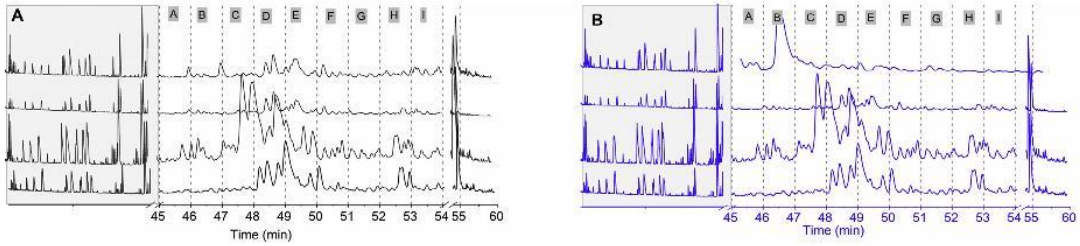

Fig. 6. HPLC profiles of β-lactoglobulin hydrolysates generated from free (A) or immobilised trypsin (B) with increasing NaCl. Samples from top to bottom are hydrolysates produced in 0.5 M, 0.1 M, 0.02 M and 0 M NaCl, respectively.

columns without a spacer linker were used as the immobilisation support, and the surface was preferentially neutral (Naldi, Černigoj, Štrancar, & Bartolini, 2017). In addition, the surface coverage ratio by trypsin molecules was high, about 65 ± 10% (Mao et al., 2017). Thus, the surface charge and hydrophobicity of the support is considered to be same as that of the formed layer of immobilised trypsin molecules. Trypsin was immobilised at pH 5.6 (Mao et al., 2017), where the overall surface charge of trypsin molecules is, in theory, highly positive. Based on the principles of electrostatic interactions, each trypsin molecule probably regulates its position to reach a charge balance with other trypsin molecules during the immobilisation. Hence, the attractive force between substrate molecules and immobilised trypsin is probably different from that for free trypsin, which is mainly dependent on electrostatic interactions (Evnin et al., 1990). Our results corroborate this prediction. For instance, negatively-charged precursor peptides f (125–141), f (125–138) and f (102–138) were much less attracted to immobilised trypsin than for free trypsin. Alternatively, the hydrophobic precursor peptides were generally preferred over hydrophilic peptides for immobilised trypsin. Therefore, hydrophobic interactions are implicated as the attracting forces at a short distance, determining the interactions between substrate molecules and immobilised trypsin. With the addition of salts, ions may provide charge shielding/electrical double layer or stoichiometric

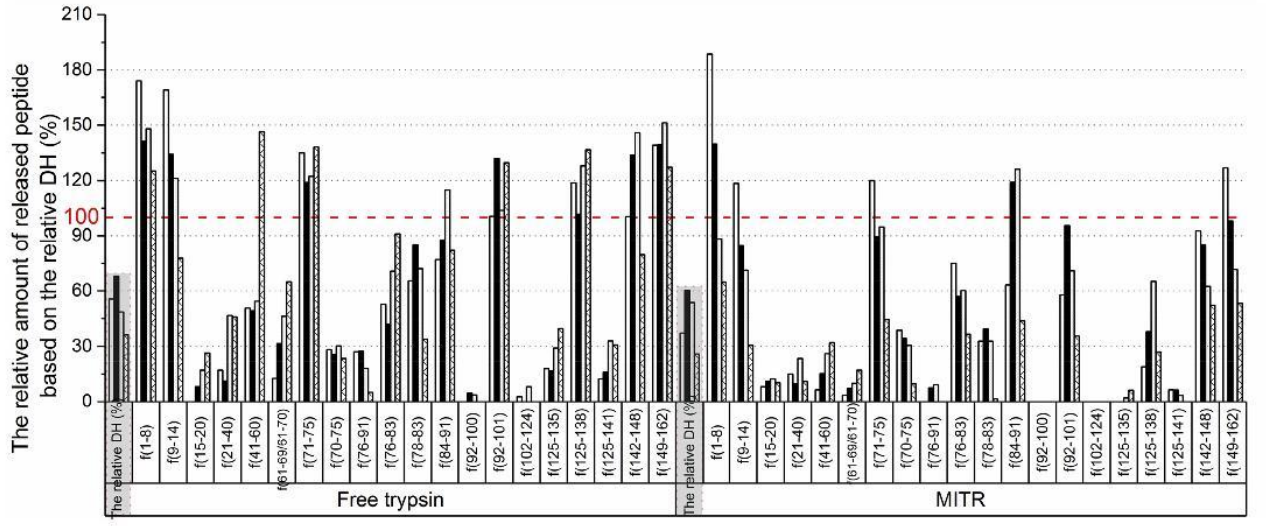

Fig. 7. Effects of NaCl on the release of specific peptides. Hollow bars, black bars, bars with dots, and bars with crossed lines represent the hydrolysis of β-lactoglobulin in 0, 0.02, 0.1 and 0.5 M NaCl, respectively.

ion binding on the support surface in MITR, which is used for column chromatography to suppress nonspecific adsorption of proteins to the column surface (Tsumoto et al., 2007). Thus, due to the ions binding on the surface of immobilisation support, this support may exert an additional repulsive force on intact protein and/or an attractive force on certain peptides.

4. Conclusions

In this study, the influence of salts was explored comparatively between free and immobilised trypsin for the hydrolysis of β-Lg. Compared with the hydrolysis without additional NaCl, DH increased faster for both forms of trypsin with the presence of 0.02 NaCl, especially for immobilised trypsin, DH increased in 0.1 M NaCl as well. Regarding the hydrolysis of intact protein, increasing NaCl concentrations significantly reduced the depletion rate for both forms of trypsin, while 0.1 M Tris had no significant influence on hydrolysing intact protein. In addition, both forms of trypsin preferentially hydrolysed certain intermediate peptides in the presence of salts, depending on the type and concentration of salts as well as on the form of trypsin. This study followed the change in peptide profiles at the early stage of hydrolysis, and provided the possibility of a partial hydrolysis of β-Lg with desired peptide compositions, for example, a hydrolysate with a maximum accumulation of certain functional intermediate peptides.

Generally, the hydrolysis efficiency and hydrolysate profiles can be regulated by adding different salts at varied concentrations, since salts significantly influence the interactions between proteins/peptides and enzymes. This study may provide some hints on the choices of buffers or salts to regulate the hydrolysis process, improve the hydrolysis efficiency or obtain desired product profiles. In future studies, the investigation of a hydrolysis medium with more complex salt compositions, such as milk salts, could be quite interesting. Milk salts contain calcium, magnesium, sodium, and potassium as the main cations and inorganic phosphate, citrate, and chloride as the main anions. The hydrolysis of milk proteins without the removal or with the addition of these salts could provide consumers with extra benefits, as these minerals are essential for bone growth and development. However, it is necessary to clarify whether these minerals will considerably influence the hydrolysis efficiency and/or the resulting hydrolysate profiles.

Acknowledgements

The first author thanks China Scholarship Council (China) for the support of her personal costs. The authors would like to thank Urh Černigoj from BIA Separations (Ajdovščina, Slovenia) for his technical help in developing the MITR. This research did not receive any specific grant from funding agencies in the public, commercial, or not-for-profit sectors.

Appendix A. Supplementary data

Supplementary data to this article can be found online at https://doi.org/10.1016/j.idairyj.2019.02.006.

References

Adler-Nissen, J. (1976). Enzymic hydrolysis of proteins for increased solubility. *Journal of Agricultural and Food Chemistry, 24*, 1090–1093.
Beierlein, F. R., Clark, T., Braunschweig, B., Engelhardt, K., Glas, L., & Peukert, W. (2015). Carboxylate ion pairing with alkali-metal ions for β-lactoglobulin and its role on aggregation and interfacial adsorption. *Journal of Physical Chemistry B, 119*, 5505–5517.
Bergmeyer, H. U., Gawehn, K., & Grassl, M. (1974). Trypsin. *Methods of Enzymatic Analysis, 1*, 515–516.
Buck, F., Vithayathil, A., Bier, M., & Nord, F. (1962). On the mechanism of enzyme action. LXXIII. Studies on trypsins from beef, sheep and pig pancreas. *Archives of Biochemistry and Biophysics, 97*, 417–424.
Butré, C. I., Sforza, S., Gruppen, H., & Wierenga, P. A. (2014). Introducing enzyme selectivity: A quantitative parameter to describe enzymatic protein hydrolysis. *Analytical and Bioanalytical Chemistry, 406*, 5827–5841.
Butré, C. I., Sforza, S., Wierenga, P. A., & Gruppen, H. (2015). Determination of the influence of the pH of hydrolysis on enzyme selectivity of *Bacillus licheniformis* protease towards whey protein isolate. *International Dairy Journal, 44*, 44–53.
Butré, C. I., Wierenga, P. A., & Gruppen, H. (2012). Effects of ionic strength on the enzymatic hydrolysis of diluted and concentrated whey protein isolate. *Journal of agricultural and food chemistry, 60*, 5644–5651.
Chaplin, M. F., & Bucke, C. (1990). *Enzyme technology*. Cambridge, UK: Cambridge University Press.
Cheison, S. C., Leeb, E., Letzel, T., & Kulozik, U. (2011a). Influence of buffer type and concentration on the peptide composition of trypsin hydrolysates of β-lactoglobulin. *Food Chemistry, 125*, 121–127.
Cheison, S. C., Leeb, E., Toro-Sierra, J., & Kulozik, U. (2011b). Influence of hydrolysis temperature and pH on the selective hydrolysis of whey proteins by trypsin and potential recovery of native alpha-lactalbumin. *International Dairy Journal, 21*, 166–171.
Duggal, S., & Bucholz, K. (1982). Effects of immobilization on intrinsic kinetics and selectivity of trypsin. *Applied Microbiology and Biotechnology, 16*, 81–87.

Endo, A., Kurinomaru, T., & Shiraki, K. (2016). Hyperactivation of α-chymotrypsin by the Hofmeister effect. *Journal of Molecular Catalysis B Enzymatic, 133*, S432–S438.
Endo, A., Kurinomaru, T., & Shiraki, K. (2018). Hyperactivation of serine proteases by the Hofmeister effect. *Molecular Catalysis, 455*, 32–37.
Evnin, L. B., Vásquez, J. R., & Craik, C. S. (1990). Substrate specificity of trypsin investigated by using a genetic selection. *Proceedings of the National Academy of Sciences, 87*, 6659–6663.
Fernández, A., & Riera, F. (2013). β-Lactoglobulin tryptic digestion: A model approach for peptide release. *Biochemical Engineering Journal, 70*, 88–96.
Fernández, A., Suárez, A., Zhu, Y., FitzGerald, R. J., & Riera, F. A. (2013). Membrane fractionation of a β-lactoglobulin tryptic digest: Effect of the pH. *Journal of Food Engineering, 114*, 83–89.
Garajova, K., Balogova, A., Dusekova, E., Sedlakova, D., Sedlak, E., & Varhac, R. (2017). Correlation of lysozyme activity and stability in the presence of Hofmeister series anions. *Biochimica et Biophysica Acta, 1865*, 281–288.
Hernández-Ledesma, B., Recio, I., & Amigo, L. (2008). β-Lactoglobulin as source of bioactive peptides. *Amino Acids, 35*, 257–265.
Hofmeister, F. (1888). Zur lehre von der wirkung der salze. *Archiv für experimentelle Pathologie und Pharmakologie, 25*, 1–30.
Kuipers, B. J., & Gruppen, H. (2007). Prediction of molar extinction coefficients of proteins and peptides using UV absorption of the constituent amino acids at 214 nm to enable quantitative reverse phase high-performance liquid chromatography–mass spectrometry analysis. *Journal of Agricultural and Food Chemistry, 55*, 5445–5451.
Leeb, E., Gotz, A., Letzel, T., Cheison, S. C., & Kulozik, U. (2015). Influence of denaturation and aggregation of beta-lactoglobulin on its tryptic hydrolysis and the release of functional peptides. *Food Chemistry, 187*, 545–554.
Mao, Y., Černigoj, U., Zalokar, V., Štrancar, A., & Kulozik, U. (2017). Production of beta-Lactoglobulin hydrolysates by monolith based immobilized trypsin reactors. *Electrophoresis, 38*, 2947–2956.
Mao, Y., Krischke, M., Hengst, C., & Kulozik, U. (2018). Comparison of the influence of pH on the selectivity of free and immobilized trypsin for beta-lactoglobulin hydrolysis. *Food Chemistry, 253*, 194–202.
Mao, Y., & Kulozik, U. (2018). Selective hydrolysis of whey proteins using a flow-through monolithic reactor with large pore size and immobilised trypsin. *International Dairy Journal, 85*, 96–104.
Mozhaev, V. V., Melik-nubarov, N. S., Sergeeva, M. V., Šikšnis, V., & Martinek, K. (1990). Strategy for stabilizing enzymes part one: Increasing stability of enzymes via their multi-point interaction with a support. *Biocatalysis and Biotransformation, 3*, 179–187.
Naldi, M., Černigoj, U., Štrancar, A., & Bartolini, M. (2017). Towards automation in protein digestion: Development of a monolithic trypsin immobilized reactor for highly efficient on-line digestion and analysis. *Talanta, 167*, 143–157.
Olsen, J. V., Ong, S.-E., & Mann, M. (2004). Trypsin cleaves exclusively C-terminal to arginine and lysine residues. *Molecular & Cellular Proteomics, 3*, 608–614.
Quan, L., Wei, D., Jiang, X., Liu, Y., Li, Z., Li, N., et al. (2008). Resurveying the Tris buffer solution: The specific interaction between tris(hydroxymethyl)aminomethane and lysozyme. *Analytical Biochemistry, 378*, 144–150.
Renard, D., Lefebvre, J., Griffin, M. C., & Griffin, W. G. (1998). Effects of pH and salt environment on the association of beta-lactoglobulin revealed by intrinsic fluorescence studies. *International Journal of Biological Macromolecules, 22*, 41–49.
Salis, A., Bilanicova, D., Ninham, B. W., & Monduzzi, M. (2007). Hofmeister effects in enzymatic activity: Weak and strong electrolyte influences on the activity of *Candida rugosa* lipase. *Journal of Physical Chemistry B, 111*, 1149–1156.
Sedlak, E., Stagg, L., & Wittung-Stafshede, P. (2008). Effect of Hofmeister ions on protein thermal stability: Roles of ion hydration and peptide groups? *Archives of Biochemistry and Biophysics, 479*, 69–73.
Selo, I., Clement, G., Bernard, H., Chatel, J., Creminon, C., Peltre, G., et al. (1999). Allergy to bovine b-lactoglobulin: Specificity of human IgE to tryptic peptides. *Clinical and Experimental Allergy, 29*, 1055–1063.
Taha, M., & Lee, M.-J. (2010). Interactions of TRIS [tris (hydroxymethyl) aminomethane] and related buffers with peptide backbone: Thermodynamic characterization. *Physical Chemistry Chemical Physics, 12*, 12840–12850.
Toro-Sierra, J., Tolkach, A., & Kulozik, U. (2011). Fractionation of α-lactalbumin and β-lactoglobulin from whey protein isolate using selective thermal aggregation, an optimized membrane separation procedure and resolubilization techniques at pilot plant scale. *Food and Bioprocess Technology, 6*, 1032–1043.
Tougu, V., Tiivel, T., Talts, P., Siksnis, V., Poyarkova, S., Kesvatera, T., et al. (1994). Electrostatic effects in trypsin reactions: Influence of salts. *European Journal of Biochemistry, 222*, 475–481.
Tsumoto, K., Ejima, D., Senczuk, A. M., Kita, Y., & Arakawa, T. (2007). Effects of salts on protein-surface interactions: Applications for column chromatography. *Journal of Pharmaceutical Sciences, 96*, 1677–1690.
Vardhanabhuti, B., & Foegeding, E. A. (2008). Effects of dextran sulfate, NaCl, and initial protein concentration on thermal stability of β-lactoglobulin and α-lactalbumin at neutral pH. *Food Hydrocolloids, 22*, 752–762.
Wesolowska, O., Krokoszynska, I., Krowarsch, D., & Otlewski, J. (2001). Enhancement of chymotrypsin-inhibitor/substrate interactions by 3 m NaCl. *Biochimica et Biophysica Acta, 1545*, 78–85.
Yu, J., & Ahmedna, M. (2012). *Functions/applications of trypsin in food processing and food science research*. Hauppauge, NY, USA: Nova Science Publishers, Inc.
Zhao, Z., Li, H., & Li, Q. (2017). Isolation of β-lactoglobulin from buffalo milk and characterization of its structure changes as a function of pH and ionic strength. *Journal of Food Measurement and Characterization, 11*, 948–955.
Žoldák, G., Sprinzl, M., & Sedlák, E. (2004). Modulation of activity of NADH oxidase from *Thermus thermophilus* through change in flexibility in the enzyme active site induced by Hofmeister series anions. *European Journal of Biochemistry, 271*, 48–57.

8.2 Oral / poster presentations

Oral presentations

Mao, Y., Kulozik, U.. Comparison of soluble and CIM monolith based immobilized trypsin for the hydrolysis of β-lactoglobulin, Awarded as the Third Prize in young researchers presentation. 7th Monolith Summer School & Symposium, Portorož, Slovenia, 05/2016.

Mao, Y., Kulozik, U.. Monolith based immobilized trypsin reactor for selective hydrolysis of ß-Lactoglobulin in a continuous flow system. Emerging Dairy Technologies, in Freising, Germany, 09/2016.

Mao, Y., Kulozik, U.. Characterization of monolith based immobilized trypsin reactors. 13th International PhD Seminar on Chromatographic Separation Science, Trifels, Germany, 02/2017

Mao, Y., Kulozik, U.. Selective hydrolysis of whey proteins by immobilized trypsin in a flow-through monolithic reactor. Participated as a lecturer. 8th Monolith Summer School & Symposium, Portorož, Slovenia, 06/2018.

Poster presentations

Mao, Y., Kulozik, U.. Selective hydrolysis of whey proteins using a flow-through monolithic reactor. CDZ-Symposium, Hohenheim, Germany, 09/2018.

8.3 Curriculum Vitae

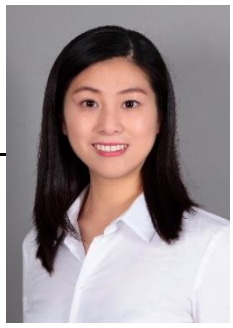

Yuhong Mao

Personal details

Date of birth	October 25th, 1988
Place of birth	Zhejiang, China
Nationality	China

Experience

Since 10/2014	Research Associate and Doctoral candidate
	Technical University of Munich, Chair of Food and Bioprocess Engineering, Freising, Germany
	Doctoral thesis: Immobilized enzyme technology for the production of whey protein hydrolysates
Since 04/2016	Global Scholar
	PreScouter, Inc., Chicago, IL, USA
	Main task: Translating academic knowledge to address technical problems
02/2012–07/2013	Part-time Lecture
	Zhejiang Pharmaceutical College, Zhejiang, China
	Main task: Teaching assistant for course Food Chemistry
09/2011–08/2012	Part-time School Counselor Assistant
	Ningbo University, School of Marine, Zhejiang, China
	Main task: Enhancing relationships with students

Education

09/2011–07/2014	Ningbo University, Zhejiang, China
	Master Thesis: Extraction and characterization of collagens from Jumbo flying squid (*Dosidicus gigas*) skin and preparation of antioxidant peptides from squid skin gelatin
	Qualification: Master in Food Science
09/2007–07/2011	Ningbo University, Zhejiang, China
	Bachelor Thesis: Antioxidant activity of shark meat hydrolysates
	Qualification: Bachelor in Food Quality and Safety
09/2004-07/2077	Huzhou High School, Zhejiang, China